AXIAL DISPERSION AND MASS TRANSFER

IN MOBILE-BED CONTACTING

by

Ram Tirth Khanna

A Thesis Submitted to the Faculty of Graduate Studies and Research in Partial Fulfilment of the requirement for the degree of Doctor of Philosophy.

Chemical Engineering Department
McGill University
Montreal

May 1971

Chemical Engineering Ph.D.

AXIAL DISPERSION AND MASS TRANSFER IN MOBILE-BED CONTACTING

Ram Tirth Khanna

ABSTRACT

A study of mobile-bed contacting with a 5.5-inch diameter column packed with low density (0.15 gm./cc.) spheres, was carried out with countercurrent gas and liquid flow rates in the range $200 < G < 3,600$ and $4,000 < L < 25,000$ lb./hr.sq.-ft. Aspects studied include hydrodynamic parameters - minimum fluidization velocity, G_{mf}, bed expansion, h, liquid holdup, and axial mixing of liquid, Pe, for four sizes of spheres, 0.5, 0.75, 1.0 and 1.5-inch, and mass transfer parameters including effective interfacial area and "true" liquid-phase mass transfer coefficients for 0.75-inch spheres.

Liquid mixing and liquid holdup were determined by pulse testing using finite bed transfer function analysis. The hydrodynamic results are presented as relationships between liquid-phase Peclet number and the stirring number, $\Delta = \frac{G - G_{mf}}{G_{mf}}$; correlations for G_{mf} and h, and graphical representation for liquid holdup.

Three separate modes of mass transfer, those for droplets, films and bubbles, were identified. The relation between the new process of mobile-bed contacting and the well-known contacting techniques in packed beds, aerated vessels, and spray columns has been established. Correlations for interfacial area and mass transfer are given for use in design.

ACKNOWLEDGMENTS

The author wishes to express his sincere appreciation for all assistance received during the course of this investigation, and in particular to the following:

- Dr. W.J.M. Douglas of the Chemical Engineering Department for counsel, guidance and encouragement.
- Pulp and Paper Research Institute of Canada for assistance in the form of equipment grants and for the extensive use of their facilities.
- McGill University for financial assistance in the form of University Graduate Fellowships.
- Graduate students and staff, both academic and technical, of the Chemical Engineering Department for their help. The stimulating discussions with Dr. Jiri Tichy concerning gas-liquid contacting were especially appreciated.

TABLE OF CONTENTS

LIST OF ILLUSTRATIONS

Page

LIST OF TABLES

LIST OF SYMBOLS

a	effective interfacial area, $cm.^2/cm.^3$
a_d	specific surface area of the packing, $cm.^2/cm.^3$
a_w	wetted area of the packing, $cm.^2/cm.^3$
A	cross sectional area of tower, sq.ft.
$[B]$	concentration of solute B in the bulk of liquid, gm.mole/liter
c	concentration in the fluid phase, gm.mole/liter
c^*	concentration of dissolved gas at the gas-liquid interface, gm.mole/liter
C	dimensionless concentration
d	diameter of packing particle (or characteristic dimension), inches
d_p	diameter of a sphere having the same volume as that of the particle, $6v_p/s_p$
d_t	column diameter, inches
D	diffusivity, also, effective dispersion coefficient, $cm.^2/hr.$
$F(s)$	transfer function
g	acceleration due to gravity, 32.2 $ft./sec.^2$
g_c	gravitational conversion factor, 32.2 $(lb.mass)(ft)/(lb.force.sec.^2)$
G	gas mass velocity, $lb./(hr.-ft.^2)$
Ga	Galileo number, $\frac{d^3 g \rho^2}{\mu^2}$, dimensionless
G_{mf}	minimum fluidization gas mass velocity, $lb./(hr.-ft.^2)$

h	dimensionless bed expansion for MBC
h_s	static bed height, ft.
H	Henry Law constant, gm.mole/liter-atmos. also, bed height, ft.
H_{op}, H_S, H_T	operating, static and total holdup, $ft.^3/ft.^3$
H_L	height of liquid phase transfer unit, $\frac{L}{k_L a\ \rho_L}$, ft.
HMU	height of mixing unit, $\frac{H}{n}$, ft.
k_2	second-order reaction velocity constant, liter/(gm.mole.sec.)
$k_G a, K_G a$	volumetric gas-phase mass transfer coefficient, $gm.mole/(sec.-atm.-cm.^3)$
k_L^o	liquid-film mass transfer coefficient in absence of chemical reaction, cm./sec.
k_L, k_{LR}	liquid-film mass transfer coefficient with chemical reaction, cm./sec., also cm./hr.
$k_L a$	volumetric liquid-phase mass transfer coefficient, (lb.mole/cu.ft.)/(hr.-lb.mole/cu.ft.)
L	liquid mass velocity, $lb./(hr.-ft.^2)$
m	equilibrium constant, $c_L = mc_G$, also a constant
M	a variable
n	number of perfectly-mixed tanks-in-series, also a constant, dimensionless
N_{OG}	number of gas-phase transfer units, $\frac{H\ \rho_G\ k_L a}{G}$, dimensionless
N_{OL}, N_{OX}	actual number of liquid phase transfer units, $\frac{H\ \rho_L\ k_L a}{L}$, dimensionless

N_{OLP}	plug flow number of liquid phase transfer units, dimensionless
N_{Pe_L}	liquid-phase Peclet number, $\frac{Ud_p}{D_L}$, dimensionless
P,Pe	Peclet number, $\frac{Ud}{D}$, dimensionless
r	specific rate of consumption of tracer, gm.mole/(sec.-cm.^{2})
R	rate of gas absorption, gm.mole/sec., also resistance of the solution in the conductivity cell, ohms
Re	Reynolds number, $\frac{dL}{u_L}$ or $\frac{dL}{u_G}$, dimensionless
s	specific rate of production of tracer, gm.mole/(sec.-cm.^{2}), also Laplace variable
s_p	surface of particle, ft.^{2}
t	time, sec.
U	mean velocity, ft./sec.
u	superficial velocity, ft./sec.
v_p	volume of particle, ft.^{3}
V	volume of the contactor, ft.^{3}
x	distance, ft.
X	dimensionless distance, x/H, also abscissa
Y	ordinate
z	stoichiometric ratio of the reaction, dimensionless
Z	reaction parameter, $\frac{z\, c^* D_A}{c_B D_B}$, dimensionless
v	volumetric flow rate, ft.^{3}/sec.

α	a constant
β	reaction factor, $\frac{k_L}{k_L^o}$, dimensionless
γ	exponent
ε	void fraction, dimensionless
θ	time, second
τ	residence time, second
ν	kinematic viscosity, $\frac{\mu}{\rho}$, ft.^{2}/sec.
μ	viscosity, lb./(ft.-hr.)
ρ	density, lb./ft.
Δ	stirring number, $\frac{G - G_{mf}}{G_{mf}}$, dimensionless
	also a differential
χ	specific rate of absorption function
ϕ	surface age distribution function
σ	surface tension, dynes/cm.

Subscripts

A,B	component A and B respectively
G	gas phase
i	component i, also i^{th} dimension
L	liquid phase
o	fixed bed condition

1. INTRODUCTION

1.1 MOBILE-BED CONTACTORS

A recently developed method of gas-liquid contacting involves countercurrent flow of these two phases through a bed of low density packing which is kept in a state of violent motion by the combined action of the gas and liquid flow. Typically the packing consists of plastic spheres of density about 0.15-g/c.c. 1 1/2-inch or less in diameter. Hollow, molded polyethylene or polypropylene spheres and foamed polystyrene balls have been used. The vigorous movement of the packing has a strongly beneficial effect on the region in the vicinity of the gas-liquid interfaces which is so important in processes involving interfacial transport. The ability of the bed to expand provides an additional advantage over contactors with fixed beds in that much higher gas and liquid mass velocities may be used. In comparison with conventional columns with fixed beds of packing it is therefore possible in mobile-bed contacting to obtain higher rates of gas absorption and heat transfer in columns of significantly smaller diameter. A practical feature of great utility is the self-cleaning feature of mobile-beds when used with gases or liquids which contain materials that deposit on the packing of fixed-bed contactors.

As a new technique, this type of operation has been described by a variety of names. The technique is known industrially primarily under two trade names, Turbulent Contact Absorbers (TCA) or Floating-Bed Wet Scrubbers (146-7).

Although Douglas and co-workers have referred to the process in the past as "turbulent-bed contacting", or "three-phase fluidization", the generic term "mobile-bed contacting" has now been adopted as the most generally descriptive name (25,29,115,149). For convenience the designation MBC will therefore be used in this thesis.

The new technique was invented by Kielback (146,148) who had been concerned with a specific gas-liquid contacting problem at the smelter of the Aluminum Company of Canada at Arvida, Quebec. During the production of aluminum by the electrolysis of alumina dissolved in cryolite and other fluorides, a hot tarry mist is evolved which contains hydrogen fluoride, carbon dioxide and particulate matter. Conventionally, the gas was treated in a large grid-packed tower which required frequent and expensive maintenance because of fouling by the particulate matter. This problem provided the stimulation for the solution conceived by Kielback of using a bed packed with low density spheres which would be kept free of fouling by the self-cleaning action of the motion of the balls. The use of low density spherical packing gave a low pressure drop, which is one of the main limitations in most scrubbing applications. Further development and application to other chemical process problems was carried out by a group at Howard Smith Paper Co., Cornwall, Ontario. Douglas et al. (147) reported a modification to Kielback's version of the contactor for use in the pulp and paper industry for the carbonation of treated sulphite liquor

in the production of vanillin, and in the preparation of various pulping liquors: sodafite, semi-chemical liquor, and the liquor for the new Magnefite process.

A number of workers (25,28-9,146-52) have published preliminary data which are helpful in the design of MBC for industrial applications. The limited design procedures available are based primarily on the operating experience of units already installed. While a good record of industrial applications has been achieved, the availability of a general calculation model would make it possible to design with greater confidence and economy for new applications, and to optimize design procedures and operating conditions.

As the majority of gas-liquid contacting operations are conducted for the purpose of effecting mass transfer between the fluid phases, and as the only mass transfer studies published for MBC are of an extremely limited nature (147,149), a thorough investigation of mass transfer in MBC was needed. Mass transfer, or any interfacial transfer operation, is affected rather sensitively by the conditions of axial mixing in the contacting vessel. Unfortunately, most published mass transfer studies do not properly account for the effect of mixing on mass transfer. Published transfer coefficients therefore frequently are strongly affected by the extent of axial mixing in the experimental equipment used. In order that this error

be avoided in the present study, an extensive study of axial mixing was carried out in the same equipment as used for the mass transfer study.

Along with the mass transfer study, the interfacial area in MBC was also determined. Knowledge of the effect of processing conditions on this variable is in itself valuable, and in addition the determination of interfacial area made it possible to obtain and examine an area-based mass transfer coefficient rather than the volumetric-based coefficient which is more commonly available.

The need to have some information on the hydrodynamics of MBC in order to carry out a sound mass transfer investigation leads to extending the determination of physical characteristics to include studies of bed expansion, minimum fluidization velocity, and liquid holdup.

These, then, were the specific features of a study which was oriented to providing the basis of a more efficient and reliable method of design of industrial mobile-bed contactors.

II. LITERATURE SURVEY

This chapter contains a brief survey of the published literature relevant to this thesis.

2.1 LIQUID HOLDUP

Liquid holdup is one of the basic liquid-side dependent variables in the operation of fixed- and mobile-bed contactors. The importance of holdup in the mass transfer process is demonstrated by the number of attempts made to correlate and explain data on the basis of liquid holdup (1-10). Holdup has been shown to have a direct influence on liquid-phase mass transfer (6-9), on loading behaviour (7) and on the gas-phase pressure gradient (7).

2.1.1 Liquid Holdup in Packed Beds

The two types of procedures by which holdup in packed beds has been measured may be designated as:

- direct method (2,9-18)
- indirect method (6,22-27)

Using the direct method, early workers identified two components of total holdup, i.e. operating and static holdup. In the more recent indirect method, the amount of liquid retained is obtained by tracer techniques with transient response, a method which gives total holdup under actual

operating conditions with the advantage of not requiring interruption of the flow.

Most of the correlations of operating holdup are dimensionally inconsistent. In 1953 Otake and Okada (20) proposed the first generalized correlation in dimensionless form as:

$$H_{op} = 1.295 \left(\frac{dL}{\mu}\right)^{0.676} \left(\frac{d^3 g \rho^2}{\mu^2}\right)^{-0.44} (a_d d) \qquad (2.1)$$

The proposed modifications of equation (2.1) which have since then been proposed by Davidson (6), Varrier and Rao (5) and Mohunta and Laddha (21) have been reviewed by Khanna (22).

The earlier holdup measurements, obtained for use in design, were not related to any theory. Recently some effort has been directed to elucidating the mechanism of flow of liquid in packed beds (6,18-9). This approach should lead to a better understanding of the hydrodynamics of packed beds, including a theoretical basis for the prediction of holdup for use in modelling for design and optimization of gas-liquid contacting in fixed and mobile beds.

2.1.2 Holdup in Mobile-Bed Contactors (MBC)

In MBC, for which the spherical packing is constantly in motion, the ratio of static to operating holdup is zero, so that the distinction which has conventionally been made between operating and total holdup effectively disappears.

Gel'prin et al. (28) have measured liquid holdup in MBC by the direct method while Chen and Douglas (29) employed the indirect method based on the transient-response tracer technique. The latter concluded that holdup is independent of gas flow rate but is primarily influenced by the liquid flow rate and diameter of the packing, as is indicated by their empirical correlation

$$H_T = 0.02 + 2.83 \times 10^{-4} (L)^{0.6} (d)^{-0.5} \qquad (2.2)$$

It is important to note that, in this correlation, H_T is based on the static height, not the expanded height, of the mobile-bed. Also, this correlation may not apply to the entire range of MBC operation as it was obtained for values of bed expansion only up to approximately $H/h_s = 2$, where h_s and H indicate the static and expanded bed height respectively. The results of Gel'prin et al. (28) for a mobile-bed in fact show that the increase in amount of liquid retained in proportion to the increase in bed expansion is considerably less than given by equation (2.2). This difference may be due to differences in the range of bed expansion for the two investigations.

2.2 INTERFACIAL AREA

Although earlier work concerning mass transfer in gas-liquid contactors involved the use of volumetric-based transfer coefficients, the trend to put mass transfer on a more theoretical foundation has brought the need to separate the interfacial area term from the more basic area-based transfer coefficient. As it is this approach which has been used in this thesis, the literature on interfacial area will now be reviewed briefly.

2.2.1 Dry, Wet and Effective Interfacial Area

For packed beds various workers (10,30-46) have estimated the wetted area per unit volume, a_w, and the effective interfacial area for mass transfer per unit volume, a. The relationship between these values and a_d, the surface area of the dry packing, is in general

$$a < a_w < a_d$$

The difference between a and a_w derives from the fact that the liquid associated with some of the wetted area remains nearly saturated and thus effectively unavailable for absorption. This difference has been reported to be greater for the case of small rings. Davidson (6) has suggested that this effect is due to the retention of a comparatively large volume of relatively stagnant liquid between the rings by surface ten-

sion forces. In a subsequent study Whitt (32) concluded that, for countercurrent air-water flow through random packed Raschig rings, the gas and liquid flow tend to separate. For 1/2- to 2-inch rings, almost complete lack of flow of one of the phases over half the total surface could occur.

2.2.2 Measurement of Interfacial Area

Interfacial areas for gas-liquid contacting have been measured by both indirect and direct methods. The indirect method (30,32,38) involves separate measurements of $k_G a$ and k_G, the ratio of which gives the area, a. For example, $k_G a$ is available from the experimental data of Fellinger (46) on absorption of ammonia in water. The gas-phase coefficient, k_G, was obtained by Shulman et al. (30) from the rate of evaporation of dry naphthalene packing, and by Whitt (32) for evaporation from porous packing saturated with water. The indirect method gives reasonably good measures of interfacial area. A complicating factor is the fact that the same mechanism which tends to make $a < a_w$ also leads to different values of effective interfacial area for absorption and evaporation. The main shortcoming of the indirect method is the need to assume that the hydrodynamic conditions for the two quite separate experiments (for $k_G a$ and for k_G) are the same. The validity of this assumption is questionable for the system noted above, and is a severe restriction in the application of this technique to other gas-liquid systems.

Among the direct measurements are various optical, photographic and chemical methods. The first two of these methods are, however, applicable primarily to gas-liquid dispersions and foams where determination of mean bubble size permits calculation of interfacial areas from geometric considerations.

The chemical method of determination of effective interfacial area involves absorption of a gas which reacts with the liquid phase. In addition to measurement of mass transfer rates under chemisorption conditions, it is necessary to have

- an exact description of the kinetics of the reaction, and
- several physico-chemical properties of the system.

This method is applicable to our system and will therefore now be discussed in greater detail.

2.2.3 Effective Interfacial Area by Absorption with Chemical Reaction

The rate of absorption is given by

$$R = \int_0^\infty \phi(\theta) \cdot \chi(\theta)\, d\theta \qquad (2.3)$$

where $\phi(\theta)$ is the surface-age distribution function and $\chi(\theta)$ is the rate of absorption per unit area at any instant θ. The function ϕ depends on the physical properties and hydrodynamics of the system. The function χ will take different forms according to the behaviour of the liquid and gas. It is in fact estimated from the solution of appropriate partial differential diffusion equations with the required boundary conditions. However, Danckwerts (47) has shown that this laborious process is not always necessary.

Both Higbie (48) and Danckwerts (49) have made postulates about the nature of the function ϕ. Higbie's assumption of a constant exposure time is improbable unless the physical nature of the contacting apparatus imposes this constraint on the system. In Danckwerts surface-renewal model, ϕ, represents the fraction of fluid elements that remain at a phase interface for a period of time θ, and the displacement of fluid elements from the interface is assumed to be completely random. This gives

$$\phi(\theta) = s\, e^{-s\theta} \tag{2.4}$$

and

$$R = \int_0^\infty \phi(\theta) \cdot \chi(\theta)\, d\theta$$

$$= s \int_0^\infty e^{-s\theta}\, \chi(\theta)\, d\theta \tag{2.5}$$

For the case of a first-order or pseudo-first-order reaction between dissolved gas and solvent, the partial differential equations representing the chemisorption process are

$$\frac{\partial c}{\partial \theta} = D \frac{\partial^2 c}{\partial x^2} - rc \tag{2.6}$$

with boundary conditions

$$\begin{aligned} c &= c_o \quad , \quad x > 0 \quad , \quad \theta = 0 \\ c &= c^* \quad , \quad x = 0 \quad , \quad \theta = 0 \\ c &< c_o \quad , \quad x = \infty \quad , \quad \theta > 0 \end{aligned} \tag{2.7}$$

Multiplying each term in the differential equation by $e^{-s\theta}$, integrating with respect to θ between 0 and ∞, and using the first boundary condition, one gets

$$sC - c_o = D \frac{d^2 C}{dx^2} - rC \tag{2.8}$$

where C, the Laplace transform of c, is defined by

$$C_{(x,s)} = \int_0^\infty e^{-s\theta} \, c(x,\theta) \, d\theta \tag{2.9}$$

The transformed boundary conditions are:

$$\begin{aligned} C &= \frac{c^*}{s} \quad , \quad x = 0 \\ C &< \frac{c_o}{s} \quad , \quad x = \infty \end{aligned} \tag{2.10}$$

The solution in terms of the transformed variable C is given by

$$C = \frac{c_o + [c^*(\frac{r+s}{s}) - c_o]\, e^{-x\sqrt{\frac{r+s}{D}}}}{(r+s)} \qquad (2.11)$$

The rate of absorption is then given by

$$R = s\int_o^\infty e^{-s\theta}\, \chi(\theta)\, d\theta$$

$$= -sD\int_0^\infty e^{-s\theta}\, (\frac{\partial c}{\partial x})_{x=0}\, d\theta$$

$$= -sD\,(\frac{dC}{dx})_{x=0}$$

$$= [c^* - c_o(\frac{s}{r+s})]\sqrt{D(r+s)} \qquad (2.12)$$

For physical absorption

$$R = (c^* - c_o)\sqrt{Ds} \qquad (2.13)$$

whence

$$k_L = \sqrt{Ds} \qquad (2.14)$$

and

$$R = [c^* - c_o\,(\frac{s}{r+s})]\sqrt{Dr + k_L^2} \qquad (2.15)$$

which for a reactive system ($c_o = 0$) leads to

$$R = c^* \sqrt{Dr + k_L^2} \qquad (2.16)$$

In cases for which

$$\sqrt{Dr} \gg 5\, k_L$$

the concentration of reactant in the neighbourhood of the interface is very little different from that in the bulk of the liquid, and the dissolved gas undergoes a pseudo-first-order reaction; equation (2.15) may be satisfactorily approximated as

$$R = c^* \sqrt{Dr} = c^* \sqrt{Dk_2[B]} \qquad (2.17)$$

Thus for these conditions the specific rate of absorption of a gas undergoing first-order or pseudo-first-order reaction becomes a unique function of the physico-chemical properties, i.e. is independent of the hydrodynamics of the system (which affects k_L only). It is this independance of absorption rate with respect to the hydrodynamics which provides the basis for the direct chemical method of determination of effective interfacial area.

Three reaction systems have been used most extensively (39-45,50-57):

- carbon dioxide-carbonate bicarbonate buffer solution
- oxygen-sodium sulphite solution, and
- carbon dioxide-sodium (or potassium) hydroxide solution

Success in the determination of effective interfacial area by this method depends entirely on the availability of reliable physico-chemical data. For example, the results of de Waal et al. (39-40) are probably in error because of the uncertain kinetics of sodium sulphite oxidation (58).

2.2.4 Influence of Liquid Properties

The dependence of effective interfacial area on fluid properties has not been studied. Sharma et al. (42-3,57) have shown that, provided the liquid properties such as viscosity, surface tension and ionic strength are kept nearly equal, the effective interfacial area as determined by the direct, chemisorption method remains practically independent of the nature of the reacting species and of the kinetics of the reaction. Detailed quantitative investigation of the influence of liquid properties is however essential before the interfacial area results presently available can be fully utilized.

2.2.5 Interfacial Area in Mobile-Bed Contacting

In addition to the measurements for fixed-bed packed columns already noted, interfacial area has been evaluated for many other types of gas-liquid contacting devices - sieve trays (52,55,56,59,60), bubble trays (52,54,61), stirred tanks (40-1,62-5), bubble columns (57), cocurrent horizontal and vertical flow (66), flow through helical coils (66), aerated mixing vessels (67-8), and spray columns (69). However, no measurements of interfacial area have yet been reported for the important new technique, mobile-bed contacting.

2.3 LIQUID-PHASE MASS TRANSFER IN PACKED BEDS

Having considered interfacial area as a separate variable, it is now appropriate to review the developments concerning area-based mass transfer coefficients.

2.3.1 Experimental Studies

The basic correlation for volumetric liquid-phase mass transfer coefficients in a packed column has been the one derived by Sherwood and Holloway from their measurements of rates of desorption of oxygen, carbon dioxide and hydrogen from water (70):

$$H_L = \frac{1}{\alpha} \left(\frac{L}{u_L}\right)^n \left(\frac{\mu}{\rho D}\right)_L^{0.5} \qquad (2.18)$$

The effects of type and size of packing are reflected in corresponding variations in α, from 80 to 550, and in n, from 0.22 to 0.46. Since in their study the interfacial area was not separated from the transfer coefficient, this correlation does not reveal the dependence of k_L^o on flow rate, L. Shulman and co-workers (30) did make this separation, using the indirect method discussed in section 2.2, thereby obtaining the following equation for k_L^o in packed columns:

$$\left(\frac{k_L^o\, d_p}{D}\right)_L = 25.1 \left(\frac{d_p L}{\mu_L}\right)^{0.45} \left(\frac{\mu}{\rho D}\right)_L^{0.5} \qquad (2.19)$$

Correlations similar to or extensions of the above (6,38,45, 71-80) have demonstrated that liquid-phase mass transfer data can be adequately represented in terms of the dimensionless variables designated as the Sherwood, Reynolds, Schmidt and Gallileo numbers. Van Krevelen and Hoftizer (73) showed from theoretical considerations that the Gallileo number, $\frac{d^3 g \rho^2}{\mu^2}$, is important in describing the nature of the liquid film flowing over the packing surface.

2.3.2 Theoretical Studies

In contrast to these semi-empirical approaches, attempts have been made more recently to predict the transfer coefficient from theoretical models of interphase mass transfer. However, the only successful description of mass transfer in liquid films flowing over random packings has been that of

Davidson (6), who predicted the mass transfer coefficient, k_L^o, from a theoretical analysis of a packed bed using the penetration model of mass transfer. Agreement between experimental data and his theory is quite good. By contrast, the recent second-order stochastic model of Schmalzer and Hoelscher (82) fails to explain mass transfer in packed beds.

Although the preceding discussion has been limited to mass transfer without chemical reaction there is great interest, because of its importance industrially, in the case of absorption with chemical reaction of the solute in the liquid phase. The extensive research of the past decade on this case is the topic of a recent book by Astarita (83), to which the interested reader is referred for an up-to-date and comprehensive treatment.

Some special features of mass transfer with simultaneous chemical reaction may be seen by reference to Figure 2.1 which illustrates the dependence of concentration profile on order and rate of reaction.

The type of chemical reaction which has received most attention is that in which the dissolved gas undergoes an irreversible second-order reaction with a reactant dissolved in the liquid. The effect of chemical reaction on the rate of absorption may be represented as Figure 2.2, where

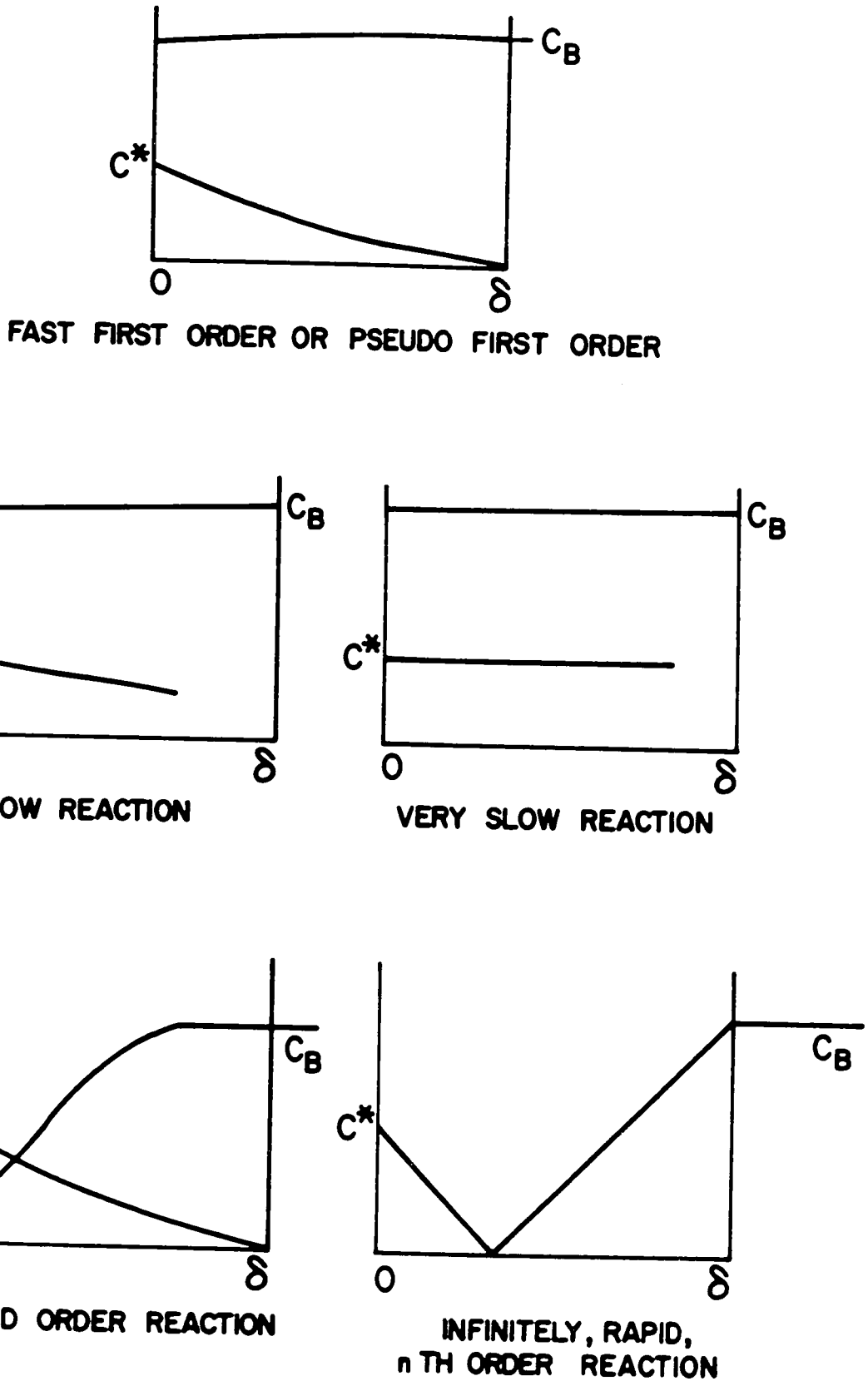

FIGURE 2.1: TYPICAL CONCENTRATION PROFILES IN THE LIQUID FILM NEAR THE GAS-LIQUID INTERFACE FOR A REACTING SYSTEM

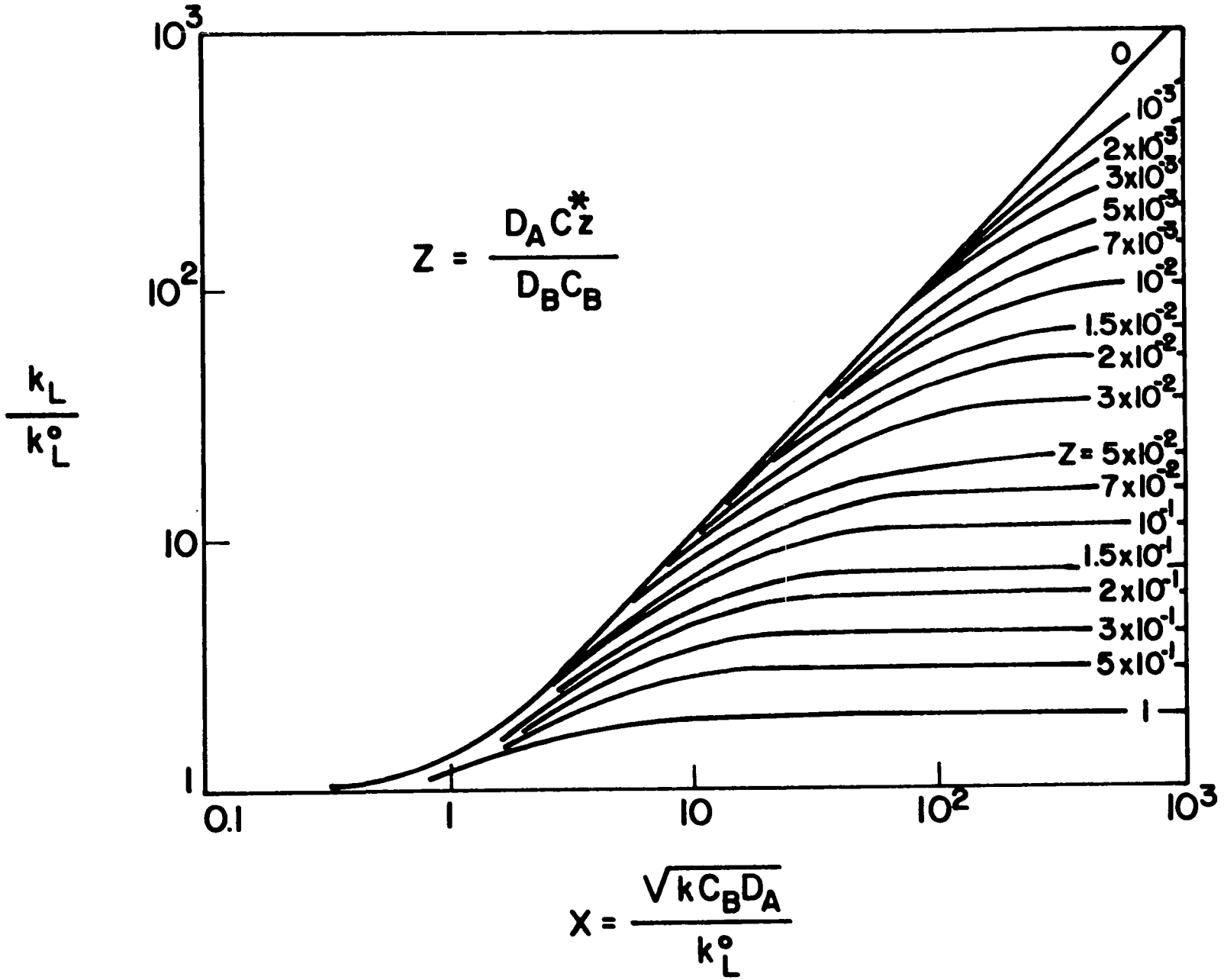

FIGURE 2.2: MASS TRANSFER WITH SECOND ORDER CHEMICAL REACTION IN THE LIQUID PHASE

$$\beta = \frac{\text{rate of absorption with chemical reaction}}{\text{rate of physical absorption}} = \frac{k_L}{k_L^o}$$

$$X = \frac{k_2 C_B D_A}{k_L^o} \quad \text{and} \quad Z = \frac{z\, c^*\, D_A}{C_B\, D_B}$$

This figure is based on numerical solutions of the film model by Van Krevelen and Hoftijzer (84-6) and of the Higbie surface-renewal model by Brian et al. (87) and Pearson (88).

These model studies are of limited use unless means are devised to apply them to the design of industrial scale equipment. The ideal cases, for which the solute concentration at the interface and bulk reactant concentration remain constant, certainly simplify the mathematical analysis of the problem, and are easy to achieve in laboratory studies. Such conditions do not of course correspond to actual operating conditions in industrial absorbers. Danckwerts and Sharma (53) have suggested that a piecewise integration be carried out over the entire column using the data given in Figure 2.2. The use of such theoretically-based methods in the design of industrial contactors where properties such as density, viscosity, surface tension, interfacial area and reaction rate may all vary significantly remains an unachieved ideal. The fact that even for commonly encountered industrial systems the physico-chemical data needed for these methods is scarce still further limits application of theory to design.

2.4 RESIDENCE TIME DISTRIBUTION AND AXIAL MIXING

The distribution of ages of the various fluid elements as they leave a process vessel is generally determined by the transient response method, the spread of residence times reflecting the phenomenon of axial mixing.

RTD does not, however, completely describe the flow. It gives the ages of the different elements but tells nothing about their history during flow through the vessel. An extensive literature has accumulated on liquid mixing in the case of single phase flow through straight pipes, packed and fluidized beds and for countercurrent gas-liquid flow through packed beds. Those aspects which are relevant to axial mixing of the liquid phase in mobile-bed contactors are now reviewed.

2.4.1 Characterization of Axial Dispersion Phenomena

A mathematical model must be constructed to describe in some simplified way the flow behaviour of the system. For most real flow systems of interest, for example, a packed bed, the flow behaviour is too complex to be described as it actually is. The formulation of a model is therefore complicated by conflicting requirements for

- a realistic representation of the actual flow behaviour, and
- ease of model parameter evaluation and of use of the model in engineering design.

Four basic models for characterization of axial dispersion are:

- Diffusion (dispersion) model - employing a modified diffusion coefficient
- CSTR model - employing mixed tanks in series corresponding to mixing cells
- Mixed model - employing combinations of blocks of simple flow systems
- Stochastic model - employing random walk in space or velocity states.

The diffusion model (also called the dispersion model), having gained the widest acceptance since it was presented by Danckwerts (89) in 1953, will be discussed in detail; only a brief description of the other models is presented for completeness. Further only the diffusion model allows representation of mass transfer in imperfectly mixed two-phase systems.

2.4.1.1 Diffusion Model

The basic premise of the dispersion model is an analogy between mixing and molecular diffusion, mixing being described as a Fickian diffusion process with an effective dispersion coefficient, D_L, superimposed on a mean convective plug flow. The material balance for a particular component over a differential section of a packed bed as shown in Figure 2.3 is

$$\text{Input} - \text{Output} = \text{Accumulation}$$

$$\left(-D_L \cdot \frac{\partial c}{\partial x} + Uc\right)_x - \left(-D_L \cdot \frac{\partial c}{\partial x} + Uc\right)_{x+\Delta x} = \frac{\partial c}{\partial t} \cdot \Delta x + r \cdot \Delta x + s \cdot \Delta x \qquad (2.20)$$

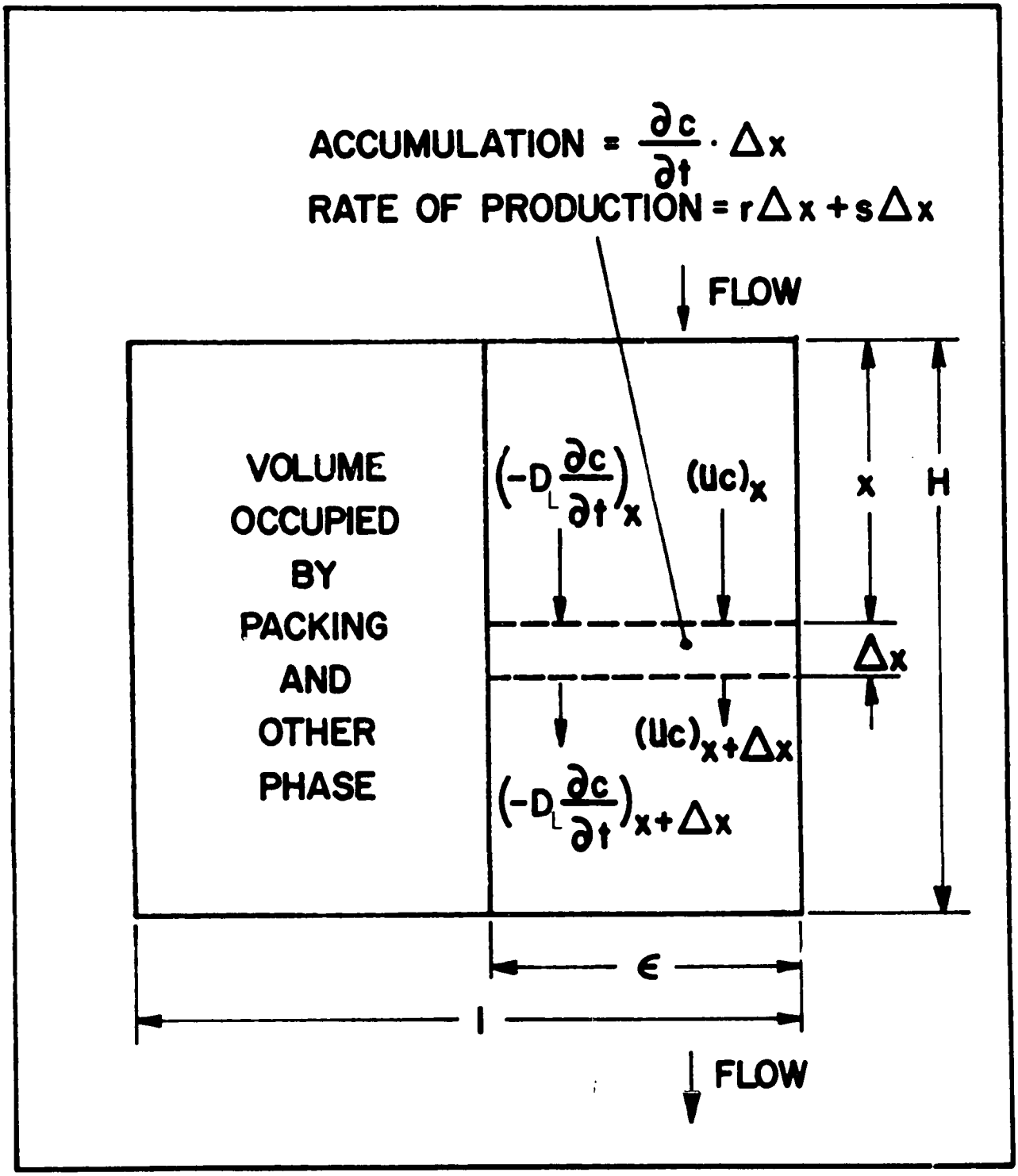

FIGURE 2.3: MATERIAL BALANCE COMPONENTS FOR THE DISPERSION MODEL

which reduces to

$$D_L \frac{\partial^2 c}{\partial x^2} - U \frac{\partial c}{\partial x} = \frac{\partial c}{\partial t} + r + s \qquad (2.21)$$

For r = 0 and s = 0 (an inert system)

$$D_L \frac{\partial^2 c}{\partial x^2} - U \frac{\partial c}{\partial x} = \frac{\partial c}{\partial t}$$

or

$$\tau \frac{\partial c}{\partial t} + \frac{\partial c}{\partial X} - \frac{1}{P} \cdot \frac{\partial^2 c}{\partial X^2} = 0 \qquad (2.22)$$

Equation (2.22) is a simplified form of a more general equation:

$$\frac{\partial c}{\partial t} = \frac{\partial}{\partial x_i} \left(D_{x_i} \frac{\partial c}{\partial x_i}\right) - U_i \frac{\partial c}{\partial x_i} + r + s \qquad (2.23)$$

where the vector-repeated index summation convention describes the multi-dimensional system.

The derivation of Equation (2.22) involves the following assumptions:

- radial concentration and velocity gradients are negligible
- material transport by axial dispersion is directly proportional to axial concentration gradient
- a single parameter, D_L, describes axial dispersion and is constant over the entire contactor length in the direction of the mean flow

- system response is independent of solute concentration, and
- there is no adsorption or chemical reaction of the component for which the material balance is written

The presence of gross flow irregularities would invalidate the first assumption. However, experimental work for single-phase systems (90-2) and two-phase systems (93-4) provide evidence that, in the absence of such flow irregularities, radial gradients are sufficiently small in comparison with axial transport that their effects are negligible. There are by now many studies to support the hypothesis that mixing in process vessels may be described adequately by the single-parameter dispersion model.

2.4.1.2 Tank-in-Series Model

In 1953 Kramers and Alberda (95) proposed a perfectly-mixed tank-in-series model to represent the axial dispersion phenomenon. Mathematically, this model corresponds to replacing the partial differential Equation (2.22) of the diffusion model by a series of ordinary differential equations with simple boundary conditions. The implied physical description of flow in packed beds according to either of these models is rather remote from the actual flow. Kramers and Alberda also showed the equivalence of the diffusion and tank-in-series

models as:

$$\frac{UH}{D_L} = 2n \qquad (2.24)$$

where n is the number of equal volume, perfectly mixed cells in series. The model was extended to the case of unequal cells-in-series by Mason and Piret (96) , and to a three-dimensional array of mixing cells by Deans and Lapidus (97).

2.4.1.3 Mixed Models

Levenspiel (98-9) presented the idea of sub-dividing a large region into a number of smaller regions, each of which could be represented by the diffusion model, dead space, by-passing, or some other simple concept of flow. This model has the advantage of great adaptability but the complimentary disadvantage is that often a non-unique set of parameters results. There is however an extensive literature on the application of this concept.

2.4.1.4 Statistical Models

Mixing in packed beds has also been described according to a number of statistical models, of which an early example was given by Einstein (100), and the most recent one by Schmalzer and Hoelscher (82). The random-walk model (100) for the flow of solid particles suspended in flowing streams

was extended by Jacques and Vermeulen (101-2) and Cairns and Prausnitz (92). This model, as well as the one based on mixing-cells, approach the simple diffusion-model at high flow rates.

The recent study of Schmalzer and Hoelscher (82) described a second-order stochastic model for a packed bed. They considered fluid packets to change velocity states according to a given set of transition probabilities. The multi-parameter nature of this model makes it particularly convenient to fit experimental mixing data.

2.4.1.5 Evaluation of Model Parameters

Considerable attention has been paid to the problem of evaluation of the parameters of models from transient response experiments. The parameters must be evaluated from some modification of the solution to the model differential equations. Methods of moments and slope at the mid-point of the breakthrough curves are easy to apply but limited in accuracy for systems with a high degree of mixing. Recent developments (103-105) extended these concepts to yield more accurate estimates even with imperfect tracer inputs. Lees (104) has proposed a simpler method of obtaining moments of the impulse response of a complex model directly from its transformed equations instead of the solution. However, these quick methods of parameter estimation are still limited to the case of infinite beds.

2.4.2 Axial Dispersion in Packed Beds

The case of single-phase flow of liquid through packed beds is now quite well documented, as is indicated by the representation of these data on Figure 2.4 Although not directly relevant to this thesis, it is at least of interest to note that the data from a number of studies of single-phase flow of gas through packed beds are also reasonably coherent. The remaining uncertainties primarily concern the effect of particle size, shape and packing arrangement.

By contrast, the present state of knowledge of axial mixing for countercurrent two-phase flow through packed beds is quite unsatisfactory. In large part, this situation reflects the considerable increase in experimental difficulty which is associated with carrying out transient response studies on one phase in the presence of a countercurrent flow of the other phase. For example, the choice of a suitable tracer material and the problem of sampling one phase from a two-phase flow system both add to the experimental difficulties. Also, the methods of analysis of transient response curves which have been available did not give very reliable estimates of the mixing parameter for RTD curves with long tails.

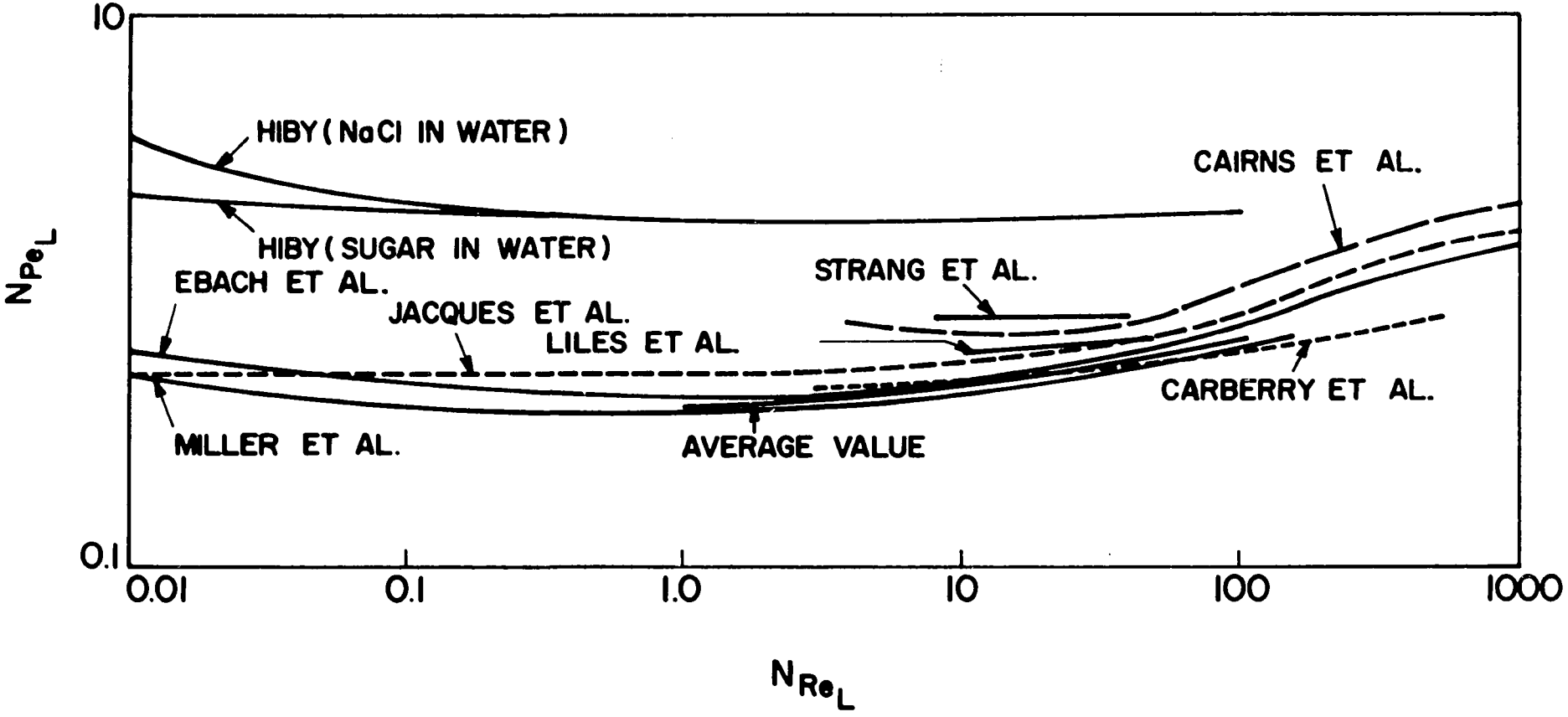

FIGURE 2.4: AXIAL DISPERSION DATA FOR LIQUIDS IN SINGLE PHASE FLOW IN RANDOM BEDS OF SPHERES, $\epsilon = 0.4$

There is considerable disagreement between the results of the relatively few studies which have been reported of axial dispersion for liquid-phase flow through packed beds. The striking differences between the results of various investigators are evident by reference to the representation of these data given on Figure 2.5. The first of these studies, that of Kramers and Alberda (95), reported the RTD in a 15-cm. diameter column packed to a height of 66-cm. with 10 mm. Raschig rings. The spread of experimental data for gas-phase dispersion for two-phase flow through packed beds is equally as wide as that for the liquid phase, thus providing further evidence of the difficulty of obtaining reliable mixing data for two-phase flow systems. For the condition of zero gas flow (often referred to as a trickle-bed contactor), they observed the packing Peclet number Ud/D_L, to increase from 0.3 to 0.5 as liquid flow rate was increased over the range 3200 to 6900 lb./(hr.-sq.ft.).

In 1958 Otake and Kunugita (16) correlated their liquid-phase mixing data in term of the dimensionless variables, Peclet, Reynolds and Gallileo numbers. For flow of water in a laboratory column filled with 7.85- and 15.5-mm. Raschig rings for the liquid phase Reynolds number range of 70-100 and gas flows from zero to 13 lb./(hr.-sq.ft.), the correlation obtained was:

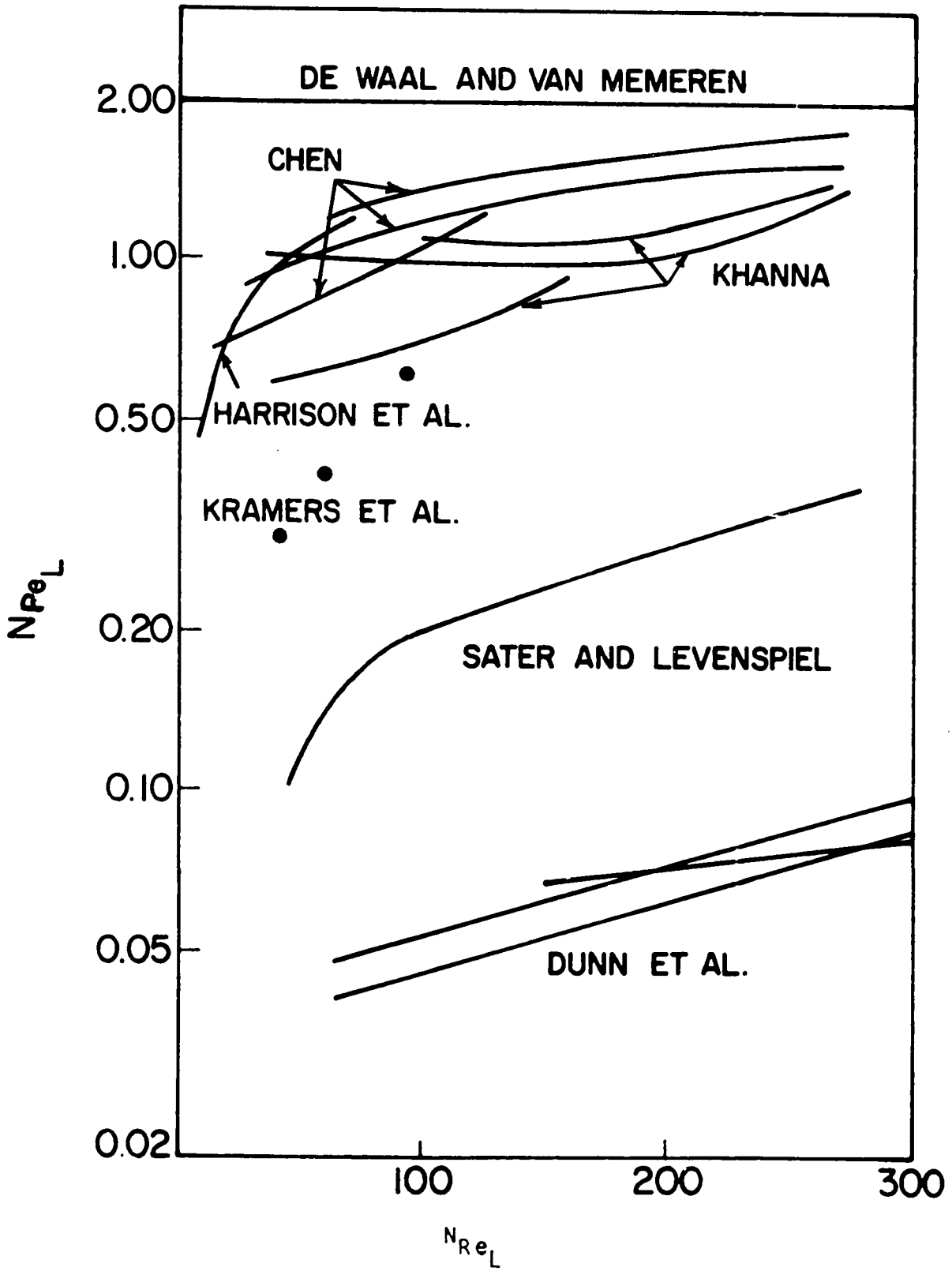

FIGURE 2.5: AXIAL DISPERSION DATA FOR LIQUID IN TWO-PHASE COUNTERCURRENT FLOW

$$\left(\frac{Ud}{D_L}\right)_L = 1.895 \left(\frac{dU\rho}{\mu}\right)_L^{0.5} \left(\frac{d^3 g \rho^2}{\mu^2}\right)^{-0.333} \qquad (2.25)$$

As the gas flow rate was always below the loading point, it is not surprising that they observed no effect of gas flow rate. They concluded that essentially plug flow prevailed for long beds, high mean liquid velocity and small packing. Hoogendorn and Lips (106) confirmed this for trickle columns of 1.33-ft. diameter and 5- and 10-ft. height packed with 1/2-inch porcelain Raschig rings. These observations are in general agreement with those of Schiesser and Lapidus (24). Hofmann (108) working with industrial size columns found the above equation to be inapplicable, and Weber (109) referred to the experiments yielding much higher values for the dispersion coefficient than those calculated from the correlation.

In 1962 Harrison et al. (110) carried out an interesting test of the use of the diffusion model for mixing in packed beds. They modelled a packed bed as a continuous vertical string of spheres and concluded that the simple diffusion model does indeed provide a fairly good representation of the axial dispersion of the liquid. Tailing of the breakthrough curves was attributed to transfer from regions of low velocity or stagnation.

Stemerding (111) in 1961 reported dispersion measurements in a 10-ft. column filled with 13 mm Raschig rings. The dispersion coefficient was observed to be essentially con-

stant for an interstitial liquid velocity of 0.2 to 1.0 cm./sec., and dependent on the air flow rate only. These results are contradicted by an almost identical study of Otake et al. (112) for which the dispersion data were correlated by an equation of the same form as used in the earlier study of Otake and Kunugita:

$$\left(\frac{Ud}{D_L}\right)_L = 1.425 \left(\frac{dU\rho}{\mu}\right)_L^{0.777} \left(\frac{d^3 g \rho^2}{\mu^2}\right)^{-0.333} \qquad (2.26)$$

Word (113) and Dunn et al. (114) measured axial dispersion in a 2-inch diameter column packed to a height of 6-ft. with 1- and 2-inch Raschig rings and 1-inch Berl saddles. The diffusion model gave a better fit than the random-walk or mixing-cell models. However, it is to be noted that the reproducibility of the data was poor and the liquid-phase Peclet numbers found are at the extreme low end of the range of the published data, as may be seen by reference to Figure 2.5. The dispersion coefficient was found to decrease with increasing liquid flow rate, but no quantitatively significant variation with gas flow rates was observed over the range 0 to 1100 lb./(hr.-sq.ft.).

In 1965 Chen and Douglas (115) correlated their results for fixed beds of 0.5, 1.0, and 1.5-inch spheres, in terms of the same variables as used by Otake et al. (112) but with considerably different constants. The Chen and Douglas

correlation is

$$\left(\frac{Ud}{D_L}\right)_L = 0.07 \left(\frac{dU\rho}{\mu}\right)_L^{0.583} \left(\frac{d^3 g \rho^2}{\mu^2}\right)_L^{-0.081} \qquad (2.27)$$

De Waal and van Mameren (40) measured RTD for liquid in a 1-ft. diameter, 10-ft. high column packed with 1-inch Raschig rings. The height of a perfectly mixed unit, HMU, was independent of gas flow rate from 1340-3750 kg./(hr.-sq.m.) and liquid flow rate from 27,000 to 69,000 kg./(hr.-sq.m.) and remained constant at one nominal packing diameter. These results are consistent with the findings of Hofmann (108) and Harrison et al. (110) but are in disagreement with those of Kunugita et al. (116).

In contrast to the above findings, Sater and Levenspiel (94),using a radioactive tracer technique,recently reported results for 1/2-inch Raschig rings and Berl saddles packed to a height of 5-ft. in a 4-inch column which were fairly close to those of Otake and Kunugita (16). They proposed the following correlation which includes the liquid phase Galileo number. The reliability of the exponents on the dimensionless groups is low because of considerable experimental scatter.

$$\left(\frac{Ud}{D_L}\right)_L = 19.4 \left(\frac{dL}{\mu}\right)_L^{0.747} \left(\frac{d^3 g \rho^2}{\mu^2}\right)^{-0.69} (ad)^{1.97} \qquad (2.28)$$

Khanna (22) working with 1-ft. diameter and 2-ft. high beds of 1- and 1.5-inch Raschig rings found results for liquid phase dispersion coefficients that were different from those of Sater and Levenspiel. The effect of gas flow was negligible and the results were expressed by the following correlation:

$$\left(\frac{Ud_p}{D_L}\right)_L = 0.789 \left(\frac{Ud_p\rho}{\mu}\right)_L^{0.383} \left(\frac{d_p^3 g \rho^2}{\mu^2}\right)_L^{-0.21} \qquad (2.29)$$

The predominant characteristic of liquid-phase mixing data for two-phase flow through packed beds is the enormous amount of disagreement between the results of different investigators. This feature may be due in considerable part to problems of scale associated with the use of laboratory-sized equipment. Another source of variation arises from the different, and sometimes inadequate, methods of data processing which have been used. This problem should not affect future data since reliable techniques are now available. However, it is probable that in some studies a considerable amount of error has been present as a consequence of inherent difficulties of sampling and determining to sufficient accuracy the concentration of the liquid phase in the presence of a gas flow in a packed bed. At this stage, therefore, it can be concluded only that additional studies are required, and that investigators must take even greater care

than in the past in order that reliable results may be obtained.

Most of the mixing studies for both single and two-phase systems have been carried out with non-reacting tracers. The results, however, are used for the cases where chemical reactions occur. The reliability of such a procedure is unknown. Pearson et al. (117) have in fact proposed that RTD be determined by measuring the conversions obtained with first-order reactions when one experimentally varies the rate constant. Lelli (118) has shown that RTD could be derived from the unsteady behaviour of chemical reacting systems. General application and testing of these more advanced concepts also remains as a problem for future work.

2.5 MASS TRANSFER CALCULATION MODELS WITH AXIAL MIXING

Past practice with respect to mass transfer was to process experimental data from laboratory packed-bed contactors in terms of a model which assumed plug flow, then use these transfer coefficients and correlations for the subsequent design of industrial packed-bed contactors, again using a design model based on plug flow. Such a procedure ignores the fact that the flow characteristics for the laboratory and industrial contactors will each differ to a different extent from the plug-flow model. During the past decade considerable effort has been directed to obtaining and testing models which allow for the occurrence of axial mixing. Such models are required in the processing of experimental data, so that the resulting mass transfer coefficients are not at the same time some kind of a measure of the specific axial mixing characteristics of the contactor used. They are required again in the use of such "true" mass transfer coefficients in the design of industrial contactors for the specific mixing conditions applicable to the latter. The more significant steps in the development of such calculation models will now be reviewed.

Both Sleicher (119) and Miyauchi and Vermeulen (93) used the diffusion model as the basis for incorporating the effect of axial mixing into a mass transfer calculation model. Consequently, they arrived at the same differential equations and boundary conditions. Sleicher presented a computer solution

in graphical form and gave an empirical formula for the ratio of the number of "apparent" transfer units to the number of "true" transfer units. Miyauchi, McMullen and Vermeulen (120) extended the concept of van Deemter, Zuiderweg, and Klinkenberg (107) for chromatographic separations to the design of mass transfer equipment with axial mixing, and developed a calculation method for countercurrent extraction systems in which the height of a true transfer unit could be obtained from a summation of those due to the apparent transfer unit (plug flow) and axial mixing. Both Sleicher and Miyauchi proposed approximate semi-empirical equations for rapid estimation of the effect of axial dispersion. Stemerding and Zuiderweg (121) and Rod (122-3) have presented further simplification of the analysis of the Sleicher-Miyauchi equations by approximating their solution in the form of a simple nomogram.

In a subsequent study Dunn et al. (114) applied a modified form of above analysis to the earlier data of both Fellinger (46) and Sherwood and Holloway (70), thereby establishing that axial mixing of liquid had occurred in both cases to an appreciable extent. For liquid-side controlled absorption the following empirical relationship was developed:

$$N_{OL} - N_{OLP} = \frac{0.96\ (N_{OLP})^2}{N_{Pe_L} + 0.63} \qquad (2.30)$$

When applied to the oxygen desorption data of Sherwood and Holloway (70) and ammonia absorption data of Fellinger (46), significant differences between the "true" and "apparent" number of transfer units was obtained. However, it should be recalled (cf. section 2.4, Figure 2.5) that experimental results for mixing in packed beds of Dunn et al. show exceptionally high degrees of liquid-phase dispersion. Although their precise results are subject to future verification, they did nonetheless provide a significant quantitative model which allows for the effect of axial mixing in the liquid phase for the case of liquid-side controlled absorption processes.

By working out two examples using the data of Tepe and Dodge (124) and Fellinger (46) Sater (125) in 1963 showed that mixing can cause a large difference between the mass transfer coefficient calculated assuming plug flow, and the "true" coefficient determined by taking into account the axial mixing by the use of dispersion model. Mecklenburgh and Hartland (126-130) have recently presented a series of papers in which they have used the diffusion model to allow for the effect of axial dispersion on mass transfer in two-phase systems. These authors have furnished a detailed analytical solution for stagewise as well as differential contactors.

Further measures of the magnitude of the effect of axial mixing on mass transfer coefficients are given by two recent studies. In applying the two-phase dispersion model to the study of distillation columns with axial mixing, Furzer and Ho (131) found that meaningful results could be obtained only when the available values of liquid-phase Peclet number were increased by a factor of 8. Sullivan et al. (132) found that in a mechanically agitated absorption tower, correction for axial mixing results in mass transfer coefficients which are 7 to 25 percent larger. There is thus ample evidence of the need in all future mass transfer studies to extract the transfer coefficients using a procedure which adequately allows for the influence of axial mixing on transfer rates.

2.6 SUMMARY

- Holdup in packed beds has been fairly well correlated on a semi-empirical basis. Recently, the prediction of holdup from basic considerations of fluid mechanics has been attempted. The holdup data for mobile-bed contactors presently available do not cover the entire range of industrial interest, and there are large differences between the results of the only two studies which have been published. Further study of holdup in mobile-bed contactors is therefore required.

- Proven methods are now available for direct measurement of effective interfacial area of mass transfer, i.e. based on absorption of a gas which undergoes a pseudo-first-order reaction on dissolution. Data are available for a variety of aqueous systems for fixed beds, but no information is available for mobile-bed contactors. There is also need for further study of the effect of fluid properties on effective interfacial area, and on the measurement of interfacial area for organic systems.

- The industrially important case of gas absorption with chemical reaction has been analysed theoretically, especially absorption with second-order chemical reaction. One of the main difficulties in application of the theory of mass transfer with chemical reaction to the design of industrial reactors is the scarcity of physico-chemical data required by the models.

- The diffusion model is the most widely-used model for representing axial dispersion in single-phase and two-phase systems. In the case of two-phase flow through packed beds, the spread of experimental results between different investigators is enormous, apparently due in large part to the extremely difficult experimental problems associated with such measurements.

- Calculation models are now available which incorporate the effect of axial mixing into the analysis of integral mass transfer equipment. The successful use of such models for two-phase contactors is however restricted by the present uncertainty concerning the quantitative results for mixing in gas-liquid contactors. This approach has not previously been applied to the important new technique, mobile-bed contacting.

III. THEORY

3.1 TRANSFER FUNCTION METHOD OF EVALUATION OF PECLET NUMBER AND RESIDENCE TIME

In 1970 Ostergaard (105) and Michelsen and Ostergaard (103) presented a transfer function analysis for the determination of Peclet number from the concentration-time records at two points in a flow system. This analysis is particularly useful in that it eliminates the need to evaluate Peclet number by the method of direct trace matching or from simplified relations obtained from the solution of model equations. Because of the boundary conditions used in their analysis however, their method is limited, in theory, to contactors which are sufficiently long that they may be adequately described mathematically with the boundary conditions for an infinite length contactor. This assumption is frequently not tenable and, in particular, is not valid in the case of mobile-bed contactors where the bed height is relatively small. The development of a transfer function analysis for finite length boundary conditions follows. The finite bed analysis is applied subsequently to the experimental program for a mobile-bed contactor, but is completely general for any flow system. It is necessary for continuity to present first the essential features of the analysis of Michelsen and Ostergaard for the infinite-bed boundary conditions, following which the extension to the finite-bed case is shown.

3.1.1 Transfer Function Analysis for Infinite Length Boundary Conditions

The differential equation for concentration of a component in a system for which the flow may be described by the dispersion model is:

$$\tau \frac{\partial c}{\partial t} + \frac{\partial c}{\partial X} - \frac{1}{P} \cdot \frac{\partial^2 c}{\partial X^2} = 0 \qquad (2.22)$$

If the flow system may be considered of infinite length and if there are no discontinuities in the concentration in the flow across the bed boundaries, the boundary conditions can be written as

$$\begin{aligned} c &= 0 \quad , \quad t < 0 \, , \quad X = 0 \\ c &= \text{finite} \, , \quad t > 0 \, , \quad X = 0 \\ c &= \text{finite} \, , \quad t > 0 \, , \quad X = \infty \end{aligned} \qquad (3.1)$$

The Laplace Transform of Equation (2.22) is

$$\tau s C + \frac{dC}{dX} - \frac{1}{P} \frac{d^2 C}{dX^2} = 0 \qquad (3.2)$$

The auxiliary equation is

$$(M^2 - P.M - \tau s P)C = 0 \qquad (3.3)$$

the two roots of which are

$$M_1, M_2 = \frac{P}{2}\left[1 \pm \sqrt{1 + \frac{4 s \tau}{P}}\right] \qquad (3.4)$$

The solution of Equation (2.22) can then be written as:

$$C = A_1 . \exp(M_1 X) + A_2 . \exp(M_2 X) \qquad (3.5)$$

Using boundary conditions (3.1), the solution in transformed form is:

$$C = C_{X=0} . \exp\left[\frac{P}{2}\left(1 - \left(1 + \frac{4 s \tau}{P}\right)^{0.5}\right)\right] X \qquad (3.6)$$

The transfer function, F(s), for a linear system is defined as

$$F(s) = \frac{C_{X=1}}{C_{X=0}} = \frac{\int_0^\infty c_2(t) . \exp(-st)\, dt}{\int_0^\infty c_1(t) . \exp(-st)\, dt} \qquad (3.7)$$

If the concentration-time records, c(t), at two measuring points across the flow system are available, numerical values of F(s) may be computed from Equation (3.7) for any arbitrary set of values of s.

Equation (3.6) can be rearranged:

$$\frac{1}{\ell n(1/F(s))} = \frac{\tau s}{(\ell n(1/F(s)))^2} - \frac{1}{P} \qquad (3.8)$$

Thus, as Michelsen and Ostergaard have shown:

$$\frac{1}{\ell n(1/F(s))} \text{ when plotted against } \frac{s}{(\ell n(1/F(s)))^2}$$

should give a straight line of slope τ and intercept $-\frac{1}{P}$ for a system obeying Equation (2.22). Therefore, when a finite length flow system may be satisfactorily approximated by the simple boundary conditions for an infinitely long system, Peclet number, P, and residence time, τ, can be evaluated from the two-point concentration-time records. A general transfer function analysis for the finite length condition is presented in the following section.

3.1.2 Transfer Function Analysis for Finite Length Boundary Conditions

Consider the case of a finite bed. The most rigorous boundary conditions for this case are those proposed by Danckwerts (89), although these have subsequently been elaborated by others (133-7). The boundary conditions for no mass transport by axial dispersion in the fore- and after-sections of any vessel are given by:

$$(Uc)_{0-} = (Uc)_{0+} - D_L \left(\frac{dc}{dx}\right)_{0+}, \quad x = 0, \quad t > 0$$

and (3.9)

$$\frac{dc}{dx} = 0 \qquad , \quad x = H, \quad t > 0$$

The boundary conditions given as Equation (3.9) do not allow for any axial dispersion in the section upstream of the system under consideration, i.e. upstream of the bed for a packed-bed contactor. For gas-liquid contactors this assumption is frequently valid, and is valid for the specific case to which the analysis will be applied in the present study by virtue of the arrangement of the inlet liquid distribution. The solution of Equation (2.22) with these boundary conditions was presented by Brenner (138), Yagi and Miyauchi (139), and others. Chen and Douglas (29) evaluated P by direct trace matching with the solution given by Brenner. Though the evaluation of P by this direct method is claimed to be accurate,the whole process is slow, tedious, and to some extent subjective.

Extension of the transfer function analysis to the case of a finite bed proceeds as follows. The initial conditions are:

$$c = 0 \quad , \quad x < 0 \quad , \quad t = 0$$
$$c = c_o \quad , \quad x > 0 \quad , \quad t = 0 \qquad (3.10)$$

The solution of Equation (2.22) in the transformed form (Equation (3.5)) can be written as:

$$C = A_1 \exp\left[\frac{P}{2}(1 + \beta)X\right] + A_2 \cdot \exp\left[\frac{P}{2}(1 - \beta)X\right] \qquad (3.11)$$

where

$$\beta = \left[1 + \frac{4 s \tau}{P}\right]^{0.5}$$

Using the finite length boundary conditions given by Equation (3.9) and simplifying, the transfer function for the case of finite bed can be written as

$$F(s) = \frac{C_{X=1}}{C_{X=0}}$$

$$= \frac{4\beta}{[(1+\beta)^2 \cdot \exp[-\frac{P}{2}(1-\beta)] - (1-\beta)^2 \cdot \exp[-\frac{P}{2}(1+\beta)]]}$$

A value of τ and P obtained from infinite-length boundary conditions as given by Equation (3.8) can be used as the initial estimate. Values of F(s) from Equation (3.12) for a particular value of s may then be computed for a large number of values of τ and P in the range around the initial estimate of τ and P. These values of F(s) are compared with the experimental value of F(s) using Equation (3.7) for the same value of s. The combination of τ and P which most closely satisfied Equation (3.12) is then computed. In this way, τ and P may be calculated digitally, thus eliminating the shortcomings of the trace-matching procedure. The method is applicable to any flow system for which the finite length boundary conditions given as Equation (3.9) apply. Details of the calculation procedure are given in Appendix V.

3.2 EVALUATION OF MASS TRANSFER COEFFICIENT IN THE PRESENCE OF AXIAL DISPERSION

A model for countercurrent gas-liquid flow with interfacial mass transfer and with axial mixing is required either for the extraction of "true" mass transfer coefficients from experimental measurements or for the application of such coefficients to the design of gas-liquid contactors. The model used in the present study is given below, along with its solution for the specific conditions which prevailed.

A composite model describing simultaneous axial dispersion and mass transfer is obtained by combining models representing the individual phenomenon. Figure 3.1 shows the individual fluxes for the three modes of material transfer, bulk flow, transport across the interface, and axial dispersion as given by the diffusion model. A material balance for each fluid phase gives basic differential equations:

For liquid phase:

$$-D_L \epsilon_L \frac{d^2 c_L}{dx^2} + \frac{L}{\rho_L} \frac{dc_L}{dx} + k_L a(c_L - mc_G) = 0 \qquad (3.13a)$$

and for gas phase:

$$D_G \epsilon_G \frac{d^2 c_G}{dx^2} + \frac{G}{\rho_G} \frac{dc_G}{dx} + k_L a(c_L - mc_G) = 0 \qquad (3.13b)$$

These equations can be rewritten with dimensionless coefficients as:

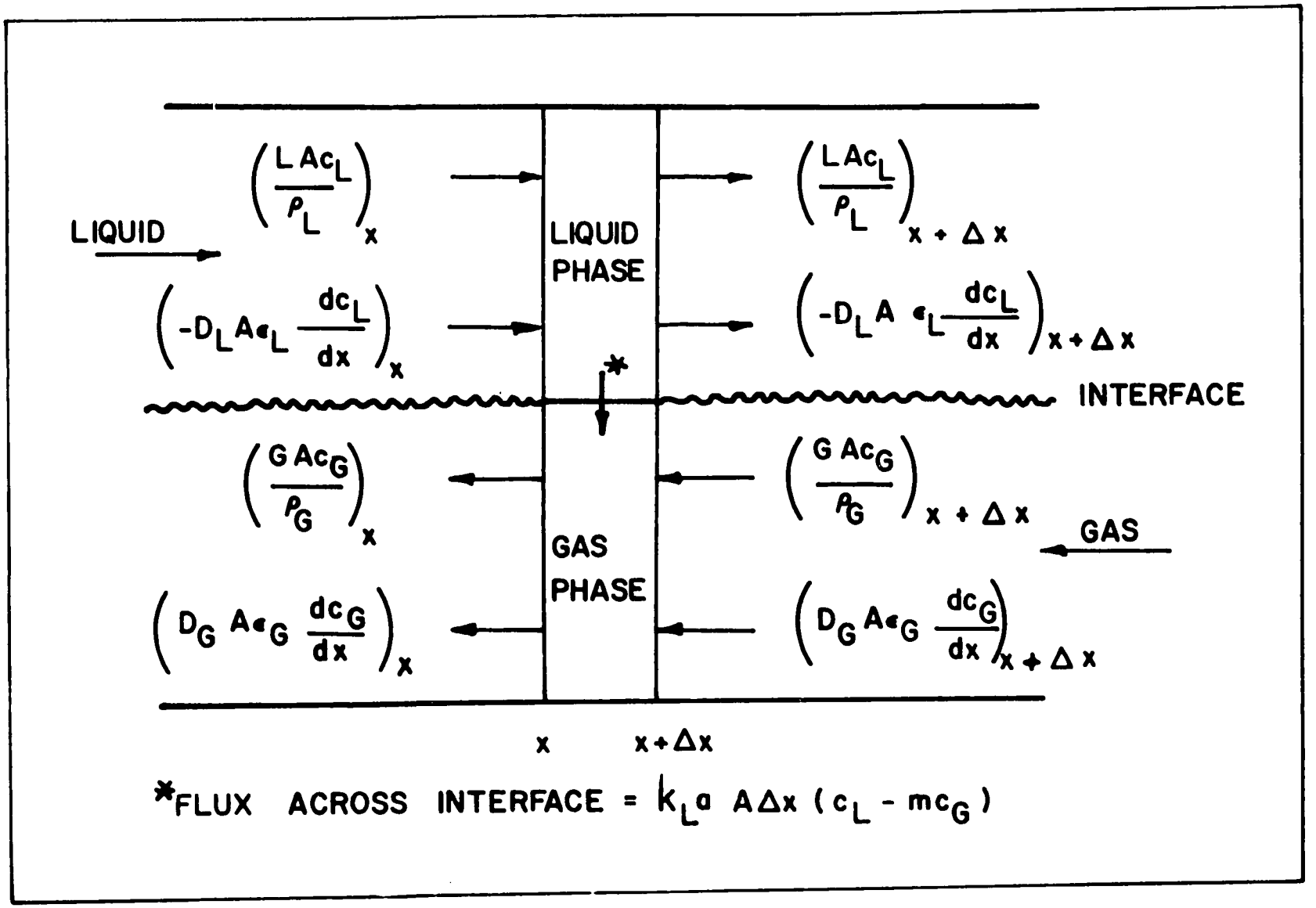

FIGURE 3.1: MATERIAL BALANCE OVER A DIFFERENTIAL SECTION OF COUNTERCURRENT TWO-PHASE FLOW SYSTEM

$$\frac{d^2C_L}{dX^2} - P_L \frac{dC_L}{dX} - N_{OL} \cdot P_L(C_L - mC_G) = 0 \qquad (3.14a)$$

and

$$\frac{d^2C_G}{dX^2} + P_G \frac{dC_G}{dX} + N_{OG} \cdot P_G(C_L - mC_G) = 0 \qquad (3.14b)$$

where

$$C_L = \frac{c_L}{c_L^o} \quad , \qquad C_G = \frac{c_G}{c_L^o}$$

$$P_L = \frac{U_L H}{D_L} \quad , \qquad P_G = \frac{U_G H}{D_G}$$

$$N_{OL} = \frac{k_L a \cdot H \cdot \rho_L}{L} \quad , \qquad N_{OG} = \frac{k_L a \cdot H \cdot \rho_G}{G}$$

$$U_L = \frac{L}{\rho_L \varepsilon_L} \quad , \qquad U_G = \frac{G}{\rho_G \varepsilon_G}$$

$$X = x/H$$

The same finite bed boundary conditions, Equation (3.9), which were used in the dispersion model for the study of liquid phase mixing should be used for both phases in the model for two-phase flow with mass transfer. The boundary conditions in dimensionless form for the gas phase which are analogous to Equation (3.9) for the liquid phase, are as follows:

$$
\begin{aligned}
(C_L)_{0^-} &= (C_L)_{0^+} - \frac{1}{P_L}\left(\frac{dC_L}{dX}\right)_{0^+} , \\
& \qquad\qquad X = 0 \\
\frac{dC_G}{dX} &= 0 , \\
& \qquad\qquad (3.15) \\
(C_G)_{H^+} &= (C_G)_{H^-} - \frac{1}{P_G}\left(\frac{dC_G}{dX}\right)_{H^-} , \\
& \qquad\qquad X = 1 \\
\frac{dC_L}{dX} &= 0 ,
\end{aligned}
$$

The application of the finite bed boundary conditions for gas flow through packed beds was tested by Wehner and Wilhelm (134) for the case of a first-order reaction in a continuous-flow reactor. Bischoff (81) has shown their validity for reactions of any order. A critical evaluation of these and alternative boundary conditions as applied to single-phase flow through tubular flow reactors has been presented by Fan and Ahn (136). Although only homogeneous single-phase reaction systems have been studied the same reasoning applies to the case of two-phase flow systems. In fact these boundary conditions have been successfully used for the cases of countercurrent extraction (141), mechanically agitated countercurrent absorption (132), and distillation columns (131).

The analytical solution of Equation (3.14) with a linear equilibrium relationship has been discussed by Sleicher (119), Miyauchi and Vermeulen (93,140-2) and Hartland and Mecklenburgh (126). The most general case for extraction of the transport coefficient from the solution of Equations (3.14) would require the axial dispersion coefficient for both phases and the experimental rates of mass transfer. For MBC, no estimate of gas mixing is available at the present time. For experimental conditions for which there is only a very small change in gas-phase composition, however, the transport coefficient, $k_L a$, can be obtained from the knowledge of liquid mixing and the experimental rates of mass transfer alone, as the influence of gas-phase mixing becomes negligible.

In the absence of any investigation of gas-phase mixing in mobile-bed contactors, the mass transfer experiments were carried out under conditions of negligible change in gas-phase concentration. For this case, therefore, the solution of Equations (3.14) with the appropriate finite-bed boundary conditions, Equations (3.9) and (3.15) can be carried out for either of the two limiting conditions of gas mixing, plug flow or perfect mixing. This simplifies the analytical solution to Equation (3.14) somewhat.

In addition to giving the general solution to Equations (3.14) with the boundary conditions given by Equations (3.9) and (3.15), Miyauchi and Vermeulen (93) also give the solution for the special case of plug flow in the gas phase, $P_G \rightarrow \infty$. The solution is

$$\frac{C_L - mC_G'}{1 - mC_G'} = \sum_{i=1}^{i=3} A_i \cdot \exp(\lambda_i X)$$

$$\frac{m(C_G - C_G')}{1 - mC_G'} = \sum_{i=1}^{i=3} a_i A_i \cdot \exp(\lambda_i X) \qquad (3.16)$$

which for the terminal condition X = 1, becomes:

$$\frac{\frac{c_L'}{c_L^o} - m\frac{c_G'}{c_L^o}}{1 - m\frac{c_G'}{c_L^o}} = \sum_{i=1}^{i=3} A_i \cdot \exp(\lambda_i) \qquad (3.17)$$

or

$$\frac{c_L' - mc_G'}{c_L^o - mc_G'} = A_1 \exp(\lambda_1) + A_2 \exp(\lambda_2) + A_3 \exp(\lambda_3)$$

where

$$A_i = D_{A_i}/D_A$$

$$D_A = D_{A_1} + \begin{vmatrix} 1 - \lambda_2/P & 1 - \lambda_3/P \\ \lambda_1.\exp(\lambda_2) & \lambda_3.\exp(\lambda_3) \end{vmatrix}$$

$$D_{A_1} = \begin{vmatrix} \lambda_2.\exp(\lambda_2) & \lambda_3.\exp(\lambda_3) \\ a_2.\exp(\lambda_2) & a_3.\exp(\lambda_3) \end{vmatrix}$$

$$D_{A_2} = \lambda_3 . \exp(\lambda_3), \quad D_{A_3} = -\lambda_2 . \exp(\lambda_2)$$

$$a_i = 1 + \lambda_i / N_{OL} - \lambda_i^2 / (N_{OL} . P), \quad i = 1,2,\text{and } 3$$

$$\lambda_1 = 0$$

$$\lambda_2, \lambda_3 = (a/2) \pm \sqrt{(a/2)^2 + b}$$

$$a = P + \Lambda . N_{OL}$$

$$b = (1 - \Lambda) . N_{OL} . P$$

and

$$\Lambda = L_M / (H . G_M)$$

H = Henry Law constant, atm/mole fraction

For the sake of convenience, P_L in the above has been replaced by P.

IV. EXPERIMENTAL

4.1 DESIGN OF EXPERIMENTS

An outline follows of the rationale behind the experimental program, and of the key factors which determine the selection of the experimental techniques of particular systems used.

4.1.1 General Determinants of the Experimental Program

Behaviour of packed columns with respect to mass transfer has generally been characterized in terms of volumetric-based transfer coefficients, $k_L a$ and $k_G a$, or their equivalent. The basic shortcoming of this procedure is that the relationship between the system variables and area-based coefficients, k_L and k_G, may be quite different from that which applies for interfacial area, a. Thus measurement of $k_G a$ and $k_L a$ determines only the composite effect which, for that reason, tends to obscure an understanding of the basic processes occurring in gas-liquid contactors. Also, different scale-up criteria may apply to interfacial area and to the area-based transfer coefficient.

Another consideration which influenced the design of the experimental program is that mass transfer theories predict the area-based transfer coefficient, k_L or k_G, for simple flows. These theories may be used as a guide in modelling transport under more complex hydrodynamic conditions. This approach requires that the functional dependence of the hydrodynamic parameters of the contactor be determined for k_L and k_G, not $k_L a$ and $k_G a$. The interfacial area, on the other hand, depends on the geometry of the packing, the physical and flow properties

of the fluids and on the mode of contacting. The fact that no generalized theoretical prediction of interfacial area appears yet to be feasible does not, however, detract from the value of determining its functional dependence on the system variables separately from that for the transfer coefficients.

The independent determination of interfacial area and an area-based transfer coefficient requires in turn that the volumetric-based mass transfer coefficient from which it is derived be properly corrected for the effect of axial mixing (section 3.2). Only by allowing for axial mixing is it possible to obtain values of the area-based transfer coefficient which reflect purely the influence of fluid flow on mass transfer. Although one study has been published of axial mixing for the liquid-phase of a mobile-bed contactor, it was done on a different sized column, using a more difficult, less accurate method of data processing than is now available, and did not cover as wide a range of mass velocities as was desired for the present mass transfer study. Thus, in order to have the required mixing data available with maximum accuracy and over the entire range of conditions of interest, the present study incorporates an extensive study of liquid-phase mixing in the same column as was used for the studies of mass transfer and interfacial area.

A 5.5-inch (I.D.) column with spheres of sizes 0.5, 0.75, 1.0 and 1.5-inches was used for all studies of the hydrodynamics of MBC. The relatively large 1.5-inch spheres were included be-

cause this is the size most used in industry and also to facilitate comparison with results of Chen. The size of the column was limited by chemical consumption and the facilities required for the mass transfer study. All mass transfer experiments were performed with 0.75-inch spheres only.

4.1.2 Basic Elements of the Experimental Program

Experiments were designed which provided:

- liquid-phase axial mixing data; since liquid holdup could be obtained from the same experiments, measurement of holdup became part of the experimental program,
- effective interfacial area of mass transfer, 'a',
- true liquid-phase volumetric mass transfer coefficient, $k_L a$, determined with appropriate allowance for the effect of axial mixing,
- area-based liquid-phase mass transfer coefficient from

$$k_L = \frac{k_L a}{a}$$

The design of each of these sub-studies is now presented.

4.1.3 Mixing and Holdup Study

Axial mixing and holdup of the liquid phase (sections 2.4.2, 2.5, 3.1) were studied by measuring the RTD of the liquid phase by the transient-response method. This technique requires selection of an input signal from the alternatives of a step, impulse, sinusoidal or random variation of some property such as color, temperature or concentration. For the present study a pulse injection of potassium chloride solution was chosen for the following reasons:

- step input gives cumulative breakthrough curves from which the information required for determination of RTD must be extracted by numerical differentiation, a process which inherently introduces inaccuracy.

- sinusoidal input requires freedom from higher harmonics, which involves the use of sophisticated injection equipment; the use of more complex input functions requires more complex analysis and offers no advantage for this system over the simpler inputs.

- the results from a pulse input give the desired data directly and accurately; the use of this input function was restricted in the past by the requirement that a satisfactorily pure pulse be produced; although it was found possible to do so in the presence case, this was not, however, essential because the method of analysis employed could use any kind of input.

- equipment for monitoring electrical conductivity of potassium chloride solutions was available from a previous study.

4.1.4 Determination of Effective Interfacial Area

Among the available systems for determination of effective interfacial area by absorption of a gas which undergoes a pseudo-first-order reaction in the liquid (section 2.2.3), the carbon dioxide-sodium hydroxide system was chosen because

- the physico-chemical constants of the reaction can be estimated with a satisfactory degree of reliability; the kinetics of oxidation of sodium sulphite, a possible alternate system, is questionable.

- the reaction velocity constant of the CO_2-OH^- reaction step, k_2, is large; the small values of k_2 which apply for the alternative system carbon dioxide-carbonate buffer solution limits the application of that previously used system to cases with a small rate of surface renewal (and thus, small mass transfer coefficient). With a low reaction rate constant and high rates of surface renewal there could be appreciable buildup of carbon dioxide in the bulk of the liquid phase such that the reaction would no longer be pseudo-first-order, as is required by the theory for this method of determination of interfacial area.

- air diluted with carbon dioxide can be used and a correction made for gas-side resistance which is not possible in other systems.

- specific rate of absorption, R, is independent of the hydrodynamics of the system and a single measurement of absorption rate is necessary. Other systems require a simultaneous variation of k_2 and the measurement of absorption rate for the evaluation of k_L before 'a' can be obtained (see Equation (2.16)).

For the system chosen, absorption of carbon dioxide from air into sodium hydroxide solutions, it is essential to allow for the gas-phase resistance. This can be done by measuring the gas-phase mass transfer coefficient for a system which is entirely gas-film controlled, such as the sulphur dioxide-alkali, acetone-water and ammonia-water systems. The system sulphur dioxide-sodium hydroxide was chosen because of the similarity of analysis procedure to that for carbon dioxide-sodium hydroxide.

The surface area may then be calculated from the expression for additivity of resistances:

$$\frac{1}{K_G a} = \frac{1}{k_G a} + \frac{1}{H k_{LR} a} \qquad (4.1)$$

with experimental values of $K_G a$ (CO_2-NaOH system) and $k_G a$ (SO_2-NaOH system), along with k_{LR} from the theory, and the physical property, H.

4.1.5 Liquid-Phase Mass Transfer Coefficient

In most systems of industrial interest the main resistance to mass transfer is in the liquid-phase. Thus a study of liquid-phase mass transfer for this new gas-liquid contacting technique was considered to have the highest priority. The system used for determination of $k_L a$ was desorption of carbon dioxide from saturated water. Actually a dilute solution of ethylene glycol in water was used so as to match the viscosity

of the liquid phase to that of the sodium hydroxide liquor used in the determination of interfacial area, thus minimizing differences in hydrodynamic effects and physical properties of the two systems. Desorption of carbon-dioxide was chosen instead of absorption because

- it is more accurate to measure large concentration changes in the liquid.
- absorption would require either pure carbon dioxide (at $\approx$ 200 cfm) or a high concentration in the air for significant absorption in the liquid. The supply of such large flows of carbon dioxide is major disadvantage.
- the absence of static holdup; differences between values of 'a' for the two cases of absorption and vaporization in packed beds are reported to be due to static holdup. As the static holdup for MBC is quite negligible relative to the operating holdup, $k_L a$ could be determined for either system.

The liquid-phase mass transfer coefficient, $k_L a$, was determined using the model which allows for the actual extent of axial mixing in the liquid phase, as determined from the mixing study. Finally, the close physical matching of the systems used for determination of interfacial area and of liquid-phase mass transfer coefficient makes it possible to determine the area-based transfer coefficient by simple combination of the results from these two extensive sub-studies , i.e. $k_L = \frac{k_L a}{a}$.

4.2 INTRODUCTION TO EXPERIMENTAL PROGRAMS

The experimental program was carried out in three parts:

1. Axial mixing investigation, involving determination of residence time distribution by the use of pulse inputs in the liquid phase.

2. Measurement of interfacial area by absorption of carbon dioxide and sulphur dioxide from air mixtures into solutions of sodium hydroxide.

3. Measurement of liquid-phase mass transfer coefficients by desorption of carbon dioxide from aqueous solution into air.

The experimental facility as used for the mixing study is described first, then those modifications which were required for the absorption and desorption experiments.

4.3 EQUIPMENT AND PROCEDURE FOR MIXING STUDIES

Figures 4.1 and 4.2 show a schematic representation and photograph of the experimental equipment. The test column was made of 6" O.D. by 1/4" thick plexiglas pipe, designed so that the spacing between grids could be varied continuously from 5.5 to a maximum of 30 inches by sliding telescopic joints. The lower supporting grid was retained between the flanges which connect the gas distribution system

FIGURE 4.1 FLOW DIAGRAM

1. COOLING AND HUMIDIFICATION COLUMN
2. BLOWER
3. AIR REGULATOR
4. GAS REGULATOR
5. GAS HOLD TANK
6. GAS CYLINDERS
7. ORIFICE METER
8. GAS DISTRIBUTOR
9. CALM SECTION
10. EXPERIMENTAL SECTION
11. LIQUID DISTRIBUTOR
12. THREE-WAY SOLENOID VALVE
13. TRACER TANK
14. NITROGEN CYLINDER
15. LIQUID ROTAMETER
16. PRESSURE RELEASE VALVE
17. LIQUID RECIRCULATING PUMP
18. RECIRCULATION TANK
19. STIRRER
20. GRIDS

P PRESSURE GAUGE

T THERMOMETER

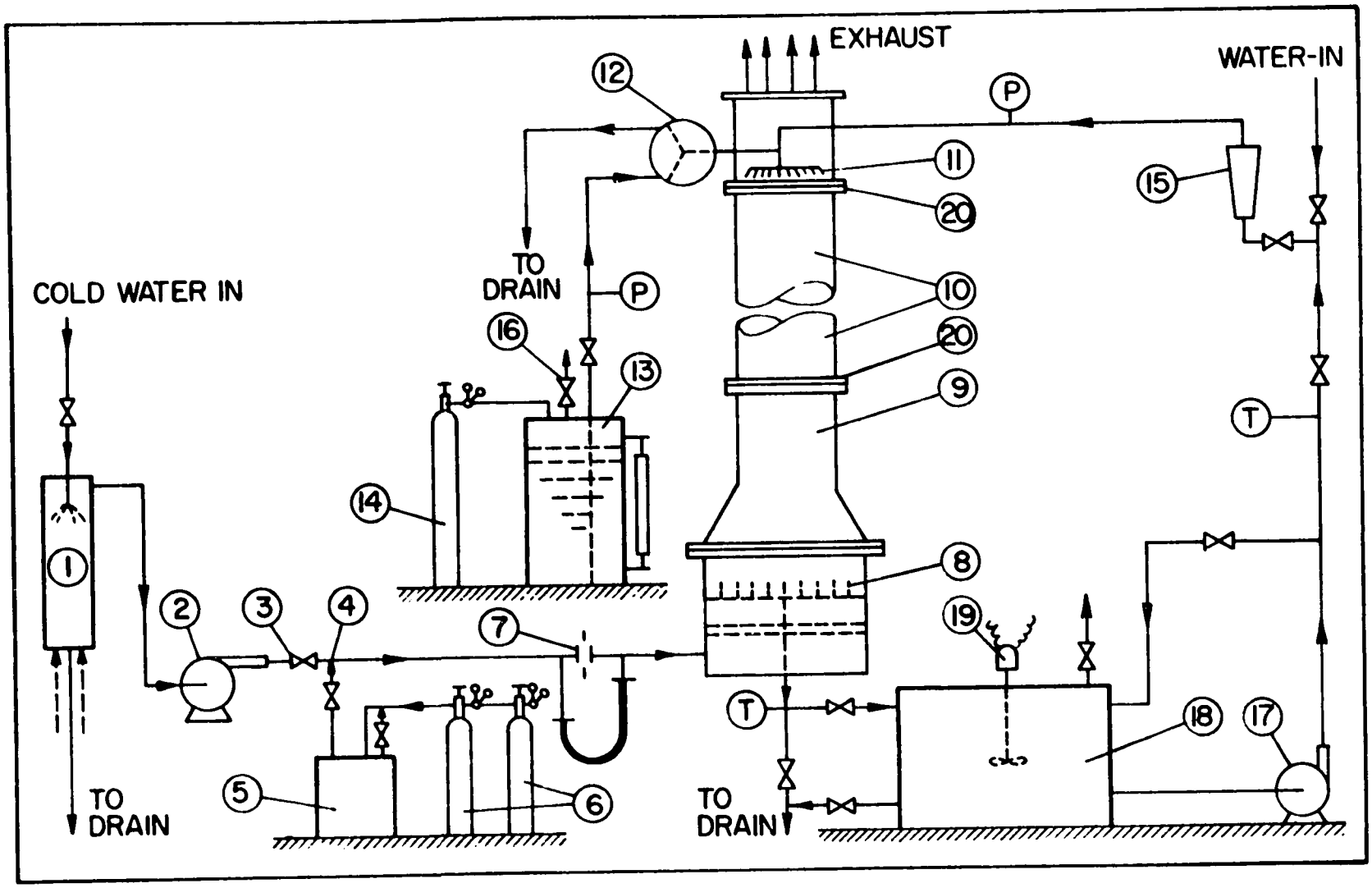

FIGURE 4.1: FLOW DIAGRAM OF THE EXPERIMENTAL SET-UP

to the test section. Both grids consisted of stainless steel wire mesh of 70% free area; mesh size for experiments with 1/2-inch spheres was 0.209 inch, and 0.42 inch for others.

4.3.1 Liquid Flow System

Water at flow rates from 3950 to 24,500 lb/(hr.-sq.ft.) could either be drawn from the mains and used on a once-through basis or could be recirculated through a 60 gallon stainless steel tank at a controlled temperature. For mixing studies water was not recirculated.

Uniform distribution of the liquid phase to the bed was obtained by the use of a specially designed 18-leg spider-type distributor, shown as Figure 4.2. The distributor was fabricated of 18, 1/8"-O.D. stainless steel tubes which were welded to a 1"-diameter by 1/2"-deep stainless steel box having a 1/2"-tube inlet for the liquid. The length of each tube was exactly the same so as to equalize the flow rate through each. The legs of liquid distributor were positioned so that each irrigated 1/18th of the column cross-section. This type of liquid distribution system has previously been used (25) with good uniformity of flow.

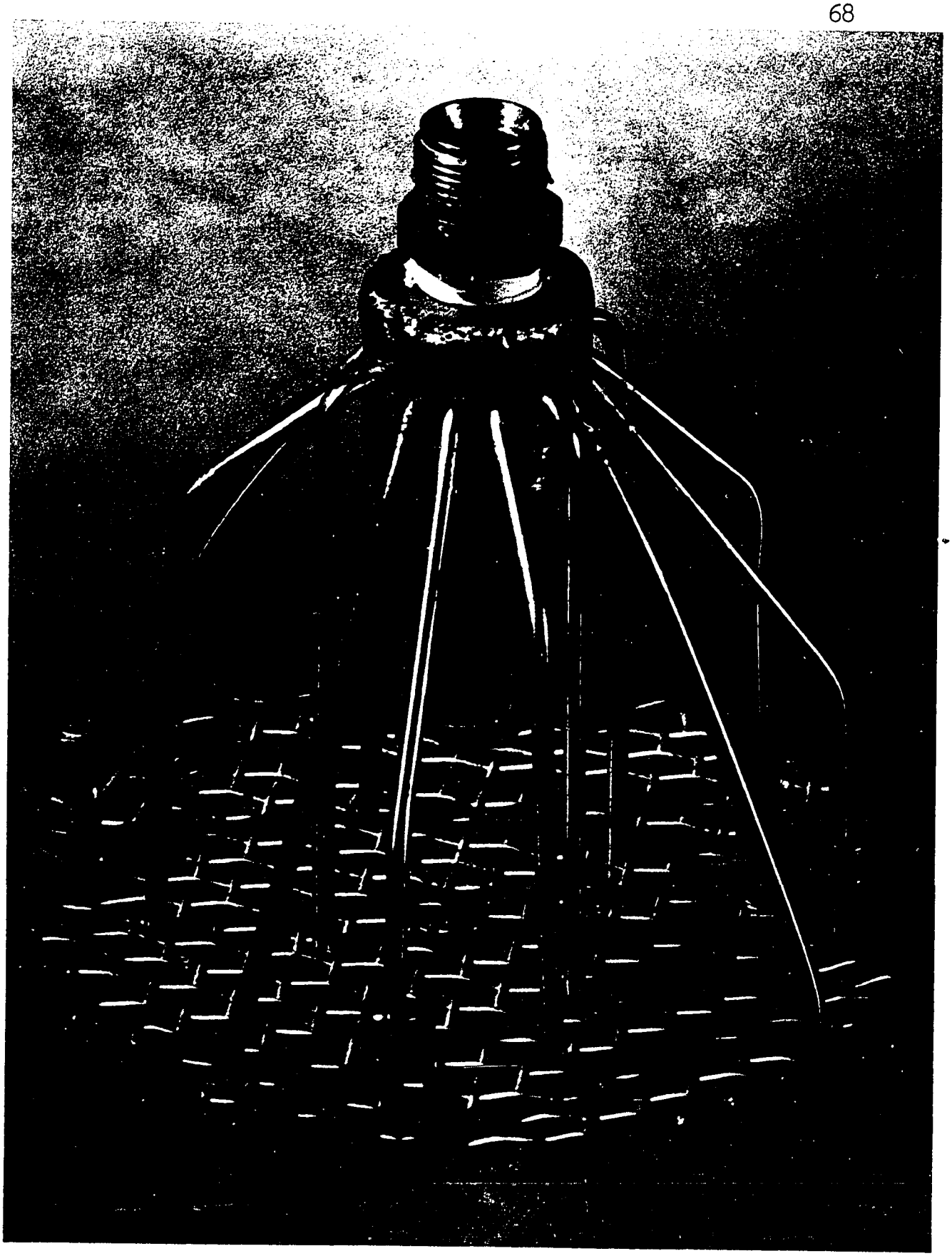

FIGURE 4.2: PHOTOGRAPH OF LIQUID DISTRIBUTOR

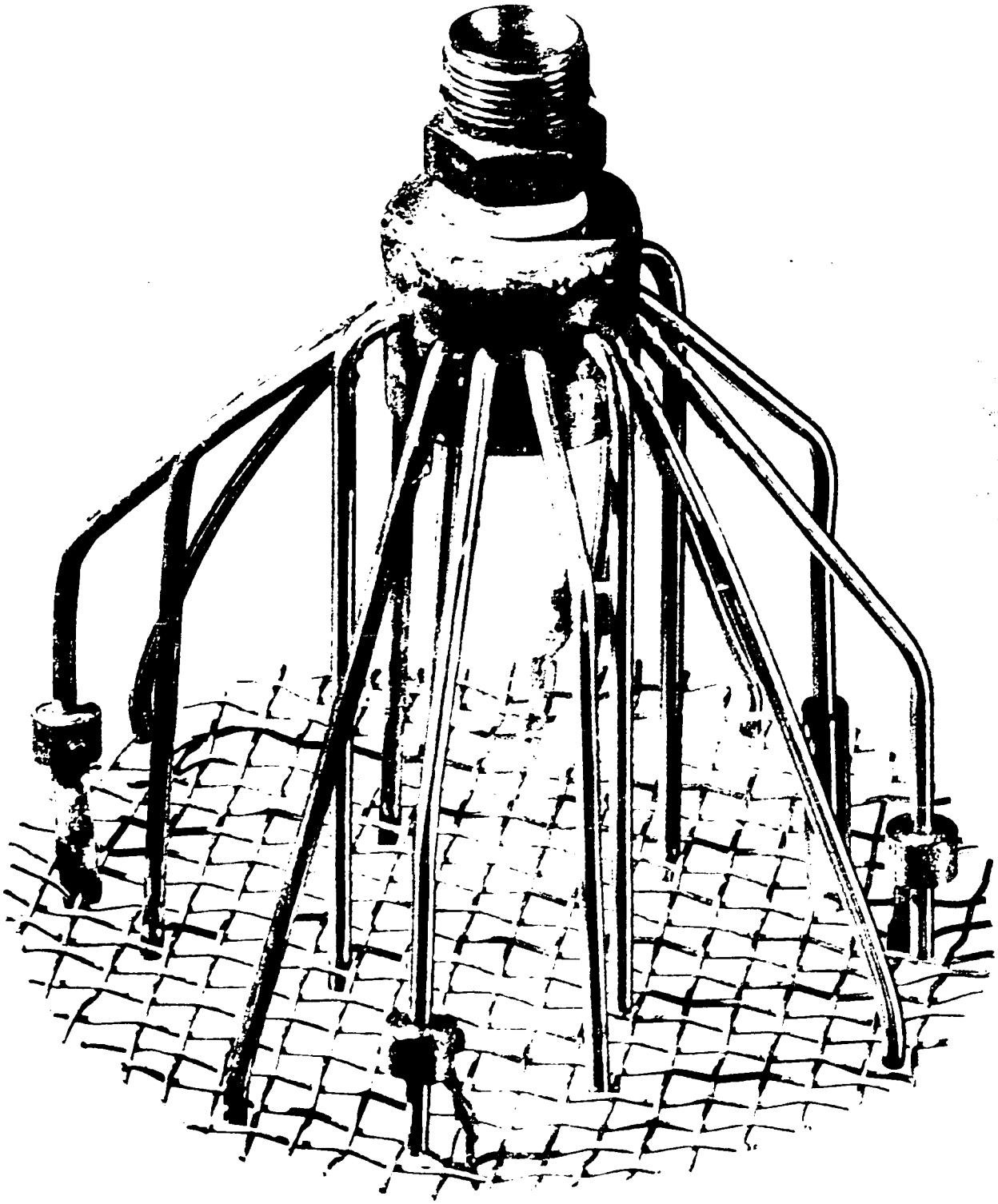

4.3.2 Gas Flow System

Air was drawn through a humidifying tower by a 5 H.P. blower and monitored by an orifice meter before it entered the gas distributing system. The humidification tower consisted of a similar MBC unit containing 1/2-inch spheres. It was provided primarily for mass transfer experiments to cool and saturate air.

The gas distribution section was designed so that a nearly flat velocity profile at the bed entrance could be obtained. The gas passed first through a cylindrical section 12-inch diameter by 12 inch high, then through a converging conical section 12 inch high. In the cylindrical section the air passed through air filters before emerging from a bundle of 32 plexiglas tubes, each 3/4-inch in diameter. The filters were made of rubber and had open cell structure. By adjusting the amount of filter material at different points on the cross-section, a uniform distribution of gas was obtained. Figure 4.3 shows typical gas flow profiles measured at the level of lower supporting grid using a standard 1/8-inch pitot tube and a pressure indicator (Barotron). The gas was exhausted through the telescoping pipes to the roof level. Gas mass velocities up to 4000 lb/(hr.-sq.ft.) could be employed.

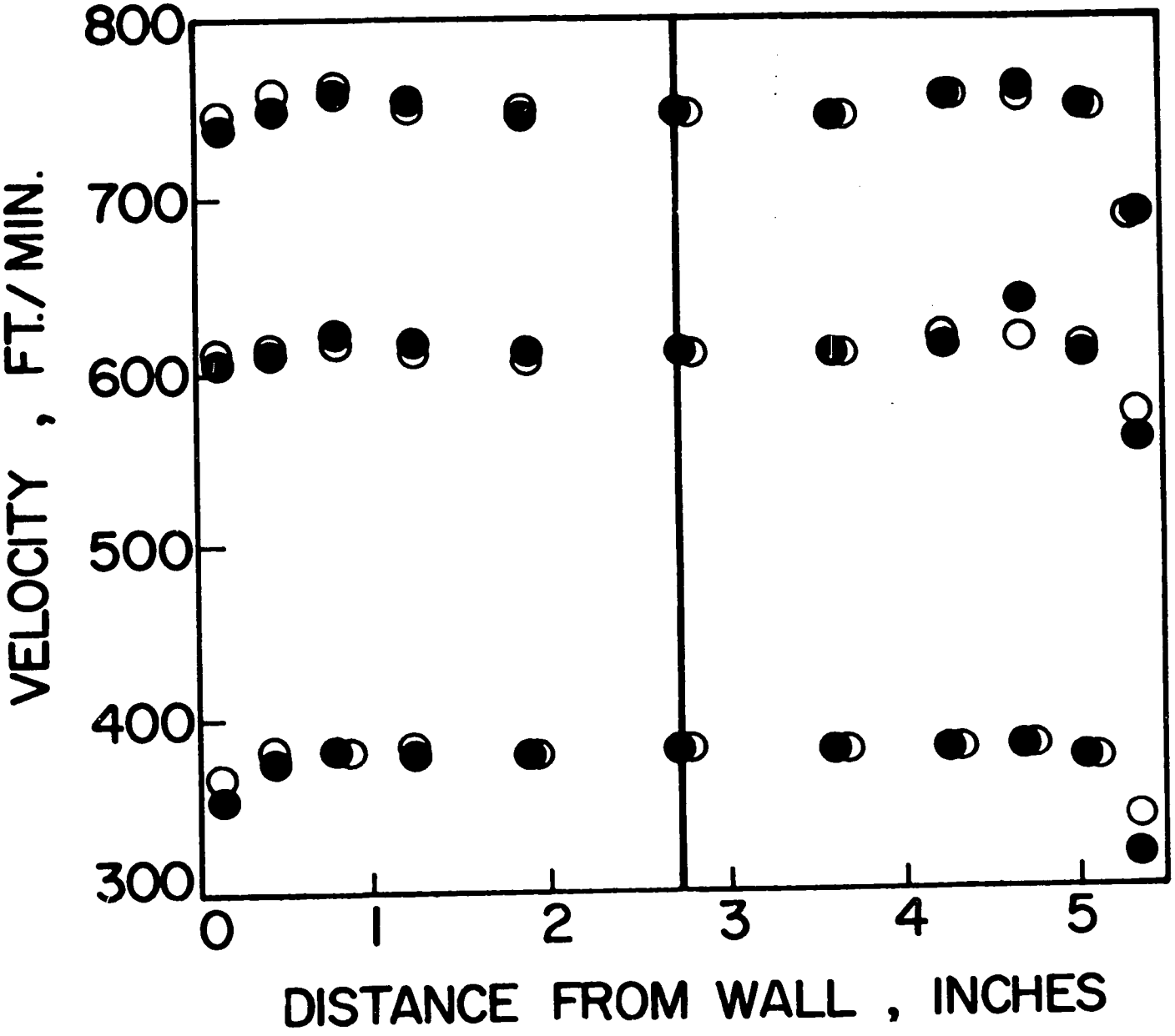

FIGURE 4.3: TYPICAL GAS FLOW PROFILES IN THE COLUMN

4.3.3 Tracer Injection System

An injection system was required for the tracer, a potassium chloride solution, which would produce in the liquid phase entering the column a sharp, smooth pulse of less than 0.1 second duration. Figure 4.4 gives a sketchmatic diagram of the system used. Potassium chloride solution from a pressurized vessel, A, was introduced into the liquid stream immediately before the liquid distributor. The flow of tracer solution was controlled by a three-way solenoid valve. When the valve was not energized, a small stream of water from the supply to the column continuously purged the line from the injection point to the solenoid valve. When the valve was energized the flow in this line reversed as tracer solution flowed into the column. The purge action after each brief energized period had the desired feature of eliminating entirely the shortcoming sometimes associated with pulse inputs, i.e. the presence of a tailing effect at the end of the input pulse. An assembly of automatic timerand a non-release relay was used to control the pulse width. An electric impulse, generated simultaneously by means of a 1.5 V flashlight battery, was fed to both the recording oscillograph and the data acquisition system to mark the exact time of tracer injection. This system entirely satisfied the required performance.

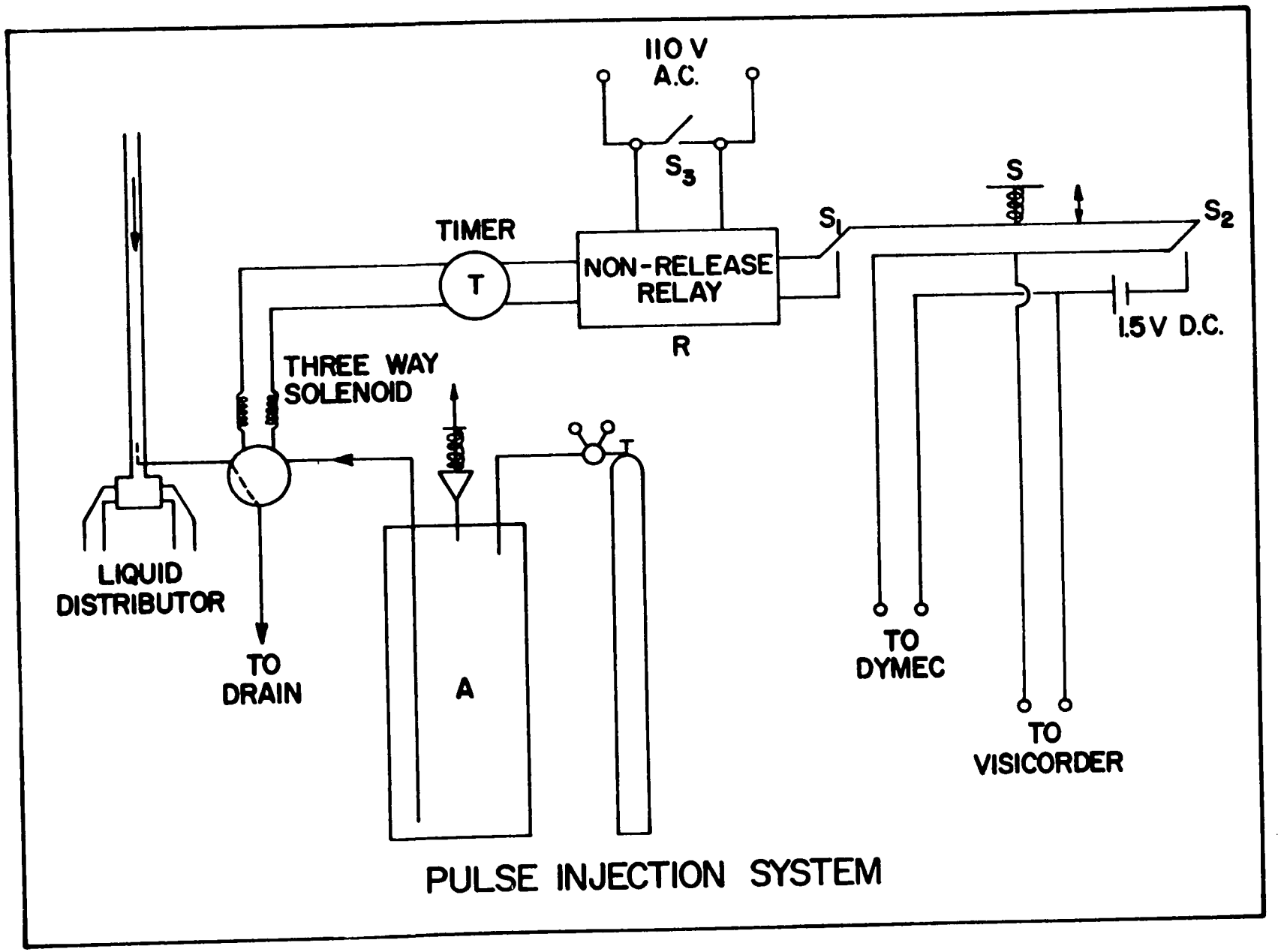

FIGURE 4.4: SKETCHMATIC REPRESENTATION OF THE TRACER INJECTION SYSTEM

4.3.4 Instrumentation

The concentration of potassium chloride was determined by the measurement of electrical conductivity. Cairns and Prausnitz (92), Hennico et al. (143), Kramers and Alberda (95) and others have used similar concentration measurement methods in their respective studies. Also, the equipment required for accurate, fast and continuous recording was available from a previous study (25).

4.3.4.1 Conductivity Cells

Each conductivity cell consisted of a pair of 1-mm. diameter platinum electrodes embedded in a 1-mm. slot of a cylindrical body, 0.5-cm. diameter x 1.3-cm. long. Each probe was constructed by immersing a U-bed of platinum wire of 1-mm. diameter x 1.2-cm. long, into liquid Epoxy resin contained in a cylindrical brass mould. The bend was positioned 2-mm. from the end of the mould. The resin setting was slotted at the U-bend,thus cutting a sharp 1-mm. wide by 5-mm. deep gap in the epoxy resin and platinum wire perpendicular to its length. In this way, pairs of plane-parallel, circular platinum electrodes of 1-mm. diameter with a gap of 1-mm. were prepared. Copper leads were soldered to the platinum wires prior to immersion in the resin.

One probe was used at each end of the test section. At the inlet section the probe was attached directly to one of the legs of the liquid distributor so that the entire amount of liquid emerging from the tube passed between the electrodes. The conductivity monitoring cell at the outlet was mounted in a liquid sampler, shown in the lower photograph of Figure 4.5. This sampler could be moved in all directions, but was positioned at the centre-line at a distance of 0.5-cm. below the supporting screen. Liquid flowed continuously through flexible tygon tubing (not shown in the photograph) attached to the lower end of liquid sampler. An adjustable pinch-cock was used to regulate the flow of liquid to the maximum value consistent with the complete exclusion of gas flow, as the presence of any gas disrupted the monitoring of liquid concentration at the electrodes. This arrangement for continuous measurement of the concentration of 1-cu.mm. elements of the liquid stream essentially eliminated time lags in the determination of the transient response of the liquid phase.

4.3.4.2 Conductivity Measuring Circuit

A basic network, such as illustrated in Figure 4.6, has been used successfully by a number of investigators (22,25,91,92,113) for the continuous measurement of electrical conductivity with fast response times. Basically the method involves connecting a constant-voltage audiorange oscillator across the electrodes and the resistor 'r'. If 'r' is chosen such that its values is small compared to the resistance of

FIGURE 4.5: PHOTOGRAPH OF CONDUCTIVITY MONITORING CELL (LOWER) AND SAMPLERS (UPPER)

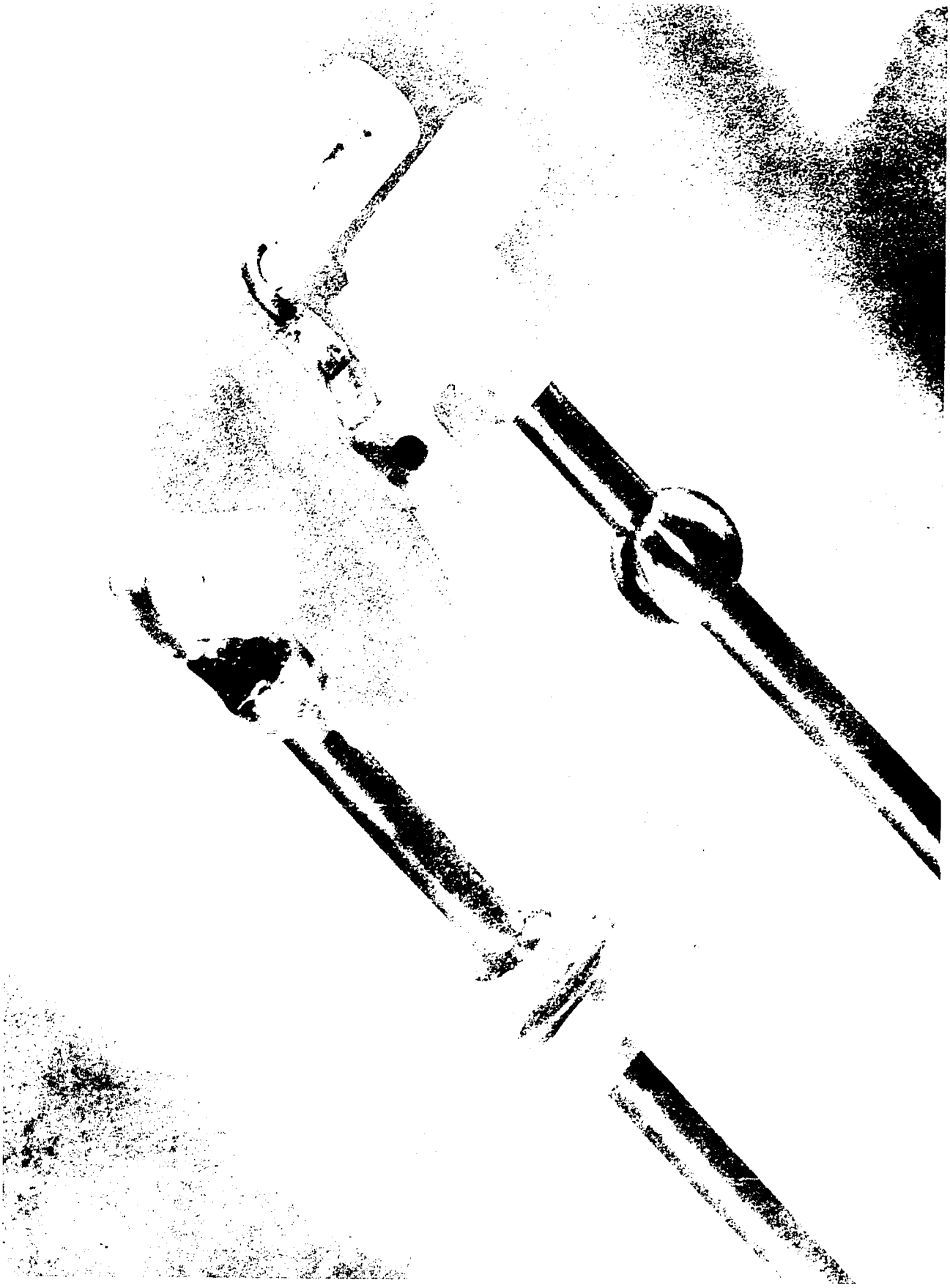

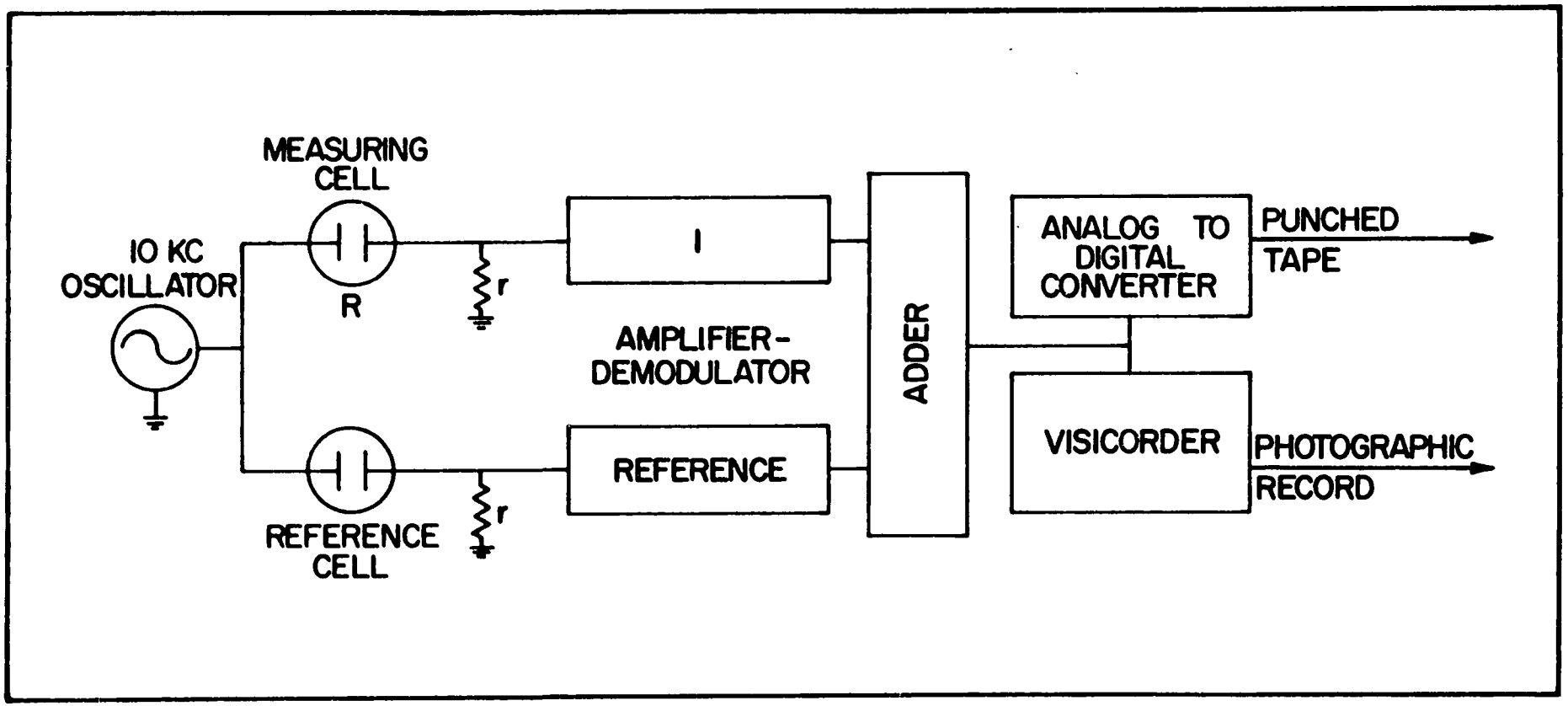

FIGURE 4.6: BASIC ELECTRONIC NETWORK FOR CONDUCTIVITY MEASUREMENTS

the solution, the potential, V_r, across 'r' becomes proportional to the current passing through it, and hence proportional to the conductance of the solution between the electrodes. Polarization of the electrodes was eliminated by using the audio range of frequency. For the present study 'r' was set at 51 ohms which was only 2% of the smallest value of cell resistance encountered during the experiments. The voltage V_r, was amplified and demodulated, thus giving a D.C. voltage directly proportional to the total conductivity of the solution. The signal from a reference channel containing an electrode dipped in tap water was subtracted from that of measuring channels to get net D.C. voltage signals which were proportional to that part of the conductivity of the solution due to the presence of salt tracer.

The time record of this conditioned signal, being proportional to tracer concentration, provides the basic data for the mixing analysis. The signal from the cell at the liquid exit from the bed was recorded digitally on analog-to-digital data acquisition system, (Dymec Model 2010B made by Hewlett-Packard) which provided two outputs, a printed record and a punched paper tape. For this purpose the unit was operated at its fastest speed, i.e. with a gate interval of 0.01 second.

The time record of the signal from the conductivity cell at the liquid inlet to the bed could, however, not be digitized directly by the data acquisition unit because its maximum speed was approximately the same as the duration of the input pulse. This signal was recorded instead with a light-beam recording oscillograph (a Heiland type, Model 916C "Visicorder", made by Honeywell). The signal from the input event marker was of course fed to both recording systems. The conditioned signal from the inlet conductivity cell drove the electromagnetically dampled moving-mirror type galvanometers which had a sensitivity of 1.2 mv./inch. The time constant of the system was adjustable by suitable choice of series and shunt resistors for the galvanometers. The galvanometers were critically damped so that a pulse as short as 11.4 milliseconds could be reproduced with amplitude fidelity.

The Visicorder was operated at a chart speed of 5-inches per second and 100 timing lines per inch. The inlet-pulse record from the Visicorder was digitized manually and the data punched on computer cards. The complete linearity of this system had been established earlier in a test by Chen (25).

4.3.5 Procedure

A warm-up period of at least one hour was allowed for all electronic equipment. The column was always packed to a static height of 5.5 inches, the bed height being controlled precisely by using the same number of plastic balls. The flow system was allowed to come to a steady-state for at least 10 minutes prior to throwing open the relay, R, of the tracer injection system (Figure 4.4) to start a run. For injecting tracer the switches S_1 and S_2 were rapidly closed. This started the following series of events:

- the input event mark was made on the Visicorder paper and the printed and punched-paper tape outputs of the data acquisition unit; the tracer injection started, then stopped after the set delay by the timer, T;
- the input pulse was recorded on the Visicorder paper;
- the output pulse was digitally recorded simultaneously on the printer and the punched paper tape; and
- a stream of water flushed the tracer line of the remaining traces of the salt after the injection stopped.

The rather good reproducibility of the total system is indicated by Figure 4.7 which shows three records for the same operating conditions. Figures 4.8 and 4.9 show the outlet response for typical liquid and gas flow rates for a trickle-bed operation and for a MBC, respectively. Table 4.1 gives the packing characteristics, flow ranges and other pertinent data.

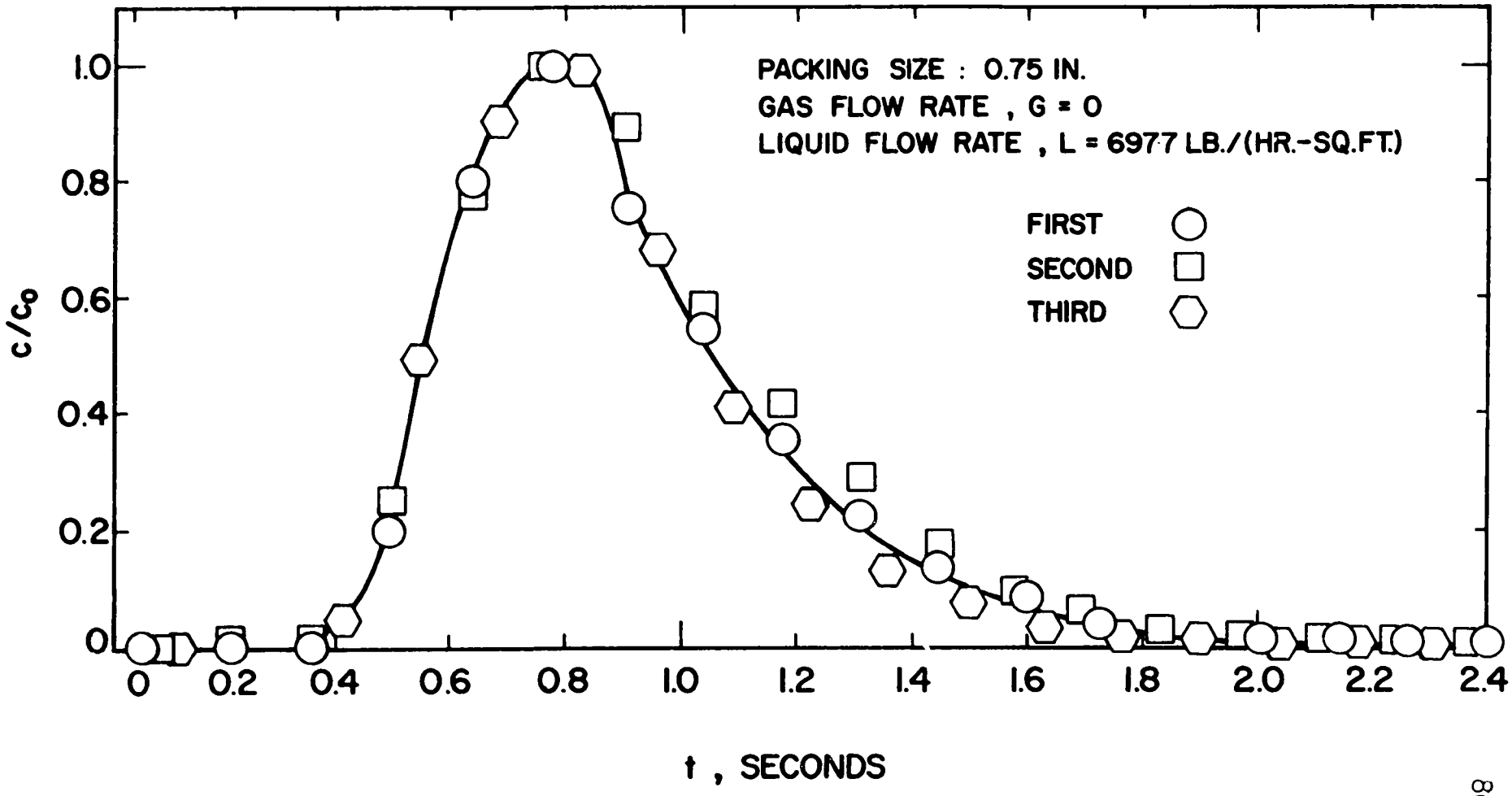

FIGURE 4.7: TYPICAL BREAKTHROUGH CURVE

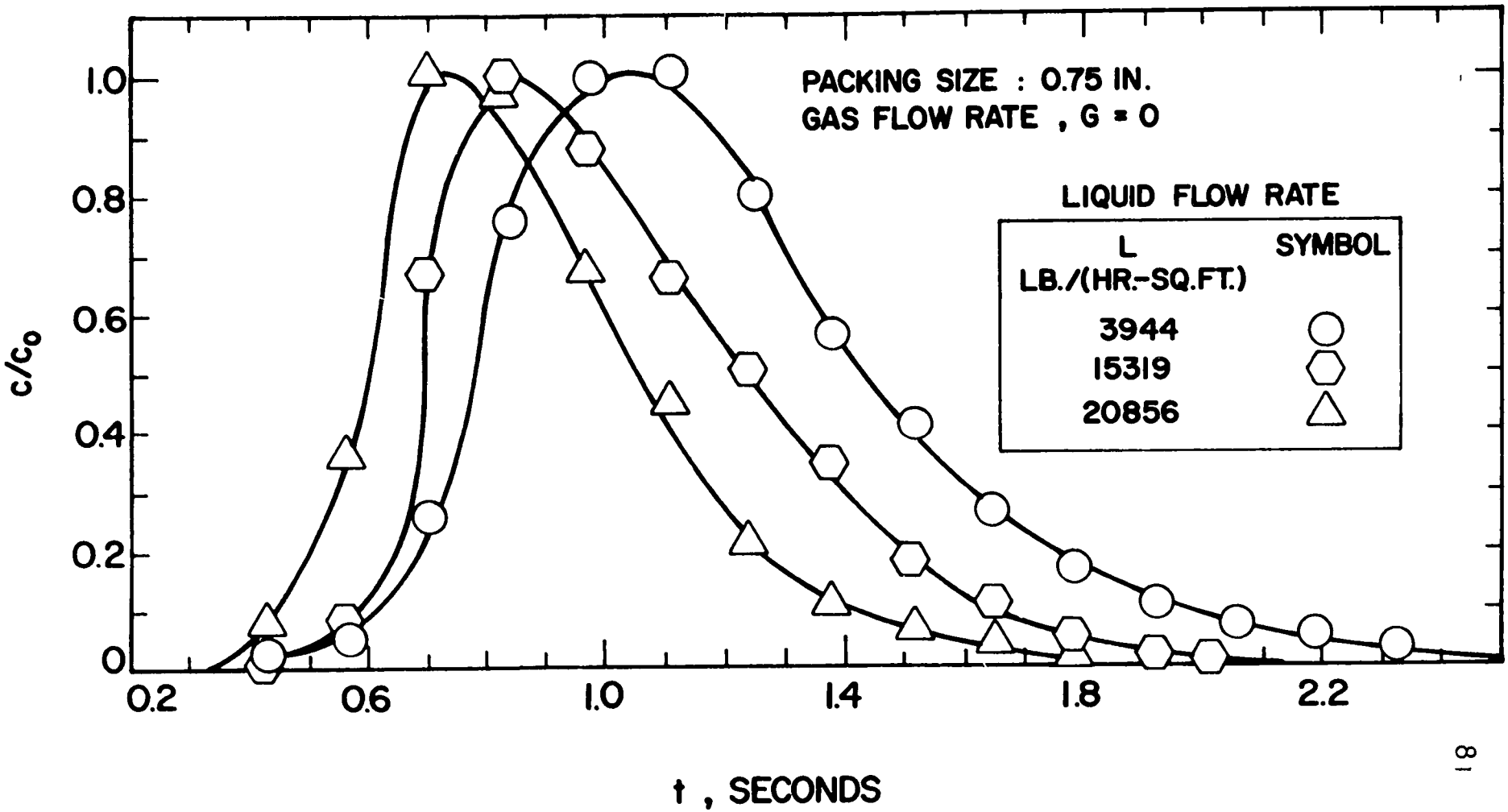

FIGURE 4.8: VARIATION OF PULSE RESPONSE WITH LIQUID FLOW RATE FOR FIXED BED OPERATION

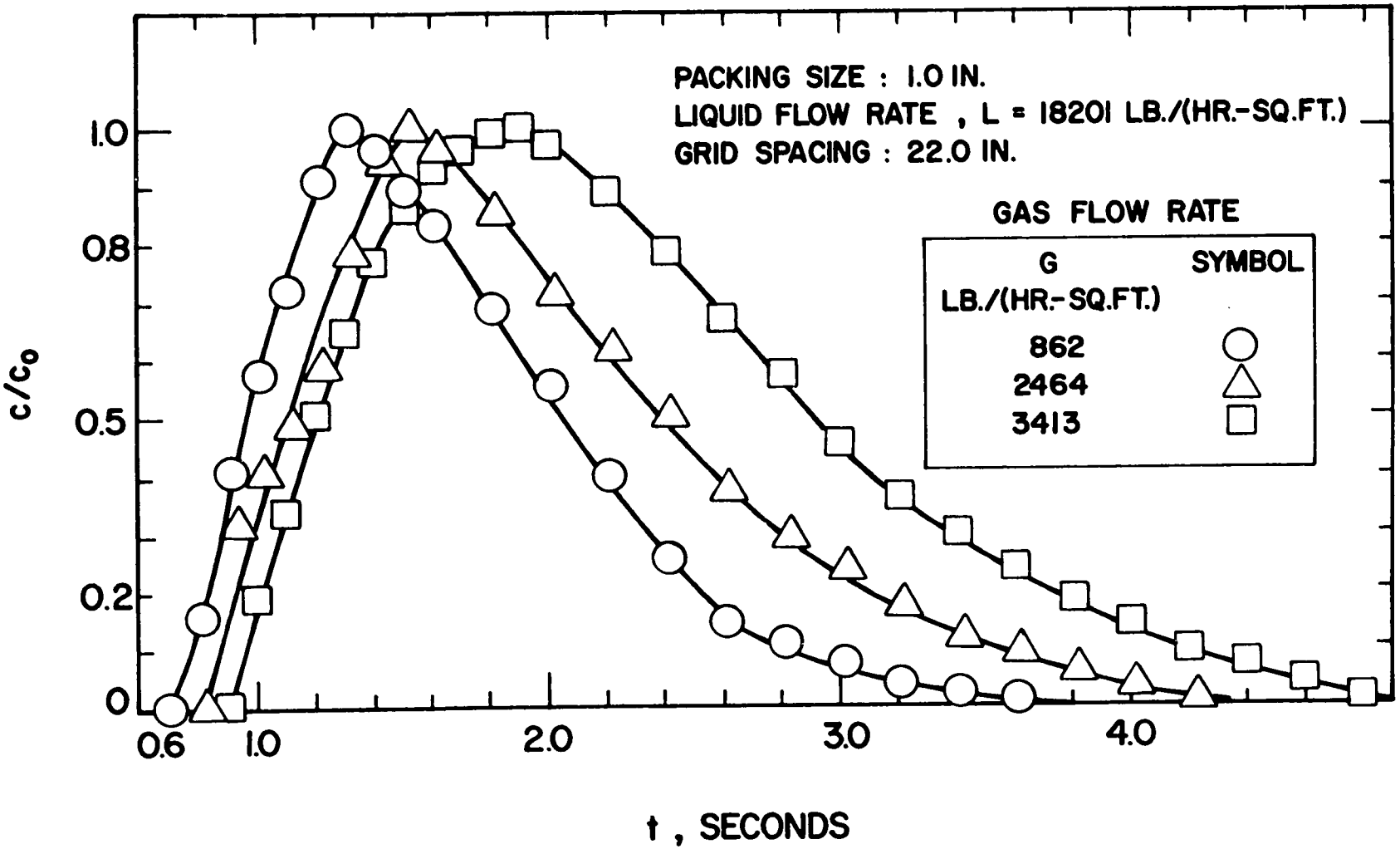

FIGURE 4.9: VARIATION OF PULSE RESPONSE WITH GAS FLOW RATE FOR MOBILE BED OPERATION

TABLE 4.1

SCOPE OF EXPERIMENTS

GAS MASS VELOCITY	0-3,600 lb./(hr.-sq.ft.)
LIQUID MASS VELOCITY	4,000-24,000 lb./(hr.-sq.ft.)
COLUMN DIAMETER	5.5 inches inside
STATIC HEIGHT	5.5 inches
FREE BOARD *	4 x Static Height
PACKING SIZE	0.5, 0.75, 1.0 and 1.5 inches
PACKING DENSITY	0.15 gm/cc, polystyrene foam
GRID FREE AREA	70%
TEMPERATURE	20-30 ^{o}C

*Free Board = Grid spacing - Static height

4.4 EQUIPMENT AND PROCEDURE FOR MASS TRANSFER STUDIES

The equipment used for the mixing study was slightly modified to accommodate the sampling and analysis systems which were required for determining the rate of desorption of carbon dioxide from aqueous solution into air and, in the determination of interfacial area, the rates of absorption of carbon dioxide and of sulphur dioxide into solutions of sodium hydroxide. Temperatures of both gas and liquid streams were kept as close as possible, preferably below 30^{o}C. The values of physico-chemical constants can be estimated more accurately below 30^{o}C. Figure 4.10 shows the control panel, the gas analysis system, the inclined-tube manometer for the inlet gas flow rate, the large rotameter for the liquid-phase and the experimental column.

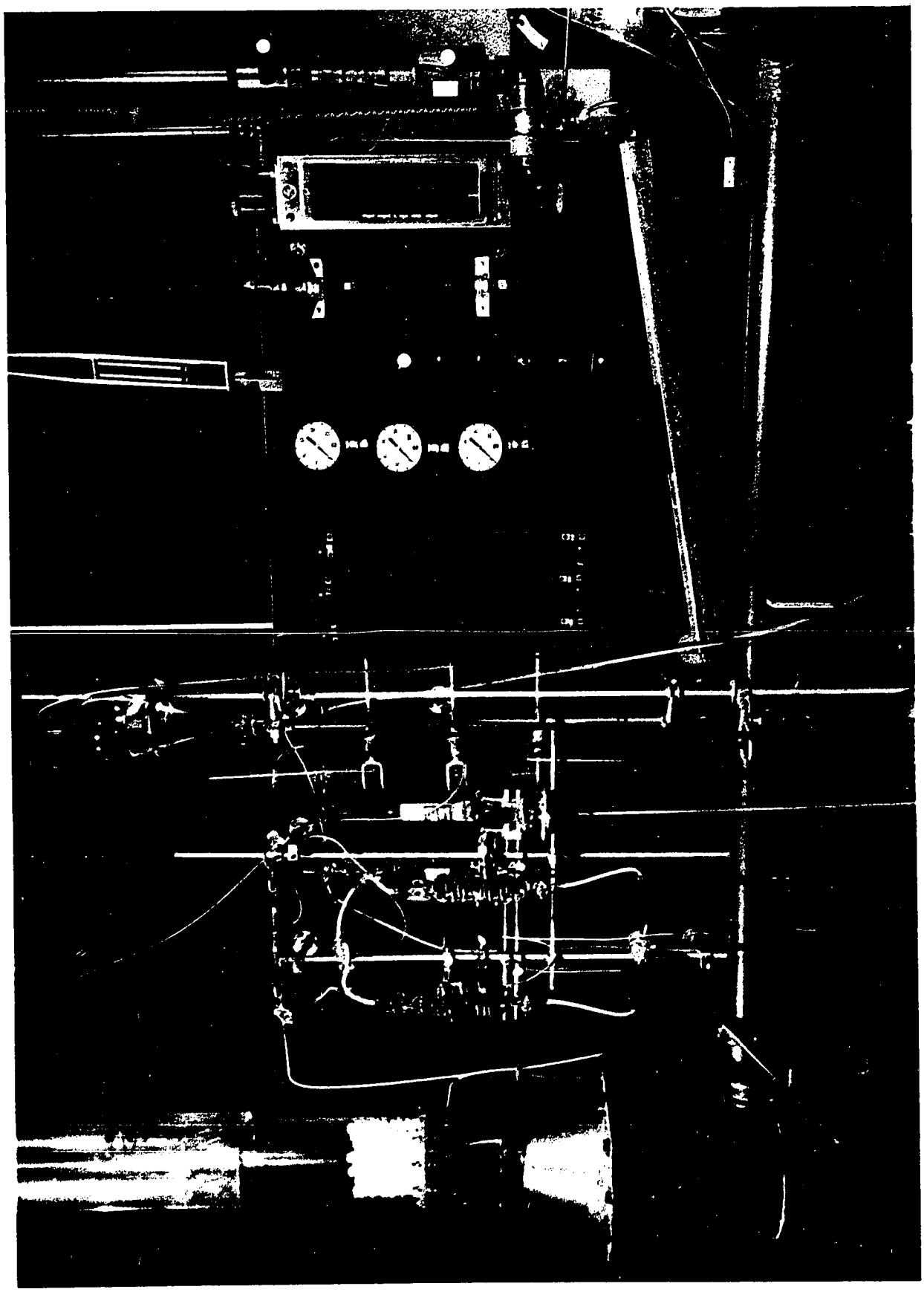

FIGURE 4.10: PHOTOGRAPH OF THE INSTRUMENT PANEL, GAS ANALYSIS SYSTEM AND THE TEST SECTION

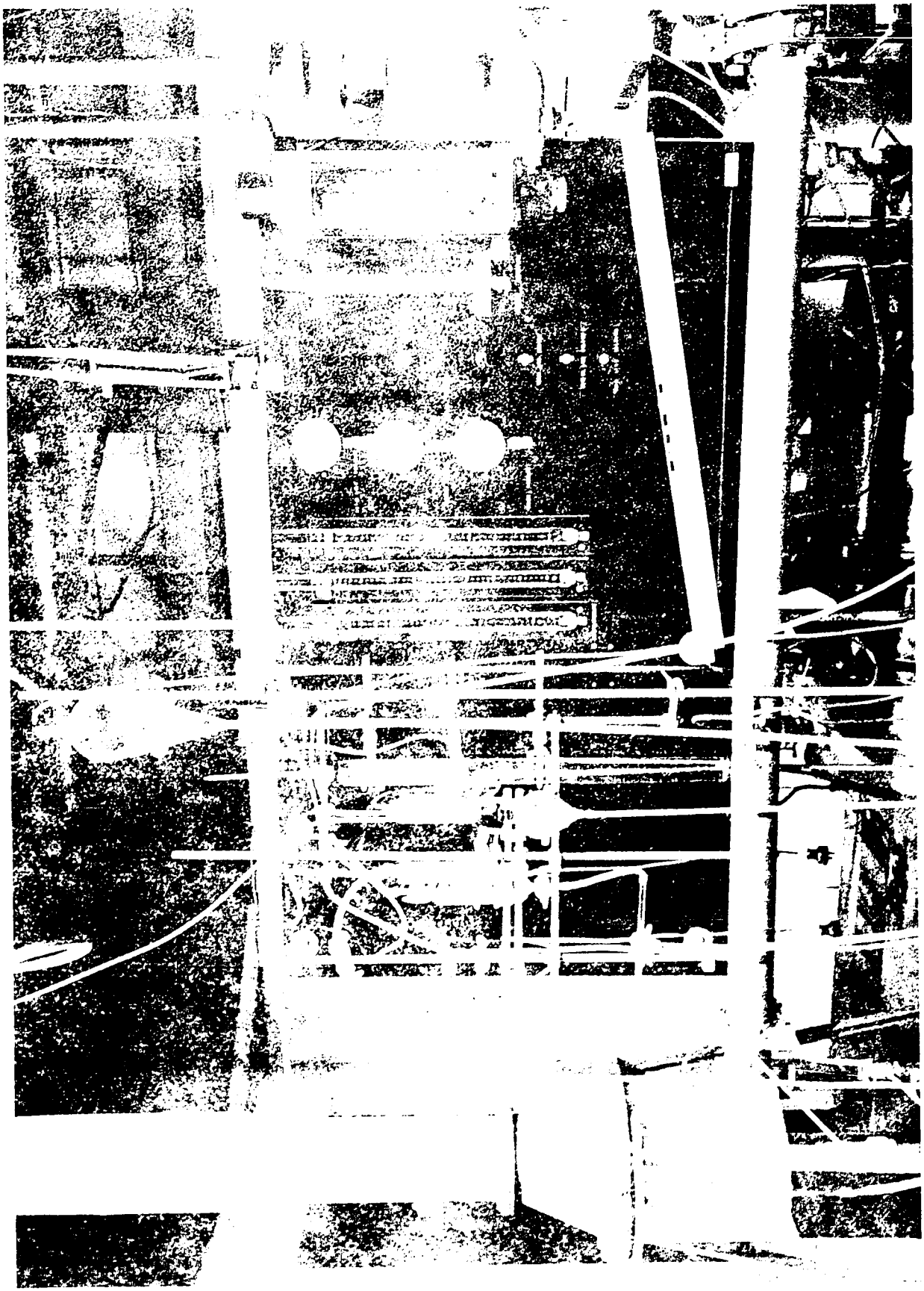

4.4.1 Liquid Flow System

The liquid flow system consisted of a 60-gallon capacity stainless-steel recirculation tank, fitted with a liquid-level indicator, cooling coils and a stirrer, and a gear pump capable of producing about 100 psig at 8 gpm. The tank was constantly purged with nitrogen when sodium hydroxide solutions were being circulated, or with carbon dioxide in the case of the desorption experiments. Chilled water from a General Electric cooling unit was circulated through the cooling coils to cool the solution.

4.4.2 Gas Flow System

Carbon dioxide and sulphur dioxide were drawn from compressed gas cylinders, metered with a gas rotameter, then introduced into the 3-inch duct at a point about 15 feet from column inlet. The exhaust from the column was led by a 20-ft high duct to the exterior above the roof level. The gas regulator on the manifold connecting a series of 11 carbon-dioxide cylinders was heated with an electric heating tape. Two cooling coils made from 50-feet of 1/4-inch copper tubing were installed in the 3-inch gas inlet pipe (upstream of the point of carbon dioxide and sulphur dioxide introduction) to cool the air. This was required for close control of reaction conditions.

4.4.3 Sampling and Analysis System

For the composition of liquid entering the test section, samples were drawn from the inlet liquid stream. The exit composition was determined on samples drawn through a small liquid sampler, which originally housed the conductivity probe, positioned at the center of the column at 0.5-cm. below the lower supporting screen. The samples were collected simultaneously at the two points in stoppered Erlenmeyer flasks which were initially flushed with dry nitrogen.

The liquid concentration was determined by volumetric analysis using automatic titration Fisher Titralyzer. In the case of carbon dioxide desorption from aqueous solutions, a known quantity of standard, carbonate-free sodium hydroxide solution was added to each sample to neutralize the dissolved gas. The concentration of sodium hydroxide in the sample and the amount of carbonate formed was determined by titration against standard hydrochloric acid in the presence of slight excess of barium chloride solution to pH values of 8.6 and 3.6, respectively (144). For the experiments involving chemisorption of carbon dioxide into solutions of sodium hydroxide, the same procedure was used to determine the amount of carbonate formed. In the case of sulphur dioxide absorption runs, the liquid sample was acidified with an excess of hydrochloric acid, then a known volume of standard iodine solution was added. The resulting solution, which had a

distinct brown colour, was titrated against standard sodium-thiosulphate solution using the dead-stop end-point technique (144). The Fisher Titralyzer was employed for this purpose also, the end-point being determined by the use of two platinum electrodes.

Gas samples were drawn through specially designed samplers mounted in the test section. The sampler at the gas inlet to the bed consisted of a 1/8-inch stainless steel tube, sealed at one end and perforated up to a 1/4-inch from the sealed end with approximately 60 holes of 1/64-inch diameter. The sample tube was placed inside a concentric plexiglas cylinder, approximately 1-cm. diameter by 2-cm. long, with one end sealed. The sampler at the gas exit was an inverted stainless steel conical cup of 1-cm. diameter at the base and 3-cm. high. The converging end was connected to a 1/4-inch stainless steel tube protruding 1/4-inch into the cone. The end of the tube was sealed and about 64 holes of 1/64-inch were drilled along the periphery in the protruding part. Both samplers were found to be satisfactory, in that completely liquid-free gas was obtained with every sample.

The gas was collected in a glass sampling tube by mercury displacement. Concentrations of carbon dioxide and sulphur dioxide were determined by standard Orsat analysis, using sodium hydroxide solutions and an accurate gas burette with an extended scale.

4.4.4 Procedure

Sodium hydroxide solutions of concentration approximately 2-Normal were prepared from distilled water and pellets with continuous stirring and cooling for about two hours. The liquid flow rate was monitored with a calibrated Schurette and Koerting Safeguard rotameter.

For experiments involving the desorption of carbon dioxide from water, the tank was filled with distilled water and the viscosity was adjusted to that of sodium hydroxide liquor of 2N concentration at the same temperature by the addition of ethylene glycol. The liquid in the circulation tank was kept saturated by pure carbon dioxide at atmospheric pressure.

For all mass transfer runs the system was allowed to come to the steady-state for 10 minutes, then gas and liquid samples were drawn simultaneously over a period of about 3-5 minutes and analyzed immediately. For the carbon dioxide desorption runs, only liquid analysis was used for computing the rate of desorption.

V. CORRELATION OF EXPERIMENTAL DATA AND DISCUSSION OF RESULTS

The results are grouped in two basic categories:

1. Hydrodynamic Effects. Liquid holdup and axial dispersion of the liquid, both determined by the impulse testing transient response technique, and expansion of the mobile bed, determined visually in the present study.

2. Mass Transfer Effects. True liquid-phase mass transfer coefficients i.e. with axial mixing appropriately allowed for, and the effective interfacial area of mass transfer.

5.1 HYDRODYNAMIC EFFECTS

The complex interaction between the solid, liquid and gas phases, all of which are in quite vigorous motion in mobile-bed contacting, determine the physical behaviour of MBC, including such measures as the degree of mixing and the holdup of each fluid phase, the bed expansion and the pressure drop. Although complicated by the additional presence of a down-flow of liquid, MBC operation is somewhat analogous to a gas fluidized bed. Based on the experience from that operation, the minimum fluidization velocity, G_{mf}, at which the bed just begins to expand from the static condition has been used also as an important correlating variable for MBC. The results for minimum fluidization velocity will be presented first as this

variable enters into subsequent correlations. The results follow for bed expansion, which is correlated in terms of minimum fluidization velocity. The bed-height correlation is in turn required for the normalization of liquid holdup data with respect to bed volume. Presentation of various hydrodynamic effects concludes with correlation of the data on axial mixing in the liquid phase.

5.1.1 Minimum Fluidization Velocity

The previous work of Chen (25,29) has established the method of determining the minimum fluidization velocity for mobile-bed contacting by extrapolation of the linear relationship between bed height and gas mass velocity to the limiting value of the static bed height. Likewise, the similarities and differences between mobile-bed contacting and the much more thoroughly studied operation, fluidization with a single fluid phase has been treated fully in the works noted above. The new data from the present study have been obtained following the pattern set by Chen, and may therefore be presented without reviewing in detail the justification for the treatment used.

The new data for height of a mobile bed are reported in full in Appendix I.1, Table III. As before, a least squares straight-line fit to the data for bed height as a function of gas velocity gives the value of minimum fluidization velocity, G_{mf}, the extrapolated value of G which corresponds to the static bed height, h_s. The height of the expanded bed was determined

visually. The values of G_{mf} obtained by this method are given in Table 5.1, while the variation of minimum fluidization gas velocity with the liquid flow rate and with packing diameter is shown on Figure 5.1

TABLE 5.1

Minimum Fluidization Velocity for MBC

Liquid Flow Rate		Minimum Fluidization Velocity, lb/(hr-ft^2)		
Rotameter Setting GPM	L, lb/(hr-ft^2)	Packing Size, Inch		
		0.75	1.0	1.5
0.5	3,944	630	1000	2000
1.0	6,977	500	860	1600
1.5	9,707	400	700	1480
2.0	12,513	340	600	1300
2.5	15,319	230	400	900
3.0	18,201	160	240	820
3.5	20,856	120	210	520
4.0	23,813	80	150	420

By extension of the work on conventional two-phase fluidization to the present operation, which may in fact be viewed as three-phase fluidization, Chen derived the form of the correlation of G_{mf} for MBC as

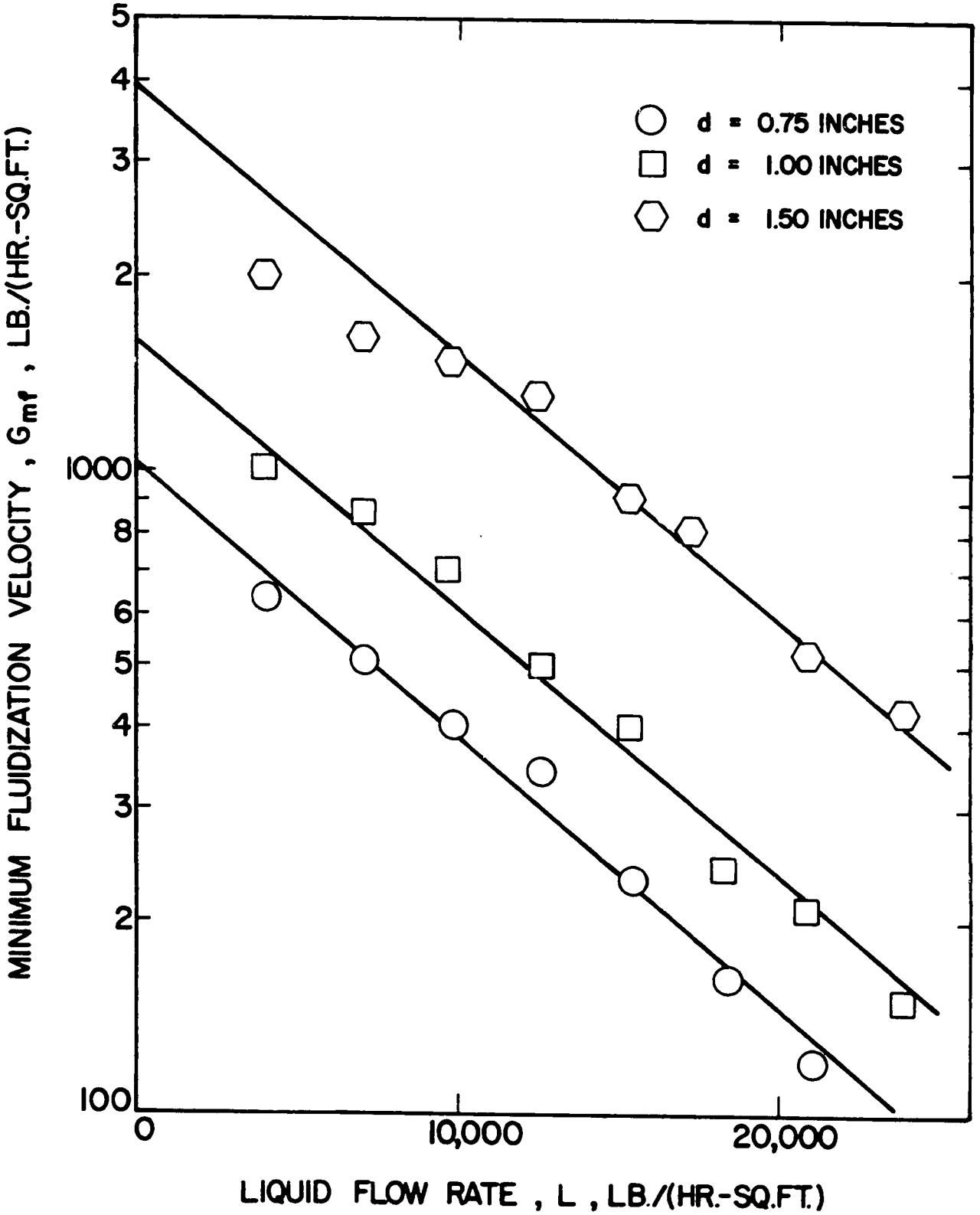

FIGURE 5.1: VARIATION OF MINIMUM FLUIDIZATION VELOCITY WITH LIQUID FLOW RATE AND PACKING SIZE FOR MOBILE BED OPERATION

$$G_{mf} = A(d)^m (10)^{-\gamma L} \qquad (5.1)$$

The presentation of data given as Figure 5.1 indicates that all the data may be adequately represented by one value of the parameter γ. For the data of the present study, a value of $\gamma = 4.3 \times 10^{-5}$ is satisfactory. Separate correlations with this value of γ for each of the three diameters of packing used would correspond to replacing the product $A(d)^m$ of Equation (5.1) by the values 1016, 1570, and 3780 for d = 0.75, 1.00 and 1.5 inches, respectively. However, Figure 5.2 indicates that not only all the data of the present study, but those from Chen's study also may be represented satisfactorily by Equation (5.1) with:

$$A = 1570$$

$$m = 1.5$$

$$\gamma = 4.3 \times 10^{-5}$$

For comparison, the constants in the corresponding correlation obtained by Chen for his data, i.e. assuming the same dependence of G_{mf} upon L for all values of d , are as follows:

$$A = 1300$$

$$m = 1.15$$

$$\gamma = 5.17 \times 10^{-5}$$

Chen obtained this correlation by first obtaining the slope for the dependence of G_{mf} upon L. The slope used was that which was best for the 1-in. spheres, the slope of the data for the 0.5-in. and 1.5-in. spheres deviating slightly on either side of this mean slope. Having thus chosen the slope, he then determined the best values of the other two parameters, A and m.

Chen's data was processed by a simple multiple regression analysis, a somewhat better procedure, by both the writer and by I. Rabin of Bechtel Corp.(153). The values of the three parameters thus obtained by both of the above for the correlation Equation (5.1) are

$$A = 1054$$

$$m = 1.067$$

$$\gamma = 3.8 \times 10^{-5}$$

It is of interest to note the considerable difference in numerical values of these parameters from those obtained by Chen.

An attempt was made to determine the minimum fluidization velocity for 0.5-inch spheres. However, the experimental scatter at the low gas velocities involved was such that the variation with liquid flow rate of the extrapolated values of G_{mf} could not be observed with reasonable accuracy. The values of G_{mf} computed from Equation (5.1) were, however,

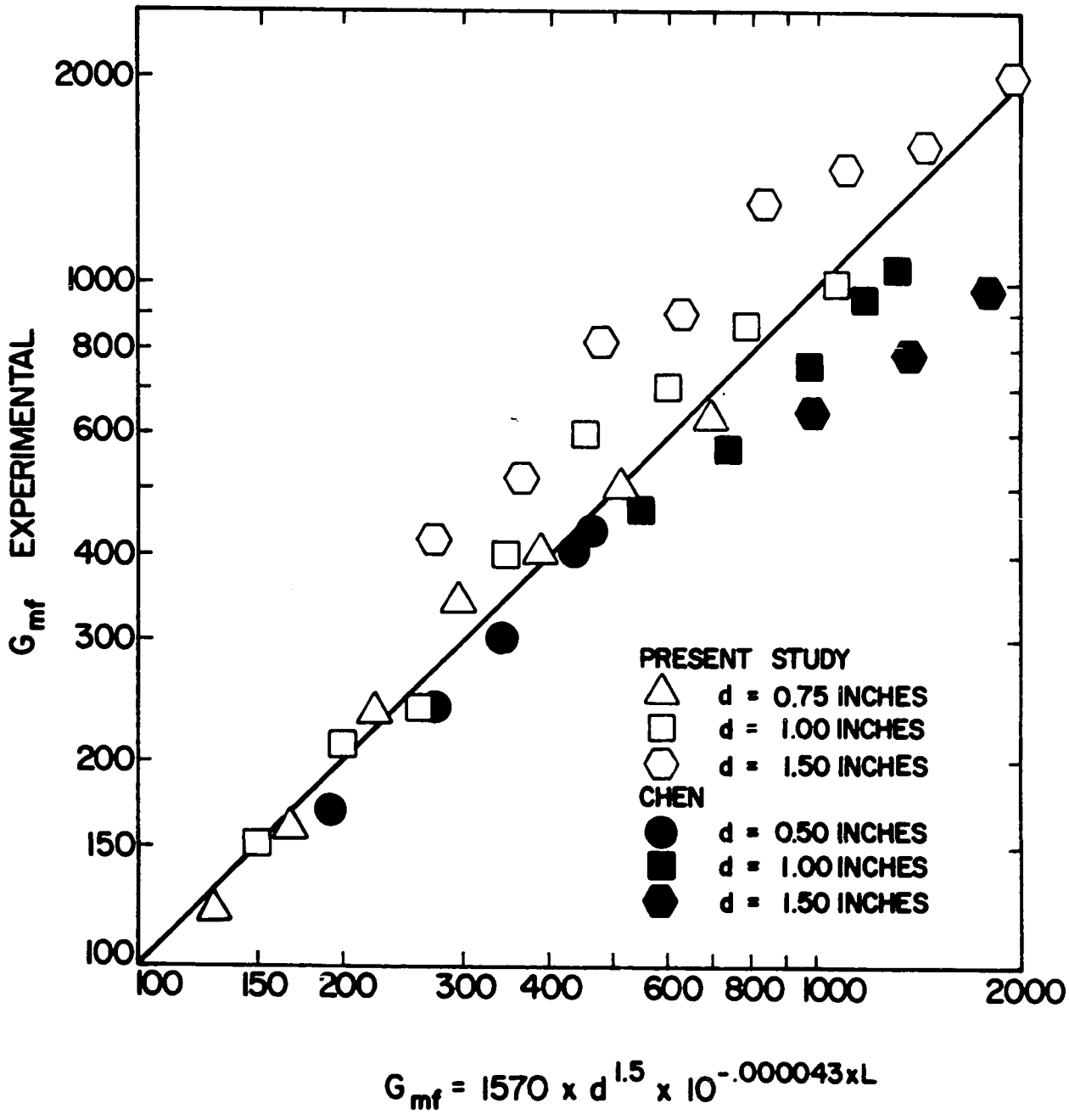

FIGURE 5.2: CORRELATION OF MINIMUM FLUIDIZATION VELOCITY FOR MOBILE BED OPERATION

judged to be sufficiently close to the experimental data that this correlation could be used where necessary for the evaluation of G_{mf} for 0.5-inch spheres.

As the column diameter in the present study was one-half that used by Chen, the new data for small packing are expected to be the closest to those of Chen. Thus the 0.75-inch packing of the present study corresponds to about the same ratio of d/d_t as the 1.5-inch packing of Chen. It may be seen from Figure 5.2 that the results for 0.75-inch spheres are indistinguishable from Chen's results, while those for 1.5-inch spheres diverge significantly. This behaviour provides strong indication of the presence of wall effect even for the relatively stationary condition at incipient fluidization.

5.1.2 Bed Expansion in Mobile-Bed Contacting

In the correlation of results for holdup, mixing, mass transfer and interfacial area it is essential to know the true height of the bed. As it is evident that bed height is also one of the important variables in design, a correlation was sought for the data obtained on bed expansion.

As bed height was found by Chen and again in the present study (Section 5.1.1) to increase linearly with the gas flow rate, the following statements may be made:

$$H \propto G$$

$$\text{For } G \leq G_{mf}, \quad H = h_s \tag{5.2}$$

$$\text{For } G > G_{mf}, \quad H = m(G - G_{mf}) + h_s$$

where m is an insensitive function of liquid flow rate and of packing diameter. For $G > G_{mf}$ the relation may be written in terms of dimensionless variables as,

$$\frac{H - h_s}{h_s} = \left(\frac{m\, G_{mf}}{h_s}\right) \frac{G - G_{mf}}{G_{mf}} \tag{5.3}$$

Neither liquid flow rate nor packing diameter appear explicitly in these correlations, but G_{mf} is of course a strong function of both.

Multiple regression analysis of the bed-expansion data for the correlation form

$$h = M \cdot \Delta^{n_1} \cdot G_{mf}^{n_2} \tag{5.4}$$

yields the following values for the parameters:

d , inch	M	n_1	n_2
0.75	7×10^{-5}	1.116	1.27
1.0	25×10^{-5}	1.0	1.16
1.5	1.1×10^{-5}	1.085	1.545

However, it is questionable whether the data justify allowing such extensive variation of parameters with packing size. A simpler, yet satisfactory correlation for dimensionless bed expansion, h, is

$$h = M \cdot \Delta \cdot G_{mf}^{1.2} \qquad (5.5)$$

where $M = 1.5 \times 10^{-4}$ for d = 0.75, 1.0 and 1.5-in.

and $M = 3.5 \times 10^{-4}$ for d = 0.5-inch

G_{mf} is given by Equation (5.1).

Figure 5.3 shows the fit of experimental data with this correlation. It is strikingly evident that bed expansion for 0.5-in. spheres differs from those for the larger sizes not only in absolute magnitude, but also because of the excessively large scatter. This difference in behaviour for the smallest packing is quite evident when observing the operation of mobile beds. The 0.5-in. spheres tended to agglomerate and to stick to the column walls. These features are presumed to result from the same underlying phenomena. Visually, the observed behaviour is as if there is an electrostatic buildup which attracts the balls to the wall and into clumps within the bed, but this possibility was discounted because the liquid phase is tap water. It is believed that the tendency to agglomerate and stick to the walls results when the surface tension forces

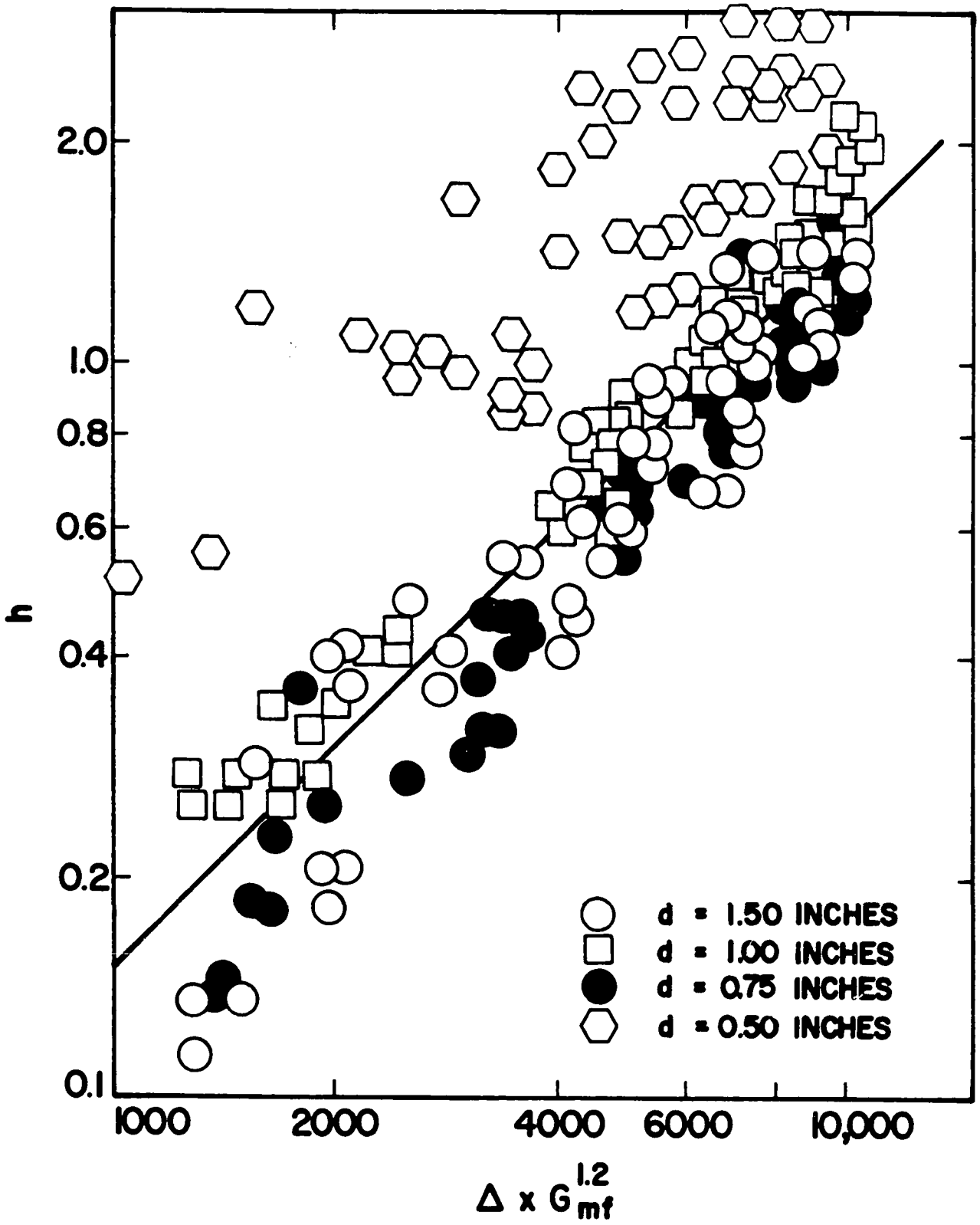

FIGURE 5.3: CORRELATION OF BED EXPANSION OF MOBILE BED CONTACTOR

in the packing-water-packing regions of contact become comparable to the weight of the sphere. Spheres only 0.5-in. diameter, of density 0.15 gm/cc, weigh only 1.29 gm. This tendency to stick together and to the column walls became much less pronounced at higher liquid flow rates. The additional liquid loading on each ball at higher liquid rates would reduce the relative importance of surface tension forces at all liquid-solid interfaces. The packing of large dimensions neither displayed this phenomenon nor gave larger than normal scatter in bed expansion, as may be seen from Figure 5.3. It is for this reason that the results for 0.5-in. packing are excluded from the general correlation given above. It is apparent from the scatter of the 0.5-in. data that the constant given for the correlating Equation (5.5) for this packing can indicate nothing more than an order-of-magnitude value of bed expansion.

The correlation for the data of the present study is compared on Figure 5.4 with the data of both Chen (25) and Blyakher et al. (150). Chen presented no correlation of his extensive observations of bed height; a straight line has been drawn through his data for the ease of comparison with the present correlation. The correlation of Chen's data is lower by 30 to 40% than that obtained in the present study. However, a comparison of Figures 5.3 and 5.4 indicates that the scatter of each set of data around the corresponding correlation (excluding the data of the present study for 0.5-in. packing)

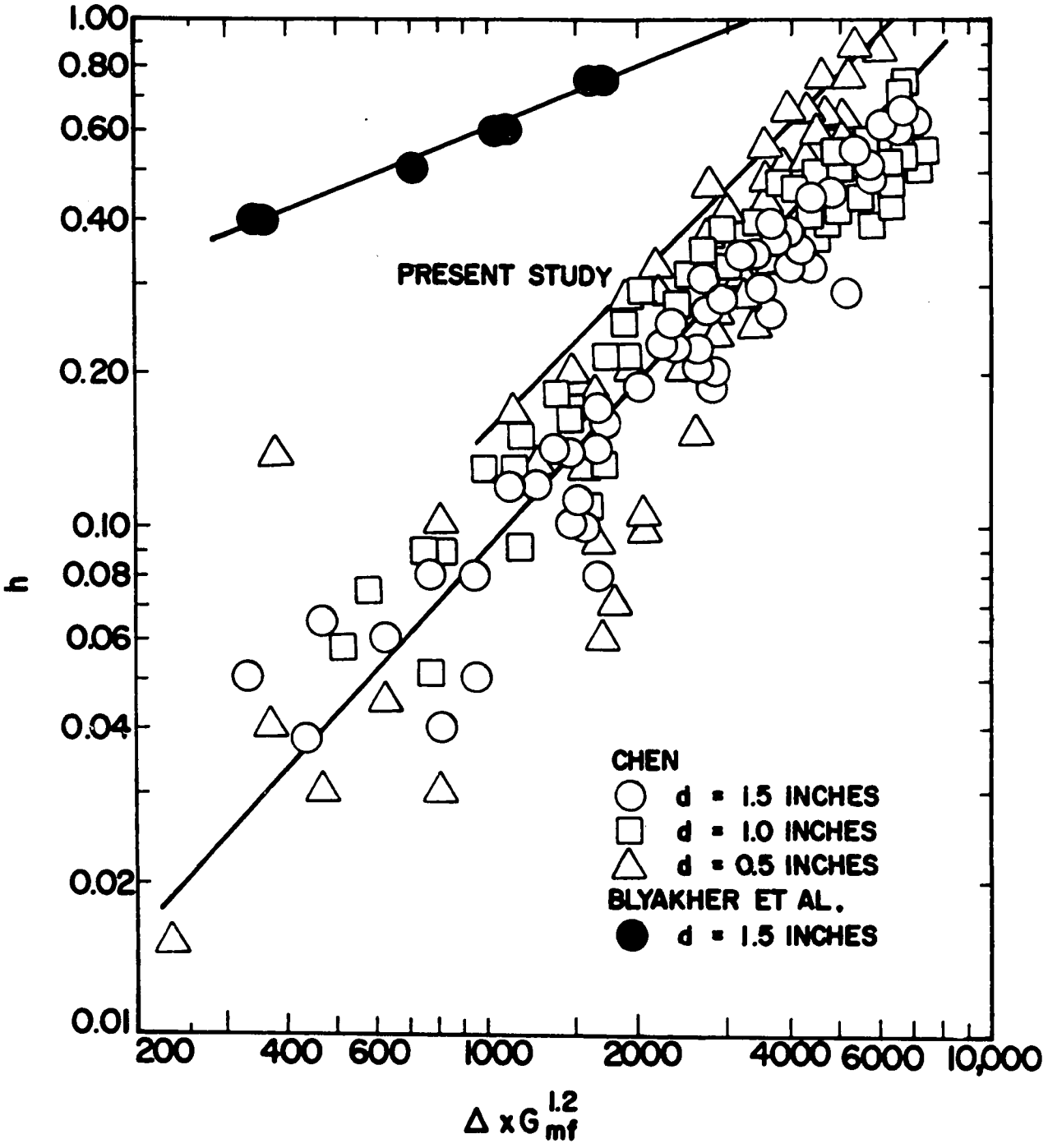

FIGURE 5.4: COMPARISON OF THE LITERATURE DATA ON BED EXPANSION OF MOBILE BED CONTACTOR AND THE PRESENT STUDY

is in fact somewhat greater than the difference between the correlations. In spite of the considerable degree of overlap for the data from the two studies, the fact that the correlation of Chen's data is appreciably lower may at least in part be due to the use of a different criterion in the measurement of bed expansion. The problem is complicated because of the fact that bed height is far from uniform across the cross-section at any instant, and it fluctuates between maximum and minimum heights. The height reported is the average of the maxima in bed height, time averaged over 5 minutes of observation. In fact, a pointer mounted on the side of the column was adjusted to correspond to average height of the top of the fluctuating bed across the entire cross-section. The height of the pointer recorded was based on 5 minutes of observation at steady-state conditions. Chen (25) notes that he averaged the bed height over a period of not less than 30 seconds. As both criteria are subjective and the fluctuation of bed height is quite large, appreciable differences between observers may be expected. Use of a quantitative criterion based on statistical fluctuations in true bed height would be preferable, but such must be based on some instrumental method of determining height of the mobile bed, as the visual method is inadequate.

The only other published data for bed expansion for the three-phase mobile-bed type of operation are those of Blyakher et al. (150). They correlated their data in the alternate form

$$\frac{H}{h_s} = 1.17 + A\,(G - G_{mf})^{1.25} \qquad (5.6)$$

in which A is a coefficient which is dependent upon the liquid loading. However, the main interest in their work is not the alternate form of correlation, but the fact that their results, expressed as dimensionless bed expansion, h, are larger by a factor of from 3 to 15 than the results of Chen or of the present study. This difference appears to be due to differences in the criteria used for bed height, large differences in the grid which supports the bed, and packing density.

The criterion probably used by Blyakher et al. is the maximum height attained at any point in the cross-section over a significantly long period of observation. If so, this criterion would correspond to decidedly higher values of bed expansion than that used for either of the other two studies. Also, there is some doubt about the packing used. They reported having used two densities of packing, 0.09 and 0.18 gm/cc, but have failed to indicate which density applies for their bed expansion observations.

Another important variable affecting bed expansion is the opening in the grid which supports the bed. In the case of Blyakher et al. the free area of the combined support and gas-distributing grids for the four different arrangements they used was 19, 30, 41 and 90%. Their upper grid had, in all cases, 90% free area. Unfortunately, it is not clear which

bottom grid was used when the bed expansion data were recorded. Based on the total open area, the linear gas velocity through the grids of Blyakher would be approximately 3.7, 2.3, 1.7, and 0.78 times that from our grid, (70% free area). Linear gas velocities, larger by such amounts, would produce significantly higher bed heights.

Chen used a supporting grid of thin wire of unspecified mesh size. However, the wire diameter of the grid was less than 0.5-mm. The free area of his grid could have been higher than the 70% which applies in the present study. The influence of reduced linear gas velocity from a grid with higher free area on the operating characteristics of MBC cannot be estimated quantitatively. But it could be a significant reason for the lower bed heights obtained by Chen.

Chen made no mention of any agglomeration or sticking behaviour for his experiments with 0.5-in. packing. The fact that there is no abnormal scatter in his bed expansion data further confirms the absence of this problem in his study. The ratio of wall surface area to bed volume for Chen's 12-in. column is slightly less than half that of the 5.5-in. column of the present study. The lower ratio of wall area to bed volume for the larger column greatly reduces the relative effect of a few balls adhering to the wall. In the 5.5-in. column by contrast, the same percentage of wall area covered by balls makes a larger reduction in column cross-section, hence causes larger fluid mass velocities in the remaining cross-section, which in

turn leads to abnormally high bed expansion.

The results for minimum fluidization velocity and for bed expansion clearly indicate the existence of two separate effects related to packing size. For the largest spheres (1.5-in.) used in the present study, for which the ratio d_t/d is only 3.7/1, it appears that the results for minimum fluidization velocity are affected by the "wall effect" as it has been understood in work on fixed-bed columns. On the other hand, the smallest spheres (0.5-in.) were not uniformly distributed in the column due to the tendency of these light weight spheres to stick to the walls of the column as well as to agglomerate into clumps of balls within the column. It will be appropriate therefore in each sub-study of the thesis to check for the presence of either or both of these effects. The results for minimum fluidization velocity and for bed expansion certainly indicate that results for any mobile-bed experiment with either 0.5 or 1.5-in. spheres in a 5.5-in. diameter column should be examined carefully for further evidence of these effects. Conversely, it appears that results of any experiment using 0.75 or 1.0-in. spheres in a 5.5-in. column may be effectively free of either effect. It is relevant in this connection to note that the 5.5-in. column was chosen to obtain high gas mass velocities with an available blower, and also because of the large consumption of chemicals for mass transfer studies in a larger unit.

5.1.3 Liquid Holdup

5.1.3.1 Liquid Holdup in Fixed Beds

As data and correlations are available for holdup in fixed beds, such data were obtained with the pulse testing technique of the present study as a test of the reliability of results prior to application of this technique to the mobile-bed contactor. Total liquid holdup was calculated from average residence time, τ, according to the relation

$$H_T = \frac{V}{\dot{V}} \cdot \tau \qquad (5.7)$$

The mean residence time was obtained from the concentration-time measurements using the transfer function analysis. Operating holdup was obtained using values of static holdup, H_S, according to the definition:

$$H_{op} = H_T - H_S \qquad (5.8)$$

The static holdup for beds of spheres required for Equation (5.8) was obtained from the work of Chen (25). The data for operating holdup determined in this way for fixed beds of spheres are compared on Figure 5.5 with Chen's data for spheres (25), Sater's data for rings and saddles (94), and with the generalized correlation of Otake (16). Although the values of liquid holdup shown on Figure 5.5 have been measured by a variety of techniques, rather good agreement exists between the different studies. With respect to the data from the present

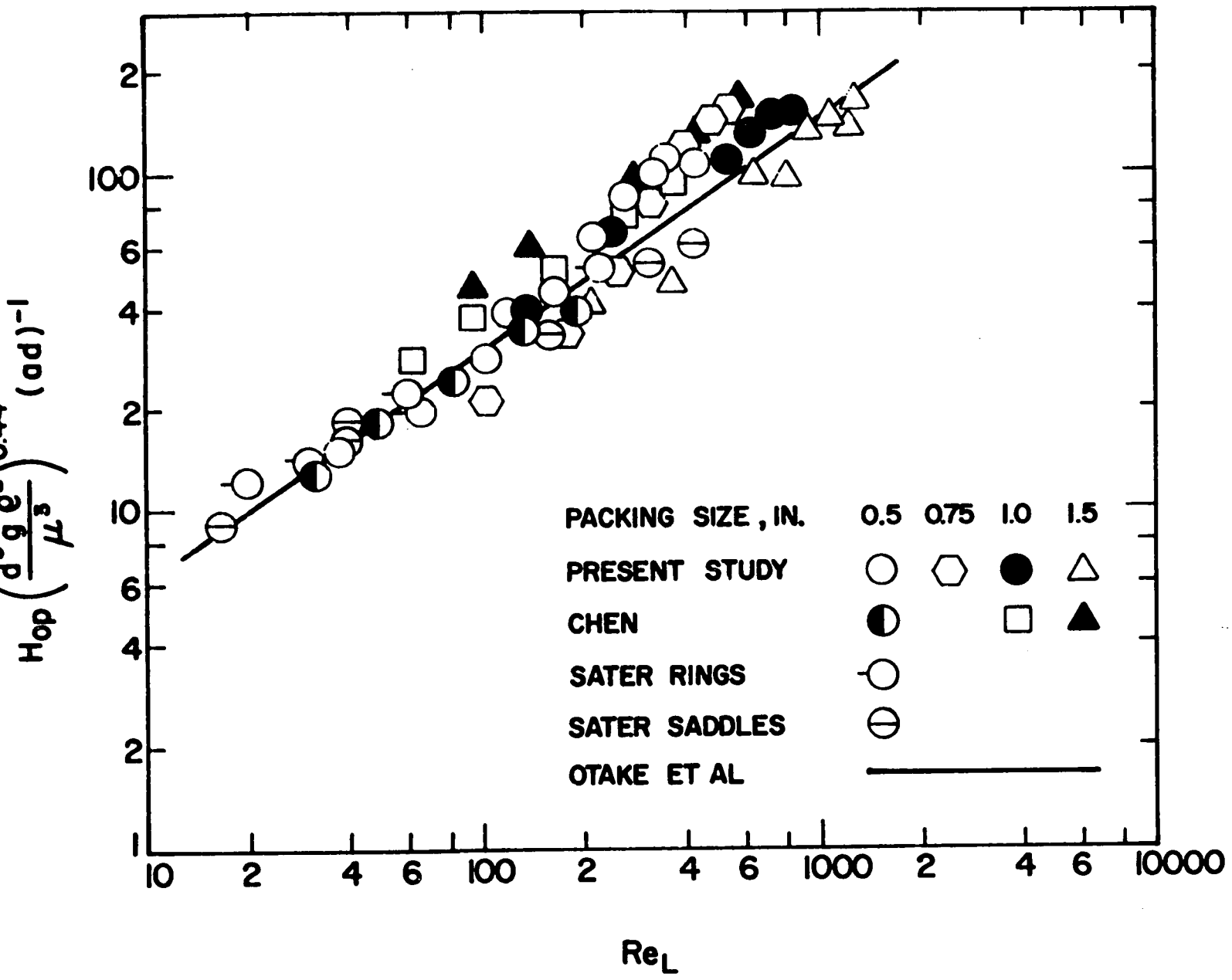

FIGURE 5.5: LIQUID HOLDUP IN PACKED BEDS

study, it is significant that there is no strong trend with respect to sphere diameter over the range 0.5 to 1.0 inches. In terms of Otake's correlation, the holdup for 1.5-in. spheres is in the order of 30% lower than for the smaller spheres. As the ratio d_t/d is only 3.7/1 for this packing, it would be surprising if holdup were not affected by the wall effect. It is interesting that this effect is in fact surprisingly small for packing which is quite large relative to the column diameter. However, as the basic objective is to study mobile beds, the main conclusion of the work with fixed beds is that the satisfactory agreement with the results of investigators who used different methods of determining holdup confirms the accuracy of the pulse testing technique as used in the present study.

5.1.3.2 Liquid Holdup in Mobile-Bed Contacting

Chen and Douglas (29) noted that in mobile-bed contacting the distinction between operating and total holdup disappears because there is in this case no static or ineffective holdup. Thus the results for holdup for MBC derive directly from Equation (5.7), the transfer function analysis of the concentration transients, and the volume of the bed, V, as determined from the correlation for bed expansion given as Equation (5.5). The designations "operating" and "total" that were used for holdup in fixed beds have been dropped in the

presentation of results in MBC. For the four packing sizes tested these results are given on the series of plots, Figure 5.6.

The new results for holdup may best be considered in detail for 1-in. packing because the results for bed expansion and minimum fluidization velocity indicate that in MBC, the hydrodynamics for 1-in. packing in a 5.5-in. column are not distorted by either of the effects which were observed for the largest and smallest spheres. While it appears that results with 0.75-in. spheres are also free from these effects, Chen obtained data for holdup in MBC for 1-in. but not for 0.75-in. spheres. Although Chen's results cover a more limited range of gas and liquid mass velocities, they provide a valuable reference for the extension made in the present study.

A central feature of the correlation for holdup in MBC by Chen and Douglas (29) is that holdup is independent of gas velocity. However, reference to the new data for 1-in. packing given on Figure 5.6 indicates a significant effect of gas velocity. The effect of liquid velocity is as before, i.e. holdup increases with increasing liquid rate. The overlap in conditions used by Chen occurs only for the lowest two of the seven values of liquid mass velocity from 6977 to 23813 lb./hr.-sq.ft., used in the present study. Although the representation by Chen and Douglas of their data for five

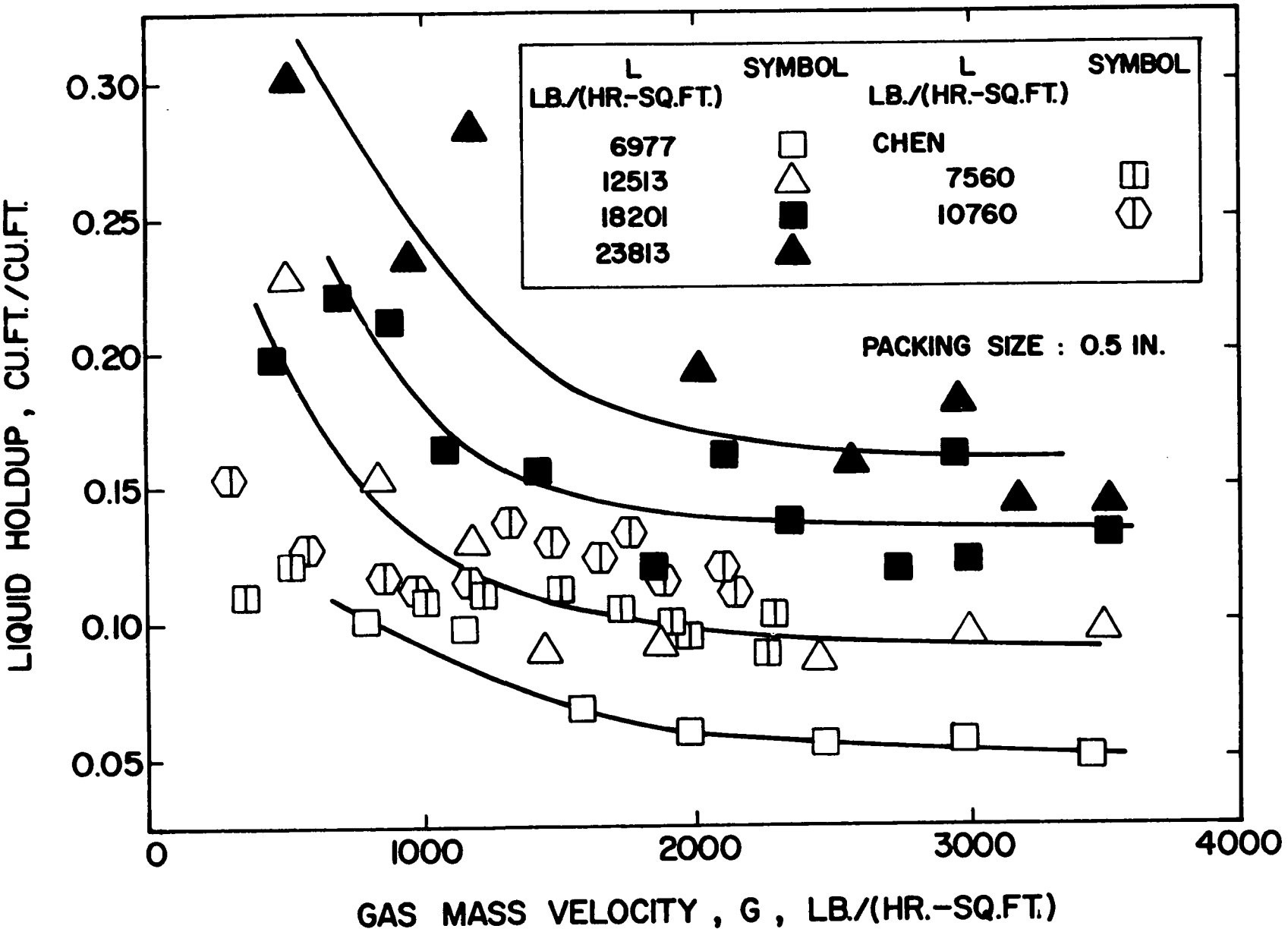

FIGURE 5.6(a): LIQUID HOLDUP IN MOBILE BED CONTACTORS
d = 0.5-inch

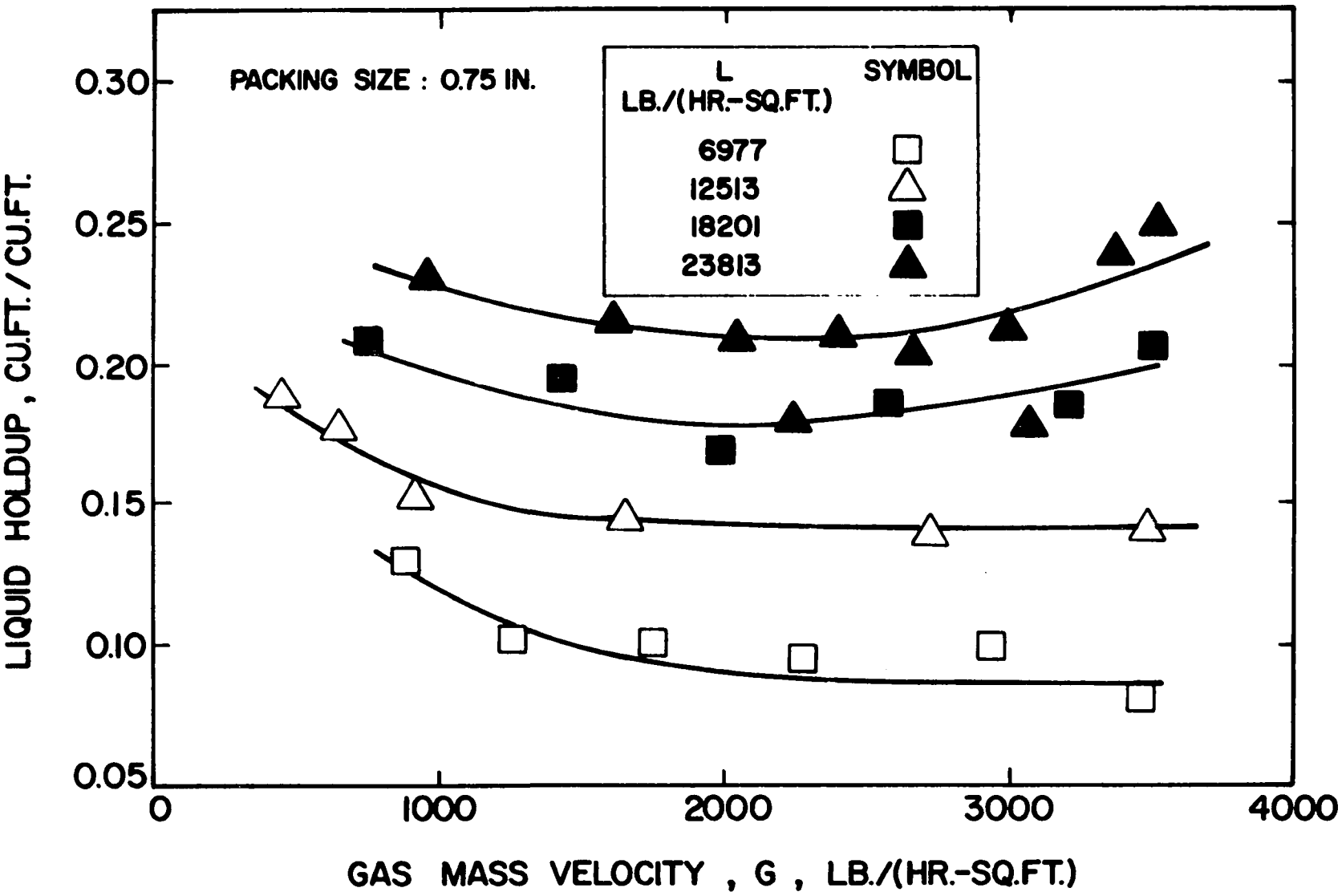

FIGURE 5.6(b): LIQUID HOLDUP IN MOBILE BED CONTACTORS
d = 0.75-inch

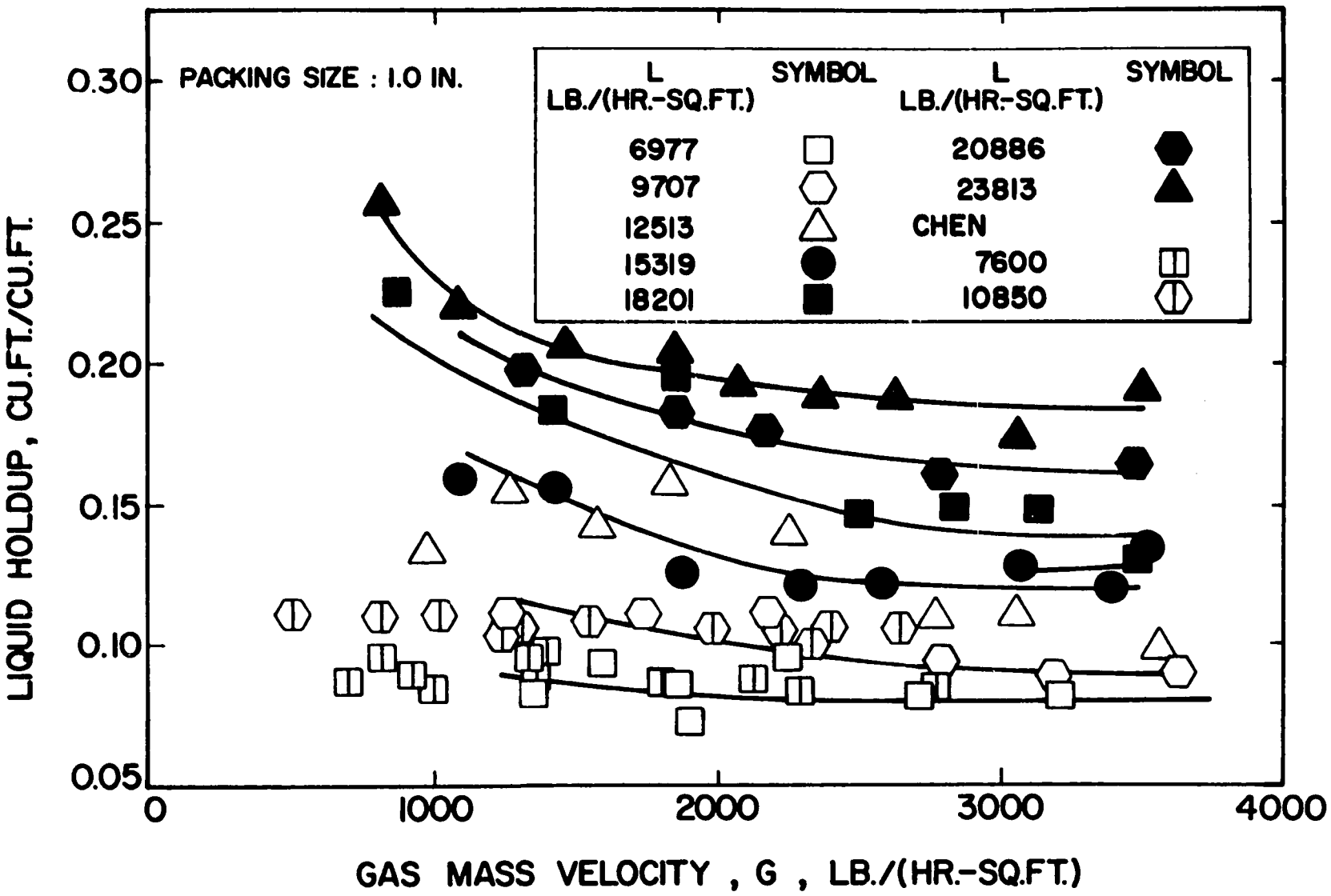

FIGURE 5.6(c): LIQUID HOLDUP IN MOBILE BED CONTACTORS
d = 1.0-inch

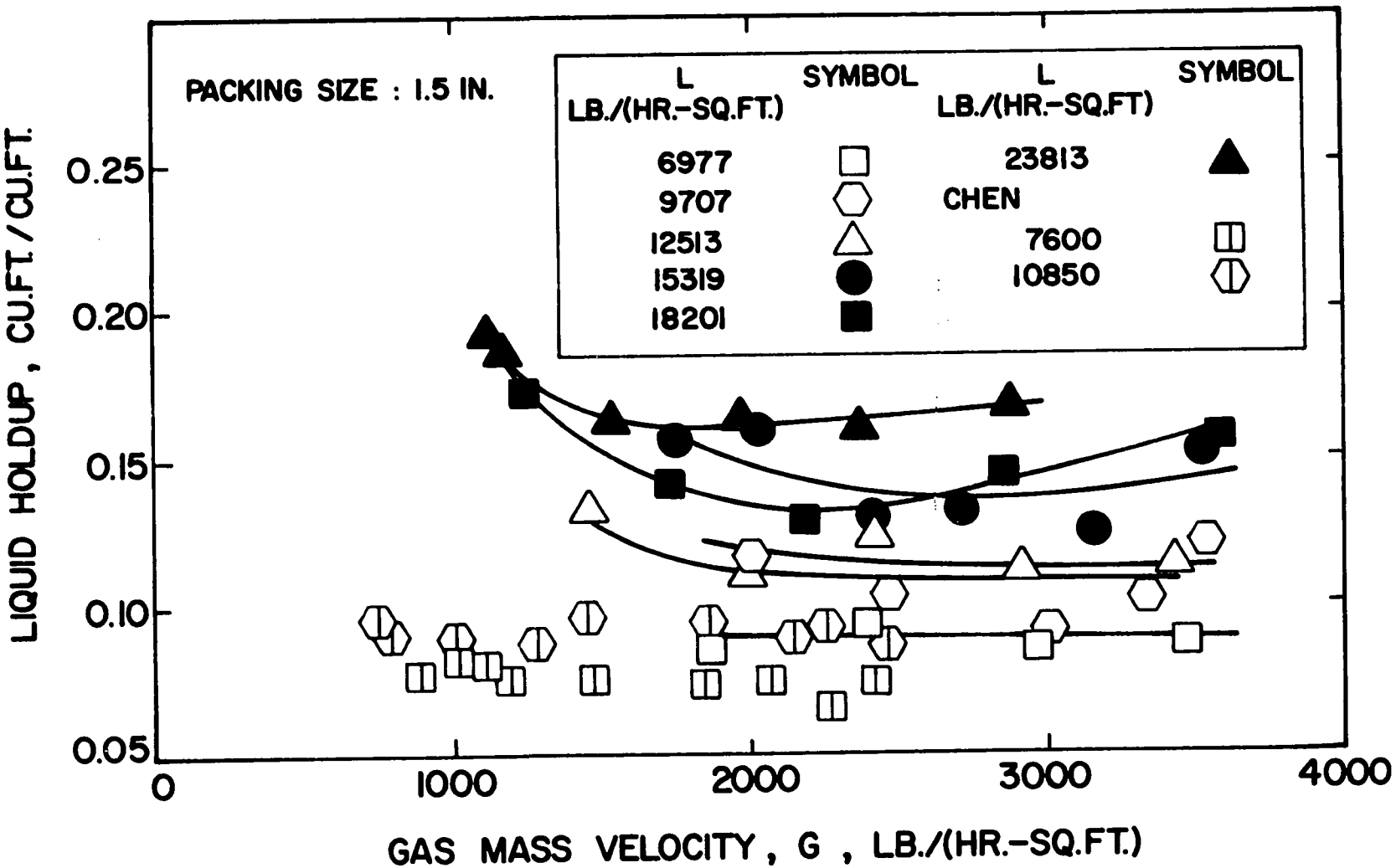

FIGURE 5.6(d): LIQUID HOLDUP IN MOBILE BED CONTACTORS
d = 1.5-inch

values of liquid rate over the range 1840 < L < 10850 as independent of gas velocity at values greater than G_{mf}. For the two lowest values of liquid rate in the present study, the moderate decrease of holdup with gas velocity is in fact not unlike that displayed by Chen's results. However, the new results at the higher liquid mass velocities which are of importance in industrial practice show clearly that holdup decreases with gas velocity at values above G_{mf}.

The same features displayed by the results for 1-in. spheres are seen also on the plot of results for 0.75-in. spheres. A new feature seen here, however, is that at the higher values of liquid velocity, the holdup passes through a shallow minimum at an intermediate value of gas velocity, then begins to increase again at higher values of gas velocity.

The results for the smallest and largest packing must now be examined critically for evidence of deviations with respect to holdup analogous to those noted in the previous sections. Because of the dependence of holdup on gas velocity, the data for 0.5-in. spheres may most conveniently be compared with that for 0.75 and 1-in. spheres by making comparison at constant values of gas velocity. At G = 2000 lb./hr.-sq.ft., for example, the liquid holdup for 0.5-in. spheres at every value of liquid velocity tested is about 3 to 4.5 volume percentage points less than for 0.75-in. spheres. Thus for L = 6977,

the volume fraction liquid holdup decreases from about 0.09 to 0.06 when the sphere diameter is reduced from 0.75 to 0.5-in. This decrease is anomalous, because the Chen and Douglas correlation for MBC shows holdup to be inversely proportional to $d^{0.5}$. It will be recalled that the bed expansion data of the present study for 0.5-in. spheres was anomalously high (Figure 5.3) due to the lack of uniform distribution of these beds. As the value for bed volume used to obtain liquid holdup on a volume fraction basis comes directly from the bed expansion data, poor performance with respect to bed expansion is reflected also in the data for holdup. Thus the holdup results for 0.5-in. spheres deviate from the predicted trend for packing diameter, and deviate in the direction expected as a result of the already noted problem of non-uniform distribution of 0.5-in. balls in the 5.5-in. column. The holdup data for 0.5-in. spheres must therefore be rejected as not indicative of holdup in a mobile-bed which has a satisfactorily uniform distribution of packing.

At the other extreme of packing size, i.e. for 1.5-in. spheres, the holdup data in the lower range of liquid velocities used appear to be affected by a wall effect. Again choosing G = 2000 lb./hr.-sq.ft. to make the comparison, the present results for L = 6977 and 9707 lb./hr.-sq.ft. indicate an increase of 1 to 1.5 percentage points in the volume percent liquid as one goes from 1 to 1.5-in. spheres. By contrast,

according to the previously observed inverse dependence of holdup with $d^{0.5}$, the holdup would be expected to decrease by about 1.5 points in volume percent. These significantly higher than expected values of holdup are believed to derive from a wall effect associated with a value of $d_t/d = 3.7$. Interestingly enough this effect on the results for holdup disappears for the higher range of liquid velocities. Thus at L = 12513 lb./hr.-sq.ft., and G = 2000, the holdup for d = 1.5-in. is no longer higher then at d = 1-in., but is essentially unchanged. At the highest values of liquid rate tested, i.e. L = 18201 and 23813 lb./hr.-sq.ft., and for G = 2000, the holdup continuously decreases as packing diameter increased from 0.75 to 1.0 to 1.5-in., in reasonable accord with the $d^{-0.5}$ dependence. Thus for 1.5-in. spheres there appears to be an appreciable wall effect which increases holdup when the bed is only moderately expanded from the fixed-bed condition. This wall effect however gradually decreases at very high liquid mass velocities which correspond to a greatly agitated mobile-bed type operation. At the condition of highly agitated bed, the movement of packing could be expected to be less influenced by the presence of the column wall.

Returning to the question of the reliability of the data for 0.75-in. packing it is significant that the change in holdup between 0.75 and 1.0-in. spheres is in all cases in general accord with the inverse $d^{0.5}$ dependence of the Chen and Douglas correlation.

Due to the complex relations apparent between the variables holdup, bed expansion, packing size, and gas and liquid mass velocities, no general correlation is offered at this time. However, the new data point out that the holdup correlation of Chen and Douglas (29) must not be used for liquid velocities outside the range for which it was derived. With respect to the new holdup data, it is believed that all of the results with 0.75 and 1.0-in. packing, some of the results with 1.5-in. packing, and none of the results for 0.5-in. packing may be taken as indicative of holdup in mobile-beds which are not significantly affected by problems of uniform distribution or wall effects.

5.1.4 Liquid Mixing

The applicability of transfer function analysis to the study of axial mixing is examined first, then the results for liquid mixing in fixed beds and in mobile-bed contacting are discussed.

5.1.4.1 Evaluation of Peclet Number and Mean Residence Time

The transfer function analysis used to compute Peclet number and mean residence time of liquid in the MBC also provides a test of the applicability of the diffusion model for liquid mixing in MBC. The concentration-time data for both inlet and outlet tracer pulses are used to evaluate the transfer function from Equation (3.7) for arbitrary values of parameter s. The ordinate and abscissa values for Equation

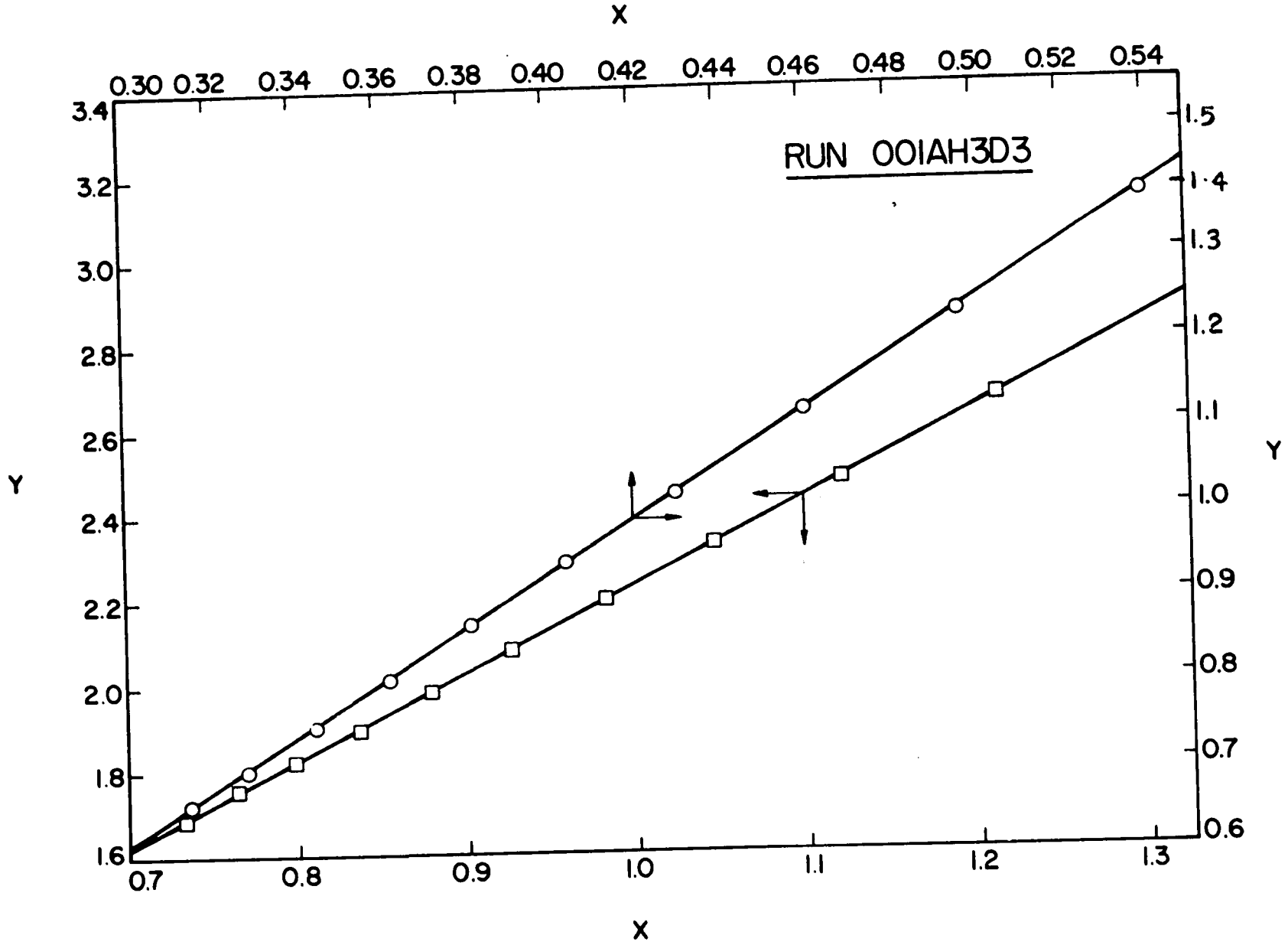

FIGURE 5.7: EVALUATION OF PECLET NUMBER USING TRANSFER FUNCTION ANALYSIS

(3.8) are evaluated from

$$Y = \frac{1}{\ell n\ (1/F(s))} \qquad (5.9)$$

and

$$X = \frac{1}{(\ell n(1/F(s)))^2}$$

for a number of arbitrarily chosen values of s. A least squares straight line was used to extract mean residence time and Peclet number from the slope and intercept of the line corresponding to Equation (3.8). A typical case for two sets of values of s is shown in Figure 5.7. The fact that the relationship between X and Y is in fact linear confirms the hypothesis that liquid mixing in MBC may be represented adequately by the diffusion model with infinite-bed boundary conditions.

Since the breakthrough curves in the present study did not show significant tailing,the magnitude of the correction for finite-bed conditions was not very significant and depended on the value of mixing parameter Pe. Maximum correction to the values of Pe for the infinite-bed correction was less than 5%. It should,however, be appreciated that the magnitude of the correction could be large for a system exhibiting high degree of mixing. Detailed computer programs and information flow charts to carry out the calculations for Peclet number and mean residence time are included in Appendices II.2 and V.

The values of Peclet number and mean residence time were corrected as outlined in Section 3.1.2. Detailed computer programs and information flow charts to carry out the calculations

for Peclet number and mean residence time are included in Appendix 11.2.

5.1.4.2 Liquid Mixing in Packed Beds

The results for liquid mixing in the trickle-bed type operation were compared in order to establish the reliability of the pulse testing technique used in the present study.

Earlier Chen (25) and Harrison et al. (110) studied liquid mixing in trickle-bed operation with packed beds of spheres using the transient response technique. The variables studied by Chen were essentially the same as in the present study; his results were correlated as

$$Pe_o = 0.07\ (Re_L)^{0.583}\ (Ga)^{-0.081} \qquad (5.10)$$

Multiple regression analysis between these dimensionless numbers and the combined data of Chen and the present study gave the following correlation for liquid mixing in trickle-bed operation through beds of spheres:

$$Pe_o = 1.06\ (Re_L)^{0.41}\ (Ga)^{-0.095} \qquad (5.11)$$

Representation of these data on Figure 5.8 indicates a reasonably good fit for correlation in this form.

The effect of packing size is of particular interest. In this connection it is to be noted that there is relatively little spread in the data of the present study for 0.5, 0.75 and 1.0-in. spheres, and within the experimental scatter there is no systematic trend with respect to packing size. As may readily be obtained from equation (5.11), the Peclet number for trickle-bed operation at constant liquid flow rate increases proportional to $d^{0.125}$.

One can visualize this increase of Peclet number with packing diameter as occurring due to the less tortuous path taken by the liquid for the larger packing. The more

direct the fluid flow path, the lower the axial dispersion coefficient, the narrower the RTD, and the closer the approach to plug flow conditions. However, it may be seen from Figure 5.8 that the values of Peclet number for 1.5-in. spheres are distinctly lower than the measurements of the present study for all smaller packing sizes. The occurrence of disproportionately high values of effective axial dispersion coefficients for 1.5-in. spheres is believed to result from channelling and/or excessive wall flow of liquid. This behaviour provides evidence of a significant wall effect for the case of 1.5-in. spheres in a 5.5-in. column, evidence in addition to that already noted from measurements of liquid holdup for both fixed and mobile-bed operation, and for minimum fluidization velocity in MBC. The data for 1.5-in. spheres has been included on Figure 5.8, but it should be remembered that these data are strongly influenced by the wall effect present for the case of $d_t/d = 3.7$.

The results of the present study for liquid mixing in trickle-bed operation may be compared with the results of others, although most of the other data available are for packed beds of raschig rings. The data of Khanna (13) for 0.5, 1.0 and 1.5-inch ceramic raschig rings in a 12-in. diameter column, Harrison et al. (110) for 1.5-in. spheres, Kramers and Alberda (95) for 10-mm. raschig rings and the present data were found to correlate by the generalized equation:

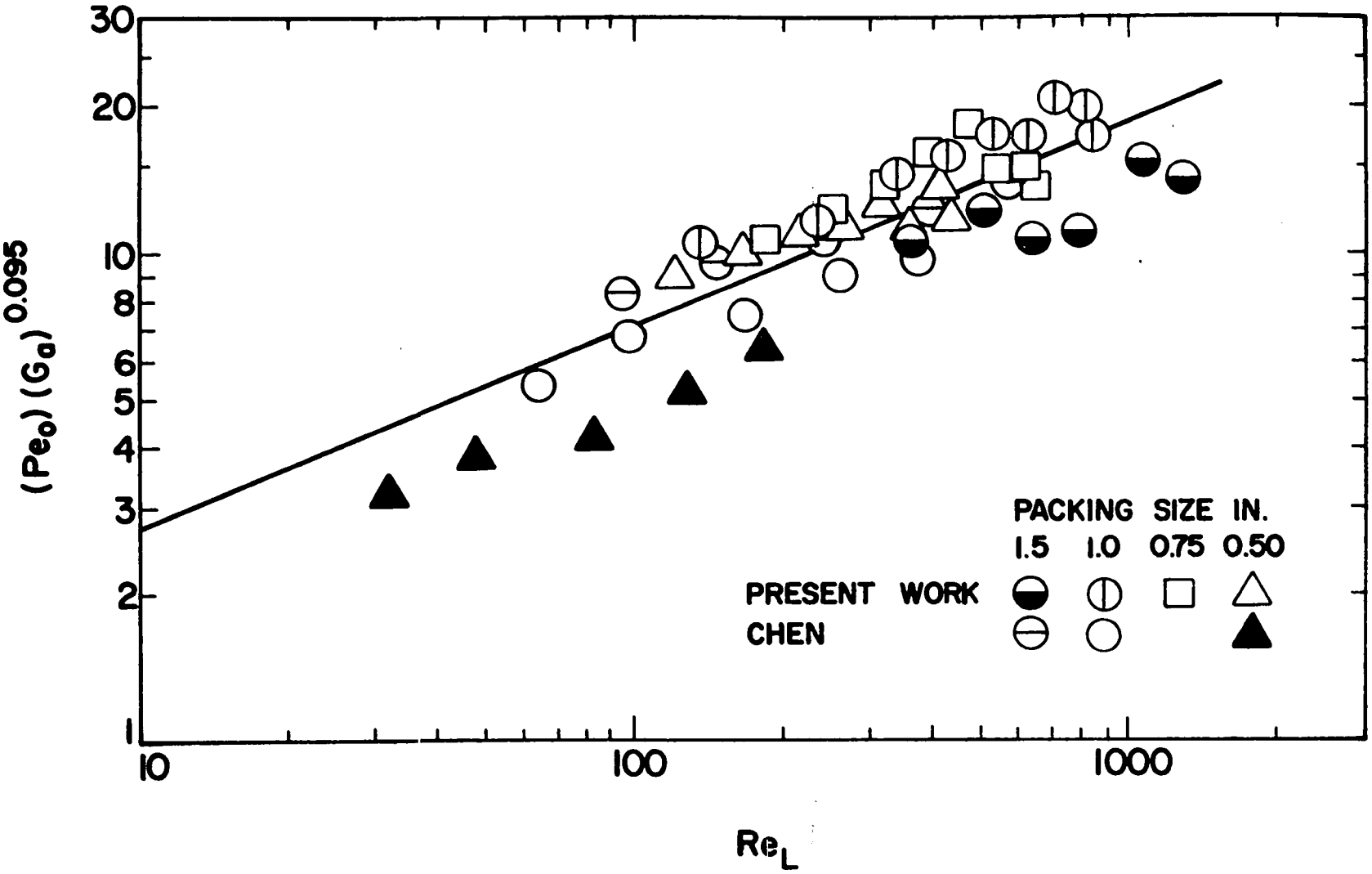

FIGURE 5.8: CORRELATION OF AXIAL MIXING FOR LIQUIDS IN TRICKLE-BED OPERATION THROUGH BEDS OF SPHERES

$$Pe_o = 1.635\ (Re_L)^{0.41}\ (Ga)^{-0.095}\ (ad)^{-0.41} \quad (5.12)$$

This correlation is essentially the same as Equation (5.11) with the additional parameter 'ad' to account for the shape of the packing. Figure 5.9 illustrates the fit of data to the proposed correlation. Although the data for 1.5-in. spheres from the present study has been included on both Figures 5.8 and 5.9, it should be remembered that these data are significant only in showing the extent of the wall effect on axial mixing for the case of $d_t/d = 3.7$. For the purpose of the present study, however, favorable comparison of the new data obtained with the pulse testing technique with results obtained by a variety of other methods for the trickle-bed operation provided further support for the use of this method to evaluate mixing in MBC.

5.1.4.3 Liquid Mixing in Mobile-Bed Contacting

Axial mixing in MBC occurs as a result of the same basic flow phenomena encountered in packed or trickle-bed operation, but with an additional contribution due to the interaction between the phases and the packing which in this case is generally in a state of vigorous motion. The following dimensionless numbers have been identified (16,112) as important in describing liquid mixing for gas-liquid flow through packed beds: Peclet number, Reynolds number of the gas and the liquid phase, Gallileo number and the diameter ratio

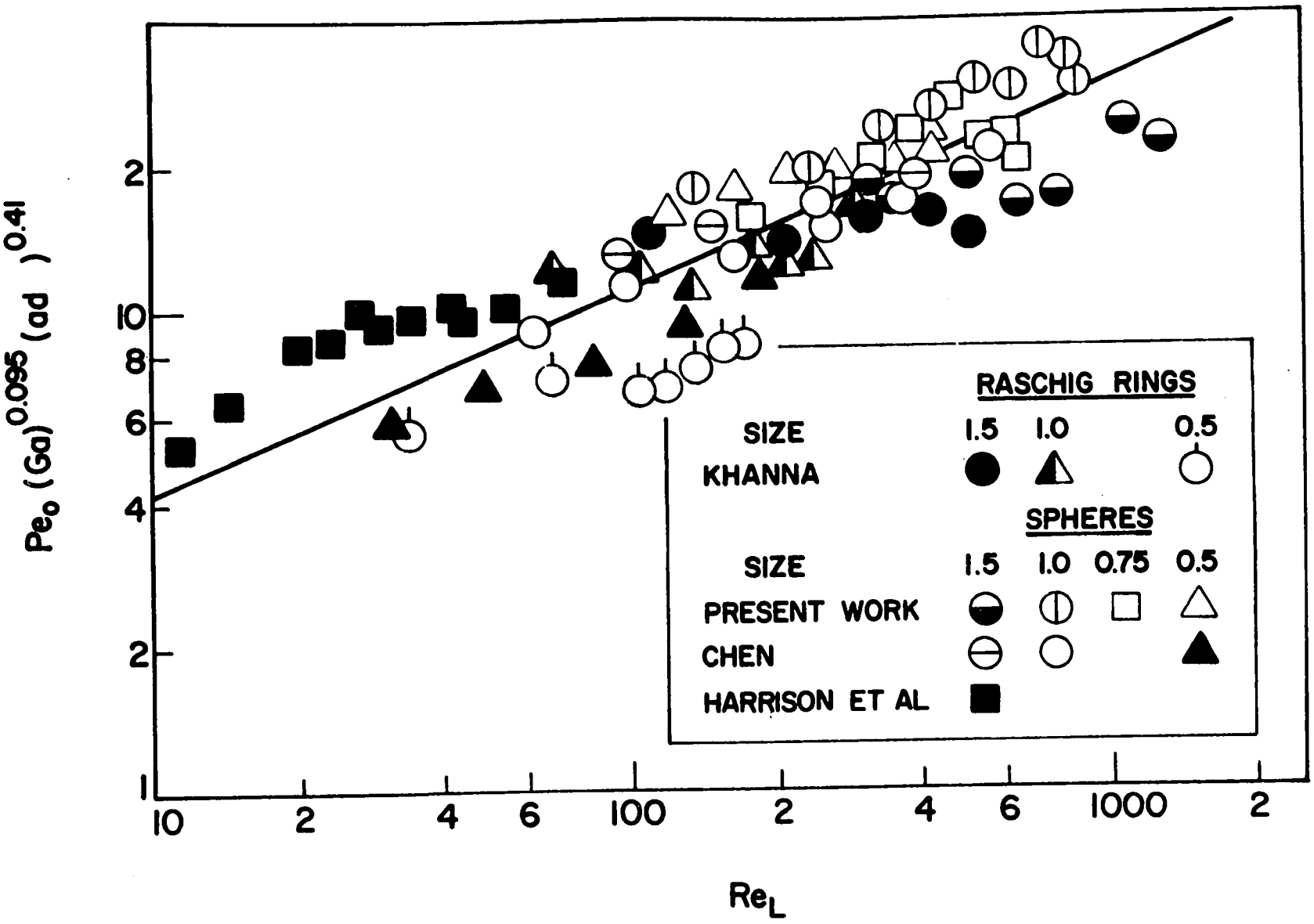

FIGURE 5.9: GENERALIZED CORRELATION OF AXIAL MIXING DATA FOR LIQUIDS IN TRICKLE-BED OPERATION

d_t/d. The liquid mixing characteristics may therefore be represented by a functional relationship between

$$Pe,\ Re_L,\ Re_G,\ Ga \text{ and } d_t/d.$$

Fox fixed beds, it has been shown (95) that the flow of gas, below loading point, does not influence mixing of the liquid phase. The gas phase Reynolds number has therefore been omitted for the case of fixed beds. Otake and Kunugita (16) investigated the effect of aspect ratios, d_t/d and H/d_t, and concluded that the influence of d_t/d between 4.3 - 6.9 and H/d_t from 14 to 24.2 on liquid mixing was not significant and proposed a correlation of the form:

$$Pe_o = 1.895\ (Re_L)^{0.5}\ (Ga)^{-0.333} \qquad (2.24)$$

Thus, for packed beds one can write,

$$Pe_o = A_1\ (Re_L)^B\ \ (Ga)^C \qquad (5.13)$$

As mobile-bed contacting may be viewed as an extension of the fixed-bed system, it may be assumed that a similar functional relationship between these dimensionless variables would apply for MBC, plus an additional parameter for the effect of gas flow. Thus, for MBC,

$$Pe = A_2\ (Re_L)^B\ \ (Ga)^C\ f(G) \qquad (5.14)$$

On dividing equations (5.14) by (5.13), one gets

$$\frac{Pe}{Pe_o} = f(G) \qquad (5.15)$$

Chen and Douglas (115) successfully used this approach in correlating their data for axial mixing of the liquid phase in mobile-bed contacting. The function f(G) was taken as the stirring number, $\Delta = \dfrac{G - G_{mf}}{G_{mf}}$.

The stirring number is the dimensionless gas flow rate above that required for incipient fluidization. It was thought that this is the gas flow variable which best represents the effects on mixing in MBC. On the basis of their successful use of this model, the same approach was used for the present study which extends considerably the range of flow rates for the MBC operation.

The results are presented in terms of both Pe, and the ratio Pe/Pe_o, on Figures 5.10 and 5.11, respectively. As the stirring number increases, the rapid increase in liquid mixing as reflected by the corresponding sharp decrease in Peclet number on Figure 5.10 is a consequence of the increased turbulent mixing in the contactor. This measured effect concurs with that anticipated from visual observation of MBC operation.

The effect of motion of the packing for the case of MBC is to give greater mixing than for a fixed-bed contactor. Thus, in the representation of results given on Figure 5.11, the data in general lie in the region $Pe/Pe_o < 1$.

The effect of packing size was of particular interest in discussion of results for trickle-bed operation, and is so again for the mobile-bed case. Referring to Figures 5.10 and 5.11, it can be seen that the results, with few exceptions, fall in the following ranges:

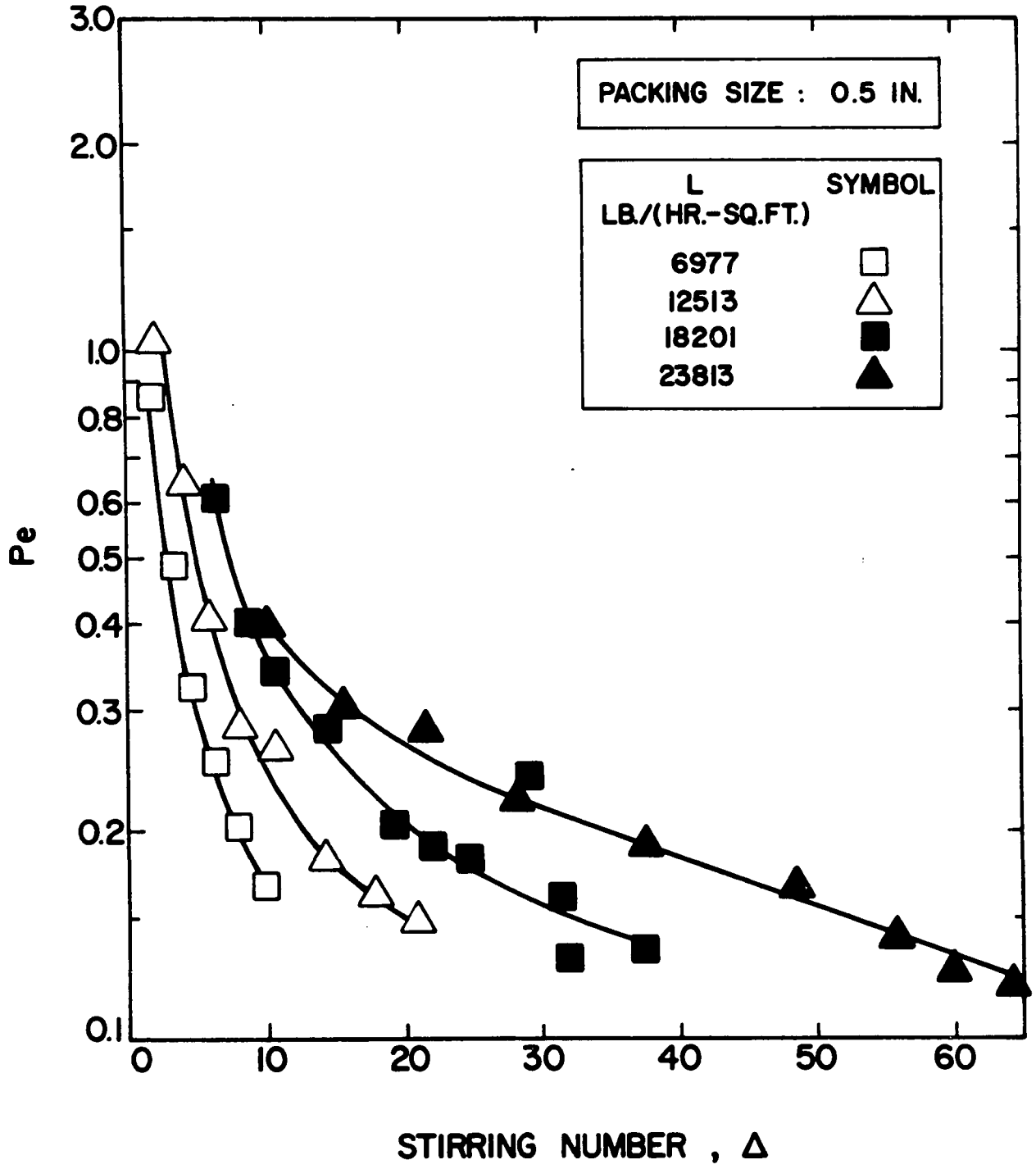

FIGURE 5.10(a): VARIATION OF LIQUID-PHASE PECLET NUMBER WITH LIQUID FLOW RATE AND PACKING SIZE FOR MOBILE-BED CONTACTING, d = 0.5-inch

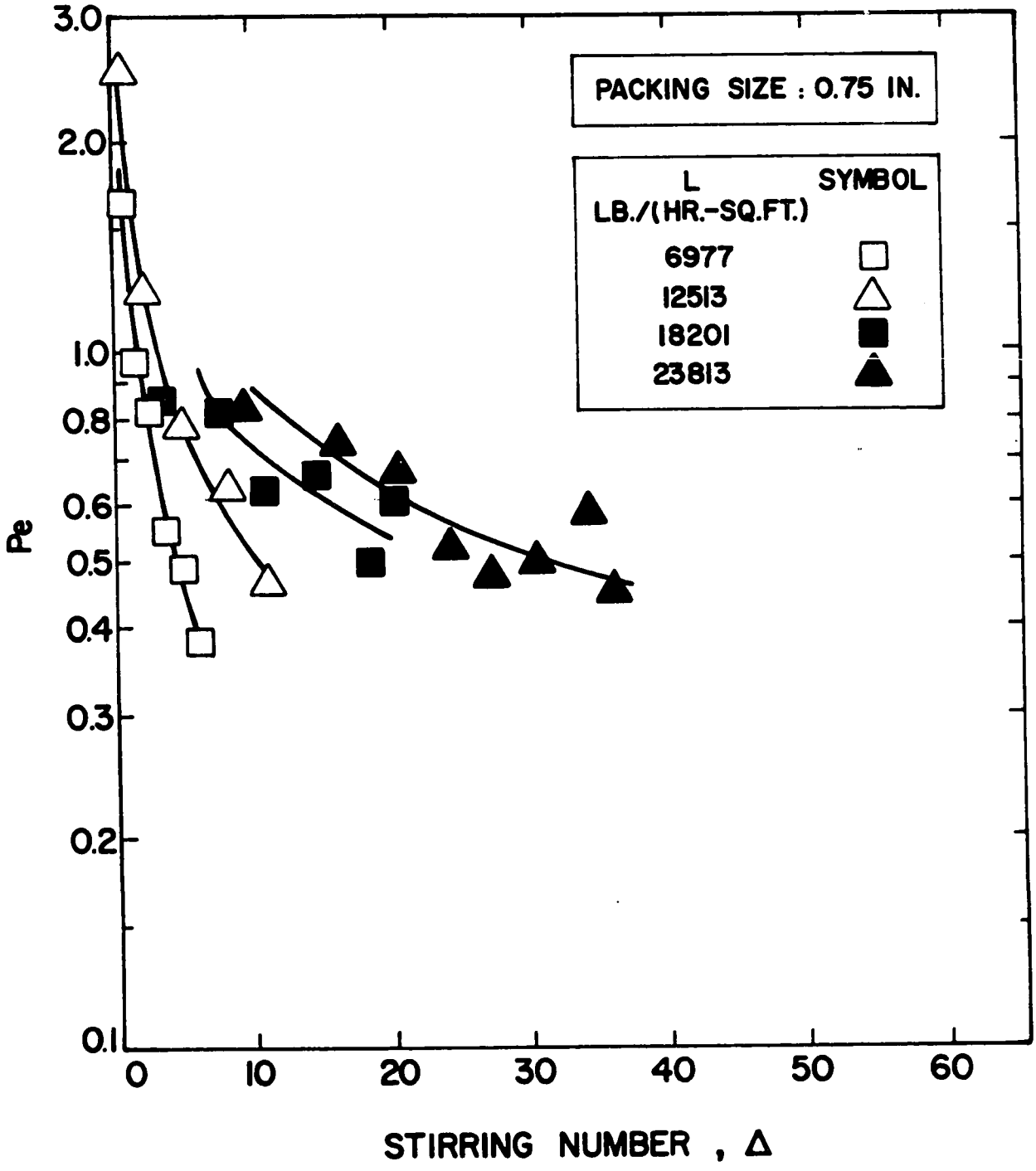

FIGURE 5.10(b): VARIATION OF LIQUID-PHASE PECLET NUMBER WITH LIQUID FLOW RATE AND PACKING SIZE FOR MOBILE-BED CONTACTING, d = 0.75-inch

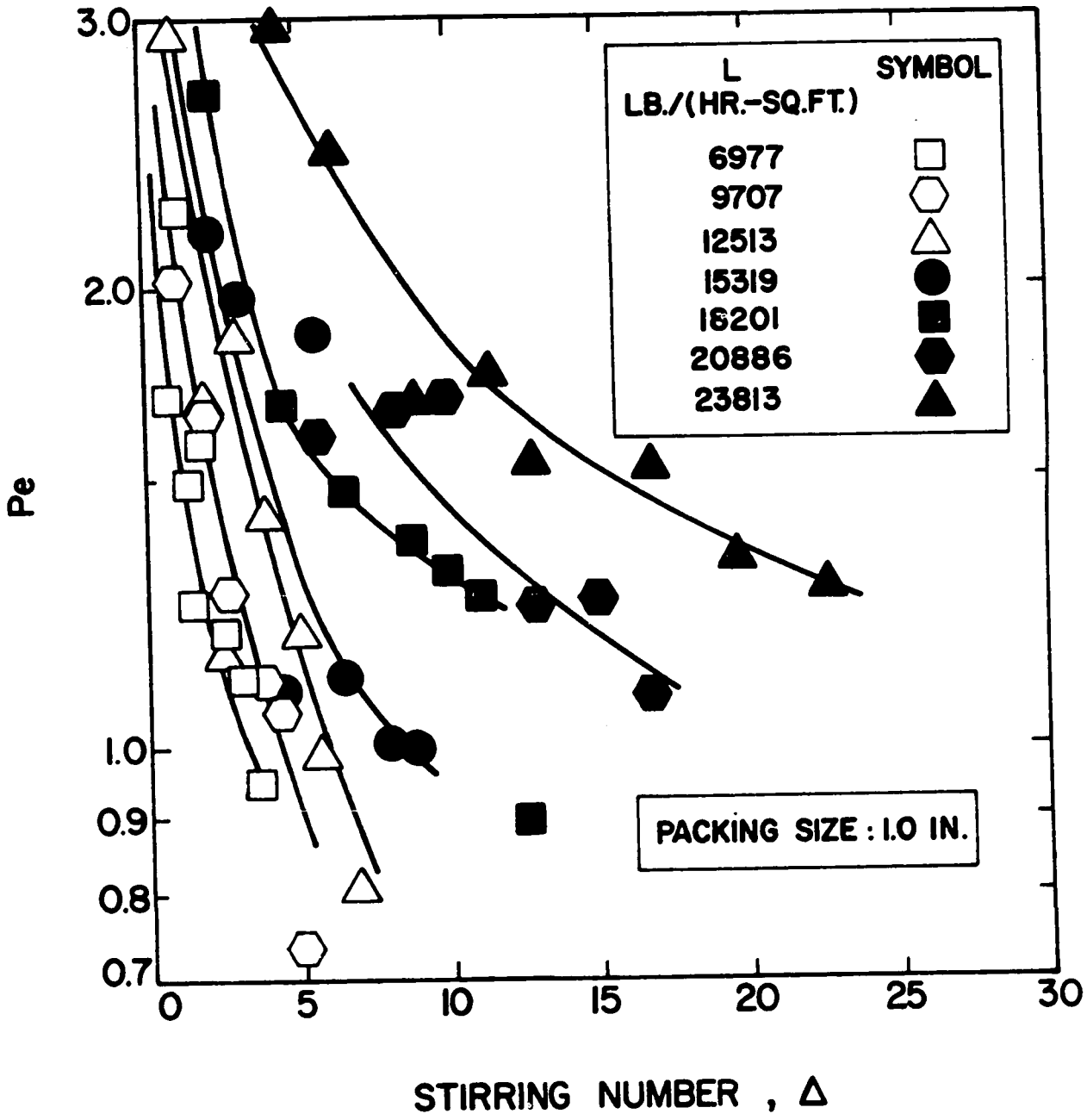

FIGURE 5.10(c): VARIATION OF LIQUID-PHASE PECLET NUMBER WITH LIQUID FLOW RATE AND PACKING SIZE FOR MOBILE-BED CONTACTING, d = 1.0-inch

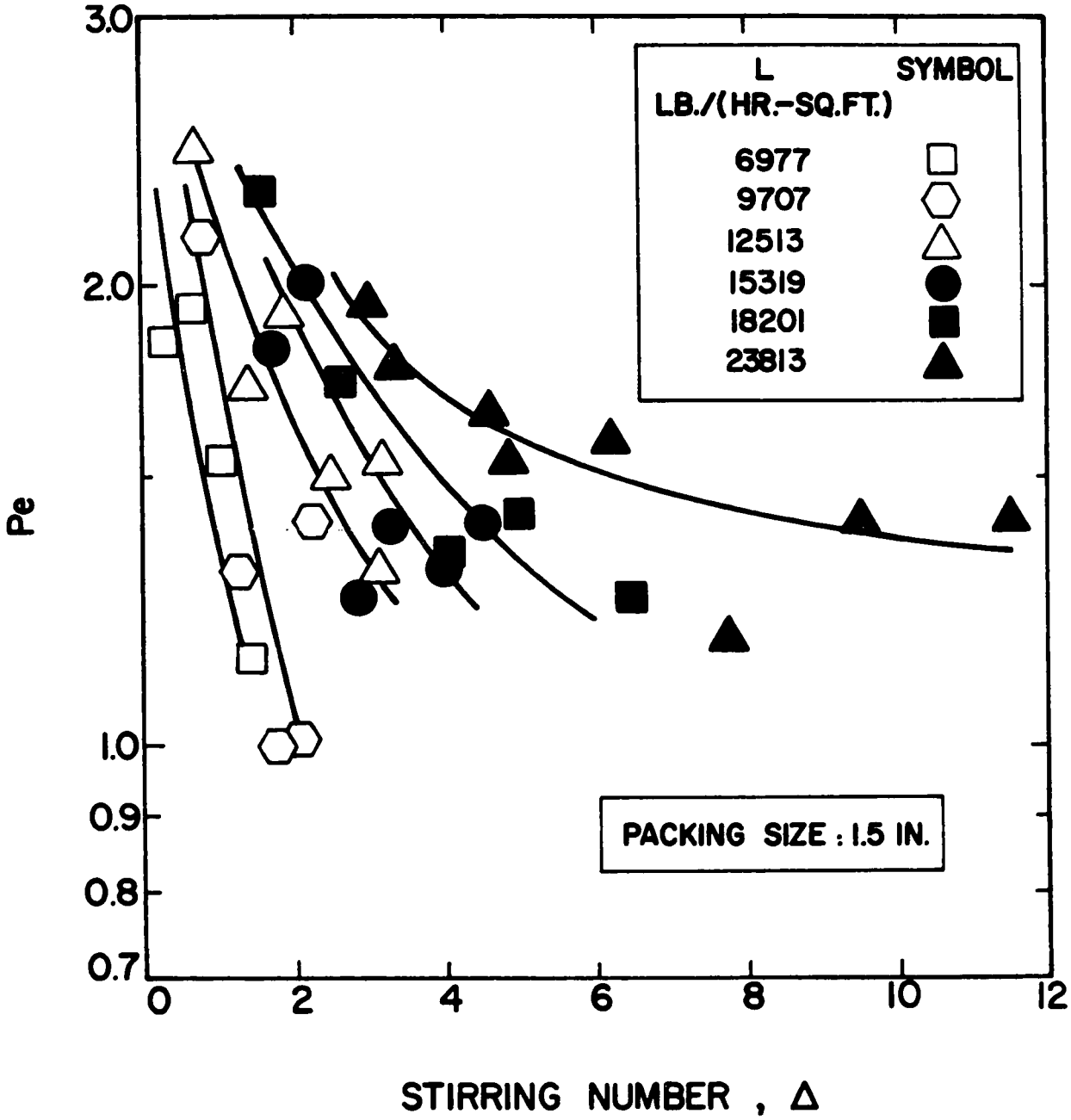

FIGURE 5.10(d): VARIATION OF LIQUID-PHASE PECLET NUMBER WITH LIQUID FLOW RATE AND PACKING SIZE FOR MOBILE-BED CONTACTING, d = 1.5-inch

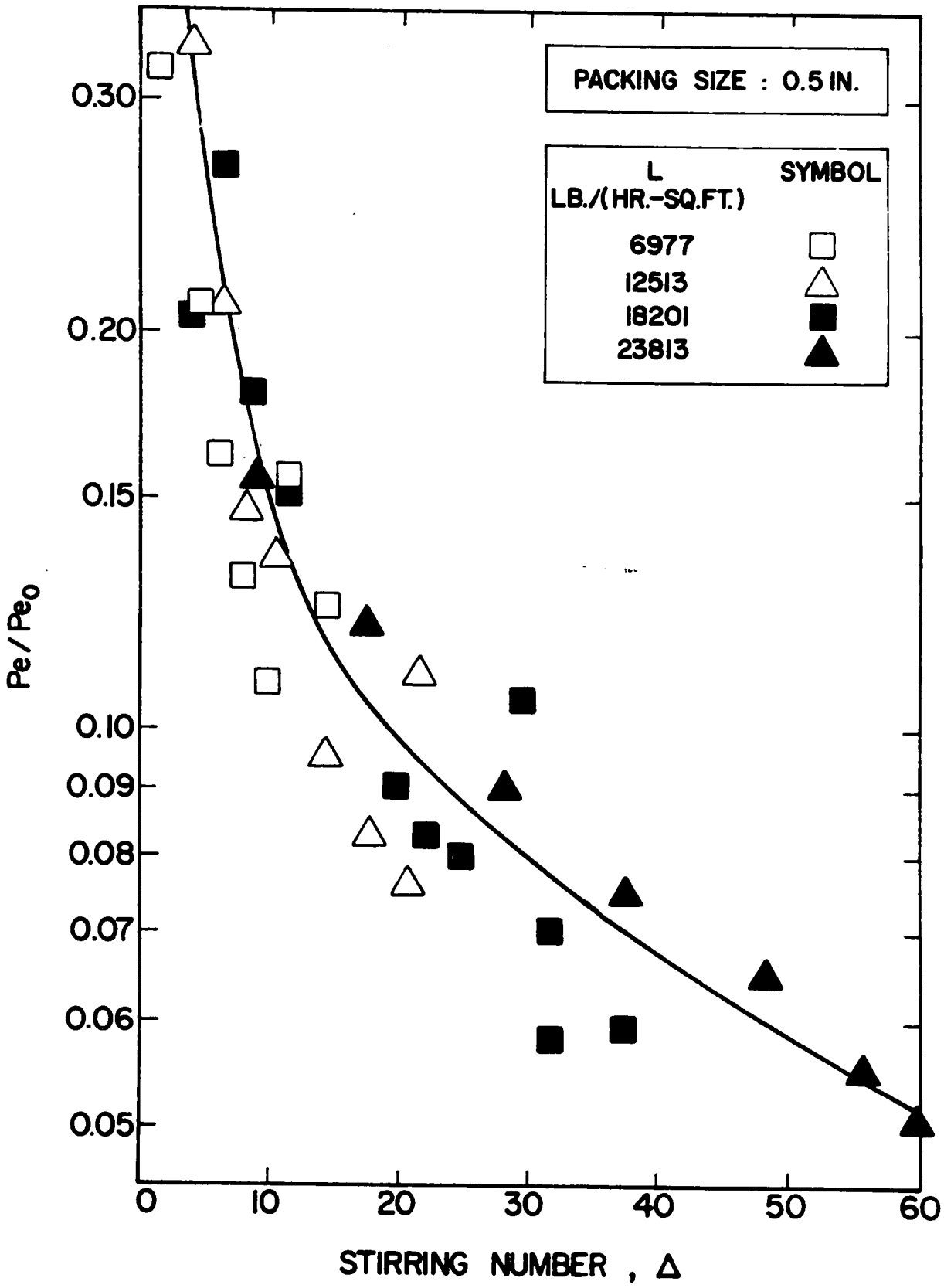

FIGURE 5.11(a): VARIATION OF THE RATIO Pe/Pe_o WITH STIRRING NUMBER AND PACKING SIZE, d = 0.5-inch

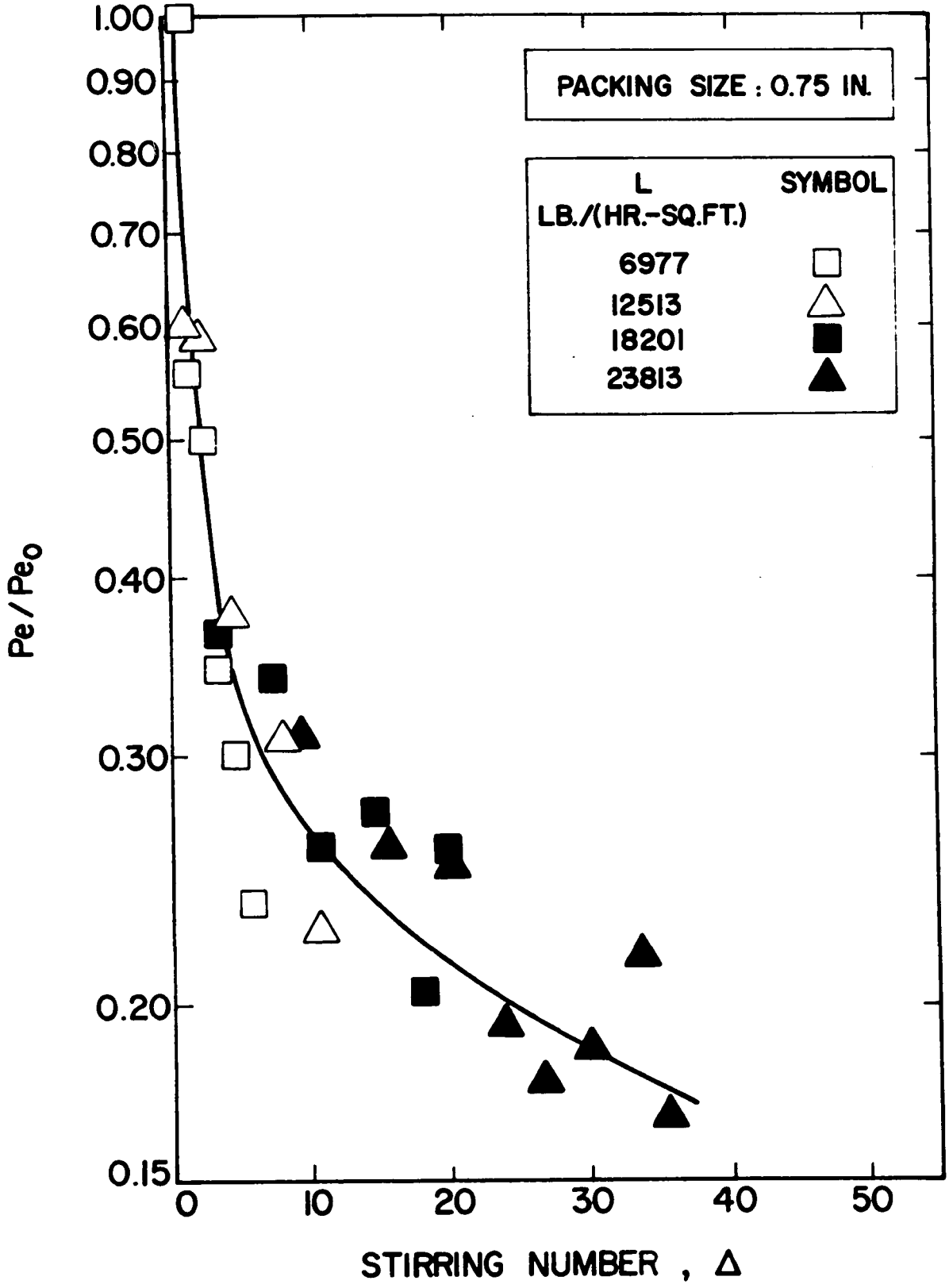

FIGURE 5.11(b): VARIATION OF THE RATIO Pe/Pe_o WITH STIRRING NUMBER AND PACKING SIZE, d = 0.75-inch

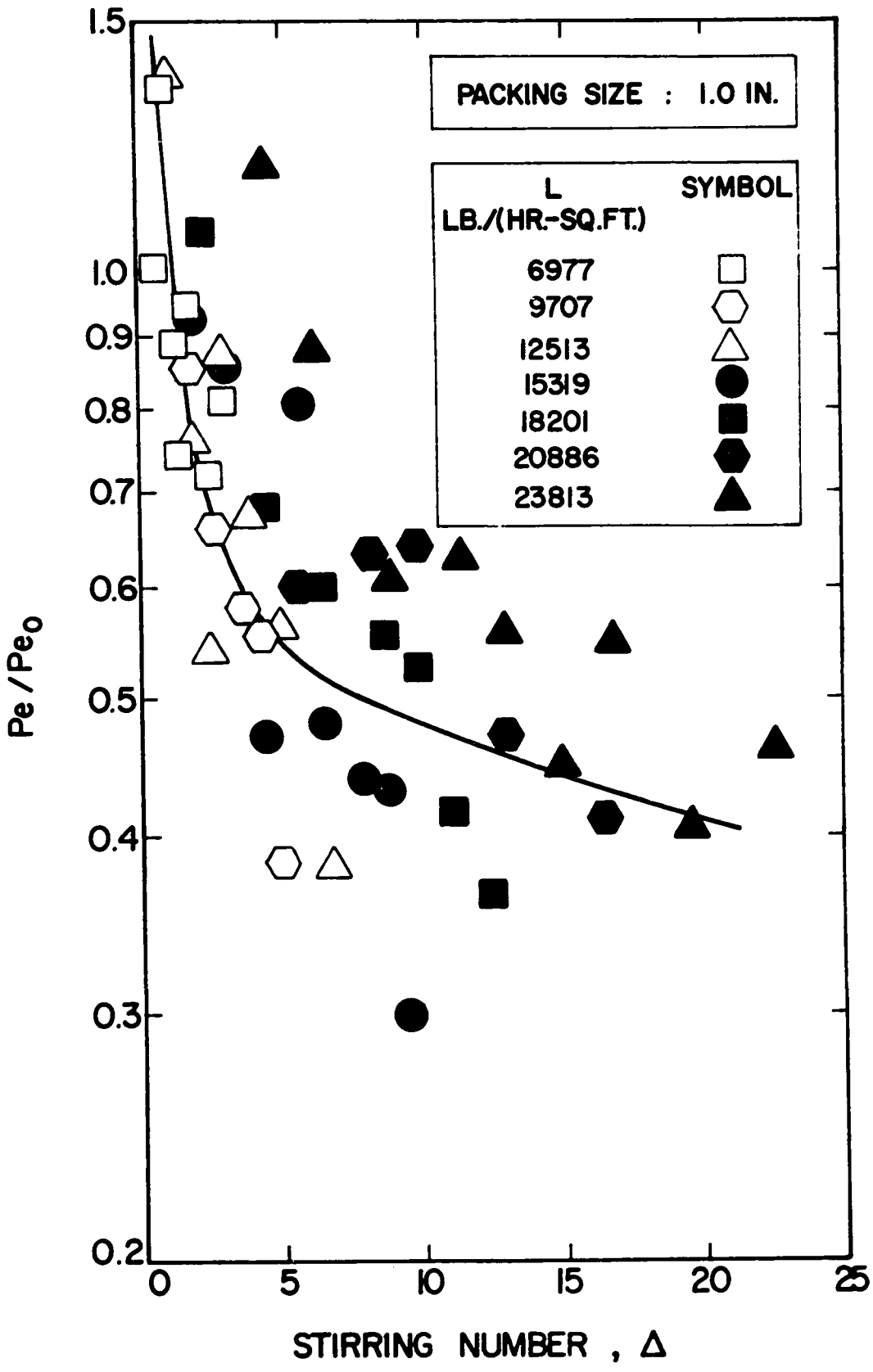

FIGURE 5.11(c): VARIATION OF THE RATIO Pe/Pe_o WITH STIRRING NUMBER AND PACKING SIZE, d = 1.0-inch

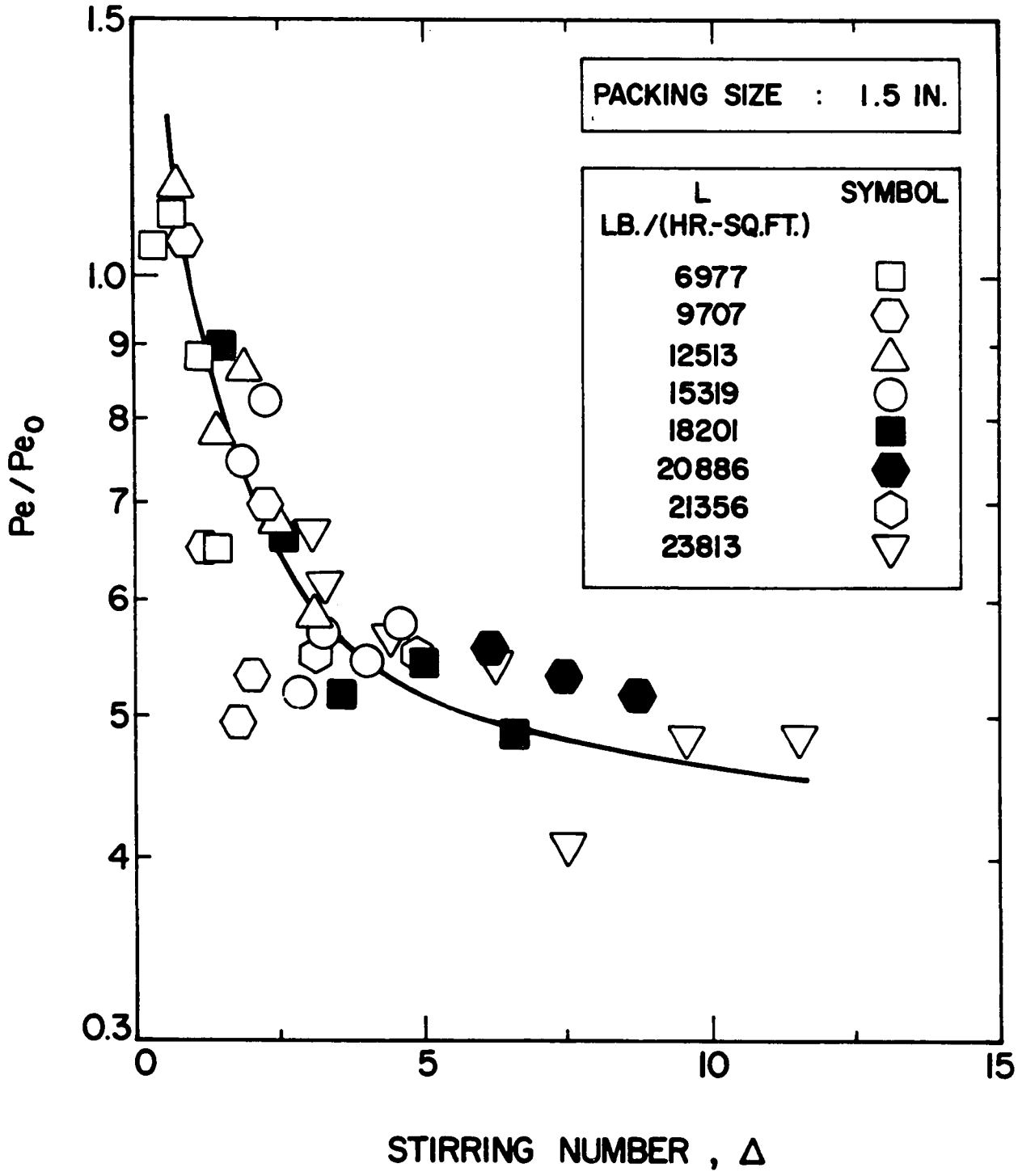

FIGURE 5.11(d): VARIATION OF THE RATIO Pe/Pe_o WITH STIRRING NUMBER AND PACKING SIZE, d = 1.5-inch

Packing Size, in.	Range of Pe	Range of Pe/Pe_o
0.5	0.15 - 1	0.05 - 0.3
0.75	0.4 - 2.5	0.17 - 1
1.0	0.7 - 3	0.4 - 1
1.5	1 - 2.5	0.5 - 1

Equation (5.11) indicates that, at constant liquid flow rate, Pe_o increases with $d^{0.125}$. The steady increase in the ratio Pe/Pe_o with packing diameter indicates that, at constant liquid flow rate, Peclet number for a mobile-bed contactor also increases with packing size, but is rather more strongly influenced by packing size than is the case for trickle-bed operation. When we recall that the effect of packing size on Peclet number for a fixed-bed appears as a consequence of a less obstructed path for liquid flow with larger packing, the trend of results for MBC is seen to form a consistent pattern because the liquid flow path becomes less obstructed yet when the bed expands in mobile-bed operation. The results reported in previous sections do in fact show that bed expansion, h, increases with packing size at constant gas and liquid flow rate. A more expanded bed allows the liquid to follow a less tortuous path, thus permitting the appreciable increase in Peclet number with packing diameter in mobile-bed type operations.

It will be recalled that for 1.5-in. spheres, mixing data for trickle-bed operation indicated a large wall

effect which causes experimental values for Peclet number to be significantly less than would be predicted by the correlation equation (5.11). The same effect is displayed for the MBC operation. In the tabulation of values of Peclet number given above, large increases in Pe with packing size may be noted over the range 0.5 to 1.0-in., whereas there is essentially no change in Pe from 1.0 to 1.5-in. spheres. It is thus apparent that there is a large wall effect in the data for MBC operation with 1.5-in. packing just as there was for the trickle-bed case. Although the continuous motion of balls acts in the direction of maintaining a uniform distribution of liquid flow over the column cross-section, the larger the balls are, the less effective they become in reducing wall flow and channelling of liquid.

For the case of 1.5-in. balls in a 5.5-in. diameter mobile bed ($d_t/d = 3.7$), therefore, the conditions unfortunately fall in the region of strong wall effect. Consequently, the data for 1.5-in. spheres on Figure 10(d) must not be taken as representative of results that would be expected for 1.5-in. balls in a larger diameter column. Likewise, the data for Pe/Pe_o for 1.5-in. spheres on Figure 11d represent the ratio of results for two experiments, both of which were strongly influenced by wall effect. Little significance should therefore be attached to this plot. Although the analysis of data for the effect of packing diameter, and thereby to the determination of wall effect for 1.5-in. diameter spheres, has proceeded on the basis of Figures 5.10 and 5.11, all conclusions reached may be substantiated by more precise com-

parisons based on the data for Peclet number, and gas and liquid mass velocities as tabulated in Appendix 1.1.

It was hoped that representation of mixing data as the ratio Pe/Pe_o on Figure 5.11 would eliminate the effect of liquid flow rate. Comparisons between Figures 5.10 and 5.11 indicate that this objective has been to a considerable extent, but not entirely achieved. For reasons which are not understood this representation is least successful for 1.0-in. spheres. Although only one curve has been shown on Figure 5.11(c), the data for liquid flow rates L = 20886 and 23813 lb./hr.-ft.^{2} and some of the data for L = 18201 lb./hr.-ft.^{2} lie in one region, above the curve shown, while the results at the lower liquid flow rates could be correlated reasonably well by a second curve located below the one shown.

For the representation of Pe/Pe_o given as Figure 11, it is of interest to note that these four plots could each show the value $Pe/Pe_o = 1$ at $\Delta = -1$, i.e., the trickle-bed condition. Work with gas-liquid flow through fixed-bed contactors indicates that the Peclet number for the liquid phase is not much affected by gas flow rate. Thus, a plot of Pe/Pe_o for operation between the trickle-bed andthe onset of the mobile-bed condition should be approximated by a horizontal line at $Pe/Pe_o = 1$ for $-1 \leq \Delta \leq 0$. Figure 11(c), for 1.0-in. spheres, thus indicates that the ratio Pe/Pe_o may pass through a maximum in the operating region just above the minimum fluidization limit. The region for which $Pe/Pe_o > 1$ corres-

ponds to conditions for which reduction in tortuosity of flow path for the liquid, resulting from a modest amount of bed expansion, is more effective in reducing axial mixing than the as yet limited amount of ball motion is in increasing mixing.

As primary industrial interest is for conditions giving a rather more expanded bed, the region of a maximum in Pe/Pe_o, and hence in Pe, will not usually be of great practical interest.

Figure 5.12 provides a comparison of results of the present study with those reported by Chen. As agreement between the two studies for trickle-bed operation was quite good, comparison in terms of Pe/Pe_o is effectively a comparison of Peclet number for the MBC operation. Two features are immediately apparent: first, the present study covers a much wider range of gas and liquid flow rates, as reflected by the value of the stirring number, Δ; second, the wide discrepancy between the results of the two investigations. There are two distinct aspects to the differences:

I. The present study indicates that liquid mixing decreases as the packing size is increased, while Chen's results indicate the opposite.

II. The magnitude of mixing in the present investigation is less by a factor of from 4 to 10 than that obtained by Chen.

The increase in liquid-phase Peclet number with increase in packing size at constant gas and liquid mass velocities may be expected because the less tortuous path

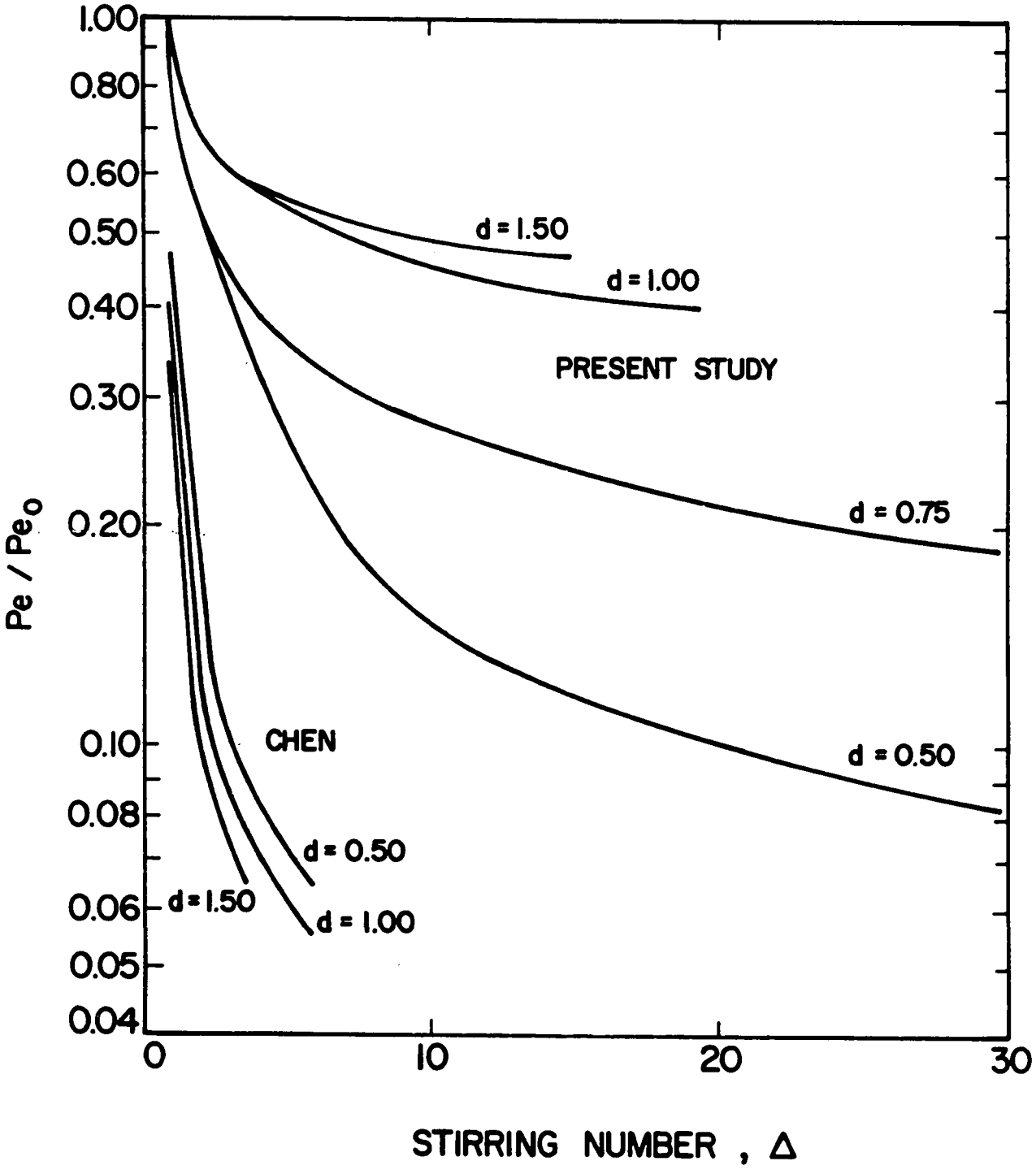

FIGURE 5.12: COMPARISON OF THE DATA ON AXIAL DISPERSION IN MOBILE-BED CONTACTING

reduced number of interactions of liquid in the case of the larger packing. The physical picture of mixing in a mobile-bed contactor is thus in agreement with the results of the present study, while those of Chen show a trend with packing diameter opposite to that which would be predicted.

Reference to Figure 5.12 indicates, however, that the spread of Chen's results with packing size is modest compared to the much larger differences between the relatively narrow region in which all his results lie and the results of the present work. Possible sources of such differences will now be examined.

Although carried out in the same laboratory, the present study was performed with a different mobile-bed facility, with a different liquid distributor, tracer injection system, design of conductivity cells, and basic data processing procedure. Any of these aspects could influence the results and, as the present study followed that of Chen's, it is believed that improvements were achieved in each. The liquid distributor used by Chen gave four times the holdup of tracer of the one now used, and as his liquid flow rates covered a range one-half that used here, there could have been some tailing in the input function which was treated as a pure step-function in his data processing. Any such effect would give results with a higher apparent value of mixing.

Based on Chen's experience, the conductivity cells and liquid sampler used in the present study were redesigned. The cells used here were one-half the diameter, the sampler one-third the diameter, and the liquid holdup in the sampler before the liquid reaches the electrodes was about one-fifth that of Chen's setup. It is relevant to note that Chen's measurements show step-input tails as long as the mean residence time in the present case. Such tailing could occur as a combination of liquid holdup and mixing in the liquid distributor and the samplers, and has the effect of indicating more mixing in the bed than actually occurs.

Development for the present study of the technique of measuring Peclet number by transfer function analysis for finite-bed boundary conditions made possible the use of simultaneous two-point measurements under actual flow conditions. At the time of Chen's study it was necessary to consider end effects as consisting only of a time delay in injection. Thus it was necessary for him to determine this correction for the trickle-bed mode of operation without gas flow, then apply this correction to the measurements for MBC operation.

There is no way of knowing whether the various improvements which were possible since the time of Chen's study have reduced any source of experimental error which was of sufficient magnitude to affect his results. What is known is that each of the changes made was in the direction

of removing a source of error which, if present, would in every case give erroneously high mixing (i.e., incorrectly low Peclet numbers). As there is a significant difference in results, the evidence is strongly in favor of the present results which have the advantage of additional development and newer techniques.

An exception is the case of results for 1.5-in. spheres, which are shown on Figure 5.12 only for comparison. As already noted, these results are incorrectly low in Peclet number because of a wall effect problem associated with the 5.5-in. diameter column.

No more general correlation of axial mixing in MBC is presented than is shown as Figure 5.12. By reference to equation (5.1) it may be seen that the effect of diameter on Peclet number enters in three ways - through liquid phase Reynolds number, Gallileo number, and stirring number. Due to the limited number of variables which have yet been studied it is considered inappropriate at this time to propose a correlation more general than the representation of Figure 5.12. Further investigation of mixing in MBC with meticulous attention to every detail is necessary to arrive at a correlation of all the variables. Reference to the enormous differences in liquid-phase mixing in packed bed shown on Figure 2.5 and discussed in the review of previous work does in fact indicate the great experimental difficulties of accurate measurement of mixing in counter-current gas-liquid flow.

5.1.5 Conclusion

A number of physical characteristics of mobile-bed contacting have been established by study of four aspects of the hydrodynamics of this process, namely, minimum fluidization velocity, G_{m_f}, bed expansion, h, liquid holdup, H_t, and liquid mixing as given by the Peclet number, Pe. New insight into the mechanism of liquid flow in MBC has thereby been provided. Also, these four important parameters of MBC can now be predicted with reasonable accuracy over the entire range of mass velocities of gas and liquid flow of industrial interest. The investigation shows that mixing conditions are considerably further in the direction of plug flow limit than had previously been thought, and this, of course, further increases the economic attractiveness of this new gas-liquid contacting technique. Liquid mixing in MBC has also been found to be more strongly dependent on size of packing than is the case for fixed-bed contactors. The scale effect associated with the importance of relative size of the packing and the column has, however, not been completely resolved. Until this effect has been investigated further, care should, therefore, be exercised in using this mixing data in the design of mobile-bed contactors of industrial size. Thus, the need remains for more mixing studies for both liquid and gas phase in MBC, in particular, the influence of size of packing, diameter of column, and effect of physical properties.

5.2 MASS TRANSFER EFFECTS

The performance of a mobile-bed contactor as a mass transfer device is presented and analyzed in this section. Effective interfacial area in MBC is considered first, then the results for "true" liquid-phase mass transfer, i.e. values of $k_L a$ corrected for effect of liquid mixing. Finally, the variation of the area-based transfer coefficient, k_L, is examined as a further indicator of the relationship between flow behaviour and mass transfer characteristics of MBC.

5.2.1 Results for Effective Interfacial Area

The central feature to a basic analysis of mass transfer behaviour in MBC is that the total effective interfacial area is the summation of three types of interfacial area, and that the mass transfer occurring across each of these types of interface contributes in a different way to the total mass transfer. The types of interfacial areas are

Bubble area - due to swarms of small gas bubbles dispersed in the liquid

Droplet area - due to liquid droplets produced by the turbulent conditions

Film area - due to liquid flowing as a film and to fragments of liquid larger than droplets.

It is important to note that the direct chemical reaction technique used in the present study measures the cumulative area due to all three types of interface. Varia-

tion in the relative importance of these types provides the key to understanding the mass transfer characteristics of MBC.

The values of effective interfacial area of mass transfer as determined by absorption of carbon dioxide from air into sodium hydroxide solutions were corrected for gas-phase resistance using the rates measured under identical flow conditions for the absorption of sulphur dioxide into sodium hydroxide solution. The techniques have been used successfully for determination of effective interfacial area (37,39,47) and were described in Sections 2.2 and 4.1.4. The computer program for calculation of physico-chemical properties of the system and processing of the data is recorded in Appendix II.3. Details of the calculation of physico-chemical data are given in Appendix IV. Bed height for the 0.75-inch spheres used was obtained from equation (5.5). The complete results for interfacial area are given in Appendix I.2, Table IV.

The experimental results for effect of gas and liquid mass velocity on interfacial area are plotted with linear and logarithmic representation on Figure 5.13(a) and (b) respectively. The large increase of interfacial area with gas and liquid flow rate is immediately evident. In the upper range the values of interfacial area may be seen from Figure 15(a) to increase continuously, the limit of which would be the conditions for which the packing would be carried to the top of the bed and the tower would flood. The

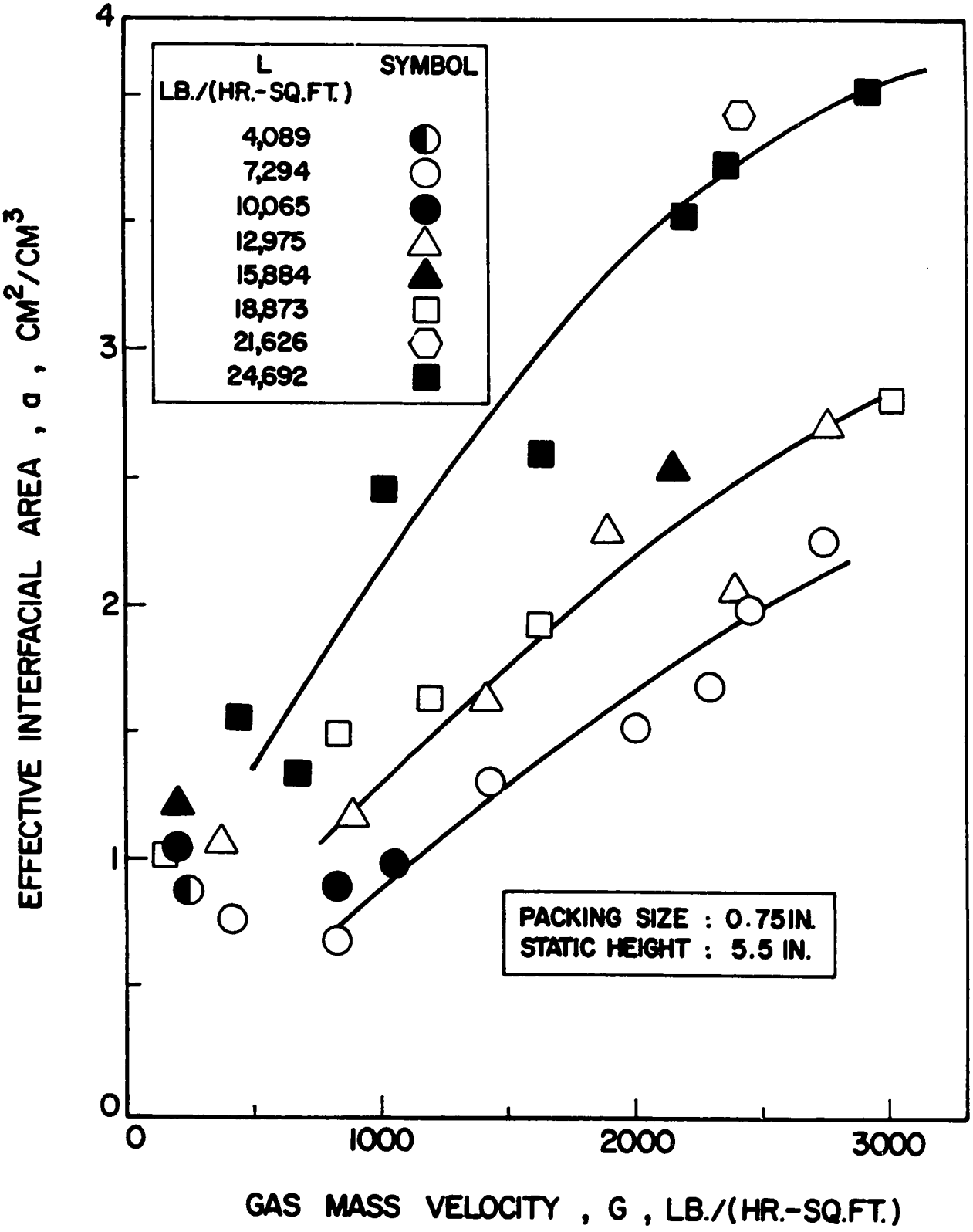

FIGURE 5.13(a): VARIATION OF EFFECTIVE INTERFACIAL AREA OF MASS TRANSFER WITH GAS AND LIQUID FLOW RATES IN MOBILE-BED CONTACTING, d = 0.75-inch (linear scale)

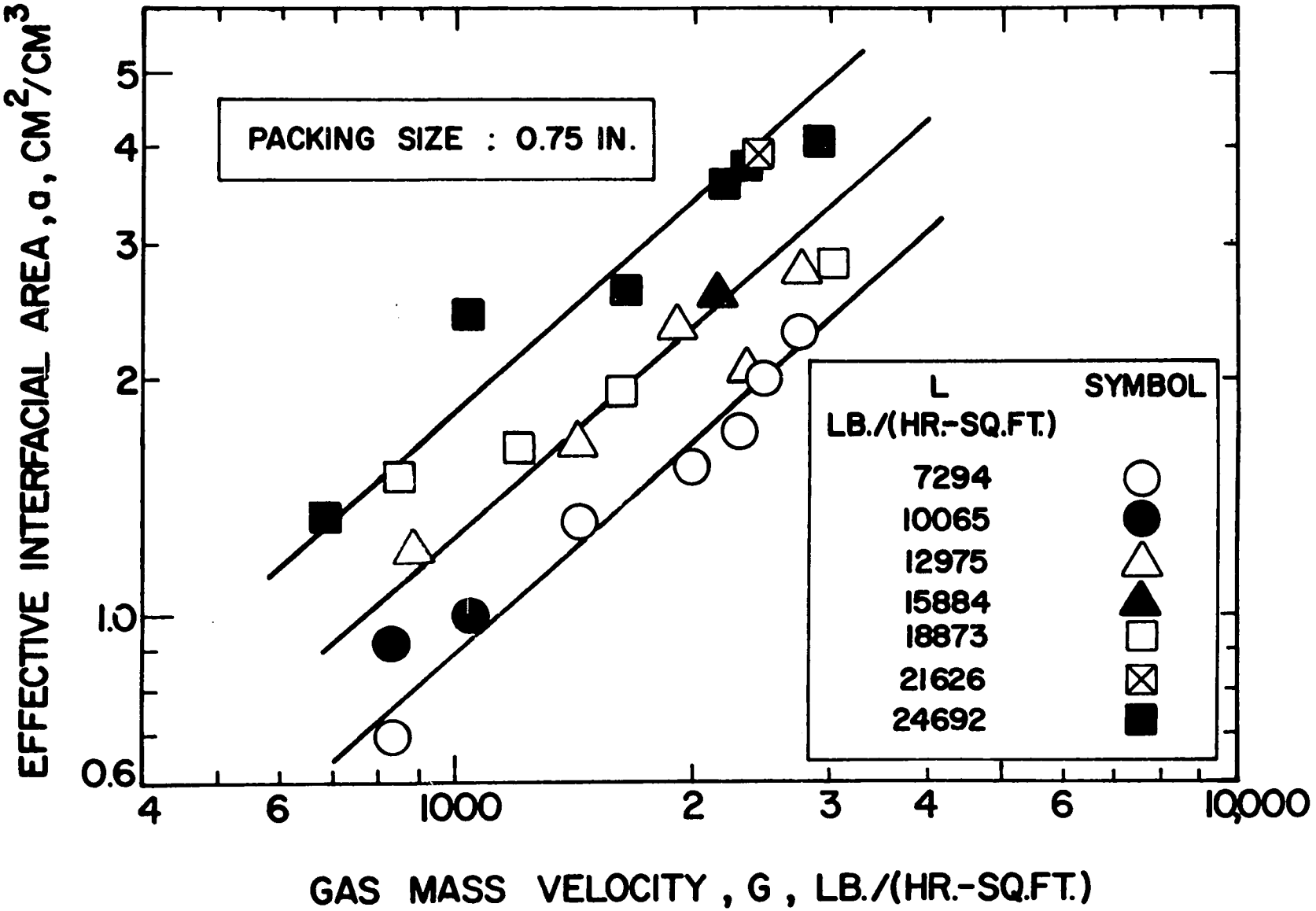

FIGURE 5.13(b): VARIATION OF EFFECTIVE INTERFACIAL AREA OF MASS TRANSFER WITH GAS AND LIQUID FLOW RATES IN MOBILE-BED CONTACTING, d = 0.75-inch (log scale)

highest gas and liquid velocities of the present study approach this limit. The effective interfacial area may be observed to increase with gas velocity continuously as this limit is approached.

The limiting condition in the region of low values of interfacial area is the trickle-bed operation, i.e. G = 0. Yoshida and Koyanagi (37) have in fact measured effective interfacial area in a sphere-packed column in trickle-bed operation. Interpolating from their results, the value of effective interfacial area of 0.84 $cm.^{-1}$ may be obtained for L = 7294 $lb./hr.-ft.^2$, which is the lowest liquid rate at which extensive area measurements are available from the present study.

From Figure 15(a) it may be seen that it would be quite consistent with the data to terminate the line for the new measurements with L = 7294 at the value of a = 0.84 $cm.^{-1}$ at G = 0. All lines shown on Figure 15(a) must of course terminate along the ordinate at the value corresponding to trickle-bed operation. The seven measurements made of interfacial area in the range G < 500 $lb./hr.-ft.^2$ may be noted on this plot. However, as these values cover the full range of liquid flow rates, 4089 < L < 24692, there is insufficient data to define interfacial area accurately in the transition region near the minimum fluidization velocity. For 0.75-inch spheres it is of interest that the range for minimum fluidization velocity is approximately 90 < G_{mf} < 700 $lb./hr.-ft.^2$

for the range of liquid flow rates used. As the transition region near $G = G_{mf}$ is not the region of primary industrial interest, it was not studied in detail, and the lines on Figure 15(a) are therefore not extended into this region.

Figure 5.13(b) shows on logarithmic scales the variation of effective interfacial area for MBC with fluid flow rates. As the seven data points for the transition region close to minimum fluidization have been omitted from Figure 5.13(b) for the reasons just noted, the straight lines which represent the data on logarithmic coordinates for the fully developed mobile-bed conditions must not be extrapolated into the transition region. The equation which corresponds to the correlation on Figure 5.13(b) is

$$a = 7.56 \times 10^{-6} \; L^{0.6} \; G^{0.9} \qquad (5.16)$$

Figure 5.14 shows the adequacy of fit of experimental data with the proposed correlation.

As noted at the outset, the interfacial area in MBC comprises the contributions of areas of gas bubbles, liquid droplets and liquid films. One can therefore interpret the results by reference to aerated liquid systems, spray columns and packed beds.

A packed bed is characterized by flow of liquid as thin films on packing surfaces while the gas phase remains as a continuous phase occupying most of the free space. Droplet and bubble formation begins to occur only in the loading

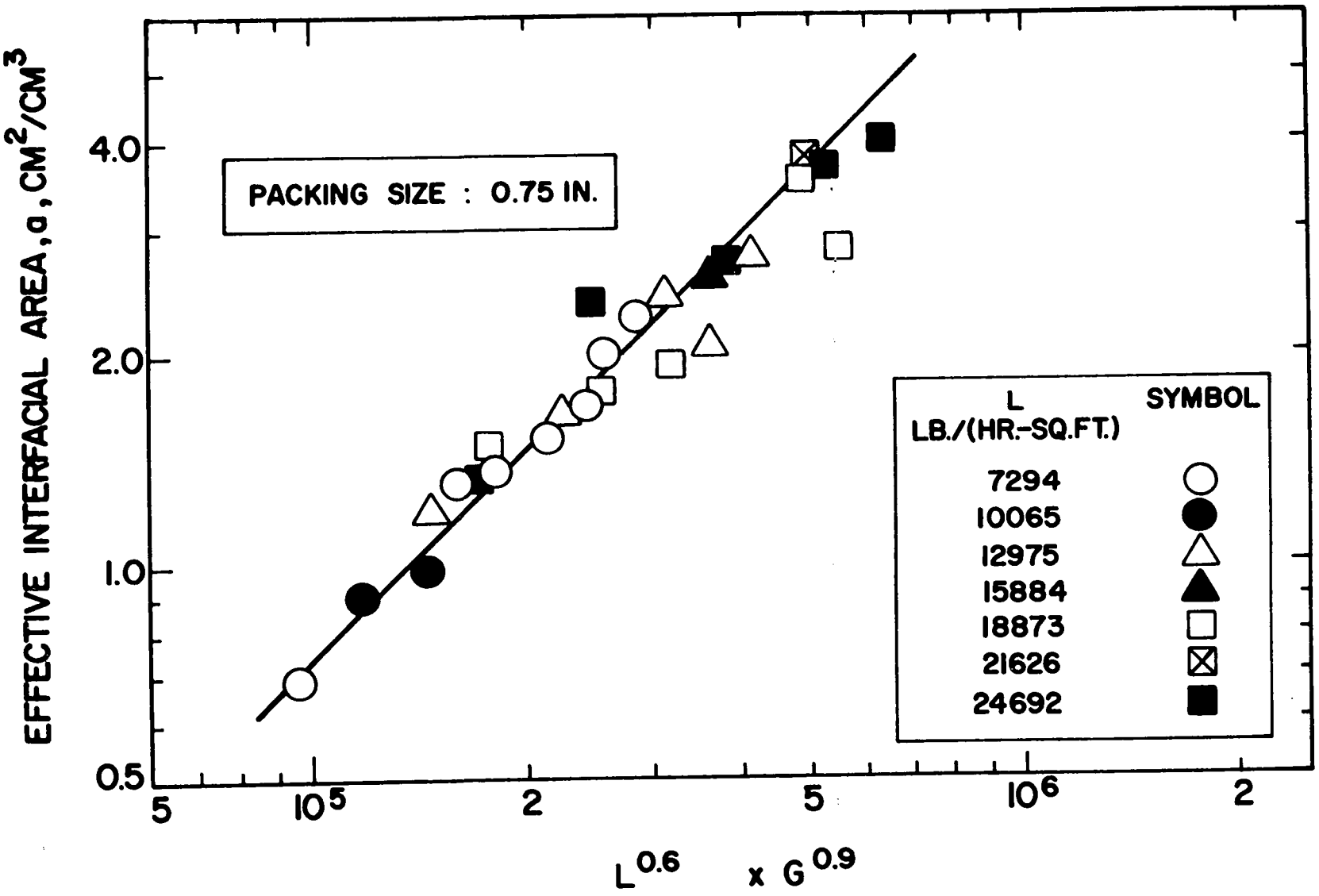

FIGURE 5.14: CORRELATION OF DATA ON EFFECTIVE INTERFACIAL AREA OF MASS TRANSFER FOR MOBILE-BED CONTACTING

region close to the flooding point. Interfacial area, as well as the transport and other properties of a packed bed below the loading point, are therefore influenced primarily by liquid flow rate, the effect of gas flow rate usually being insignificant (37,42,47).

Danckwerts and Sharma (53) have summarized for a number of packings the data for effective interfacial area, a, and liquid phase mass transfer coefficient, k_L, for absorption of carbon dioxide. Typically, the effective interfacial area increases relatively rapidly with liquid flow rate, in the low range of flows, probably due to difficulty with fixed-bed contactors of wetting all the packing surface. Effective interfacial area approached that of dry packing below the loading point while at high flow rates, beyond the loading point, effective interfacial area may eventually be greater than that of the dry packing. It is probable that some droplet and bubble formation occurs for the rather unstable conditions above the loading point. The region for fixed-bed contactors near the flooding point has not however been adequately studied.

An interesting point of comparison for the results of the present study may be made at L = 7294 lb./hr.-ft.^{2} At this liquid flow rate the review of Danckwerts and Sharma (47) indicates that effective interfacial area for columns packed with various industrial packings (rings and saddles) is in the range of 1 to 3.5 cm.$^{-1}$. This comparison is somewhat mis-

region close to the flooding point. Interfacial area, as well as the transport and other properties of a packed bed below the loading point, are therefore influenced primarily by liquid flow rate, the effect of gas flow rate usually being insignificant (37,42,47).

Danckwerts and Sharma (47) have summarized for a number of packings the data for effective interfacial area, a, and liquid phase mass transfer coefficient, k_L, for absorption of carbon dioxide. Typically, the effective interfacial area increases relatively rapidly with liquid flow rate, in the low range of flows, probably due to difficulty with fixed-bed contactors of wetting all the packing surface. Effective interfacial area approached that of dry packing below the loading point while at high flow rates, beyond the loading point, effective interfacial area may eventually be greater than that of the dry packing. It is probable that some droplet and bubble formation occurs for the rather unstable conditions above the loading point. The region for fixed-bed contactors near the flooding point has not however been adequately studied.

An interesting point of comparison for the results of the present study may be made at L = 7294 lb./hr.-ft.^{2} At this liquid flow rate the review of Danckwerts and Sharma (47) indicates that effective interfacial area for columns packed with various industrial packings (rings and saddles) is in the range of 1 to 3.5 cm.$^{-1}$. This comparison is somewhat mis-

leading, however, in that it is only possible to reach interfacial areas in the order of 3.5 $cm.^{-1}$ with 0.5-inch packing, and such small packing has rather restricted application because of the correspondingly low flooding velocities. Interestingly enough, the interfacial area at L = 7294 is effectively the same for 0.75-inch spheres in mobile beds near the minimum fluidization condition, as it is for 1.5-inch Raschig rings in fixed beds. As liquid flow rate increases above this value, interfacial area increases more rapidly for the MBC, and liquid rate for MBC can of course be increased to much higher values before flooding (L > 25000 $lb./hr.-ft.^2$) than is the case for a fixed-bed column.

The dependence of interfacial area on liquid flow rate provides another point of comparison between mobile-bed and fixed-bed contactors. The correlation of results proposed here, equation (5.16), indicates that interfacial area in MBC increases with $L^{0.6}$, while Shulman et al. (30) report that the exponent for a fixed-packed column is 0.45. As MBC is characterized by much more highly turbulent flow conditions than those in a packed bed, it is not surprising to obtain a higher exponent for liquid flow rate in our case.

The dependence of interfacial area on liquid flow rate may also be compared with the variation of liquid holdup with liquid flow rate. The results for 0.75-inch spheres given in Section 5.1.3.2 indicate that liquid holdup in MBC increases approximately proportional to $L^{0.7}$. The fact that

the dependence on liquid flow rate in the case of interfacial area is somewhat less than it is for holdup is in fact a reflection of the same phenomena which cause the reduction in axial mixing of the liquid as liquid flow rate increases (cf. Section 5.1.4). Thus although liquid holdup increases approximately with $L^{0.7}$, interfacial area does not increase in direct proportion to the increase in holdup because the liquid flow conditions are changing in the direction of less axial mixing associated with less tortuous flow path provided by the more expanded bed. The result is less interfacial area per unit amount of holdup, and thus a lower exponent for interfacial area.

The contribution and effect of that fraction of the interfacial area which is contributed by droplets will next be examined. The recent results of Mehta and Sharma (69) for interfacial area in a spray column are reproduced in Table 5.2; the results tabulated for mass transfer coefficients will be discussed in the subsequent section. It may be noted that interfacial area in a spray column is relatively low and not strongly dependent on either gas or liquid flow rate. An estimate of the importance of droplet interfacial area may be obtained from an order of magnitude calculation. Typical values for holdup of the liquid and solid phases in MBC are 0.15 and 0.3 volume fraction, respectively, which correspond to 0.55 volume fraction for gas-phase holdup. If 1 $cm.^{-1}$ is taken as a generously high estimate of droplet interfacial

TABLE 5.2

MASS TRANSFER AND EFFECTIVE INTERFACIAL AREA IN A SPRAY COLUMN (69)

COLUMN DIAMETER = 7.9 cm.

COLUMN HEIGHT = 134.0 cm.

SHOWER TYPE NOZZLE:
DISC DIAMETER = 12.5 mm.
ORIFICE DIAMETER = 1.2 mm.
NUMBER OF HOLES = 69

LIQUID FLOW RATE lb./hr.-ft.^{2}	GAS VELOCITY cm./sec.	k_La hr.$^{-1}$	k_L cm./hr.	a cm.^{2}/cm.^{3}
9,950	1-15	32.4	65.5	0.495
9,950	25	38.2	65.5	0.584
15,930	1-15	47.9	85.5	0.57
15,930	25	61.2	91.8	0.666
15,930	42			0.800

area in a spray column at high gas and liquid velocitires, and it is assumed that droplet concentration in the gas space in MBC is as high as in a spray column, then an upper bound of 0.55 $cm.^{-1}$ follows for the contribution of interfacial area from droplets in MBC. As experimental values of total interfacial area for MBC would be about 3 $cm.^{-1}$ for flow conditions corresponding to those for which the value of 0.55 $cm.^{-1}$ has been estimated, it is apparent that area from droplets contributes a rather small amount to the total interfacial area. Thus, in view of the low percentage of total area which derives from droplets, combined with the relative insensitivity of this contribution to gas and liquid flow rate, it may be concluded that the strong effect observed for gas flow rate on total interfacial area ($a \propto G^{0.9}$) must originate from the third source of interfacial area, namely, from bubbles. Interfacial area from liquid films as they occur in normal packed bed operation cannot of course provide any significant amount of this dependency on gas flow rate because, as already noted, liquid phase behaviour in packed beds (holdup, axial mixing, interfacial area) is essentially independent of gas velocity.

Gas bubbles are the source of interfacial area for the general class of equipment referred to as aerated contactors. This class of contactor may be taken as including sparged reactors, bubble columns, sieve and bubble trays where gas bubbles rise through a continuous liquid phase. In

this case, the gas-liquid contact area is in fact the area of tiny bubble swarms. Bubble phenomena observed in these systems have been extensively studied by Calderbank and co-workers (63,67). The interfacial area was found to increase with gas flow rate. The relationship for sieve plates with holdup ratios less than 7% (for gas velocity, u_G, below 1.5 cm./sec.) is given by

$$a \propto u_G^{0.704} \tag{5.17}$$

This is in good agreement with the exponent of 0.715 obtained by Quigley's correlation (68) which was developed by measuring bubble diameters and gas-phase holdup for this range of gas flow rates. An empirical correlation:

$$a \propto u_G^{0.9} \tag{5.18}$$

was given (63) for values of gas holdup up to 40%, with gas velocity, u_G, ranging from 12 to 100 ft./min. These gas flow rates are low by comparison with MBC, for which interfacial area was measured at gas velocities up to 3100 lb./hr.-ft.^{2} i.e. for superficial velocities up to 580 ft./min. The above relationship was later confirmed for foams with gas holdup up to 80%. For sieve trays (67) interfacial area continues to increase until it reaches a maximum of about 8 cm.$^{-1}$ when it remains almost constant. For bubble columns Sharma and Mashelkar(57) measured interfacial areas in the range 1.5 to 3.5 cm.$^{-1}$ for superficial gas velocities from 15 to 40 cm./sec. Also, they consistently found interfacial area to vary with

the 0.7 power of gas velocity.

In the operation of aerated mixing vessels, as well as sieve plate columns, mechanical energy is dissipated in stirring the fluid phases. The magnitude of transport properties and effective interfacial area, therefore, depends on the amount of energy input to the system. Calderbank (67) suggested the following correlation as suitable for non-agitated aerated mixing vessels as well as for sieve plate columns:

$$a = C \frac{(P/V)^{0.4} \rho_L^{0.2}}{\sigma^{0.6}} \cdot u_G^{0.5} \qquad (5.19)$$

where C is a dimensional constant, and the specific power input for non-agitated systems is defined as

$$P/V = \frac{u_G \rho_L g}{g_c} \qquad (5.20)$$

This relation again predicts that interfacial area should be proportional to $u_G^{0.9}$. All of the experimental evidence for dependence of interfacial area of bubbles in aerated vessels supports the conclusion that the observed dependence with $G^{0.9}$ derives from the fact that area of bubbles makes a large contribution to total interfacial area in MBC.

In summary, recognition of three types of interfacial area in MBC - bubble, droplet, and film area - leads to relating this new contacting technique to aerated processes, spray columns, and packed beds, respectively. At onset

of mobile-bed type operation at the condition of minimum fluidization, total interfacial area is in the order of 1 $cm.^{-1}$, essentially all of which is film area. At the upper end of the physical limit of operation of MBC, total interfacial area is about 4 $cm.^{-1}$, of which film area may have increased to somewhat greater than 1 $cm.^{-1}$ due to strong shearing action of the solid and gas phase on the liquid films and large globs of liquid in the much expanded bed. As an order of magnitude analysis indicates that droplet area may reach a maximum of 0.5 $cm.^{-1}$ for high gas and liquid flow rates, bubble area is therefore expected to reach a maximum of close to 2.5 $cm.^{-1}$. The two dominant influences, area of liquid films and of gas bubbles, is reflected in the experimentally determined dependence of total interfacial area, i.e. $a \propto (L)^{0.6}(G)^{0.9}$. The dependence on $L^{0.6}$ derives primarily from area of liquid films, while the contribution from gas bubbles is the main source of the $G^{0.9}$ variation.

The results for interfacial area thus indicate that in the lower range of fluid flow rates, not far removed from the minimum fluidization condition, MBC may be viewed primarily as a modified packed bed which, by virtue of the ability of the bed to expand, is able to operate in a completely stable manner in a state analogous to the unstable loading-flooding region of a fixed-bed contactor. In the other limit of operation for MBC, i.e. near the maximum fluid flow conditions possible, the bed behaves to a large extent

as an aerated vessel with swarms of bubbles entrained in the liquid, although the region of the expanded bed still has attributes of a packed bed to a reduced extent, and also has an appreciable concentration of droplets in the gas space in the manner of a spray column. The mass transfer results to be presented next will be interpreted in the light of the relative importance and effect of the three types of interfacial area across which the transport occurs.

5.2.2 RESULTS FOR LIQUID-PHASE MASS TRANSFER

The study of effective interfacial area has identified the three modes of mass transfer; film, droplet and bubble. An indication of the relative proportion of the three types of interfacial area was obtained, but this information reveals nothing about the conditions on the liquid-phase side of each of these three types of interfaces. Measurement of liquid-phase mass transfer should therefore provide further information concerning the characteristics of the process of mobile-bed contacting.

5.2.2.1 Evaluation of Volumetric Liquid-Phase Mass Transfer Coefficients

Mass transfer coefficients for desorption of carbon dioxide from water in a mobile-bed contactor with 0.75-in. spheres were calculated with appropriate allowance for the effect of axial mixing in the liquid phase. Equation (3.17) gives outlet liquid composition as a function of liquid Peclet number, P, and the number of mass transfer units, N_{OL}. Effective height of the mobile bed was computed from Equation (5.5) and Peclet numbers were obtained from Figure 5.11(b). Iterations were performed by changing N_{OL} to converge at the measured value of liquid concentration at the exit from the bed. The computer program for calculation of mass transfer results is included in Appendix II.4; complete results are tabulated in Appendix I.3, Table V.

Equation (3.17) with the assumption of plug flow in the gas phase has been used as the calculation model. It is, however, important to appreciate that the use of this model does not imply that there is no back-mixing of the gas phase in a MBC, nor that this back-mixing does not affect the performance of the contactor, including the mass transfer coefficient. It is just that for the case of negligible overall change in gas phase concentration, as for the conditions of this investigation, back-mixing in the gas phase does not affect the driving force for mass transfer. Axial mixing of gas is no doubt present, and the calculated values of transfer

coefficients do correctly allow for whatever effect this mixing has on the transfer coefficients. Thus it is quite valid to apply the transfer coefficients obtained here to cases for which there are appreciable changes in gas composition from inlet to outlet and gas-phase mixing therefore exerts an appreciable effect on the driving force for mass transfer.

5.2.2.2 Correlation and Discussion of $k_L a$ Data

Mass transfer in MBC occurs across three types of interfaces, those for films, bubbles and droplets. These interfacial areas are characterized by the nature of mass transfer process occurring through them which can give an order of magnitude estimate of mass transfer coefficients associated with them. The contribution of these three types of areas varies from one limit which applies for operation near the point of minimum fluidization, where most of the transport occurs across film area, to the strongly turbulent region at high flow rates where bubble area predominates, but where film and droplet area also contribute. Since $k_L a$ measured in the present study is the cumulative result, one can write

$$k_L a = k_{LD} a_D + k_{LF} a_F + k_{LB} a_B$$

where a_D, a_F and a_B are effective interfacial areas and k_{LD}, k_{LF} and k_{LB} are area-based liquid-phase mass transfer coefficients for drops, films and bubbles, respectively. Repre-

sentation of the overall transfer coefficient in this manner is the key feature of the analysis and interpretation of results for liquid-phase mass transfer.

Figures 15(a) and 15(b) show linear and logarithmic variation of $k_L a$ with flow rates in a mobile bed packed with 0.75-inch spheres. Before analyzing the results in detail, however, it is interesting to compare the mass transfer coefficients for MBC with those of other gas-liquid contactors. Thus Tables 5.3 and 5.4 show typical data for spray, bubble and packed columns while additional mass transfer data for spray columns appear in Table 5.2 given earlier. The following general characteristics become apparent form these figures and tables:

a) volumetric mass transfer coefficients for MBC are considerably larger than those for packed beds or other gas-liquid contactors (Tables 5.2, 5.3 and 5.4),

b) volumetric mass transfer coefficients for MBC increase strongly with liquid flow rate but are only slightly dependent on gas flow rate. After decreasing somewhat with gas velocity in the lower range of velocities, there is some indication that at high gas flow rates, the volumetric transfer coefficients may approach a constant value which is characteristic of the liquid flow rate used.

An empirical correlation was developed by cross-plotting the experimental data (Figure 5.13(b)) and is given by

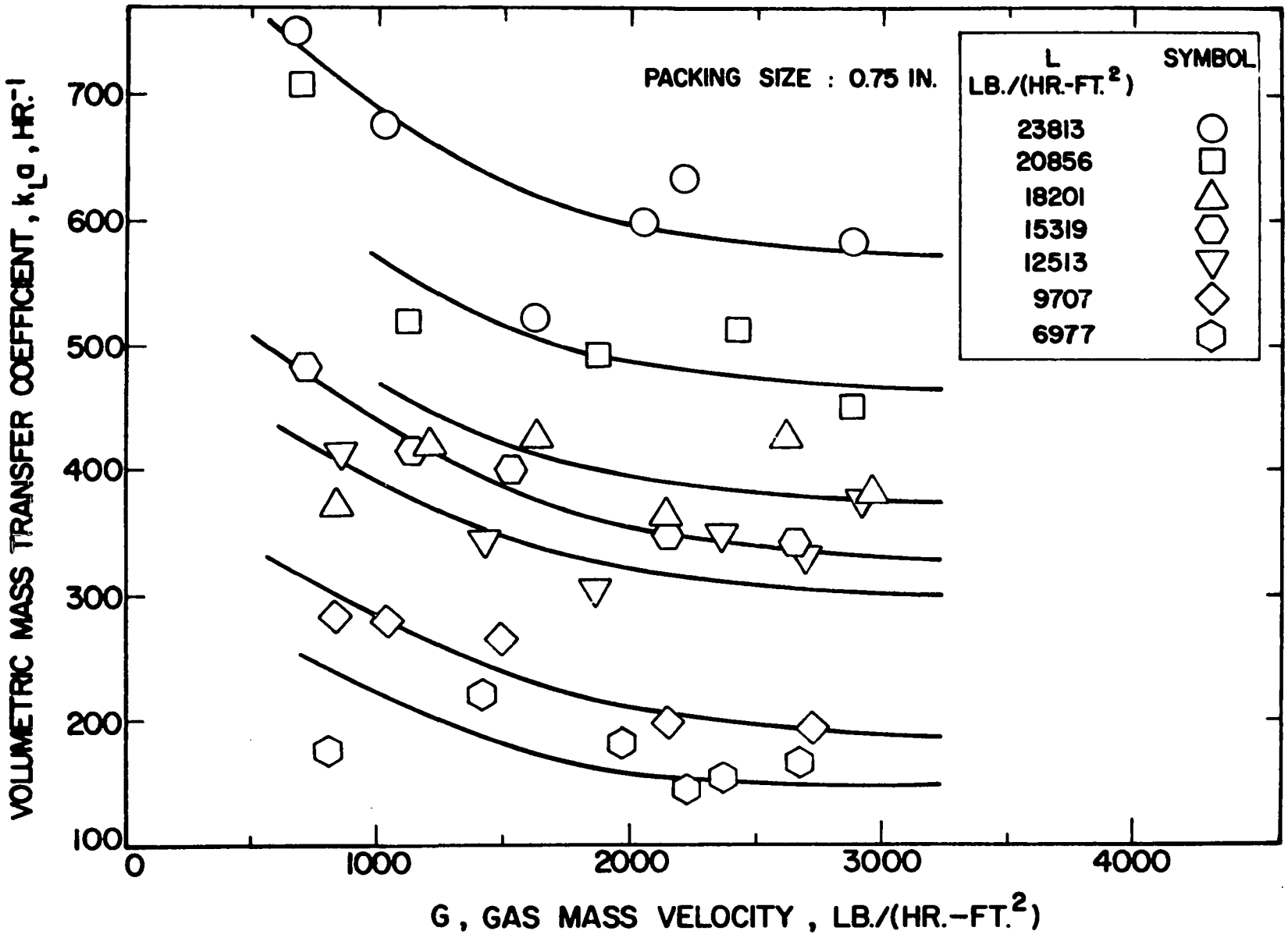

FIGURE 5.15(a): VARIATION OF VOLUMETRIC MASS TRANSFER COEFFICIENT, $k_L a$, WITH GAS AND LIQUID FLOW RATES IN MOBILE-BED CONTACTING (linear scale)

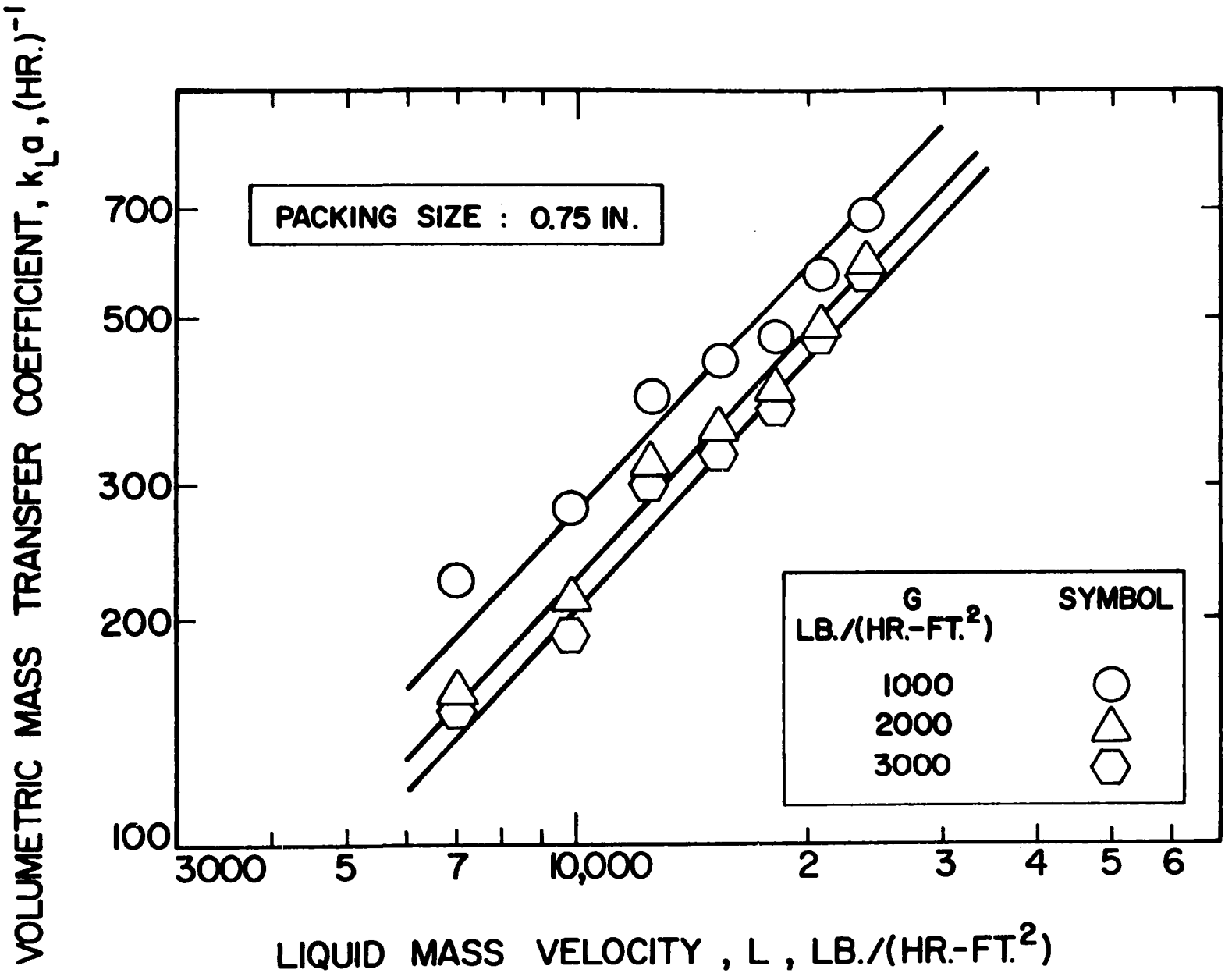

FIGURE 5.15 (b): VARIATION OF VOLUMETRIC MASS TRANSFER COEFFICIENT, $k_L a$, WITH GAS AND LIQUID FLOW RATES IN MOBILE-BED CONTACTING (log scale)

TABLE 5.3

TYPICAL MASS TRANSFER DATA FOR CONVENTIONAL CONTACTORS

Contactor	L lb./hr.-ft.^{2}	G lb./hr.-ft.^{2}	$k_L a$ hr.$^{-1}$	Remarks	Ref.
Spray Tower	800	450	10.66		154
Packed Tower	800	450	15.28	2" - R Rings	154
Packed Tower	20,000	No effect	183	0.75" sphere packed (interpolated)	70
Packed Tower	6,140	No effect	10.32	0.75" sphere packed (calculated from correlation)	78
Bubble Column	No effect	18.1	15	1 mm particle	105
Bubble Column	No effect	18.1	95	No particle	105
Bubble Column	No effect	18.1	190	6 mm particle	105

TABLE 5.4

LIQUID PHASE MASS TRANSFER IN BUBBLE COLUMNS (152)

LIQUID FLOW RATE	GAS FLOW RATE	MASS TRANSFER COEFFICIENT	ESTIMATED INTERFACIAL AREA	ESTIMATED MASS TRANSFER COEFFICIENT
LB./HR.-SQ.FT.		$HR.^{-1}$	$CM.^{-1}$	CM./HR.
L	G	k_La	a	k_L
1,000	18.7-74.2(55)	33-58 (40)	2-5(3)	7-30 (13)
10,000	18.7-74.2(42)	165-270(205)	2-5(3)	13-145(70)
24,000*	18.7-74.2(38)	205-315(240)	2-5(3)	40-155(80)
40,000	18.7-74.2(33)	248-362(280)	2-5(3)	50-180(90)

Values in parantheses indicate, for G, the value at transition, and for k_La, a, and k_L, the constant value of the variable above transition.

* INTERPOLATED

$$k_L a = 0.113\ L^{1.08}\ G^{-0.31} \qquad (5.21)$$

Figure 5.16 shows the fit of experimental data with the above equation. It should be remembered that this correlation represents the cumulative effect of the changing proportion of three modes of mass transfer. This feature will now be considered in greater detail.

The effective interfacial area for mass transfer in MBC varies between one limit where it is mostly film area, to the other limit of highly dispersed gas-liquid flow, where droplet and bubble area predominate. One can expect that the mass transfer characteristics will vary in a similar manner. Thus, for the mass transfer behaviour of MBC, there is not a single analogue but three - spray, bubble and packed columns. The mass transfer characteristics of these contactors are, therefore, briefly discussed below.

Liquid-phase mass transfer in fixed-bed packed columns is insensitive to gas flow rate below loading point. Onda, Sida, Kido and Tanaka (78) studied the absorption of pure carbon dioxide into water. The capacity coefficients were related for $1{,}000 < L < 30{,}000$ kg./(m^2.-hr.) by the equation

$$k_L a = AL^B \qquad (5.22)$$

where A and B are constants given in Table 5.5.

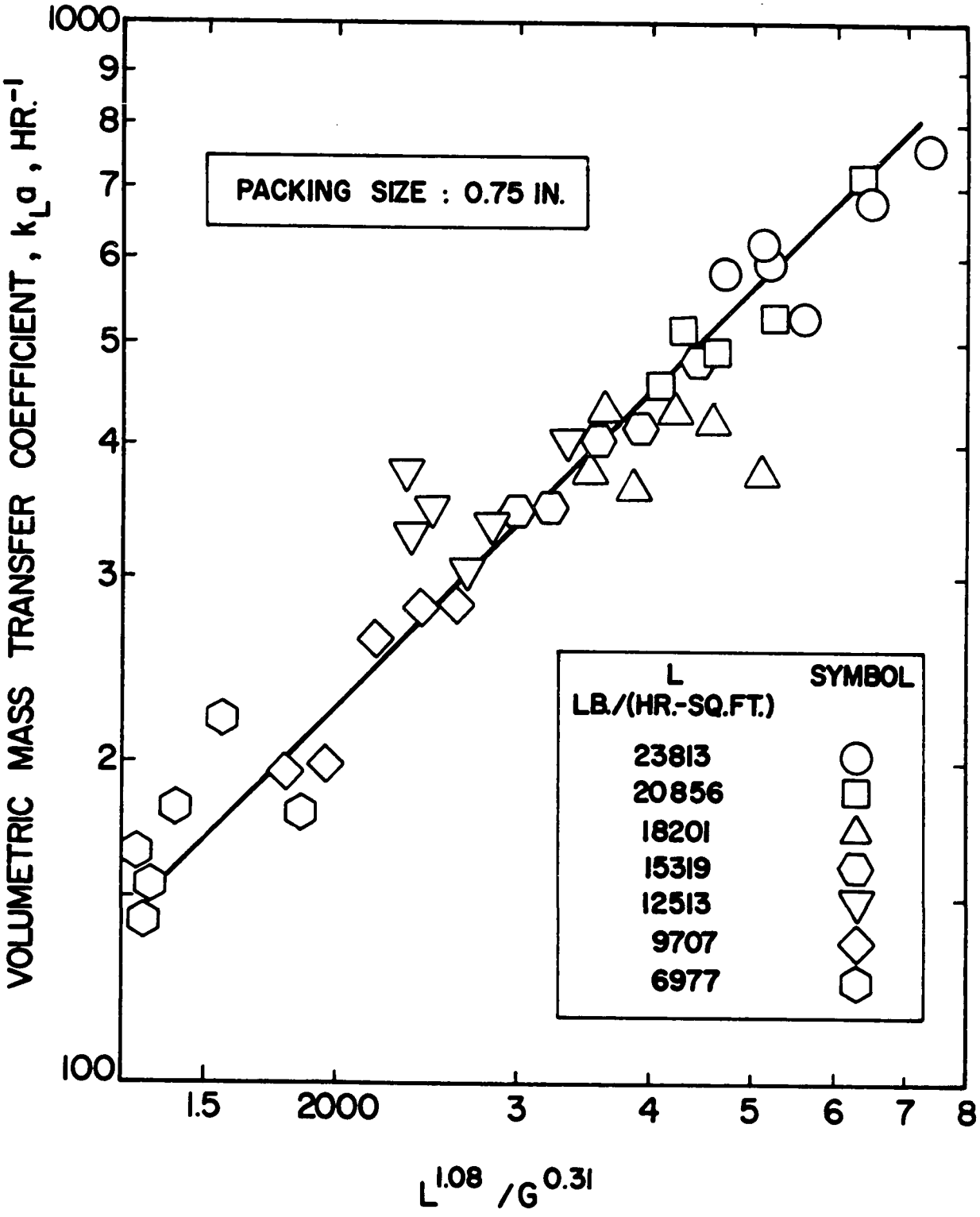

FIGURE 5.16: CORRELATION OF DATA ON VOLUMETRIC MASS TRANSFER COEFFICIENT FOR MOBILE-BED CONTACTING

TABLE 5.5

CONSTANTS AND EXPONENTS IN EQUATION (5.22)

Packing	A	B
0.5-inch Ceramic spheres	1.35×10^{-3}	0.90
1.0-inch Ceramic spheres	0.944×10^{-3}	0.87
1.33-inch Ceramic spheres	1.23×10^{-3}	0.86

Interpolating for 0.75-inch spheres, one arrives at the following equation:

$$k_L a = 1.15 \times 10^{-3} \; L^{0.885} \qquad (5.23)$$

where liquid mass velocity, L, is kg./m^2.-hr. and volumetric mass transfer coefficient, $k_L a$, is $hr.^{-1}$ The fact that the exponents for L in Equations (5.21) and (5.22) are quite close indicates that the effect of liquid flow rate in MBC is essentially similar to that for packed columns. The mass transfer interfaces in packed beds are constantly renewed by a combination of film phenomena. The liquid films in MBC are apparently considerably more turbulent than is the case in a packed bed, this effect being reflected by the much higher values of $k_L a$ than in a packed bed.

Bubble columns are characterized by no external mixing, low gas velocity (≈2 fpm) and in most cases practically zero liquid flow. However, Shulman and Molstad (152) examined the mass transfer characteristics of bubble columns in which there was a large downflow of water as the liquid phase. The specific system studied was absorption and desorption of carbon dioxide. The results are summarized in Table 5.4. Two distinctly different regions were observed. At low gas velocities, the rate of mass transfer increased with increasing gas velocity, but at high gas velocities, $k_L a$ became independent of gas velocity. The transition between the two regimes is characterized by a decrease in mass transfer rate, as may be noted from Table 5.4. The behaviour in the region of high gas flows could be partly due to effective reduction in the level of turbulence in the liquid adjacent to the bubble surfaces because of the onset of slug flow of the gas. Also, the mass transfer rates were of the same order of magnitude as packed beds at low liquid flow rates, and much higher mass transfer rates at high liquid flow rates. The increase in liquid flow rate results in more intense gas-liquid interaction which causes $k_L a$ to increase significantly.

Spray columns are characterized by liquid drops dispersed in a continuous gas phase. As can be seen from Table 5.2, liquid-phase transfer coefficients in spray columns are not strongly affected by large variations in gas velocity,

although $k_L a$ does increase significantly with liquid flow rate. However, more significant yet is the fact that the range of values of $k_L a$ for spray columns is very low, in the range 10 to 60 hr^{-1}. This low magnitude of $k_L a$ values is due to the very low level of fluid motion in the interior of tiny drops.

Thus, analysis of available data for liquid-phase mass transfer indicates that $k_L a$ can be varied over a wide range for both packed and bubble columns, depending upon the intensity of turbulence in the liquid phase. The rate of liquid-phase mass transfer in drops is, however, small. The observed behaviour of MBC as a mass transfer device can be interpreted as the result of a combination of the flow conditions typical of bubble columns, packed beds and spray columns.

Only two studies for mass transfer in MBC have been reported, and these are of very limited scope (147,149). Also, these studies were for systems for which gas-side resistance to mass transfer was predominant. Douglas et al. (147) observed that volumetric gas-phase mass transfer coefficients, $k_G a$, for MBC were 80-130 times higher than those for a large coke packed absorption tower which had been used for the same service. However, a large part of this improvement was no doubt due to the difficulty of wetting all the packing in the fixed-bed tower. Similar results were obtained by Douglas (149) in the study of ammonia absorption in water.

More insight into the mechanism of mass transfer in MBC can be obtained by studying the area-based mass transfer coefficient, k_L. As was done for effective interfacial area and volumetric mass transfer coefficient, the behaviour of k_L also will be analyzed in terms of the contributions to total mass transfer from the three types of gas-liquid interfaces present in MBC. Thus k_L may be expressed in terms of the coefficients and areas for drops, films and bubbles as follows:

$$k_L = \frac{k_L a}{a} = \frac{k_{LD} a_D + k_{LF} a_F + k_{LB} a_B}{a} \qquad (5.24)$$

As order of magnitude estimates for the three components of effective interfacial area in MBC are now available, and estimates can be made of the values of the transfer coefficients for each type of interface, the mass transfer results for MBC will be examined by comparison with predictions based on this approach.

Experimental values of k_L were obtained by dividing the corresponding values of volumetric mass transfer coefficient, $k_L a$, by effective interfacial area, a, as calculated from Equation (5.16). The results are shown in Figure 5.17(a) and (b) for the range of flow rates studied. An empirical correlation for estimating k_L was obtained by dividing Equation (5.21) by Equation (5.16):

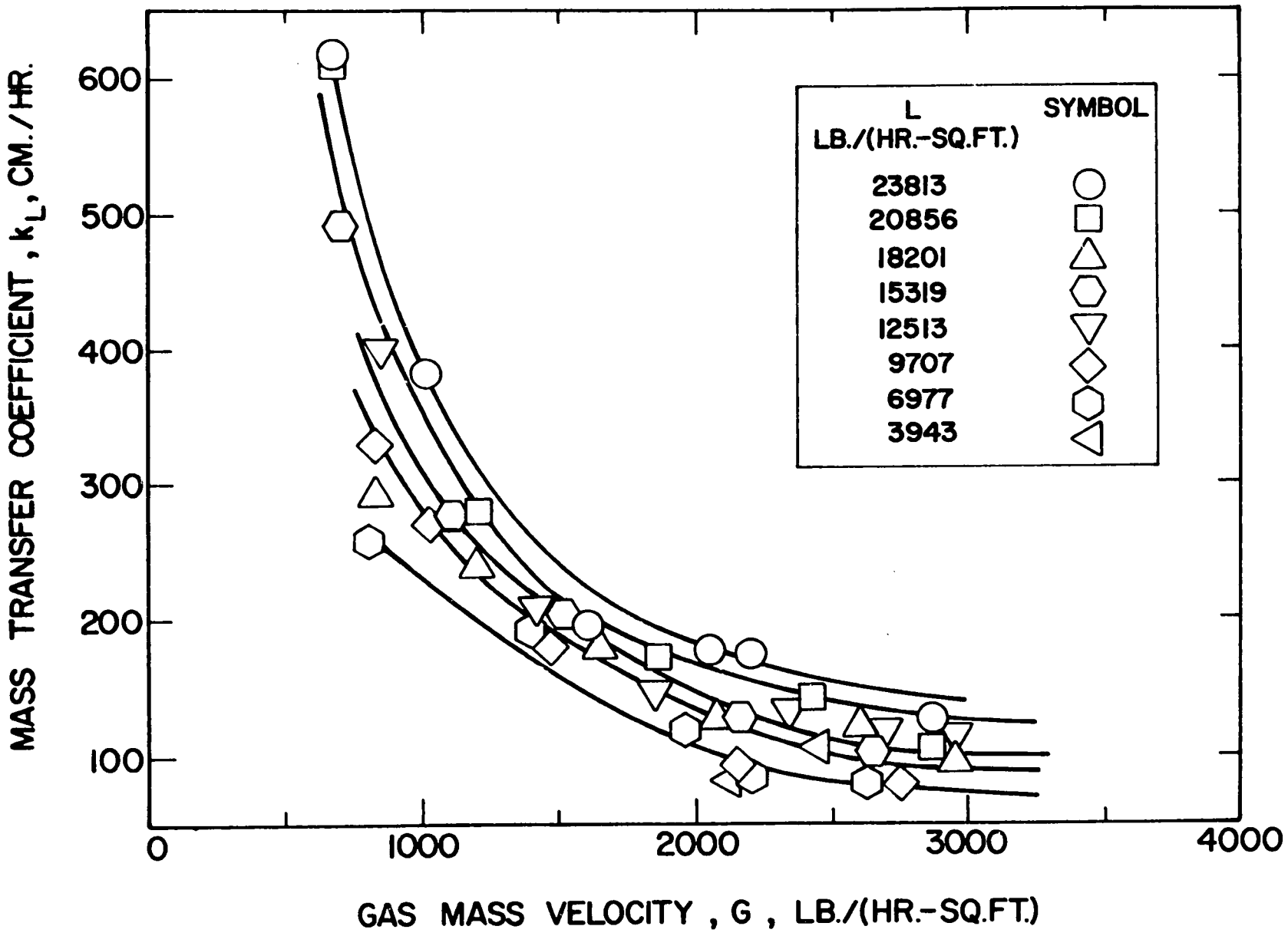

FIGURE 5.17(a): VARIATION MASS TRANSFER COEFFICIENT, k_L, WITH GAS AND LIQUID FLOW RATES IN MOBILE-BED CONTACTING (linear scale)

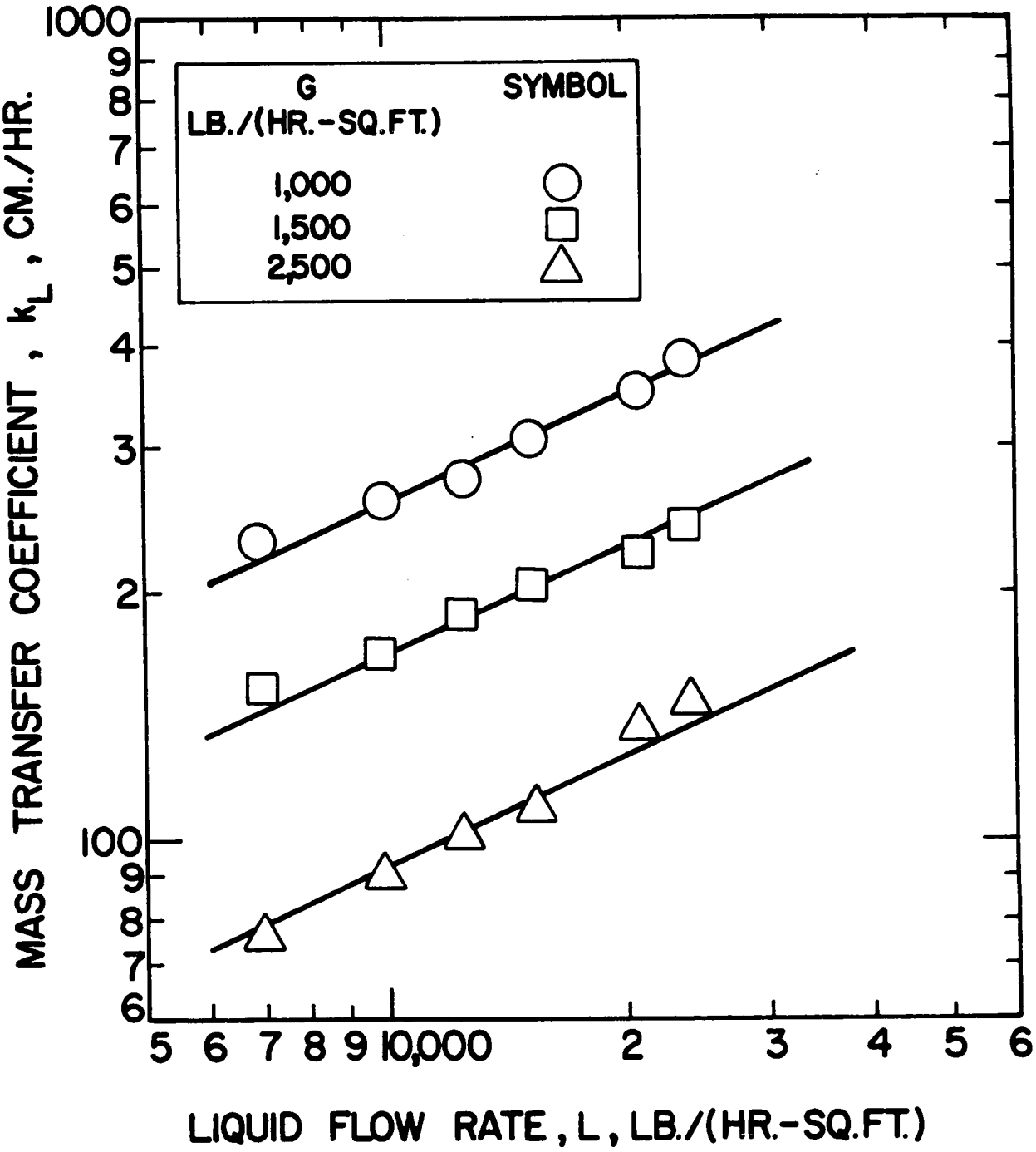

FIGURE 5.17(b): VARIATION MASS TRANSFER COEFFICIENT, k_L, WITH GAS AND LIQUID FLOW RATES IN MOBILE-BED CONTACTING (log scale)

$$k_L = 1.51 \times 10^4 \; L^{0.48} \; G^{-1.21} \qquad (5.25)$$

Figure 5.18 gives a comparison of experimental results with those obtained from Equation (5.25).

It is essential to recognize that the k_L shown on Figures 5.17(a) and (b) and given by Equation (5.25) represents an area-averaged value of k_L for the three different modes of mass transfer, as indicated by Equation (5.24). Because the proportionality between the three types of interfacial area changes appreciably over the range of flow conditions for which the equation applies, the exponents on L and G in Equation (5.25) bear no relationship to the corresponding exponents for any of the three contributing modes of mass transfer. The exponents of Equation (5.25) are in fact a direct reflection of the changing weighting factors for the three modes of transfer over the range of operation of MBC. The data presented in Tables 5.2 and 5.4 show small increases in mass transfer coefficients of drops, k_L, with gas flow in spray columns, a positive dependence of mass transfer coefficient due to bubbles, k_{LB}, on gas flow through bubble columns and almost zero dependence of mass transfer coefficient due to films, k_{LF}, on the gas flow through packed columns. However, in spite of positive or zero coefficients for the dependence on L for each of the component modes of transport, the weighted average k_L of Equation (5.25) shows a high negative coefficient on L due to variation in the weighting factors for the three modes.

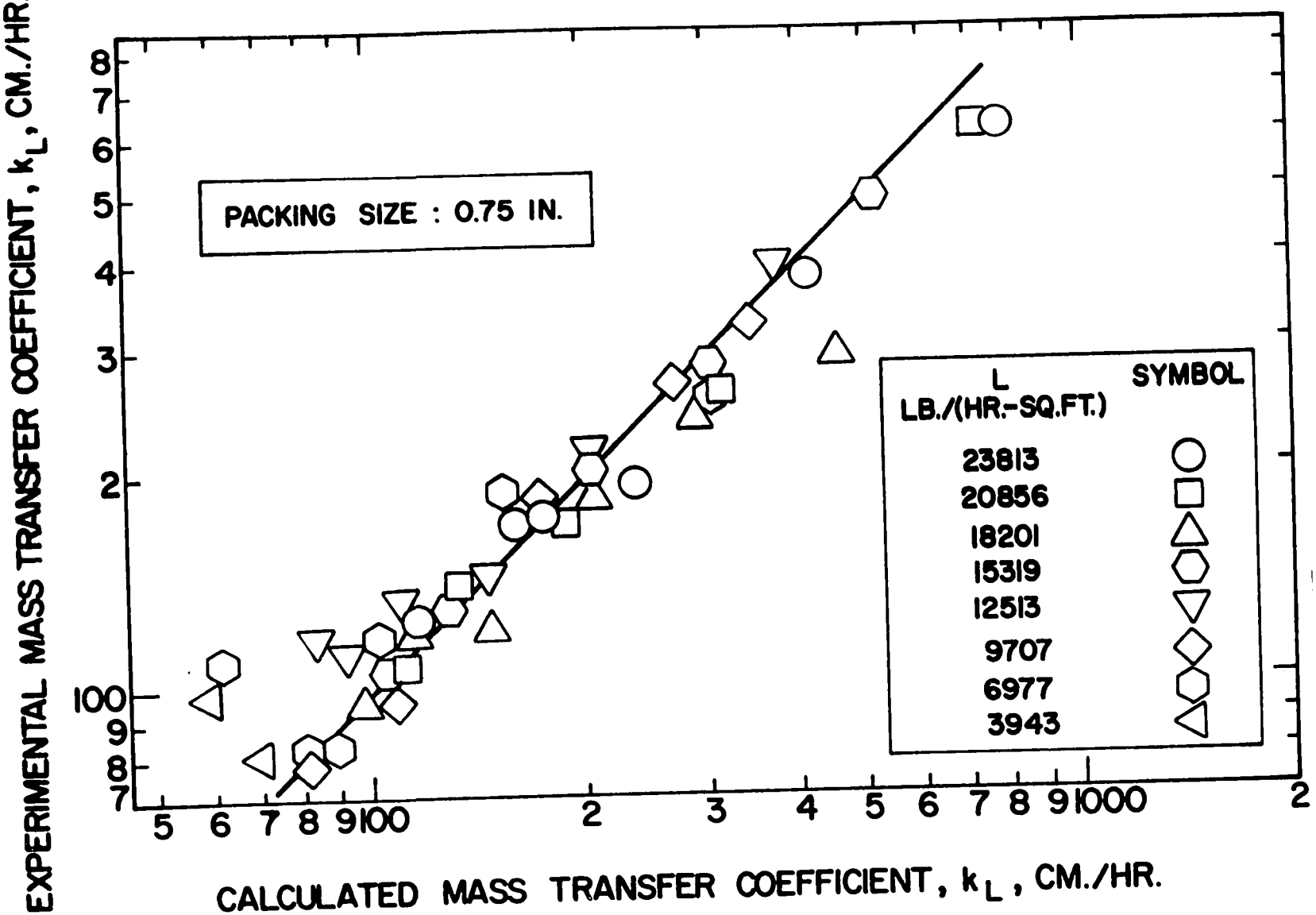

FIGURE 5.18: COMPARISON OF EXPERIMENTAL VALUES OF MASS TRANSFER COEFFICIENT, WITH CALCULATED VALUES FROM PROPOSED CORRELATION

Before proceeding further with analysis of mass transfer in MBC based on the application of Equation (5.24) it is necessary to estimate the values of k_{LD}, k_{LF} and k_{LB} which would apply for conditions in a mobile bed.

For a rigid sphere model of small drops

$$k_{LD} = 6.58 \frac{D}{d} \tag{5.26}$$

while for Kronig and Brink circulating large drops

$$k_{LD} = 17.90 \frac{D}{d} \tag{5.27}$$

Experimental rates have been found to vary from those for rigid spheres in the case of highly viscous liquids, upto three or four times the Kronig and Brink rate for fluids of low viscosities. The mass transfer coefficients for small non-circulating drops is generally an order of magnitude smaller than for turbulent liquid flims. The values of k_L shown in Tables 5.2 and 5.3 confirm this behaviour. The data given in Table 5.2 are used to estimate k_L for drops.

The magnitude of the transfer coefficient in the case of turbulent liquid films depends on the rate of surface renewal and is given for Danckwert's model of mass transfer as $k_L \propto \sqrt{Ds}$. The experimentally measured values given in Table 5.3 indicate that small values of k_L of 10-180 $hr.^{-1}$ occur for the relatively calm conditions of a packed bed. As liquid flow conditions in MBC are much more turbulent, one should expect a significantly higher mass transfer coefficient.

Figure 5.17(a) shows that this is indeed so at low gas velocities where the liquid flows primarily as liquid films, the contributions due to drop and bubble phenomena being still quite small.

A further complication with respect to estimating the value of k_{LF} results from the presence of swarms of tiny gas bubbles dispersed in the liquid. The extent of this effect is appreciable as indications are that, at high rates of fluid flow, more than half of the interfacial area may be present in this form. The presence of small bubbles no doubt alters the structure of turbulence in the liquid phase, including the interfacial region. If the presence of bubbles acts as a turbulence suppressor in the liquid, the film mass transfer coefficient could be appreciably reduced in the case of MBC.

The behaviour with respect to liquid-phase mass transfer of bubble columns for which there is a significant downflow of liquid is given in Table 5.4. The range of variation of k_{LB} is very large, from 7 to 180 cm./hr. The estimates for transfer coefficients in agitated and non-agitated gas-sparged reactors which are shown in Table 5.6 indicate a range of k_{LB} from 12 to 110 cm/hr. It is particularly significant to note that when high shear rates are applied to the liquid by means of mechanical agitation, the increase in k_L is strongly determined

TABLE 5.6

MASS TRANSFER IN AERATED SYSTEMS

Bubble Size	G lb./hr.-sq.ft.	Agitation	$k_L a$ $hr.^{-1}$	Estimated a cm^{-1}	Estimated k_L cm./hr.
small (< 2 mm)	25	No	48	4	12
large (> 2 mm)	25	No	48	3	16
large	250	No	450	4	110
small	25	High	192	6	32
large	25	High	480	5	96

by the bubble diameter. For the agitation used, k_L increases by a factor of about 2.5 for small bubbles (diameter < 2 mm.) but by about a factor of 6 for larger bubbles. It is believed that the bubbles present in MBC operation are in the small range, less than 2 mm. in diameter. Thus the mass transfer coefficient, k_{LB}, for the bubble area in MBC is probably not strongly dependent on the mixing conditions which prevail.

An order-of-magnitude estimate can now be made for MBC. For conditions just above minimum fluidization, the interfacial area is believed to be mostly film area in a quite turbulent state such that $a_F = 1$ cm.$^{-1}$ and $k_{LF} = 600$ cm/hr. $= k_L$. For MBC conditions approaching the upper limit of possible fluid flow rates considerable drop and bubble phenomena occur, and one can estimate

$$k_{LD} = 100 \text{ cm/hr.}, \quad a_D = 0.5 \text{ cm.}^{-1}$$

$$k_{LF} = 600 \text{ cm/hr.}, \quad a_F = 1 \text{ cm.}^{-1}$$

$$k_{LB} = 80 \text{ cm/hr.}, \quad a_B = 2.5 \text{ cm.}^{-1}$$

whence from Equation (5.24),

$$k_L = \frac{100 \times 0.5 + 600 \times 1.0 + 80 \times 2.5}{(0.5 + 1.0 + 2.5)}$$

$$= 212 \text{ cm/hr.}$$

This estimate is probably somewhat high because of the assumption that the value of $k_{LF} = 600$ cm/hr. does not decrease as the bubble population increases. No quantitative basis is available for estimating this effect. If it were estimated that

k_{LF} = 400 cm./hr., the weighted average value of k_L would be 162 cm./hr. for MBC at high flow rates. From Figure 17(a) it can be seen that at L = 24000, G = 3000 lb./hr.-sq.ft., the value of k_L is about 150 cm./hr. Errors enter the prediction due to lack of complete and appropriate data for liquid-phase mass transfer for films, droplets and bubbles, and to the further difficulty of definition of flow conditions affecting these modes of transfer within a mobile bed. However, such close agreement between the actual and predicted values, considering the difficulties associated with the prediction, confirms the validity of the basic approach. This analysis of the mass transfer results also confirms that the apparent effect of gas and liquid flow rate on the mass transfer coefficient for MBC is in fact only reflection of the changing relative importance of transport across the quite different interfaces of films, bubbles, and droplets all of which co-exist within a mobile bed.

5.2.3 CONCLUSION

Three modes of mass transfer in MBC have been identified. The mass transfer which occurs across liquid films is similar to that in a packed bed, except that the combined effects of the shearing action of the moving balls and the higher rates of countercurrent gas-liquid flow produce more turbulent conditions with a higher rate of surface renewal and

thereby, larger values of k_L. The other two modes of transport correspond to those for droplets in spray towers and bubbles in gas-sparged vessels or bubble columns. The area-based transfer coefficients for both these modes are much less than for liquid films. As the proportion of dispersed area, as bubbles and drops, increases with gas flow rate in a mobile-bed, the effect on the mass transfer coefficient which measures the cumulative mass transfer is for a strong decrease in k_L at limiting values of high gas rate. The increase of total interfacial area with gas flow rate due to small droplets and swarms of bubbles produced is however sufficiently large that the volumetric mass transfer coefficient, k_La, decreases only moderately with increasing gas velocity. The net effect is that liquid-phase mass transfer rates are much higher in mobile-bed contacting than for other gas-liquid contactors.

VI. SUMMARY AND CONTRIBUTION TO KNOWLEDGE

Mobile-bed contacting was studied in a 5.5-inch diameter column over the range of gas and liquid flow rates $200 < G < 3{,}600$ and $4000 < L < 25{,}000$ lb./hr.-ft.^{2} with packing of density 0.15 gm./cc. The results are of two types:

- HYDRODYNAMIC EFFECTS; including minimum fluidization velocity, bed expansion, liquid holdup and axial mixing of the liquid, and
- MASS TRANSFER EFFECTS; including effective interfacial area and liquid-phase mass transfer coefficient.

The important features of this study can be summarized as follows:

1. The determination of residence time distribution by the method of transfer function analysis, as presented recently by Ostergaard (105) and Michelsen and Ostergaard (103), has been extended to include the case of finite-bed boundary conditions which give a better representation of a real system. With this extension, the method has been applied in determining axial mixing of the liquid phase in a mobile-bed contactor. The dispersion model is found to give a good representation of the liquid flow. Axial mixing in MBC was determined for four sphere sizes, 0.5, 0.75, 1.0 and 1.5-inch. The results for 1.5-inch spheres are not reliable as they are significantly influenced by

wall effect. Liquid mixing, characterized as Peclet number, changes in the direction of plug flow when either liquid flow rate or sphere diameter is increased, and towards a more completely mixed state when gas flow rate is increased, The increase in Peclet number with packing size or liquid rate is interpreted as resulting from a decrease in the tortuosity of the liquid flow path. Increased gas rate on the other hand increases the stirring action, hence leads to decreased Peclet numbers. A graphical correlation of Peclet number as a function of these variables is presented. An aspect of the results which is of direct relevance to the economics of industrial application is that the general level of mixing conditions in MBC is appreciably closer to plug flow than was indicated by a previous study of more limited scope.

2. Minimum fluidization velocity, G_{mf}, was studied and a correlation is presented for use in the design of MBC:

$$G_{mf} = 1570\, d^{1.5} \times 10^{-4.3} \times 10^{-5L}$$

for $4{,}000 < L < 25{,}000$ lb./hr.-ft.^{2}

This correlation predicts values of G_{mf} which are in good agreement up to sphere size of 1.0 in.; some deviation from the predicted values is observed for the case of 1.5-inch spheres because of wall effect.

2. Bed expansion for MBC is correlated by:

$$h = 1.5 \times 10^{-4} \Delta G_{mf}^{1.2}$$

where $h = \frac{H - h_s}{h_s}$, and $\Delta = \frac{G - G_{mf}}{G_{mf}}$

This correlation is valid for 0.75- and 1.0-inch spheres, and would probably apply for 0.5-inch spheres in a larger column. In the 5.5-inch diameter column there was a severe problem of the 0.5-inch balls sticking to the walls and agglomerating within the bed, so the bed expansion results for 0.5-inch spheres are not considered representative. The magnitude of the wall effect for 1.5-inch spheres did not seem as serious for bed expansion as in the case of the other measurements.

For systems using similar packing of 0.15 gm./cc. density and a supporting grid of 70% free area, both G_{mf} and bed expansion can be predicted with reasonable accuracy.

4. Liquid holdup was determined for all sphere sizes,but results for the smallest and largest spheres (0.5 and 1.5-inch) are unreliable for the reasons noted in connection with the bed expansion data. Liquid holdup increases with liquid flow rate and decreases with packing size. With gas flow rate, holdup decreases as gas velocity increases above the minimum fluidization velocity and either approaches a constant value or, in some cases, begins to increase again at high gas velocity. Graphical representation of holdup data is presented.

5. For trickle-bed operation (no gas flow) liquid holdup and liquid-phase mixing were determined for spherical packing by the same technique as used for the MBC study, i.e. by pulse testing using simultaneous two-point measurements. The results in both

cases agree well with those of other workers except for the case of the 1.5-inch packing which give anomalously low values of holdup and high values of dispersion coefficient because of the presence of wall effect.

6. The various hydrodynamics results taken together form a consistent pattern of the physical behaviour of a mobile-bed contactor. Some limits have been established for conditions of operation as a uniformly mobile bed and without significant wall effect. Large differences between the liquid mixing results of Chen and Douglas on a 1.5-inch diameter column and the present investigation with a 5.5-inch column indicate that until further study resolves the disagreement, care must be exercised in applying laboratory results for scale-up to larger units. As large discrepancies exist in the numerous results for mixing in countercurrent gas-liquid flow through fixed-bed contactors, it is not surprising that the hydrodynamics of the much more recent mobile-bed technique remain as yet imperfectly understood.

7. Three distinct types of interfacial areas, droplet, film and bubble area, have been identified as contributing to the total effective interfacial area in MBC. At the condition of minimum fluidization, total interfacial area is about 1 cm^{-1}., most of which is area of liquid films. For high fluid flow rates near the upper physical limit of operation of MBC the total interfacial area is about 4 $cm.^{-1}$, and this is now

believed to be distributed approximately as 2.5 $cm.^{-1}$ from bubbles, 1.0 $cm.^{-1}$ from films, and 0.5 $cm.^{-1}$ from droplets. The dependence of total interfacial area

$$a = 7.56 \times 10^{-6} L^{0.6} G^{0.9} \quad \text{(0.75-inch spheres)}$$

is consistent with the effect of gas and liquid flow on the three components of total interfacial area.

This finding indicates that MBC has attributes to a varying extent of three older classes of gas-liquid contactors - packed beds, spray columns, and aerated processes such as bubble columns and gas-sparged vessels. Thus MBC operation varies from a lower limit which is similar to a packed bed in the loading region with continuous liquid film flow, to the other extreme of a highly dispersed gas (as bubbles) and liquid (as droplets) system.

8. Liquid-phase mass transfer in MBC, determined with appropriate allowance for the effect of axial dispersion in the liquid phase, has been analysed on the basis of the contributions made by mass transfer in droplets, films and bubbles. The liquid-phase volumetric mass transfer coefficients are correlated by

$$k_L a = 0.113 L^{1.08} G^{-0.31}$$

and the area-based mass transfer coefficient as

$$k_L = 1.51 \times 10^{4} L^{0.48} G^{-1.21}$$

These correlations are valid over the entire range of stable operation of MBC and result from the continuous changes in contribution to total mass transfer made by drop, film and bubble phenomena with changing gas and liquid flow rate. Order-of-magnitude calculations show that the overall values of mass transfer coefficient which were measured are in general agreement with predictions based on the contributions by mass transfer through bubbles, films, and droplets, where the contributions are weighted according to the relative proportions of each type of area. This analysis of the mass transfer behaviour reinforces the interpretation of MBC as having varying degrees of similarity to three other classes of gas-liquid contactor - packed beds, aerated processes, and spray columns. Finally, mass transfer rates in MBC are found to be superior to the older contacting processes.

SUGGESTIONS FOR FUTURE WORK

Hydrodynamic behaviour of MBC appears to be strongly influenced by the size of the unit and the packings used. One of the important parameters that could provide some insight into the flow behaviour of MBC is the pressure drop. It would be interesting to examine the relationship between pressure drop and physical parameters like bed expansion, minimum fluidization velocity, properties of the fluids, packing size and density and geometry of the supporting grid. Less subjective criteria for measurement of bed expansion and minimum fluidization velocity are needed.

In reacting systems the extent of mixing in the gas phase determines the conversion that would be obtained in an MBC reactor. Knowledge of the flow behaviour of gas in MBC is therefore required. Since the residence time of gas in MBC is very short ($\approx$ 0.1 sec.) it is rather difficult to determine the residence time distribution in a two-phase flow system by transient response experiments. However, it may be feasible to obtain RTD for the gas phase from steady-state conversion obtained for a system where gas undergoes a chemical reaction of accurately known kinetics.

Although the diffusion model has been quite satisfactory in the present study, there is need for better models for characterizing mixing. The statistical approach to this problem may be applicable in future studies.

REFERENCES

1. Fenske, M.R., C.O. Tongberg and D. Quiggle, Ind. Eng. Chem., 26, 1169 (1934).

2. Furnas, C.C. and F.M. Bellinger, Trans. A.I.Ch.E., 34, 251 (1938).

3. Shulman, H.L., C.F. Ullrich and N. Wells, A.I.Ch.E.J., 1, 247 (1955).

4. Onda, K., E. Sada and Y. Murase, A.I.Ch.E.J., 52, 235 (1959).

5. Varrier, C.B.S. and K.R. Rao, Trans. Indian Inst. Chem. Engrs., 13, 29 (1960-61).

6. Davidson, J.F., Trans. Inst. Chem. Engrs., (London), 37, 131 (1959).

7. Uchida, S. and S. Fujita, J. Soc. Chem. Ind. (Japan), 39, 876, 432B (1936)., 40, 538, 238B (1937), 41, 563, 275B (1938).

8. Shulman, H.L., C.G. Savini and R.V. Edwin, A.I.Ch.E.J., 9, 479 (1963).

9. Cooper, C.M., R.J. Christl and L.C. Perry, Trans. A.I.Ch.E., 37, 979 (1941).

10. Mayo, F., T.G. Hunter and A.W. Nash, J. Soc. Chem. Ind. (London), 54, 375T (1935).

11. Payne, J.W. and B.F. Dodge, Ind. Eng. Chem., 24, 630 (1932).

12. Simmons, C.W. and H.B. Osborn, Jr., Ind. Eng. Chem., 26, 529 (1934).

13. Elgin, J.C. and F.B. Weiss, Ind. Eng. Chem., 31, 435 (1939).

14. Elgin, J.C. and B.W. Jesser, Trans. A.I.Ch.E., 39, 377 (1943).

15. Shulman, H.L., C.F. Ullrich, N. Wells and A.Z. Proulx, A.I.Ch.E.J., 1, 259 (1955).

16. Otake, T. and E. Kunugita, Chem. Eng. (Japan), 22, 144 (1958).

17. White, A.M., Trans. A.I.Ch.E., 31, 390 (1935).

18. Buchanan, J.E., Ind. Eng. Chem. Fundamentals, 6, 400 (1967).

19. Gelbe, H., Chem. Eng. Sci., 23, 1401 (1968).

20. Otake, T. and K. Okada, Kagaku Kogaku, 17, 176 (1953).

21. Mohunta, D.M. and G.S. Laddha, Chem. Eng. Sci., 20, 1069 (1965).

22. Khanna, R.T., McGill Univ., Master's Thesis, April 1966.

23. De Maria, F. and R.R. White, A.I.Ch.E., 6, 473 (1960).

24. Schiesser, W.E. and L. Lapidus, A.I.Ch.E.J., 7, 163 (1961).

25. Chen, B.H., Ph.D. Thesis, McGill Univ., April 1965.

26. Hwa, C.S. and R.B. Beckman, A.I.Ch.E.J., 6, 359 (1960).

27. Standish, N., Ind. Eng. Chem. Fundamentals, 7, 312 (1968).

28. Gel'prin, N.T., V.Z. Grishko, V.I. Savchenko and V.M. Shchedro, Chem. and Pet. Eng., 1, 36 (1966).

29. Chen, B.H. and W.J.M. Douglas, Can. J. Chem. Eng., 245 (1968).

30. Shulman, H.L., C.F. Ullrich, A.Z. Proulx and J.O. Zimmerman, A.I.Ch.E.J., 1, 253 (1955).

31. Whitt, F.R., Brit. Chem. Eng., 1, 43 (1956).

32. Whitt, F.R., Brit. Chem. Eng., 3, 179 (1960).

33. Fujita, S. and S. Sakuma, Chem. Eng. (Japan), 18, 64(1954).

34. Hikita, H. and T. Kataoka, Chem. Eng. (Japan), 20, 528 (1956).

35. Hikita, H. and T. Kataoka, Chem. Eng. (Japan), 24, 2 (1960).

36. Onda, K., Chem. Eng. (Japan), 24, 490 (1960).

37. Yoshida, F. and T. Koyanagi, Ind. Eng. Chem., 50, 365 (1958).

38. Yoshida, F. and T. Koyanagi, A.I.Ch.E.J., 8, 309 (1962).

39. De Wall, K.J.A. and W.J. Beek, Chem. Eng. Sci., 22, 585 (1967).

40. De Wall, K.J.A., A.C. van Mameren and P.V. Rottenburg, Transport Phenomena, Inst. of Chem.Engrs. (London), Sym. Series, 6, 60 (1965).

41. Danckwerts, P.V. and A.J. Gillham, Trans. Inst. Chem. Engrs. 44, T42 (1966).

42. Vidwans, A.D. and M.M. Sharma, Chem. Eng. Sci., 22, 673 (1967).

43. Jhaveri, A.S. and M.M. Sharma, Chem. Eng. Sci., 23, 669 (1968).

44. Mannford-Doble, M., Ph.D. Thesis, University of Cambridge (1966).

45. Yoshida, F. and Y. Miura, A.I.Ch.E.J., 9, 331 (1963).

46. Fellinger, L., Sc.D. Thesis, Mass. Inst. Tech., Mass. (1941).

47. Danckwerts, P.V., Ind. Eng. Chem., 43, 1460 (1951).

48. Higbie, R., Trans. A.I.Ch.E., 31, 365 (1935).

49. Danckwerts, P.V., Trans. Farad. Soc., 47, 1014 (1951).

50. Richards, G.M., G.A. Ratcliff and P.V. Danckwerts, Chem. Eng. Sci., 19, 325 (1964).

51. Porter, K.E., Trans. Inst. Chem. Engrs., 44, T25 (1966).

52. Sharma, M.M., R.A. Mashlekar and V.D. Mehta, Brit. Chem. Eng., 14, 70 (1969).

53. Danckwerts, P.V. and M.M. Sharma, Trans. Inst. Chem. Engrs., 44, CE244 (1966).

54. Porter, K.E., Trans. Inst. Chem. Engrs., 41, 320 (1963).

55. Rodionov, A.I. and A.A. Vinter, Intnl. Chem. Eng., 7, 468 (1967).

56. Pohorecki, R., Chem. Eng. Sci., 23, 1447 (1968).

57. Sharma, M.M. and R.A. Mashelkar, Tripartite Chem. Eng. Conf., Sym. on Mass Transfer with Chemical Reaction, Montreal, Session 2, 14 (1968).

58. Astarita, G., G. Marcucci and L. Coliti, Li Chimica Industries,46, 9 (1964).

59. Francis, R.C. and J.C. Berg, Chem. Eng. Sci., 22, 685 (1967).

60. Eben, C.D. and R.L. Pigford, Chem. Eng. Sci., 20, 9 (1965).

61. Porter, K.E., M.B. King and K.C. Varshney, Trans. Inst. Chem. Engrs., 44, T274 (1966).

62. Calderbank, P.H., Trans. Inst. Chem. Engrs., 36, 443 (1958).

63. Ibid, 37, 173 (1959).

64. Dillon, G.B. and I.J. Harris, Can. J. Chem. Eng., 44, 307 (1966).

65. Westerterp, K.R., L.L. van Dierendonck, and de Kraa, Chem. Eng. Sci., 18, 157 (1963).

66. Banerjee, S., Ph.D. Thesis, University of Waterloo, Waterloo, Ont. (1968).

67. Calderbank, P.H., F. Evans, and J. Rennie, Part I and II, Proceedings of the International Symposium on Distillation, Brighton, Inst. Chem. Engrs., London, May 1960.

68. Quigley, C.J., A.I. Johnson, B.L. Harris, Chem. Eng. Progr., Sym. Series., 51 (16), 31 (1955).

69. Mehta, K.C. and M.M. Sharma, Brit. Chem. Eng., 15(11), 1440-44(1970), 15, (12), 1556-58 (1970).

70. Sherwood, T.K. and F.A.L. Holloway, Trans. A.I.Ch.E., 36, 39 (1940).

71. Molstad, M.C., J.F. McKinney and R.G. Abbey, Trans. A.I.Ch.E., 39, 605 (1943).

72. Deed, D.W., P.W. Schultz and T.B. Drew, Ind. Eng. Chem., 39, 766 (1947).

73. Van Krevelen, D.W. and P.J. Hoftijzer, Rec. Trav. Chim., 66, 49 (1947).

74. Fujita, S. and T. Hayakawa, Chem. Eng. (Japan), 20, 113 (1956).

75. Hikita, H., Chem. Eng. (Japan), 26, 725 (1962).

76. Onda, K., E. Sada and Y. Murase, A.I.Ch.E.J., 5, 235 (1959).

77. Onda, K., E. Sada and M. Saito, Chem. Eng. (Japan), 25, 820 (1961).

78. Onda, K., E. Sada, C. Kido and A. Tanaka, Chem. Eng. (Japan), 27, 140 (1963).

79. Vivian, J.E. and D.W. Peaceman, A.I.Ch.E.J., 2, 437 (1956).

80. Mada, J. and H. Shinohara, Kagaku Kogaku, 28, 159 (1964).

81. Bischoff, K.B., Chem. Eng. Sci., 12, 69 (1960).

82. Schmalzer, D.K. and H.E. Hoelscher, A.I.Ch.E.J., 17, 1, 104-110 (1971).

83. Astarita, G., "Mass Transfer with Chemical Reaction", Elsevier Publishing Company, New York (1967).

84. Van Krevelen, D.W. and P.J. Hoftijzer, Rec. Trav. Chim., 67, 133 (1948).

85. Van Krevelen, D.W. and P.J. Hoftijzer, Chem. Eng. Sci., 2, 145 (1953).

86. Van Krevelen, D.W., Chem. Ing. Techn., 30, 551 (1958).

87. Brian, P.L.T., J.F. Hurley and E.H. Hasseltine, A.I.Ch.E.J., 7, 226 (1961).

88. Pearson, J.R.A., Appl. Scient. Res., AX1, 321 (1963).

89. Danckwerts, P.V., Chem. Eng. Sci., 2, 1 (1953).

90. Carberry, J.J. and R.H. Bretton, A.I.Ch.E.J., 4, 367 (1958).

91. Cairns, E.J. and J. Prausnitz, A.I.Ch.E.J., 6, 400 (1960).

92. Cairns, E.J. and J. Prausnitz, Chem. Eng. Sci., 12, 20 (1960).

93. Miyauchi, T. and T. Vermeulen, Ind. Eng. Chem. Fundamentals, 2, 113 (1963).

94. Sater, V.E. and Levenspiel, Ind. Eng. Chem. Fundamentals, 5, 86 (1966).

95. Kramers, H. and G. Alberda, Chem. Eng. Sci., 2, 173 (1953).

96. Mason, D.R. and E.L. Piret, Ind. Eng. Chem., 42, 817 (1950).

97. Deans, H.A. and L. Lapidus, A.I.Ch.E.J., 6, 656 (1960).

98. Levenspiel, O, C.J.Ch.E., 40, 135 (1962).

99. Levenspiel, O. and K.B. Bischoff, "Advan. in Chem. Eng.", 4, 95-198 (1963).

100. Einstein, H.A., Ph.D. Thesis, Eidg. Techn. Hochschule, Zurich (1937).

101. Vermeulen, T., Lawrence Radiation Laboratory Report,UCRL-8658, Univ. of Calif., Berkeley, April 1959.

102. Jacques, G.L. and T. Vermeulen, Lawrence Radiation Laboratory, Univ. of Calif., Berkeley, Report UCRL-8029 (1958).

103. Michelsen, M.L. and K. Ostergaard, Chem. Eng. Sci., 25, 583-592 (1970).

104. Lees, F.P., Chem. Eng. Sci., 24, 1607-1613 (1969).

105. Ostergaard, K., "Studies of Gas-Liquid Fluidization", I Kommission Hos Teknisk Forlag (1969).

106. Hoogendoorn, C.S. and J. Lips, C.J.Ch.E., 43, 125 (1965).

107. Van Deemter, J.J., F.J. Zuiderweg and A. Klinkenberg, Chem. Eng. Sci., 5, 271 (1956).

108. Hofmann, H., Chem. Eng. Sci., 14, 193 (1961).

109. Weber, H.H., Untersuchungen uber die Verweilzeiteilung in Aufstromkolonnen. Diss., Tech. Hochschule, Darmstadt, Germany, 1961.

110. Harrison, D., M. Lane and D.J. Walne, Tran. Inst., Chem. Engrs., 40, 214 (1962).

111. Stemerding, S., Chem. Eng. Sci., 14, 209 (1961).

112. Otake, T., E. Kunugita and T. Yamanishi, Chem. Eng. (Japan), 26, 800 (1962).

113. Word, T.T., Lawrence Radiation Laboratory, University of California, Berkeley, Report UCRL-9844, September (1961).

114. Dunn, W.E., T. Vermeulen, C.R. Wilkie and T.T. Words, Lawrence Radiation Laboratory Report UCRL-10394, Univ. of Calif., Berkeley, July 1962.

115. Chen, B.H. and W.J.M. Douglas, C.J.Ch.E., 47, 113 (1969).

116. Kunugita, E.T., T. Otake and K. Yoshii, Chem. Eng. (Japan), 26, 672 (1962).

117. Pearson, J.R.A., G.M. Richards and H. Skoczylas, Chem. Eng. Sci., 19, 82 (1964).

118. Lelli, U., Ind. Eng. Chem. Fundamentals, 4, (3), 360 (1965).

119. Sleicher, C.A., A.I.Ch.E.J., 5, 145 (1959).

120. Miyauchi, T., A.K. McMullen and T. Vermeulen, UCRL-3911, Rev. 1960 (Washington: U.S. Atomic Energy Commission).

121. Stemerding, S. and F.J. Zuiderweg, Trans. Instn. Chem. Engrs., 41, CE 156 (1963).

122. Rod, V., Brit. Chem. Eng., 9, 300 (1964).

123. Ibid., 11, 483 (1966).

124. Tepe, J.B. and B.F. Dodge, Trans. A.I.Ch.E., 39, 255 (1943).

125. Sater, V.E., Ph.D. Thesis, Illinois Institute of Technology, Chicago, Ill., p. 127, January 1963.

126. Hartland, S. and J.C. Mecklenburgh, Chem. Eng. Sci., 21, 1209 (1966).

127. J.C. Mecklenburgh and S. Hartland, Chem. Eng. Sci.,23 57 (1968).

128. Ibid., 23, 67 (1968).

129. Ibid., 23, 81 (1968).

130. Ibid., 23, 1421 (1968).

131. Furzer, I.A. and G.E. Ho, Chem. Eng. Sci., 25, 1297-1300 (1970).

132. Sullivan, G.A. and R.E. Treybal, The Chemical Engineering Journal, 1, 302-10 (1970).

133. Van der Laan, E.T., Chem. Eng. Sci., 7, 187 (1958).

134. Wehner, J.F. and R.H. Wilhelm, Chem. Eng. Sci., 6, 89 (1956).

135. Ibid., 8, 309 (1958).

136. Fan, L.T. and Y.K. Ahn, CEP Sym. Series, 59, 946 (1963).

137. Van Cauwenberghe, A.R., Chem. Eng. Sci., 21, 203-5 (1966).

138. Brenner, H., Chem. Eng. Sci., 17, 229 (1962).

139. Yagi, S. and T. Miyauchi, Chem. Eng. (Japan), 17, 382 (1953).

140. Miyauchi, T., Lawrence Radiation Laboratory, University of California, Berkeley, Report UCRL-3911 (1957).

141. McMullen, A.K., T. Miyauchi and T. Vermeulen, Lawrence Radiation Laboratory, Univ. of California, Berkeley, Report UCRL-3911 Supplement (1958).

142. Miyauchi, T. and T. Vermeulen, Ind. Eng. Chem. Fundamentals, 2, 304 (1963).

143. Hennico, A., G. Jacques, and T. Vermeulen, UCRL-10696 (1963).

144. Vogel, A.I., A Text-Book of Quantitative Inorganic Analysis, 2nd Ed., Longmans (1957).

145. Remilleux, par J., A.T.I.P. Bull. No. 2, 19, 94 (1965).

146. Kielback, A.W., Chem. Eng. Prog.,Symp. Ser.,57 (35), 51 (1961).

147. Douglas, H.R., I.W.A. Snider and G.H. Tomlinson, Chem. Eng. Prog., 59 (12), 85 (1963).

148. Kielback, A.W., Paper Presented at A.I.Ch.E. Meeting, December 1960.

149. Douglas, W.J.M., Chem. Eng. Prog., 60 (7), 66 (1964).

150. Blyakher, I.G., L. Ya. Zhivaikin and N.A. Yurovakaya, Intnl. Chem. Eng., 7, 485 (1967).

151. Levsh, I.P., N.I. Krainev and M.I. Niyazov, Intnl. Chem. Eng., 8, 311 (1968).

152. Shulman, H.L. and M.C. Molstad, Ind. Eng. Chem., 42, 1058 (1950).

153. Rabin, I., Bechtel Corp., Private Communication.

154. Perry, R.H., Chemical Engineer's Handbook, p. 700, 3rd. Ed., 1948.

155. Nijsing, R.A.T.O., R.H. Hendriksz, and H. Kramers, Chem. Eng. Sci., 10, 88 (1959).

156. Thomas, W.J. and M.J. Adams, Trans. Faraday Society, 61, 668 (1965).

157. van Krevelen, D.W. and P.V. Hoftyzer, Chimie et Industrie: Numéro Spéciale du XXIe Congrès International de Chimie Industrielle, Bruxelles, Sept., 168 (1948).

158. Roberts, D. and P.V. Danckwerts, Chem. Eng. Sci., 17, 961 (1962).

159. Nijsing, R.A.T.O. and H. Kramers, Chem. Eng. Sci., 8, 81 (1958).

AUTHOR INDEX

APPENDIX I

EXPERIMENTAL DATA AND CALCULATED RESULTS

I.1 Axial Dispersion Data

TABLE I Axial Dispersion Data for Fixed Bed

TABLE II Axial Dispersion Data for Mobile Bed

TABLE III Bed Height Data for Mobile Bed

I.2 TABLE IV Interfacial Area Data

I.3 TABLE V Physical Mass Transfer Data

TABLE I EXPERIMENTAL DATA AND CALCULATED RESULTS
FIXED BED RUNS

DIAMETER OF PACKING 0.50 INCHES
GALLELEI NUMBER 0.20E 08

STATIC HOLDUP 0.029
Y = HOP * GA**0.44 * AD**-1

RUN NUMBER	LIQUID FLOW RATE LBM/(HR-FT**2)	COLUMN PECLET NUMBER	PACKING PECLET NUMBER	RESIDENCE TIME SECS.	LIQUID HOLDUP	PEO * GA**0.095	Y
1H1D2	6977.1	19.58	1.78	1.74	0.1181	8.79	38.0
2H1D2	9707.3	21.78	1.98	1.43	0.1349	9.78	45.3
3H1D2	12513.4	23.42	2.13	1.50	0.1823	10.52	65.6
4H1D2	15319.4	23.84	2.17	1.51	0.2251	10.70	84.0
5H1D2	18201.3	26.93	2.45	1.50	0.2648	12.09	101.0
6H1D2	20855.6	24.82	2.26	1.38	0.2786	11.14	106.9
7H1D2	23813.3	29.15	2.65	1.20	0.2783	13.09	106.8
8H1D2	24799.2	24.47	2.22	1.20	0.2896	10.99	111.6

TABLE I EXPERIMENTAL DATA AND CALCULATED RESULTS
FIXED BED RUNS (CONTINUED)

DIAMETER OF PACKING 0.75 INCHES
GALLELEI NUMBER 0.68E 08

STATIC HOLDUP 0.025
Y = HOP * GA**0.44 * AD**-1

RUN NUMBER	LIQUID FLOW RATE LBM/(HR-FT**2)	COLUMN PECLET NUMBER	PACKING PECLET NUMBER	RESIDENCE TIME SECS.	LIQUID HOLDUP	PEO * GA**0.095	Y
1H1D3	3943.6	19.57	2.67	1.17	0.0449	14.90	21.0
2H1D3	6977.1	13.45	1.83	0.83	0.0562	10.17	33.0
3H1D3	9707.3	15.73	2.14	0.78	0.0731	11.89	50.8
4H1D3	12513.4	21.17	2.89	0.86	0.1042	16.00	83.6
5H1D3	15319.4	20.41	2.78	0.94	0.1394	15.43	120.8
6H1D3	18201.3	23.86	3.25	0.91	0.1601	18.04	142.6
7H1D3	20855.6	19.15	2.61	0.82	0.1670	14.47	149.9
8H1D3	23813.3	19.55	2.67	0.97	0.2236	14.78	209.6
9H1D3	24799.2	18.05	2.46	0.95	0.2284	13.65	214.7

TABLE I EXPERIMENTAL DATA AND CALCULATED RESULTS
FIXED BED RUNS (CONTINUED)

DIAMETER OF PACKING 1.00 INCHES
GALLELEI NUMBER 0.16E 09

STATIC HOLDUP 0.022
Y = HOP * GA**0.44 * AD**-1

RUN NUMBER	LIQUID FLOW RATE LBM/(HR-FT**2)	COLUMN PECLET NUMBER	PACKING PECLET NUMBER	RESIDENCE TIME SECS.	LIQUID HOLDUP	0.095 PED * GA	Y
1H1D4	3943.6	10.74	1.95	1.37	0.0525	11.75	36.0
2H1D4	6977.1	9.53	1.73	1.13	0.0769	10.42	64.7
3H1D4	9707.3	12.89	2.34	0.97	0.0911	14.10	81.4
4H1D4	12513.4	13.54	2.46	0.88	0.1070	14.82	100.2
5H1D4	15319.4	15.61	2.84	0.76	0.1130	17.08	107.3
6H1D4	18201.3	15.99	2.91	0.73	0.1295	17.50	126.7
7H1D4	20855.6	16.98	3.09	0.73	0.1474	18.58	147.7
8H1D4	23813.3	17.06	3.10	0.64	0.1486	18.67	149.1
9H1D4	24799.2	16.55	3.01	0.63	0.1520	18.10	153.2

TABLE I EXPERIMENTAL DATA AND CALCULATED RESULTS
FIXED BED RUNS (CONTINUED)

DIAMETER OF PACKING 1.50 INCHES
GALLELEI NUMBER 0.54E 09

STATIC HOLDUP 0.018
Y = HOP * GA**0.44 * AD**-1

RUN NUMBER	LIQUID FLOW RATE LBM/(HR-FT**2)	COLUMN PECLET NUMBER	PACKING PECLET NUMBER	RESIDENCE TIME SECS.	LIQUID HOLDUP	0.095 PED * GA	Y
1H1D6	3943.6	6.57	1.65	0.90	0.0475	11.16	70.0
2H1D6	6977.1	5.68	1.55	0.55	0.0370	10.47	45.1
3H1D6	9707.3	5.81	1.58	0.37	0.0349	10.70	39.9
4H1D6	12513.4	5.65	1.54	0.45	0.0543	10.40	86.3
5H1D6	15319.4	4.97	1.36	0.42	0.0619	9.16	104.1
6H1D6	18201.3	6.25	1.70	0.43	0.0766	11.51	139.3
7H1D6	20955.6	7.49	2.04	0.39	0.0790	13.78	145.0
8H1D6	23813.3	6.22	1.70	0.34	0.0793	11.45	145.8
9H1D6	24799.2	7.49	2.04	0.35	0.0840	13.80	156.9

TABLE II EXPERIMENTAL DATA AND CALCULATED RESULTS
MOBILE BED RUNS

DIAMETER OF PACKING 0.50 INCHES
GALLELEI NUMBER 0.20E 08
DENSITY OF PACKING 0.167 GRAMS / CC.
PEO = 1.06 * (REL**0.41) * (GA**(-0.095))

RUN NUMBER	LIQUID MASS VELOCITY	GAS MASS VELOCITY	MINIMUM FLUIDIZATION VELOCITY	DELTA	PACKING PECLET NUMBER	RESIDENCE TIME SEC.	PE/PEO	LIQUID HOLDUP
1D2	6977.1	794.6	278.2	1.86	0.85	2.27	0.555	0.0980
2D2	6977.1	1151.4	278.2	3.14	0.49	2.78	0.319	0.0970
3D2	6977.1	1578.5	278.2	4.67	0.32	2.34	0.210	0.0657
4D2	6977.1	1974.4	278.2	6.10	0.25	2.48	0.162	0.0535
5D2	6977.1	2486.9	278.2	7.94	0.20	2.75	0.131	0.0550
6D2	6977.1	2997.0	278.2	9.77	0.17	3.25	0.109	0.0560
7D2	6977.1	3450.8	278.2	11.40	0.24	3.35	0.156	0.0513
8D2	12513.4	506.4	160.8	2.15	1.03	2.50	0.532	0.2279
9D2	12513.4	846.9	160.8	4.27	0.64	2.06	0.331	0.1515
10D2	12513.4	1189.8	160.8	6.40	0.41	2.12	0.211	0.1294

TABLE II EXPERIMENTAL DATA AND CALCULATED RESULTS
MOBILE BED RUNS (CONTINUED)

DIAMETER OF PACKING 0.50 INCHES
GALLELEI NUMBER 0.20E 08
DENSITY OF PACKING 0.167 GRAMS / CC.
PEO = 1.06 * (REL**0.41) * (GA**(-0.095))

RUN NUMBER	LIQUID MASS VELOCITY	GAS MASS VELOCITY	MINIMUM FLUIDIZATION VELOCITY	DELTA	PACKING PECLET NUMBER	RESIDENCE TIME SEC.	PE/PEO	LIQUID HOLDUP
11D2	12513.4	1457.2	160.8	8.06	0.29	1.63	0.147	0.0830
12D2	12513.4	1879.8	160.8	10.69	0.26	2.02	0.136	0.0922
13D2	12513.4	2459.1	160.8	14.29	0.19	2.30	0.095	0.0855
14D2	12513.4	3012.6	160.8	17.74	0.16	2.95	0.083	0.0953
15D2	12513.4	3504.6	160.8	20.80	0.15	3.36	0.076	0.0945
16D2	18201.3	458.4	91.6	4.01	0.47	1.45	0.209	0.1948
17D2	18201.3	699.4	91.6	6.64	0.51	1.89	0.270	0.2194
18D2	18201.3	896.4	91.6	8.79	0.41	2.01	0.188	0.2172
19D2	18201.3	1083.6	91.6	10.84	0.35	1.71	0.153	0.1628
20D2	18201.3	1416.4	91.6	14.47	0.28	1.88	0.124	0.1546

TABLE II EXPERIMENTAL DATA AND CALCULATED RESULTS
MOBILE BED RUNS (CONTINUED)

DIAMETER OF PACKING 0.50 INCHES
GALLELEI NUMBER 0.20E 08
DENSITY OF PACKING 0.167 GRAMS / CC.
PEO = 1.06 * (REL**0.41) * (GA**(-0.095))

RUN NUMBER	LIQUID MASS VELOCITY	GAS MASS VELOCITY	MINIMUM FLUIDIZATION VELOCITY	DELTA	PACKING PECLET NUMBER	RESIDENCE TIME SEC.	PE/PEO	LIQUID HOLDUP
21D2	18201.3	1845.9	91.6	19.16	0.20	1.79	0.090	0.1262
22D2	18201.3	2106.1	91.6	22.00	0.19	2.42	0.083	0.1561
23D2	18201.3	2353.9	91.6	24.71	0.18	2.27	0.080	0.1355
24D2	18201.3	2746.4	91.6	29.00	0.24	2.51	0.106	0.1190
25D2	18201.3	2964.9	91.6	31.38	0.16	3.16	0.070	0.1605
26D2	18201.3	2996.0	91.6	31.72	0.13	2.41	0.058	0.1215
27D2	18201.3	3522.5	91.6	37.47	0.13	2.98	0.059	0.1328
28D2	23813.3	520.5	52.5	8.91	0.39	1.86	0.155	0.3031
29D2	23813.3	972.6	52.5	17.52	0.30	1.73	0.120	0.2334
30D2	23813.3	1187.7	52.5	21.61	0.28	2.30	0.111	0.2821

TABLE II EXPERIMENTAL DATA AND CALCULATED RESULTS
MOBILE BED RUNS (CONTINUED)

DIAMETER OF PACKING 0.50 INCHES
GALLELEI NUMBER 0.20E 08
DENSITY OF PACKING 0.167 GRAMS / CC.
PEO = 1.06 * (REL**0.41) * (GA**(-0.095))

RUN NUMBER	LIQUID MASS VELOCITY	GAS MASS VELOCITY	MINIMUM FLUIDIZATION VELOCITY	DELTA	PACKING PECLET NUMBER	RESIDENCE TIME SEC.	PE/PEO	LIQUID HOLDUP
31D2	23813.3	1537.4	52.5	28.27	0.23	1.97	0.090	0.2127
32D2	23813.3	2028.3	52.5	37.61	0.17	2.11	0.076	0.1939
33D2	23813.3	2594.3	52.5	48.39	0.16	2.15	0.065	0.1572
34D2	23813.3	2978.0	52.5	55.69	0.14	2.56	0.055	0.1813
35D2	23813.3	3200.4	52.5	59.93	0.13	2.14	0.051	0.1445
36D2	23813.3	3525.6	52.5	66.12	0.12	2.28	0.046	0.1433

TABLE II EXPERIMENTAL DATA AND CALCULATED RESULTS
MOBILE BED RUNS (CONTINUED)

DIAMETER OF PACKING 0.75 INCHES
GALLELEI NUMBER 0.68E 08
DENSITY OF PACKING 0.103 GRAMS / CC.
PED = 1.06 * (REL**0.41) * (GA**(-0.095))

RUN NUMBER	LIQUID MASS VELOCITY	GAS MASS VELOCITY	MINIMUM FLUIDIZATION VELOCITY	DELTA	PACKING PECLET NUMBER	RESIDENCE TIME SEC.	PE/PED	LIQUID HOLDUP
1D3	6977.1	462.4	511.1	-0.10	1.34	1.48	0.831	0.1001
2D3	6977.1	881.3	511.1	0.72	1.61	2.20	1.001	0.1291
3D3	6977.1	1262.5	511.1	1.47	0.95	2.09	0.588	0.1016
4D3	6977.1	1753.6	511.1	2.43	0.81	2.45	0.503	0.1008
5D3	6977.1	2281.9	511.1	3.46	0.55	2.70	0.344	0.0950
6D3	6977.1	2924.5	511.1	4.72	0.49	3.30	0.302	0.0938
7D3	6977.1	3468.9	511.1	5.79	0.38	3.03	0.236	0.0807
8D3	12513.4	445.3	295.4	0.51	2.51	1.55	1.228	0.1881
9D3	12513.4	649.7	295.4	1.20	1.24	1.69	0.607	0.1759
10D3	12513.4	920.1	295.4	2.11	1.22	1.61	0.597	0.1519

TABLE II EXPERIMENTAL DATA AND CALCULATED RESULTS
MOBILE BED RUNS (CONTINUED)

DIAMETER OF PACKING 0.75 INCHES
GALLELEI NUMBER 0.68E 08
DENSITY OF PACKING 0.103 GRAMS / CC.
PED = 1.06 * (REL**0.41) * (GA**(-0.095))

RUN NUMBER	LIQUID MASS VELOCITY	GAS MASS VELOCITY	MINIMUM FLUIDIZATION VELOCITY	DELTA	PACKING PECLET NUMBER	RESIDENCE TIME SEC.	PE/PED	LIQUID HOLDUP
11D3	12513.4	1665.7	295.4	4.64	0.77	1.94	0.377	0.1443
12D3	12514.5	2684.8	295.4	8.09	0.63	2.42	0.308	0.1399
13D3	12513.4	3500.3	295.4	10.85	0.46	2.89	0.227	0.1403
14D3	15319.4	379.4	223.7	0.70	1.44	1.68	0.648	0.2497
15D3	18201.3	748.8	168.2	3.45	0.83	1.47	0.350	0.2094
16D3	18201.3	1430.1	168.2	7.50	0.40	1.67	0.338	0.1944
17D3	18201.3	1986.2	168.2	10.81	0.61	1.67	0.258	0.1673
18D3	18201.3	2582.2	168.2	14.35	0.65	2.10	0.274	0.1850
19D3	18201.3	3200.6	168.2	18.03	0.49	2.38	0.204	0.1849
20D3	18201.3	3511.7	168.2	19.88	0.62	2.82	0.259	0.2077

TABLE II EXPERIMENTAL DATA AND CALCULATED RESULTS
MOBILE BED RUNS (CONTINUED)

DIAMETER OF PACKING 0.75 INCHES
GALLELEI NUMBER 0.68E 08
DENSITY OF PACKING 0.103 GRAMS / CC.
PEO = 1.06 * (REL**0.41) * (GA**(-0.095))

RUN NUMBER	LIQUID MASS VELOCITY	GAS MASS VELOCITY	MINIMUM FLUIDIZATION VELOCITY	DELTA	PACKING PECLET NUMBER	RESIDENCE TIME SEC.	PE/PEO	LIQUID HOLDUP
21D3	18656.3	2251.3	160.8	13.00	0.76	1.85	0.318	0.1794
22D3	23813.3	967.5	96.5	9.03	0.82	1.34	0.309	0.2307
23D3	23813.3	1622.1	96.5	15.81	0.71	1.47	0.269	0.2165
24D3	23813.3	2040.4	96.5	20.14	0.67	1.56	0.252	0.2096
25D3	23813.3	2399.5	96.5	23.87	0.51	1.69	0.194	0.2101
26D3	23813.3	2668.4	96.5	26.65	0.47	1.72	0.177	0.2028
27D3	23813.3	2992.3	96.5	30.01	0.50	1.91	0.186	0.2121
28D3	23813.3	3073.7	96.5	30.85	0.33	1.61	0.124	0.1761
29D3	23813.3	3369.2	96.5	33.91	0.59	2.30	0.217	0.2393
30D3	23813.3	3522.1	96.5	35.50	0.44	2.46	0.167	0.2495

TABLE II EXPERIMENTAL DATA AND CALCULATED RESULTS
MOBILE BED RUNS (CONTINUED)

DIAMETER OF PACKING 1.00 INCHES
GALLELEI NUMBER 0.16E 09
DENSITY OF PACKING 0.181 GRAMS / CC.
PEO = 1.06 * (PEL**0.41) * (GA**(-0.095))

RUN NUMBER	LIQUID MASS VELOCITY	GAS MASS VELOCITY	MINIMUM FLUIDIZATION VELOCITY	DELTA	PACKING PECLET NUMBER	RESIDENCE TIME SEC.	PE/PEO	LIQUID HOLDUP
1D4	4095.3	2331.2	1046.7	1.23	1.13	2.61	0.846	0.0595
2D4	4095.3	3045.6	1046.7	1.91	0.91	2.76	0.677	0.0498
3D4	6977.1	1349.3	786.8	0.71	1.69	1.61	1.012	0.0829
4D4	6977.1	1593.7	786.8	1.03	2.27	2.02	1.362	0.0939
5D4	6977.1	1893.6	786.8	1.41	1.48	2.09	0.887	0.0869
6D4	6977.1	1916.2	786.8	1.44	1.24	1.72	0.743	0.0709
7D4	6977.1	2251.4	786.8	1.86	1.57	2.39	0.944	0.0946
8D4	6977.1	2720.4	786.8	2.46	1.20	2.52	0.717	0.0812
9D4	6977.1	3222.9	786.8	3.09	1.02	2.89	0.611	0.0822
10D4	6977.1	3567.0	786.8	3.53	0.84	2.75	0.502	0.0723

TABLE II EXPERIMENTAL DATA AND CALCULATED RESULTS
MOBILE BED RUNS (CONTINUED)

DIAMETER OF PACKING 1.00 INCHES
GALLELEI NUMBER 0.16E 09

DENSITY OF PACKING 0.181 GRAMS / CC.
PEO = 1.06 * (REL**0.41) * (GA**(-0.095))

RUN NUMBER	LIQUID MASS VELOCITY	GAS MASS VELOCITY	MINIMUM FLUIDIZATION VELOCITY	DELTA	PACKING PECLET NUMBER	RESIDENCE TIME SEC.	PE/PEO	LIQUID HOLDUP
11D4	9707.3	1259.4	600.5	1.10	2.09	1.57	1.092	0.1102
12D4	9707.3	1743.3	600.5	1.90	1.63	1.91	0.855	0.1113
13D4	9707.3	2182.1	600.5	2.63	1.27	2.19	0.663	0.1113
14D4	9707.3	2791.9	600.5	3.65	1.11	2.15	0.582	0.0927
15D4	9707.3	3191.4	600.5	4.31	1.06	2.14	0.556	0.0842
16D4	9707.3	3583.7	600.5	4.97	0.73	2.46	0.382	0.0890
17D4	12513.4	970.9	454.8	1.13	2.93	1.38	1.384	0.1327
18D4	12513.4	1265.5	454.8	1.78	1.60	1.78	0.753	0.1537
19D4	12513.4	1577.6	454.8	2.47	1.15	1.94	0.544	0.1421
20D4	12513.4	1812.2	454.8	2.98	1.85	2.19	0.872	0.1566

TABLE II EXPERIMENTAL DATA AND CALCULATED RESULTS
MOBILE BED RUNS (CONTINUED)

DIAMETER OF PACKING 1.00 INCHES
GALLELEI NUMBER 0.16E 09

DENSITY OF PACKING 0.181 GRAMS / CC.
PEO = 1.06 * (REL**0.41) * (GA**(-0.095))

RUN NUMBER	LIQUID MASS VELOCITY	GAS MASS VELOCITY	MINIMUM FLUIDIZATION VELOCITY	DELTA	PACKING PECLET NUMBER	RESIDENCE TIME SEC.	PE/PEO	LIQUID HOLDUP
21D4	12513.4	2261.0	454.8	3.97	1.43	2.22	0.673	0.1399
22D4	12513.4	2708.1	454.8	4.95	1.19	1.93	0.563	0.1391
23D4	12513.4	3056.5	454.8	5.72	0.94	2.14	0.463	0.1119
24D4	12513.4	3563.2	454.8	6.83	0.90	2.10	0.379	0.0986
25D4	15319.4	1095.3	344.5	2.18	2.15	1.44	0.935	0.1577
26D4	15319.4	1426.0	344.5	3.14	1.97	1.55	0.858	0.1543
27D4	15319.4	1866.4	344.5	4.42	1.08	1.52	0.471	0.1249
28D4	15319.4	2290.5	344.5	5.65	1.85	1.59	0.809	0.1213
29D4	15319.4	2580.9	344.5	6.49	1.10	1.70	0.479	0.1215
30D4	15319.4	3074.7	344.5	7.93	1.01	2.02	0.437	0.1296

TABLE II EXPERIMENTAL DATA AND CALCULATED RESULTS
MOBILE BED RUNS (CONTINUED)

DIAMETER OF PACKING 1.00 INCHES
GALLELEI NUMBER 0.16E 09
DENSITY OF PACKING 0.181 GRAMS / CC.
PEO = 1.06 * (REL**0.41) * (GA**(-0.095))

RUN NUMBER	LIQUID MASS VELOCITY	GAS MASS VELOCITY	MINIMUM FLUIDIZATION VELOCITY	DELTA	PACKING PECLET NUMBER	RESIDENCE TIME SEC.	PE/PEO	LIQUID HOLDUP
31D4	15319.4	3395.6	344.5	8.86	0.99	2.00	0.430	0.1205
32D4	15319.4	3582.8	344.5	9.40	0.68	2.31	0.297	0.1340
33D4	18201.2	861.7	259.0	2.33	2.66	1.62	1.078	0.2252
34D4	18201.2	1411.1	259.0	4.45	1.68	1.58	0.682	0.1835
35D4	18201.2	1941.8	259.0	6.50	1.48	1.84	0.598	0.1845
36D4	18201.2	2497.1	259.0	8.64	1.37	1.65	0.553	0.1445
37D4	18201.2	2827.8	259.0	9.92	1.30	1.83	0.528	0.1499
38D4	18201.2	3129.9	259.0	11.09	1.27	1.92	0.513	0.1470
39D4	18201.2	3497.0	259.0	12.50	0.88	1.84	0.357	0.1318
40D4	18595.6	3002.3	249.1	11.05	1.03	1.90	0.415	0.1528

TABLE II EXPERIMENTAL DATA AND CALCULATED RESULTS
MOBILE BED RUNS (CONTINUED)

DIAMETER OF PACKING 1.00 INCHES
GALLELEI NUMBER 0.16E 09
DENSITY OF PACKING 0.181 GRAMS / CC.
PEO = 1.06 * (REL**0.41) * (GA**(-0.095))

RUN NUMBER	LIQUID MASS VELOCITY	GAS MASS VELOCITY	MINIMUM FLUIDIZATION VELOCITY	DELTA	PACKING PECLET NUMBER	RESIDENCE TIME SEC.	PE/PEO	LIQUID HOLDUP
41D4	20855.6	1305.0	199.1	5.55	1.56	1.44	0.599	0.1976
42D4	20855.6	1841.0	199.1	8.25	1.65	1.55	0.634	0.1836
43D4	20855.6	2169.9	199.1	9.90	1.67	1.61	0.641	0.1758
44D4	20855.6	2783.7	199.1	12.98	1.23	1.66	0.472	0.1590
45D4	20855.6	3499.5	199.1	16.58	1.08	1.97	0.412	0.1647
46D4	23813.3	816.9	148.6	4.50	3.30	1.41	1.198	0.2565
47D4	23813.3	1079.8	148.6	6.27	2.44	1.30	0.886	0.2190
48D4	23813.3	1479.8	148.6	8.96	1.67	1.39	0.605	0.2084
49D4	23813.3	1855.4	148.6	11.50	1.74	1.51	0.632	0.2059
50D4	23813.3	2074.4	148.6	12.96	1.54	1.47	0.557	0.1996

TABLE II EXPERIMENTAL DATA AND CALCULATED RESULTS
MOBILE BED RUNS (CONTINUED)

DIAMETER OF PACKING 1.00 INCHES
GALLELEI NUMBER 0.16E 09

DENSITY OF PACKING 0.181 GRAMS / CC.
PEO = 1.06 * (REL**0.41) * (GA**(-0.095))

RUN NUMBER	LIQUID MASS VELOCITY	GAS MASS VELOCITY	MINIMUM FLUIDIZATION VELOCITY	DELTA	PACKING PECLET NUMBER	RESIDENCE TIME SEC.	PE/PEO	LIQUID HOLDUP
5104	23813.3	2374.2	148.6	14.98	1.24	1.55	0.449	0.1892
5204	23813.3	2632.5	148.6	16.72	1.53	1.64	0.555	0.1881
5304	23813.3	3059.5	148.6	19.59	1.13	1.65	0.411	0.1749
5404	23813.3	3519.1	148.6	22.69	1.27	1.97	0.461	0.1921

TABLE II EXPERIMENTAL DATA AND CALCULATED RESULTS
MOBILE BED RUNS (CONTINUED)

DIAMETER OF PACKING 1.50 INCHES
GALLELEI NUMBER 0.54E 09

DENSITY OF PACKING 0.152 GRAMS / CC.
PEO = 1.06 * (REL**0.41) * (GA**(-0.095))

RUN NUMBER	LIQUID MASS VELOCITY	GAS MASS VELOCITY	MINIMUM FLUIDIZATION VELOCITY	DELTA	PACKING PECLET NUMBER	RESIDENCE TIME SEC.	PE/PEO	LIQUID HOLDUP
106	6977.1	1870.6	1445.5	0.29	1.34	1.59	1.049	0.0846
206	6977.1	2399.2	1445.5	0.66	1.95	2.26	1.111	0.0949
306	6977.1	2979.7	1445.5	1.06	1.55	2.50	0.893	0.0851
406	6977.1	3478.4	1445.5	1.41	1.14	3.01	0.651	0.0843
506	9707.3	2000.1	1103.1	0.81	2.14	1.92	1.047	0.1171
606	9707.3	2471.0	1103.1	1.24	1.30	1.99	0.650	0.1026
706	9707.3	3030.1	1103.1	1.75	1.00	2.09	0.496	0.0904
806	9707.3	3319.0	1103.1	2.01	1.07	2.57	0.531	0.1031
906	9707.3	3559.6	1103.1	2.23	1.40	3.21	0.698	0.1213
1006	12513.4	1457.2	835.5	0.74	2.45	1.49	1.102	0.1332

TABLE II EXPERIMENTAL DATA AND CALCULATED RESULTS
MOBILE BED RUNS (CONTINUED)

DIAMETER OF PACKING 1.50 INCHES
GALLELEI NUMBER 0.54E 09
DENSITY OF PACKING 0.152 GRAMS / CC.
PEO = 1.06 * (REL**0.41) * (GA**(-0.095))

RUN NUMBER	LIQUID MASS VELOCITY	GAS MASS VELOCITY	MINIMUM FLUIDIZATION VELOCITY	DELTA	PACKING PECLET NUMBER	RESIDENCE TIME SEC.	PE/PEO	LIQUID HOLDUP
11D6	12513.4	1991.5	835.5	1.39	1.73	1.57	0.776	C.1143
12D6	12513.4	2404.4	835.5	1.88	1.92	1.95	0.860	0.1248
13D6	12513.4	2907.9	835.5	2.48	1.50	2.01	0.673	C.1115
14D6	12513.4	3436.7	835.5	3.11	1.30	2.37	0.584	C.1149
15D6	15319.4	1750.7	632.9	1.77	1.81	1.68	0.750	C.1555
16D6	15319.4	2023.2	632.9	2.20	1.99	1.88	0.823	0.1598
17D6	15319.4	2410.2	632.9	2.81	1.25	1.70	0.517	C.1292
18D6	15319.4	2716.1	632.9	3.29	1.39	1.87	0.572	C.1307
19D6	15319.4	3155.4	632.9	3.99	1.32	1.99	0.546	C.1245
20D6	15319.4	3528.0	632.9	4.57	1.40	2.61	0.579	C.1504

TABLE II EXPERIMENTAL DATA AND CALCULATED RESULTS
MOBILE BED RUNS (CONTINUED)

DIAMETER OF PACKING 1.50 INCHES
GALLELEI NUMBER 0.54E 09
DENSITY OF PACKING 0.152 GRAMS / CC.
PEO = 1.06 * (REL**0.41) * (GA**(-0.095))

RUN NUMBER	LIQUID MASS VELOCITY	GAS MASS VELOCITY	MINIMUM FLUIDIZATION VELOCITY	DELTA	PACKING PECLET NUMBER	RESIDENCE TIME SEC.	PE/PEO	LIQUID HOLDUP
21D6	18201.2	1243.3	475.8	1.61	2.32	1.36	0.892	C.1723
22D6	18201.2	1727.5	475.8	2.63	1.73	1.29	0.665	C.1330
23D6	18201.2	2194.6	475.8	3.59	1.32	1.36	0.509	C.1279
24D6	18201.2	2853.4	475.8	5.00	1.42	1.83	0.545	C.1456
25D6	18201.2	3589.0	475.8	6.54	1.25	2.30	0.460	C.1562
26D6	20855.6	2604.1	365.8	6.12	1.53	1.73	0.557	C.1672
27D6	20855.6	3073.4	365.8	7.40	1.47	1.76	0.534	C.1535
28D6	20855.6	3561.5	365.8	8.74	1.41	2.19	0.515	C.1733
29D6	21386.5	1440.7	347.1	3.15	1.53	1.23	0.550	C.1671
30D6	21386.5	2027.8	347.1	4.84	1.55	1.59	0.557	C.1823

TABLE II EXPERIMENTAL DATA AND CALCULATED RESULTS
MOBILE BED RUNS (CONTINUED)

DIAMETER OF PACKING 1.50 INCHES
GALLELEI NUMBER 0.54E 09

DENSITY OF PACKING 0.152 GRAMS / CC.
PED = 1.06 * (REL**0.41) * (GA**(-0.095))

RUN NUMBER	LIQUID MASS VELOCITY	GAS MASS VELOCITY	MINIMUM FLUIDIZATION VELOCITY	DELTA	PACKING PECLET NUMBER	RESIDENCE TIME SEC.	PE/PED	LIQUID HOLDUP
31D6	23813.3	1112.9	272.9	3.08	1.95	1.15	0.671	C.1920
32D6	23813.3	1531.3	272.9	4.61	1.66	1.11	0.573	C.1630
33D6	23813.3	1965.5	272.9	6.20	1.59	1.21	0.548	C.1617
34D6	23813.3	2386.2	272.9	7.74	1.17	1.37	0.403	C.1604
35D6	23813.3	2870.4	272.9	9.52	1.41	1.59	0.485	C.1678
36D6	23813.3	1160.9	272.9	3.25	1.79	1.13	0.613	C.1850
37D6	23813.3	3426.3	272.9	11.55	1.40	2.11	0.483	C.1949

TABLE III BED HEIGHT DATA FOR MOBILE BED

GMF - LBS. / (HR.-FT**2)
DP = 0.50 INCHES

H - INCHES

L		1	2	3	4	5	6	7	8	9	10
3944.	G	1526.	2196.	2690.	3225.	3539.	793.	1439.	2488.	3213.	3534.
	H	10.25	12.25	14.50	16.25	17.00	8.50	10.37	14.75	19.00	20.75
6977.	G	840.	1387.	2238.	2946.	3575.	707.	1481.	2407.	3096.	3555.
	H	8.25	10.50	12.50	15.75	17.75	7.25	10.50	14.25	18.25	22.50
9707.	G	653.	1128.	1990.	2934.	3557.	563.	1374.	2341.	3016.	3542.
	H	7.00	9.75	12.00	16.75	22.50	7.13	11.50	14.75	19.25	22.75
12513.	G	432.	984.	2126.	2973.	3317.	445.	1123.	2254.	2959.	3418.
	H	7.00	10.25	13.50	18.25	21.50	7.13	10.13	14.00	17.75	21.50
15319.	G	354.	1249.	2154.	2782.	3167.	347.	1076.	2015.	2769.	3220.
	H	7.13	10.88	14.50	18.13	22.50	7.13	10.75	13.75	18.50	22.00
18201.	G	370.	1092.	1950.	2536.	2846.	512.	1195.	1736.	2278.	2789.
	H	7.63	11.25	14.50	20.25	22.50	8.25	11.25	13.25	15.25	21.75
20856.	G	328.	1010.	2023.	2340.	2765.	206.	1151.	1777.	2170.	2607.
	H	7.88	11.50	17.00	19.50	23.50	7.50	12.00	15.63	18.00	22.00
23813.	G	294.	760.	1397.	2032.	2493.					
	H	9.00	12.00	14.75	18.75	22.50					

TABLE III (CONTINUED) BED HEIGHT DATA FOR MOBILE BED

GMF - LBS. / (HR.-FT**2)
DP = 0.75 INCHES

H - INCHES

L		1	2	3	4	5	6	7	8	9	10	11	12
3943.	G	817.	1320.	1974.	2484.	3083.							
	H	6.00	7.00	8.75	10.25	11.25							
6977.	G	834.	1429.	1930.	2477.	2978.	3395.	805.	1375.	1927.	2460.	2964.	3462.
	H	5.88	7.25	8.50	10.00	11.75	13.25	5.75	7.13	9.00	10.00	10.75	12.25
9707.	G	825.	1345.	1945.	2480.	2962.	3428.						
	H	6.38	7.55	9.25	9.75	10.75	13.00						
12513.	G	840.	1467.	1950.	2449.	3006.	3458.	784.	1391.	1939.	2447.	2967.	3379.
	H	5.50	7.88	9.00	10.00	11.00	12.75	6.25	7.25	9.25	10.50	11.25	12.75
15319.	G	775.	1391.	1950.	2491.	3002.	3396.						
	H	6.50	8.00	9.00	10.25	12.00	13.75						
18201.	G	876.	1444.	1929.	2560.	3019.	3446.	771.	1403.	1932.	2459.	3008.	3384.
	H	5.88	8.00	8.88	10.00	11.50	14.25	6.75	7.75	9.50	10.75	12.75	14.25
20856.	G	329.	1372.	1901.	2499.	2985.	3422.						
	H	7.00	8.00	9.00	10.50	12.50	14.50						
23813.	G	909.	1335.	1949.	2515.	3041.							
	H	7.50	8.00	9.00	11.00	13.25							

TABLE III (CONTINUED) BED HEIGHT DATA FOR MOBILE BED

GMF - LBS. / (HR.-FT**2) H - INCHES
DP = 1.00 INCHES

L		1	2	3	4	5	6	7	8	9	10
3943.	G	1416.	2114.	2627.	3227.	3503.	1505.	2051.	2551.	3046.	3533.
	H	7.38	9.75	11.50	13.75	17.50	7.38	9.13	10.75	12.50	14.50
6977.	G	1441.	2151.	2844.	3168.	3529.	1240.	1884.	2403.	3002.	3491.
	H	7.75	10.50	13.00	14.75	17.25	7.00	9.00	10.25	12.88	14.13
9707.	G	1043.	1870.	2532.	3158.	3497.	1035.	1952.	2520.	3104.	3535.
	H	6.88	8.88	11.00	12.75	14.00	7.00	10.00	12.13	13.75	16.50
12513.	G	1035.	1943.	2573.	3196.	3550.	992.	1899.	2516.	3162.	3482.
	H	7.25	10.25	11.50	15.00	17.25	6.88	8.75	11.00	12.25	14.50
15319.	G	1143.	1892.	2513.	3083.	3521.	849.	1881.	2511.	3013.	3477.
	H	7.87	10.13	11.50	13.75	16.00	6.88	9.00	10.13	12.00	14.50
18201.	G	815.	1625.	2503.	3118.	3505.	1064.	1817.	2651.	3066.	3511.
	H	7.00	8.75	10.75	12.75	14.00	7.75	9.63	12.50	13.75	15.13
20856.	G	856.	1741.	2438.	3105.	3490.	694.	1838.	2715.	3124.	3532.
	H	7.00	9.25	10.75	12.75	14.75	6.88	9.75	12.00	13.25	14.75
23813.	G	607.	1820.	2422.	3060.	3503.					
	H	7.00	9.75	11.00	12.75	15.00					

TABLE III (CONTINUED) BED HEIGHT DATA FOR MOBILE BED

GMF - LBS. / (HR.-FT**2) H - INCHES
DP = 1.50 INCHES

L		1	2	3	4	5	6	7	8	9	10
3943.	G	2334.	2796.	3191.	3503.	2457.	2909.	3211.	3514.		
	H	6.75	8.50	10.75	13.00	7.75	9.25	10.50	12.00		
6977.	G	2132.	2577.	2948.	3380.	2262.	2797.	3153.	3522.		
	H	8.13	10.00	10.75	13.25	7.75	9.88	10.75	12.25		
9707.	G	1944.	2745.	3189.	3511.	1971.	2493.	3057.	3490.		
	H	7.75	9.50	11.75	13.25	7.50	8.88	10.00	12.25		
12513.	G	2112.	2868.	3176.	3497.	1310.	1970.	2613.	3102.	3484.	
	H	8.50	11.75	12.50	13.75	6.38	7.50	9.75	11.00	13.50	
15319.	G	1236.	1943.	2559.	3115.	3500.	1254.	1962.	2667.	3149.	3499.
	H	6.13	7.75	9.25	11.25	12.75	6.25	7.75	9.25	11.25	13.25
18201.	G	1211.	1950.	2668.	3190.	3483.	1157.	1911.	2644.	2698.	3508.
	H	6.25	8.00	10.25	11.75	13.00	6.25	8.13	10.00	11.38	13.25
20856.	G	1085.	1866.	2628.	3193.	3503.	1115.	1965.	2645.	3175.	3535.
	H	6.50	8.50	10.00	11.25	12.75	6.63	8.75	10.25	11.75	13.50
23813.	G	1000.	1911.	2615.	3161.	3501.					
	H	6.63	8.50	9.75	11.50	12.75					

TABLE IV INTERFACIAL AREA DETERMINATION
EXPERIMENTAL DATA

ABSORPTION OF CARBON DIOXIDE IN SODIUM HYDROXIDE SOLUTION
IN MOBILE BED CONTACTOR
DP = 0.75 INCHES

RUN NUMBER	LIQUID FLOW	GAS FLOW	RATE OF ABSORPTION	LIQUID CONCN.	LIQUID TEMP	GAS TEMP	LOG MEAN GAS CONCENTRATION
	LBS/HR-FT**2		GM-MOL/SEC	GM-MOL/L.	C	C	%
1	7234.5	832.3	0.7520E-03	1.48	16.0	22.1	4.972
2	7234.5	1439.2	0.1743E-02	1.48	16.4	21.1	4.789
3	7234.5	2007.5	0.2269E-02	1.50	13.5	19.1	4.780
4	7234.5	2296.9	0.2655E-02	1.48	14.4	19.9	4.682
5	7234.5	2460.6	0.2855E-02	1.72	14.7	20.2	3.915
6	7234.5	2752.6	0.3973E-02	1.69	15.3	20.7	4.462
7	10065.2	832.4	0.6387E-03	1.78	16.3	19.8	3.018
8	10065.2	1047.3	0.1231E-02	1.79	17.4	19.4	4.779

TABLE IV INTERFACIAL AREA DETERMINATION
EXPERIMENTAL DATA (CONTINUED)

ABSORPTION OF CARBON DIOXIDE IN SODIUM HYDROXIDE SOLUTION
IN MOBILE BED CONTACTOR
DP = 0.75 INCHES

RUN NUMBER	LIQUID FLOW	GAS FLOW	RATE OF ABSORPTION	LIQUID CONCN.	LIQUID TEMP	GAS TEMP	LOG MEAN GAS CONCENTRATION
	LBS/HR-FT**2		GM-MOL/SEC	GM-MOL/L.	C	C	%
9	12974.8	884.2	0.1408E-02	1.80	19.0	20.4	4.655
10	12974.8	1431.4	0.1754E-02	1.80	19.3	20.3	3.398
11	12974.8	1912.2	0.3879E-02	1.77	16.7	20.9	5.039
12	12974.8	2418.8	0.3473E-02	1.77	18.2	20.6	4.308
13	12974.8	2765.3	0.5824E-02	1.77	19.5	20.5	4.979
14	15884.4	2147.4	0.4032E-02	2.01	16.8	21.3	4.488
15	18872.7	841.6	0.1875E-02	1.96	21.9	24.4	4.488
16	18872.7	1202.5	0.2986E-02	2.05	24.1	25.0	5.510

TABLE IV INTERFACIAL AREA DETERMINATION
EXPERIMENTAL DATA (CONTINUED)

ABSORPTION OF CARBON DIOXIDE IN SODIUM HYDROXIDE SOLUTION
IN MOBILE BED CONTACTOR
DP = 0.75 INCHES

RUN NUMBER	LIQUID FLOW	GAS FLOW	RATE OF ABSORPTION	LIQUID CONCN.	LIQUID TEMP	GAS TEMP	LOG MEAN GAS CONCENTRATION
	LBS/HR-FT**2		GM-MOL/SEC	GM-MOL/L.	C	C	%
17	18872.7	1641.4	0.3003E-02	2.10	24.5	23.1	4.144
18	18872.7	3018.6	0.5989E-02	1.78	19.1	21.8	4.741
19	21625.7	2420.8	0.6664E-02	2.01	18.9	21.1	4.425
20	24691.8	677.9	0.1454E-02	2.07	23.1	23.4	3.970
21	24691.8	1019.9	0.4020E-02	2.06	23.2	23.2	5.440
22	24691.8	1640.2	0.4588E-02	2.06	23.8	22.7	4.949
23	24691.8	2191.7	0.6950E-02	1.99	15.7	21.8	5.944
24	24691.8	2374.6	0.7722E-02	2.00	15.7	20.4	5.924
25	24691.8	2935.1	0.5928E-02	2.00	17.2	21.5	3.657

TABLE IV INTERFACIAL AREA DETERMINATION
EXPERIMENTAL DATA (CONTINUED)

ABSORPTION OF CARBON DIOXIDE IN SODIUM HYDROXIDE SOLUTION
IN FIXED BED CONTACTOR
DP = 0.75 INCHES

RUN NUMBER	LIQUID FLOW	GAS FLOW	RATE OF ABSORPTION	LIQUID CONCN.	LIQUID TEMP	GAS TEMP	LOG MEAN GAS CONCENTRATION
	LBS/HR-FT**2		GM-MOL/SEC	GM-MOL/L.	C	C	%
26	4088.5	229.5	0.1726E-02	2.05	23.3	28.6	9.691
27	7234.5	419.4	0.1051E-02	2.05	20.3	26.2	6.921
28	10065.2	222.9	0.1963E-02	2.05	22.0	28.3	8.653
29	12974.8	382.3	0.1945E-02	2.05	20.6	26.5	8.564
30	15884.4	203.7	0.2454E-02	2.05	21.4	28.1	9.516
31	18872.7	202.7	0.1215E-02	2.05	19.1	26.2	5.846
32	24691.8	456.0	0.2453E-02	2.05	18.4	25.1	6.291

TABLE IV INTERFACIAL AREA DETERMINATION
EXPERIMENTAL DATA

ABORPPTION OF SULPHER DIOXIDE IN 2N SODIUM HYDROXIDE SOLUTION
IN MOBILE BED CONTACTOR
DP = C.75 INCHES

RUN NUMBER	LIQUID FLOW	GAS FLOW	RATE OF ABSORPTION	LIQUID TEMP	GAS TEMP	LOG MEAN GAS CONCENTRATION
	LBS/HR-FT**2		GM-MOL/SEC	C	C	%
1	7234.5	855.8	0.3447E-01	23.7	24.7	3.182
2	7234.5	1445.6	C.5061E-01	23.3	25.2	3.322
3	7234.5	2007.8	C.6233E-C1	26.0	28.3	2.778
4	7234.5	2163.7	C.7962E-01	36.9	30.7	3.751
5	7234.5	2503.9	0.1071E 00	41.3	26.8	3.282
6	7234.5	2628.9	0.1026E CC	42.3	26.7	2.863
7	10065.2	867.0	C.2605E-01	24.8	24.6	1.555
8	10065.2	1119.3	0.4069E-01	27.4	24.9	2.554

TABLE IV INTERFACIAL AREA DETERMINATION
EXPERIMENTAL DATA (CONTINUED)

ABORPPTION OF SULPHER DICXIDE IN 2N SODIUM HYDROXIDE SOLUTION
IN MOBILE BED CONTACTOR
DP = 0.75 INCHES

RUN NUMBER	LIQUID FLOW	GAS FLOW	RATE OF ABSORPTION	LIQUID TEMP	GAS TEMP	LOG MEAN GAS CONCENTRATION
	LBS/HR-FT**2		GM-MOL/SEC	C	C	%
9	12974.8	746.5	C.3799E-01	28.1	25.7	1.438
10	12974.8	1454.1	C.6083E-01	30.6	26.8	2.132
11	12974.8	1898.8	C.9848E-01	34.5	26.8	3.370
12	12974.8	2433.3	C.1098E CC	38.8	31.4	3.100
13	12974.8	2671.5	0.1097E CC	40.7	26.5	3.015
14	15884.4	2186.4	C.1161E CC	33.1	24.8	3.842
15	18872.7	834.8	0.2416E-01	23.3	26.0	0.920
16	18872.7	1239.3	0.6123E-01	27.4	25.9	1.404

TABLE IV INTERFACIAL AREA DETERMINATION
EXPERIMENTAL DATA (CONTINUED)

ABSORPTION OF SULPHER DIOXIDE IN 2N SODIUM HYDROXIDE SOLUTION
IN MOBILE BED CONTACTOR
DP = 0.75 INCHES

RUN NUMBER	LIQUID FLOW	GAS FLOW	RATE OF ABSORPTION	LIQUID TEMP	GAS TEMP	LOG MEAN GAS CONCENTRATION
	LBS/HR-FT**2		GM-MOL/SEC	C	C	%
17	18872.7	1765.6	0.9031E-01	32.0	26.1	1.845
18	18872.7	3111.1	0.1884E 00	41.5	24.0	1.655
19	21625.7	2495.9	0.7954E-01	34.0	25.7	1.704
20	24691.8	677.8	0.5014E-01	32.0	25.7	1.943
21	24691.8	1024.0	0.4673E-01	33.5	25.9	1.193
22	24691.8	1670.4	0.9242E-01	41.5	26.2	2.239
23	24691.8	2200.1	0.7683E-01	39.9	24.7	1.067
24	24691.8	2483.8	0.1701E 00	45.9	25.3	1.400
25	24691.8	2984.4	0.1796E 00	41.5	25.7	1.253

TABLE IV INTERFACIAL AREA DETERMINATION
EXPERIMENTAL DATA (CONTINUED)

ABSORPTION OF SULPHER DIOXIDE IN 2N SODIUM HYDROXIDE SOLUTION
IN FIXED BED CONTACTOR
DP = 0.75 INCHES

RUN NUMBER	LIQUID FLOW	GAS FLOW	RATE OF ABSORPTION	LIQUID TEMP	GAS TEMP	LOG MEAN GAS CONCENTRATION
	LBS/HR-FT**2		GM-MOL/SEC	C	C	%
26	4088.5	211.6	0.4064E-02	24.5	25.4	2.890
27	7234.5	402.1	0.4719E-02	23.3	23.3	2.483
28	10065.2	218.7	0.6244E-02	23.4	24.4	1.504
29	12974.8	373.3	0.7220E-02	23.7	23.3	1.774
30	15884.4	217.2	0.4113E-02	23.0	23.7	0.801
31	18872.7	241.4	0.3203E-02	23.2	23.3	0.716
32	24691.8	972.9	0.8667E-01	41.5	25.9	2.257

TABLE IV INTERFACIAL AREA DETERMINATION

EXPERIMENTAL DATA AND CALCULATED RESULT FOR ABSORPTION
IN MOBILE BED CONTACTOR
DP = 0.75 INCHES

RUN NUMBER	LIQUID FLOW	GAS FLOW	KG (CO2)	KG (SO2)	LIQUID SOLUBILITY CONCN	DIFFUSIVITY	REACTION VELOCITY CONSTANT	INTERFACIAL AREA
					GM-MOL/L	10**5		
	LBS/HR-FT**2	GM-MOL/(SEC ATM CM**3)			GM-MOL/L-ATM	CM**2/SEC	L/GM-MOL-SEC	CM**2/CM**3
1	7234.	832.	0.60E-05	0.45E-03	1.48	0.0269	1.10	6596.6	0.690
2	7234.	1439.	0.11E-04	0.50E-03	1.48	0.0265	1.11	6811.0	1.314
3	7234.	2007.	0.12E-04	0.61E-03	1.50	0.0287	1.01	5419.8	1.538
4	7234.	2297.	0.14E-04	0.55E-03	1.48	0.0281	1.05	5801.2	1.696
5	7234.	2461.	0.17E-04	0.78E-03	1.72	0.0258	1.01	6390.7	1.994
6	7234.	2753.	0.19E-04	0.82E-03	1.69	0.0256	1.04	6644.0	2.282
7	10065.	832.	0.80E-05	0.66E-03	1.78	0.0242	1.05	7391.4	0.905
8	10065.	1047.	0.89E-05	0.58E-03	1.79	0.0233	1.08	8097.7	0.983

TABLE IV INTERFACIAL AREA DETERMINATION
(CONTINUED)

EXPERIMENTAL DATA AND CALCULATED RESULT FOR ABSORPTION
IN MOBILE BED CONTACTOR
DP = 0.75 INCHES

RUN NUMBER	LIQUID FLOW	GAS FLOW	KG (CO2)	KG (SO2)	LIQUID SOLUBILITY CONCN	DIFFUSIVITY	REACTION VELOCITY CONSTANT	INTERFACIAL AREA
					GM-MOL/L	10**5		
	LBS/HR-FT**2	GM-MOL/(SEC ATM CM**3)			GM-MOL/L-ATM	CM**2/SEC	L/GM-MOL-SEC	CM**2/CM**3
9	12975.	884.	0.11E-04	0.10E-02	1.80	0.0222	1.13	9200.5	1.192
10	12975.	1431.	0.16E-04	0.91E-03	1.80	0.0221	1.14	9418.0	1.648
11	12975.	1912.	0.21E-04	0.81E-03	1.77	0.0239	1.06	7610.7	2.322
12	12975.	2419.	0.19E-04	0.87E-03	1.77	0.0230	1.11	8566.0	2.050
13	12975.	2765.	0.26E-04	0.83E-03	1.77	0.0221	1.15	9488.5	2.723
14	15884.	2147.	0.23E-04	0.79E-03	2.01	0.0221	1.03	8254.6	2.552
15	18873.	842.	0.15E-04	0.10E-02	1.96	0.0195	1.19	12090.6	1.498
16	18873.	1202.	0.18E-04	0.15E-02	2.05	0.0178	1.23	14723.7	1.639

TABLE IV INTERFACIAL AREA DETERMINATION
(CONTINUED)

EXPERIMENTAL DATA AND CALCULATED RESULT FOR ABSORPTION
IN MOBILE BED CONTACTOR
DP = 0.75 INCHES

RUN NUMBER	LIQUID FLOW	GAS FLOW	KG (CO2)	KG (SO2)	LIQUID CONCN	SOLUBILITY	DIFFUSIVITY	REACTION VELOCITY CONSTANT	INTERFACIAL AREA
					GM-MOL/L		10**5		
	LBS/HR-FT**2	GM-MOL/(SEC ATM CM**3)			GM-MOL/L-ATM		CM**2/SEC	L/GM-MOL-SEC	CM**2/CM**3
17	18873.	1641.	0.21E-04	0.15E-02	2.10	0.0174	1.22	15403.6	1.919
18	18873.	3019.	0.27E-04	0.25E-02	1.78	0.0223	1.14	9230.3	2.816
19	21626.	2421.	0.37E-04	0.12E-02	2.01	0.0208	1.09	9750.1	3.944
20	24692.	678.	0.14E-04	0.10E-02	2.07	0.0182	1.19	13728.5	1.345
21	24692.	1020.	0.26E-04	0.14E-02	2.06	0.0182	1.20	13807.3	2.463
22	24692.	1640.	0.27E-04	0.13E-02	2.06	0.0179	1.22	14426.4	2.605
23	24692.	2192.	0.31E-04	0.20E-02	1.99	0.0229	1.00	7527.5	3.534
24	24692.	2375.	0.33E-04	0.32E-02	2.00	0.0228	1.00	7545.1	3.738
25	24692.	2935.	0.37E-04	0.34E-02	2.00	0.0218	1.04	8506.9	4.039

TABLE IV INTERFACIAL AREA DETERMINATION
(CONTINUED)

EXPERIMENTAL DATA AND CALCULATED RESULT FOR ABSORPTION
IN FIXED BED CONTACTOR
DP = 0.75 INCHES

RUN NUMBER	LIQUID FLOW	GAS FLOW	KG (CO2)	KG (SO2)	LIQUID CONCN	SOLUBILITY	DIFFUSIVITY	REACTION VELOCITY CONSTANT	INTERFACIAL AREA
					GM-MOL/L		10**5		
	LBS/HR-FT**2	GM-MOL/(SEC ATM CM**3)			GM-MOL/L-ATM		CM**2/SEC	L/GM-MOL-SEC	CM**2/CM**3
26	4089.	230.	0.83E-05	0.69E-04	2.05	0.0182	1.21	13847.8	0.888
27	7234.	419.	0.71E-05	0.93E-04	2.05	0.0198	1.12	10990.7	0.774
28	10065.	223.	0.11E-04	0.20E-03	2.05	0.0189	1.17	12540.2	1.081
29	12975.	382.	0.10E-04	0.19E-03	2.05	0.0196	1.13	11251.8	1.073
30	15884.	204.	0.12E-04	0.25E-03	2.05	0.0192	1.15	11968.3	1.240
31	18873.	203.	0.95E-05	0.21E-03	2.05	0.0204	1.08	10035.2	1.027
32	24692.	456.	0.15E-04	0.15E-02	2.05	0.0208	1.07	9484.5	1.579

TABLE V LIQUID-SIDE MASS TRANSFER COEFFICIENT DETERMINATION FOR MOBILE BED CONTACTOR

EXPERIMENTAL DATA AND CALCULATED RESULTS FOR DESORPTION OF CARBONDIOXIDE FROM WATER

RUN NUMBER	LIQUID FLOW L	GAS FLOW G	LIQUID CONCENTRATION XIN	LIQUID CONCENTRATION XOUT	TRANSFER UNITS N OX	TRANSFER UNITS N OXP	MASS TRANSFER COEFFICIENT K A L	HEIGHT OF TRANSFER UNITS H OL
	LBS/HR-FT**2		10**2 GM-MOL/L.				HR**(-1)	FT
1	23813.	667.	1.5426	0.5798	1.109	0.979	760.9	0.502
2	23813.	1007.	1.8288	0.6956	1.092	0.967	678.1	0.563
3	23813.	1606.	1.3143	0.5393	0.994	0.891	528.8	0.722
4	23813.	2048.	1.5195	0.5087	1.245	1.094	599.0	0.637
5	23813.	2206.	1.4922	0.4574	1.349	1.176	627.6	0.608
6	23813.	2873.	2.0000	0.5773	1.429	1.243	583.5	0.654
7	20856.	684.	1.5740	0.5500	1.169	1.051	710.6	0.470
8	20856.	1205.	2.0943	0.8387	1.020	0.915	521.5	0.641
9	20856.	1851.	2.1406	0.7767	1.138	1.014	492.0	0.679
10	20856.	2429.	2.0505	0.6303	1.340	1.180	511.2	0.654
11	20856.	2865.	1.5914	0.5070	1.290	1.144	451.4	0.741

TABLE V LIQUID-SIDE MASS TRANSFER COEFFICIENT DETERMINATION FOR MOBILE BED CONTACTOR

EXPERIMENTAL DATA AND CALCULATED RESULTS FOR DESORPTION OF CARBONDIOXIDE FROM WATER

(CONTINUED)

RUN NUMBER	LIQUID FLOW L	GAS FLOW G	LIQUID CONCENTRATION XIN	LIQUID CONCENTRATION XOUT	TRANSFER UNITS N OX	TRANSFER UNITS N OXP	MASS TRANSFER COEFFICIENT K A L	HEIGHT OF TRANSFER UNITS H OL
	LBS/HR-FT**2		10**2 GM-MOL/L.				HR**(-1)	FT
12	18201.	833.	2.0149	1.0066	0.751	0.694	374.1	0.780
13	18201.	1190.	1.4194	0.6046	0.942	0.853	419.9	0.695
14	18201.	1619.	1.8023	0.6832	1.081	0.970	428.2	0.681
15	18201.	2135.	1.6675	0.6501	1.042	0.942	364.1	0.801
16	18201.	2612.	1.9529	0.5864	1.361	1.203	428.3	0.681
17	18201.	2949.	1.9893	0.6303	1.289	1.149	379.5	0.769
18	15319.	700.	2.0803	0.7643	1.092	1.001	483.1	0.568
19	15319.	1107.	2.2490	0.8553	1.071	0.967	412.4	0.595
20	15319.	1517.	2.5228	0.8817	1.177	1.051	401.1	0.612
21	15319.	2149.	2.2392	0.7610	1.205	1.079	348.5	0.704
22	15319.	2645.	2.3491	0.7138	1.340	1.191	346.4	0.709

TABLE V LIQUID-SIDE MASS TRANSFER COEFFICIENT DETERMINATION FOR MOBILE BED CONTACTOR

EXPERIMENTAL DATA AND CALCULATED RESULTS FOR DESORPTION OF CARBONDIOXIDE FROM WATER

(CONTINUED)

RUN NUMBER	LIQUID FLOW L	GAS FLOW G	LIQUID CONCENTRATION XIN	LIQUID CONCENTRATION XOUT	TRANSFER UNITS N OX	TRANSFER UNITS N OXP	MASS TRANSFER COEFFICIENT K A L	HEIGHT OF TRANSFER UNITS H OL
	LBS/HR-FT**2		10**2 GM-MOL/L.				HR**(-1)	FT
23	12513.	848.	1.9297	0.6476	1.191	1.092	413.8	0.485
24	12513.	1410.	2.1258	0.7204	1.205	1.082	346.6	0.579
25	12513.	1859.	2.2531	0.7659	1.205	1.079	304.5	0.659
26	12513.	2349.	2.2598	0.5740	1.567	1.370	349.6	0.574
27	12513.	2686.	1.7775	0.4334	1.613	1.411	333.1	0.602
28	12513.	2929.	2.0546	0.3879	1.942	1.667	380.6	0.527
29	9707.	821.	1.5932	0.6576	1.009	0.946	282.3	0.551
30	9707.	1020.	1.9405	0.7039	1.093	1.014	283.0	0.550
31	9707.	1484.	2.5112	0.8412	1.207	1.094	265.8	0.585
32	9707.	2148.	2.7006	1.0074	1.086	0.986	197.2	0.789
33	9707.	2705.	2.3780	0.7792	1.241	1.116	196.4	0.792

TABLE V LIQUID-SIDE MASS TRANSFER COEFFICIENT DETERMINATION FOR MOBILE BED CONTACTOR

EXPERIMENTAL DATA AND CALCULATED RESULTS FOR DESORPTION OF CARBONDIOXIDE FROM WATER

(CONTINUED)

RUN NUMBER	LIQUID FLOW L	GAS FLOW G	LIQUID CONCENTRATION XIN	LIQUID CONCENTRATION XOUT	TRANSFER UNITS N OX	TRANSFER UNITS N OXP	MASS TRANSFER COEFFICIENT K A L	HEIGHT OF TRANSFER UNITS H OL
	LBS/HR-FT**2		10**2 GM-MOL/L.				HR**(-1)	FT
34	6977.	801.	2.2713	1.0256	0.840	0.795	178.0	0.628
35	6977.	1410.	2.8512	0.8511	1.328	1.209	220.4	0.507
36	6977.	1962.	2.5823	0.7974	1.306	1.175	181.3	0.617
37	6977.	2216.	1.7535	0.6369	1.113	1.013	143.7	0.778
38	6977.	2368.	1.7916	0.5873	1.238	1.115	153.4	0.729
39	6977.	2684.	2.0207	0.5616	1.444	1.280	165.0	0.677
40	6977.	3010.	1.9388	0.2622	2.399	2.001	254.0	0.440
41	3943.	2149.	2.7155	0.8660	1.264	1.143	96.3	0.656
42	3943.	2450.	3.0017	0.5277	2.028	1.738	141.5	0.447

APPENDIX II

COMPUTER PROGRAMS

II.1 Smoothening of the Experimental Pulse Testing

II.2 Flow Diagram and Calculation of Liquid Mixing Results

II.3 Calculation of Interfacial Areas of Mass Transfer

II.4 Calculation of Physical Mass Transfer Coefficients

VI.1. SMOOTHING OF THE EXPERIMENTAL PULSE TESTING DATA

```
C
C     NOMENCLATURE
C
C
C     KKK       TOTAL NUMBER OF RESPONSE PULSES
C     NA        NUMBER OF POINTS PER RESPONSE PULSE
C     NB        NUMBER OF POINTS PER INPUT FORCING PULSE
C     N         NUMBER OF POINTS IN THE SMOOTHED RESPONSE PULSE AT EQUAL
C               TIME INTERVALS
C     X'S       NAME OF INPUT FORCING PULSE ARRAY
C     Y'S       NAME OF RESPONSE PULSE ARRAY
C     DIAP      DIAMETER OF PACKING
C     HITE      COLUMN HEIGHT USED
C     RUN       RUN NUMBER
C     FLOL      LIQUID FLOW RATE
C     TEMP      TEMPERATURE OF AIR ENTERING THE COLUMN
C     PS        STATIC PRESSURE OF AIR IN THE LINE
C     ORIF      ORIFICE PRESSURE DIFFERENTIAL
C     WBTP      WET BULB AIR TEMPERATURE
C     ISUB      NUMBER OF SUBSETS FOR EACH RUN
C     IXN       DEAD TIME FOR INPUT FORCING PULSE IN MULTIPLES OF 0.01 SEC.
C     XN        DEAD TIME FOR RESPONSE PULSE FROM THE INSTANT OF INPUT IN SEC.
C
      DIMENSION NA(550),A1(100, 70),Y2(100),Y(100),AN(15),   A6(100,70),
     1NB(15),IXN(15),X(100,15),A2(100,70),A3(100,70),A4(100,70),
     2A5(100,70),A7(100,70),A8(100,70)
C
C     THIS PROGRAM READS, ARRANGES, SMOOTHENS AND PUNCHES 'KKK'
C     SETS OF DATA ON TO COMPUTER CARDS IN SEQUENCE
C
      KKK = 542
      READ( 5 , 1 ) ( NA(I) , I = 1 , KKK )
    1 FORMAT(40I2)
      DIAP = 0.75
      HITE =27.50
      MM = 0
      LLL = 0
      ISUM = 0
      MMMM = 0
      IIIII = 0
C
C     READ ALL THE RESPONSE PULSES FROM PUNCHED CARDS OBTAINED FROM
C     ANALOG TO DIGITAL CONVERTER
C
C
      DO 2 J = 1 , KKK
      L = NA(J)
      I = 1 + J/70
      IF(I - 2) 31 , 32 , 33
   31 READ( 5 , 3 ) ( A1 (II , J ) , II = 1 , L )
      GO TO 42
   32 J1 =  J - 70
      READ( 5 , 3 ) ( A2 (II , J1) , II = 1 , L )
      GO TO 42
   33 IF(I - 4)  34 , 35 , 36
   34 J2 =  J - 140
      READ( 5 , 3 ) ( A3 (II , J2) , II = 1 , L )
      GO TO 42
   35 J3 =  J - 210
      READ( 5 , 3 ) ( A4 (II , J3) , II = 1 , L )
      GO TO 42
   36 IF(I - 6)  37 , 38 , 39
   37 J4 =  J - 280
      READ( 5 , 3 ) ( A5 (II , J4) , II = 1 , L )
      GO TO 42
   38 J5 =  J - 350
      READ( 5 , 3 ) ( A6 (II , J5) , II = 1 , L )
      GO TO 42
   39 IF(I - 8)  40 , 41 , 42
   40 J6 = J - 420
      READ( 5 , 3 ) ( A7 (II , J6) , II = 1 , L )
      GO TO 42
   41 J7 = J - 490
      READ( 5 , 3 ) ( A8 (II , J7) , II = 1 , L )
   42 CONTINUE
    2 CONTINUE
C
    3 FORMAT(11F7.0)
      NUM = 1
C
C
C     TAKE OUT ONE SET OF RESPONSE PULSES AT A TIME AND PROCEED
C
C
      DO 30 IJ = 1 , 542
      L = NA(IJ)
C
      DO 5 II = 1 , L
      I = 1 +IJ/70
      IF(I - 2) 51 , 52 , 53
   51 Y(II) = A1(II ,IJ)
      GO TO 5
   52 IJ1 = IJ - 70
      Y(II) = A2(II ,IJ1)
      GO TO 5
   53 IF(I - 4) 54 , 55 , 56
   54 IJ2 = IJ - 140
      Y(II) = A3(II ,IJ2)
      GO TO 5
   55 IJ3 = IJ - 210
      Y(II) = A4(II ,IJ3)
      GO TO 5
   56 IF(I - 6) 57 , 58 , 59
   57 IJ4 = IJ - 280
      Y(II) = A5(II ,IJ4)
      GO TO 5
   58 IJ5 = IJ - 350
      Y(II) = A6(II ,IJ5)
```

```
      GO TO 5
   59 IF(I - 8) 60 , 61 , 5
   60 IJ6 = IJ - 420
      Y(II) = A7(II ,IJ6)
      GO TO 5
   61 IJ7 = IJ - 490
      Y(II) = A8(II ,IJ7)
    5 CONTINUE
C
      N = L
C
C     IF ANY POINT IS POSITIVE, REJECT THE SET
C     POSITIVE NUMBERS APPEAR WHEN A BUBBLE ENTERS THE
C     CONDUCTIVITY PROBE.  THE CIRCUITS HAVE BEEN SO DESIGNED
C     THAT ALL OTHER VOLTAGES EITHER FROM THE CONDUCTIVITY
C     CELL OR FROM THE INPUT EVENT MARKER ARE NEGATIVE.
C
      DO 300 I = 1, N
      IF(Y(I) - 200.) 300, 501, 501
  300 CONTINUE
      GO TO 1000
  501 WRITE(6,4)
      NNNN = NNNN + 1
    4 FORMAT('POSITIVE NUMBER SET REJECTED')
C
C     FIND THE POINT OF INJECTION
C
 1000 DO 302 I = 1 , 15
      IF(Y(I) + 200.) 301, 301, 302
  302 CONTINUE
  301 IF(I - 1) 304, 304, 303
  303 NI = I - 1
      A = Y(NI)
      K1 = NI + 1
      DO 305 I = K1, N
      K4 = I - NI
      Y(K4) = Y(I) - A
  305 Y2(K4) = Y(K4)
      N = N - NI
      L = N
      GO TO 310
  304 A = Y(N)
      DO 325 I = 1, N
      Y(I) = Y(I) - A
  325 Y2(I) = Y(I)
  310 AMAX = 0.
      IF(Y(4) + 125.) 373 , 373 , 374
  373 IF(Y(5) +100.)  709 , 709 , 710
  709 Y(5) = Y(6)
  710 Y(4) = Y(5)
  374 C = Y(4)
      DO 344 I = 1 , 3
  344 Y(I) = Y(I) - C
C
C     FIND THE MAXIMUM RESPONSE VALUE, OTHER THAN THE SIGNAL INPUT FROM CELL
C
      DO 307 I = 4 , N
      Y(I) = Y(I) - C
      IF(Y(I) - Y(I+1)) 306, 306, 307
  306 IF(Y(I) - AMAX) 308, 308, 307
  308 AMAX = Y(I)
      M = I
  307 CONTINUE
C
C     SMOOTHEN THE CURVE BY EXTRAPOLATION, IF NECESSARY
C
      K2 = M - 1
      K10 = N - 1
      K30 = M + 1
      K40 = N - 3
      DO 392 J = K30 , K40
      IF(Y(J) - Y(J + 1)) 392 , 392 , 720
  720 IF(Y(J) - Y(J + 2)) 392 , 392 , 721
  721 IF(Y(J) - Y(J + 3)) 392 , 392 , 722
  722 Y(J) = ( Y( J - 1 ) + Y ( J + 1 ))/2.
  392 CONTINUE
C
      DO 309 J = 4,K2
      AK = 1.
      IP = 0
      E =  7.*Y(J)
      IF(Y(J))390 , 391 , 391
  391 IF(Y(J + 1) + E) 380 , 380 , 381
  390 IF(Y(J +1) - E)  380 ,  380 , 381
  380 IF(Y(J + 1) - Y(J + 2)) 399 , 381 , 381
  399 Y(J + 1) = Y(J)
      GO TO 309
  381 IF(Y(J) - Y(J + 1)) 319, 319, 309
  319 IF(J - 4) 327 , 327, 311
  311 IF(J.EQ.K2) GO TO 22
      IF(Y(J) - Y(J + 2)) 330 , 334 , 334
  334 IF(Y2(J) - Y(J + 1)) 393 , 309 , 309
  393 Y(J + 1 ) = ( Y(J) + Y( J + 2 ))/2.
      GO TO 309
  330 Y(J + 1) = Y(J) + Y(J) - Y(J - 1)
  395 IF(Y(J + 1) - Y(J + 2)) 397 , 309 , 309
  397 AK = AK*2.
      IP = IP + 1
      Y(J + 1 ) = Y(J) + ( Y(J) - Y(J - 1 ))/AK
      IF(IP.GT.10) GO TO 309
      GO TO 395
  327 K5 = J + 1
      Y(K5) = Y(J)
      GO TO 309
   22 IF(Y(K2) - Y( J - 1 )) 309, 309 , 23
   23 Y(K2) = Y(J - 1) - 1.
  309 CONTINUE
C
```

```
C
      DO 313 J = M , K10
      AK = 1.
      IP = 0
      IF(Y(J) - Y(J + 1)) 313, 312, 312
  312 IF(Y(J) - Y(J + 2)) 335 , 335 , 328
  335 Y(J + 1) = (Y(J) + Y(J + 2))/2.
      GO TO 313
  328 IF(Y2(J) - Y(J + 1)) 365 , 365 , 366
  366 Y(J + 1) = Y(J) + Y(J) - Y(J - 1)
  396 IF(Y(J + 1 ) - Y( J + 2 )) 313 , 313 , 394
  394 AK = AK*2.
      IP = IP + 1
      Y(J + 1 ) = Y(J) + (Y(J) - Y(J - 1 ))/AK
      IF(IP.GT.10) GO TO 313
      GO TO 396
  365 IF(Y( J + 1) - Y2(N)) 313 , 313 , 388
  313 CONTINUE
C
      GO TO 398
  388 N = J + 1
      K10 = N - 1
  398 DO 375 J = 5 , K2
      IF(Y(J) - Y(J + 1)) 371 , 375 , 375
  371 Y(J) = (Y(J - 1) + Y(J + 1))/2.
  375 CONTINUE
      DO 378 J =K30, K10
      IF(Y(J) - Y(J + 1)) 378 , 378 , 372
  372 Y(J) = (Y(J - 1) + Y(J + 1))/2.
  378 CONTINUE
      DO 707 J = 3 , M
      IF(Y(J)) 707 , 707 , 708
  708 Y(J)  = 0.
  707 CONTINUE
C
C     TERMINATE THE DATA WHEN THE END VALUE IS LESS THAN THE 0.1%
C     OF THE MAXIMUM PULSE HEIGHT
C
      BN=N - M
      IF(N.EQ.M) GO TO 66
      GO TO 67
   66 WRITE( 6 , 68 ) IJ
   68 FORMAT(1H , //, 50X, ' HERE M EQUALS N, CHECK '  )
      IIIII = IIIII + 1
   67 B = Y(N)/BN
      K9 = M + 1
      DO 314 I =K9 , N
      AI = I - M
  314 Y(I) = Y(I) -AI*B
      DO 315 I = M, N
      IF(Y(I) - 0.001*AMAX) 315, 316, 316
  315 CONTINUE
      IF(Y(I)) 329 , 316 , 329
  329 I = I + 1
  316 Y(I) = 0.
      N=I
      YMAX = 0.
      DO 355 I = 1 , 3
      IF(Y(I) - YMAX) 356 , 355 , 355
  356 YMAX = Y(I)
      K20 = I
  355 CONTINUE
      Y(3) = 0.
      IF(YMAX +  13500.)376 , 376 , 377
  377 YMAX = -13500.
  376 XN = Y(1)/(YMAX*10.) + 0.05 + 0.03
      IF(K20.EQ.1) GO TO 8
      GO TO 62
    8 XN = XN + 0.015
   62 K7 = N - 2
      DO 326 I = 1 , K7
      K6 = I + 2
      Y(I) = Y(K6)
  326 CONTINUE
      N = N - 2
      DO 343 I = 1 , M
      IF( Y(I)+ 10.) 343 ,  343 , 347
  347 Y(I) = 0.
  343 CONTINUE
      DO 317 I = 1, N
  317 Y(I) = ABS(Y(I))/10.
      MM = MM + 1
      IF(MM - ISUB) 13 , 13 , 6
    6 MM = 1
      IF(NUM.EQ.1) GO TO 27
      GO TO 28
   27 READ( 5 , 29 ) HITE
C
C     READ EACH SET OF PUNCHED DATA FOR INPUT PULSES AT A TIME
C
   28 READ( 5,7 )RUN,FLOL,TEMP,PS,GDIF,WBTP,ISUB,NUM
   29 FORMAT(F5.2)
    7 FORMAT(A3,F4.3,F3.1,F3.0,F6.4,F3.1,I2,I1)
      READ( 5 , 9 ) (AN(J) , J = 1 , ISUB )
    9 FORMAT(15A1)
      READ( 5 , 10 ) (NB(J) , IXN(J) , J = 1 , ISUB )
   10 FORMAT(4012)
      DO 12 JJ = 1 , ISUB
      LL = NB(JJ)
      READ( 5 , 11 ) (X(I , JJ) , I = 1 , LL )
   11 FORMAT(25F3.1)
   12 CONTINUE
C
C     WRITE AND PUNCH ALL THE DATA AND EXPERIMENTAL CONDITIONS IN
C     SEQUENCE
C
   13 WRITE(6,25) IJ
      NA(IJ) = N
```

```
      LL = NR(MM)
      WRITE( 6 , 14 )
   14 FORMAT( 50X ,   /, 47X, ' ORIGINAL PUNCHED PULSE ',/)
      WRITE( 6 , 15 ) (Y2(I) , I = 1 , L )
   15 FORMAT(1H , 20X, 11F7.0, / )
      WRITE( 6 , 16 ) L
   16 FORMAT(100X, I10,  /, 40X, 'SMOOTHED PULSE AT OUTLET OF COLUMN')
      WRITE( 6 , 17 ) (Y(I) , I = 1 , N )
   17 FORMAT(/,1H , 20X , 11F7.2)
      WRITE( 6 , 18 ) N
   18 FORMAT(100X, I10, //, 52X, 'INLET PULSE',/)
      WRITE( 6 , 19 ) (X(I ,MM) , I = 1 , LL )
   19 FORMAT(1H , 36X , 4F10.1 )
      WRITE( 6 , 20 ) LL
   20 FORMAT(100X,I10, //,45X,'EXPERIMENTAL CONDITIONS'/)
      WRITE( 6 , 24 )RUN,AN(MM),FLOL,TEMP,PS,ODIF,WBTP,ISUB,DIAP,HITE,N,
     1IXN(MM),LL,NUM,IJ,XN
   24 FORMAT(1H ,15X,A3,A1,F8.3, F8.1, F8.1, F10.4,F8.1, I3,2F7.2,
     1514,F10.7)
   25 FORMAT(1H1,//,50X,'PAGE NUMBER #2, I3)
   21 WRITE( 7 , 26 ) RUN, AN(MM),FLOL, TEMP, PS, ODIF,WBTP, DIAP, HITE,
     1N,IXN(MM),LL, NUM,IJ,XN, (Y(I) , I = 1 , N ),(X(I,MM),I = 1 , LL)
   26 FORMAT(A3,A1,F7.3,F5.1,F5.0,F10.4,F6.1,F5.2,F6.2,4I3,I4,F9.7,/
     1(12F6.2))
   30 CONTINUE
C
C
      WRITE(6 , 65 ) MMMM
      WRITE( 6 , 63) ( NA(I) , I = 1 , 542 )
      WRITE(7 , 64) (NA(I) , I = 1 , KKK )
   63 FORMAT( 30X, 10I7)
   64 FORMAT(40I2)
   65 FORMAT(1H1,///,50X, 'NUMBER OF SETS WITH POSITIVE NUMBERS = ', I2)
      STOP
      END
```

MAIN

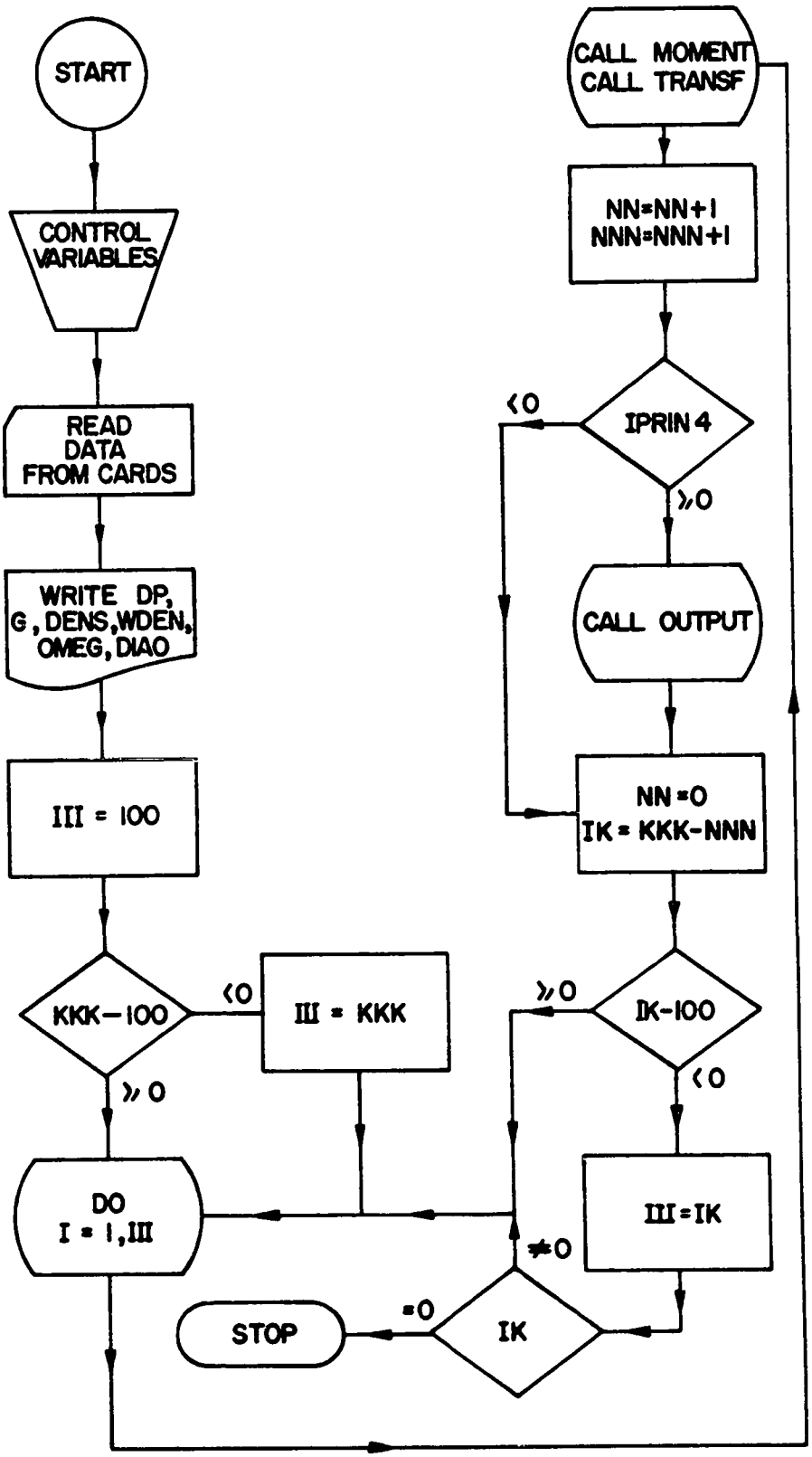
START
CONTROL VARIABLES
READ DATA FROM CARDS
WRITE DP, G, DENS, WDEN, OMEG, DIAO
III = 100
KKK-100
<0
III = KKK
>0
DO I = 1, III
CALL MOMENT
CALL TRANSF
NN=NN+1
NNN=NNN+1
IPRIN 4
<0
>0
CALL OUTPUT
NN=0
IK = KKK-NNN
IK-100
>0
<0
III=IK
≠0
IK
=0
STOP

MOMENT

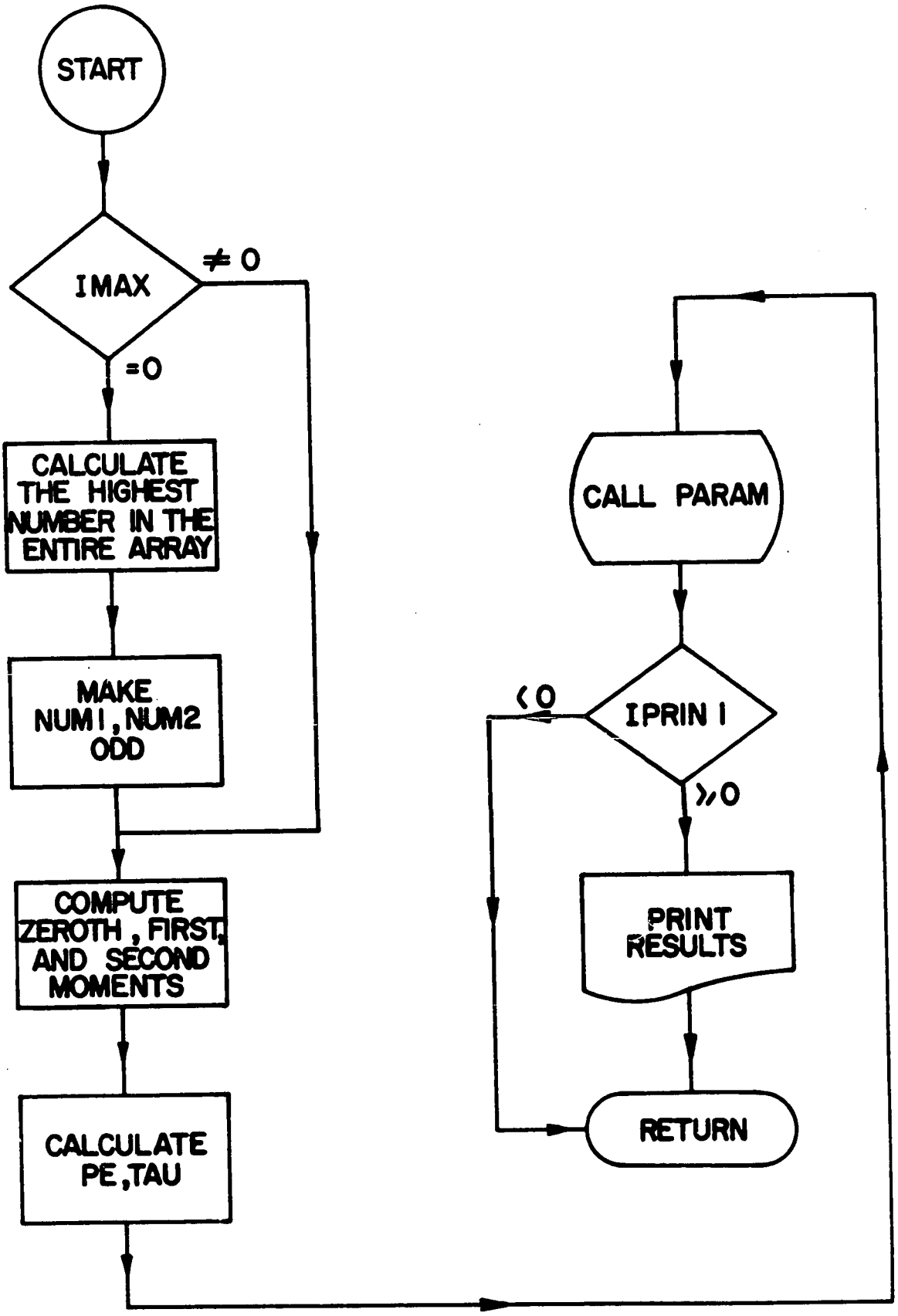
START
IMAX
≠ 0
=0
CALCULATE THE HIGHEST NUMBER IN THE ENTIRE ARRAY
MAKE NUM1, NUM2 ODD
COMPUTE ZEROTH, FIRST, AND SECOND MOMENTS
CALCULATE PE, TAU
CALL PARAM
IPRIN I
< 0
>, 0
PRINT RESULTS
RETURN

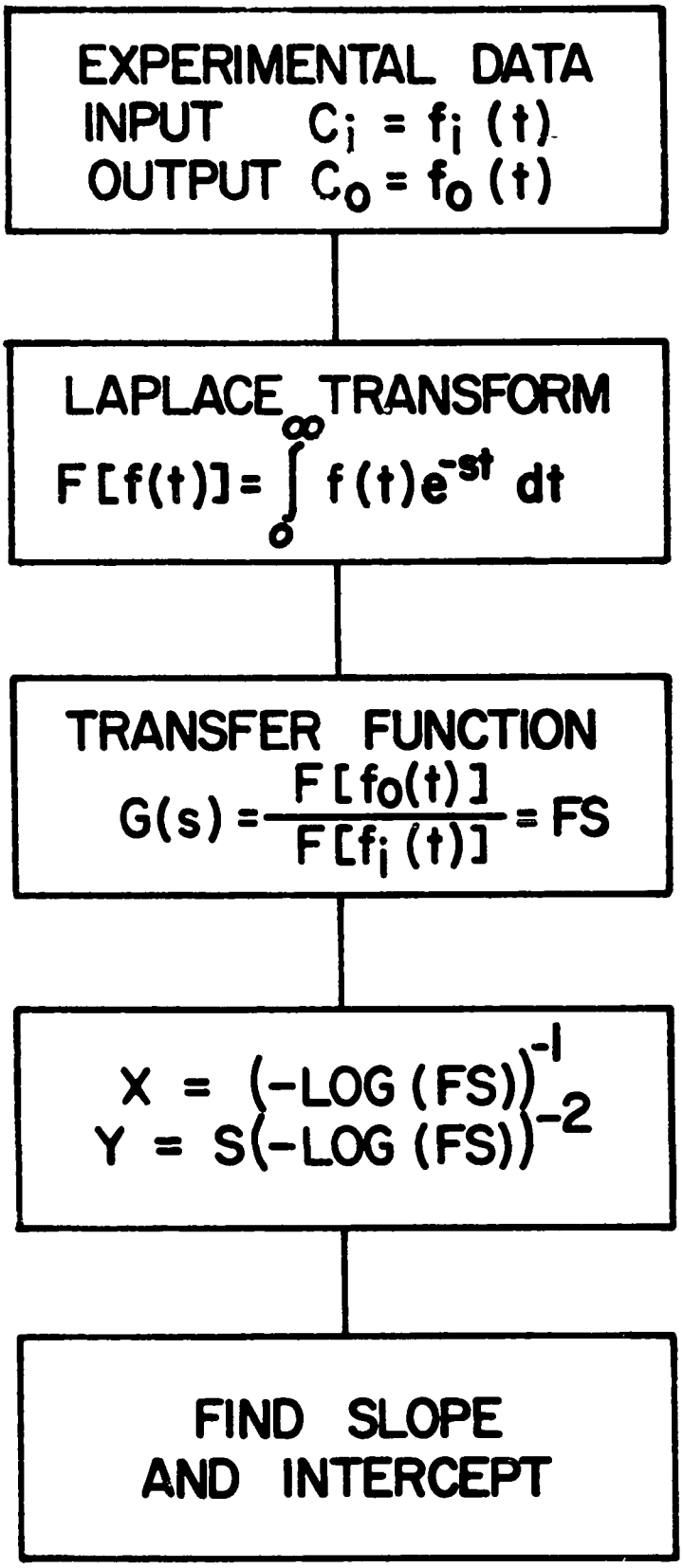

TRANSFER FUNCTION ANALYSIS

TRANSF

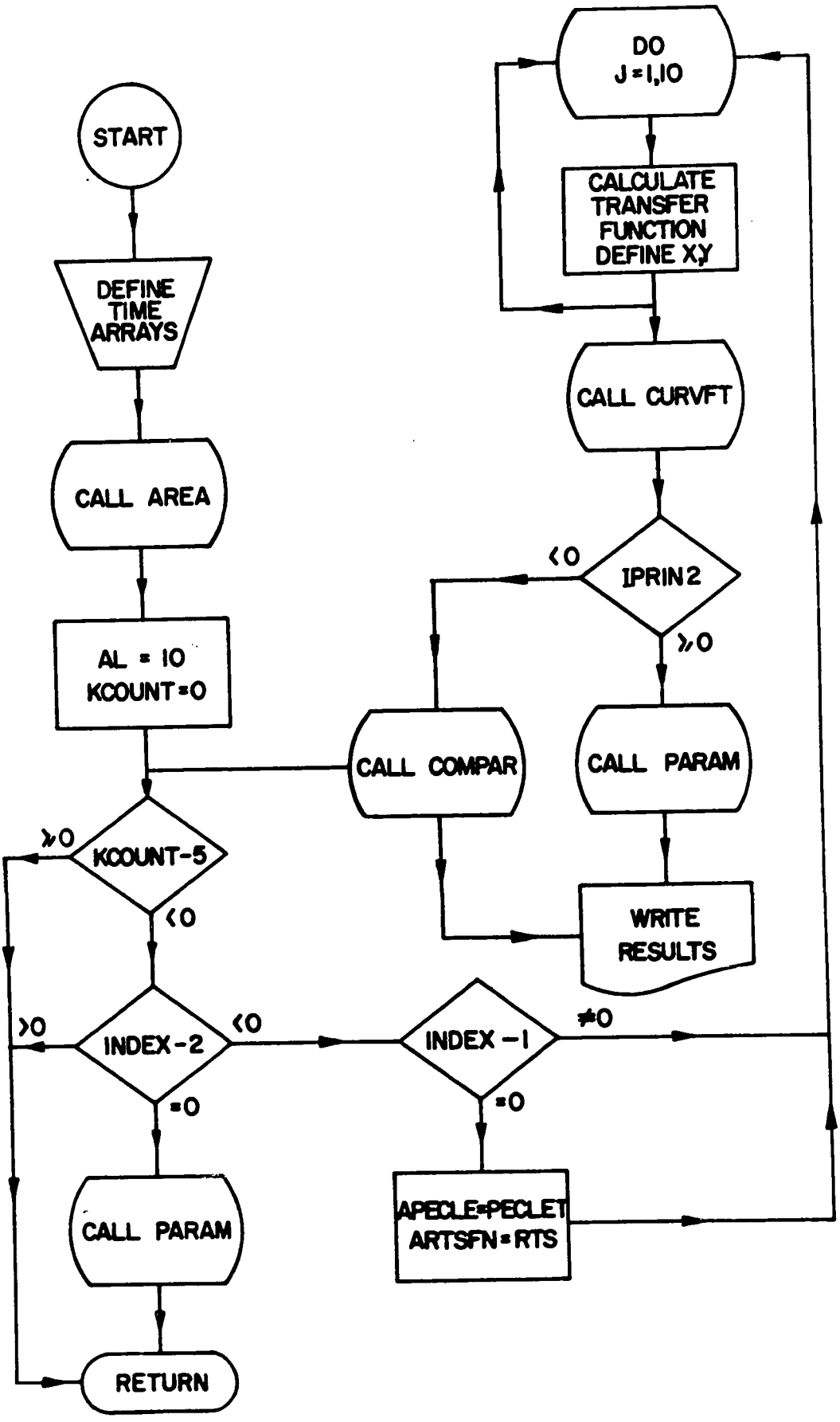
START
DEFINE TIME ARRAYS
CALL AREA
AL = 10
KCOUNT=0
KCOUNT-5
≥0
<0
INDEX-2
>0
<0
=0
CALL PARAM
RETURN
CALL COMPAR
DO J=1,10
CALCULATE TRANSFER FUNCTION DEFINE X,Y
CALL CURVFT
IPRIN2
<0
≥0
CALL PARAM
WRITE RESULTS
INDEX-1
≠0
=0
APECLE=PECLET
ARTSFN=RTS

COMPAR

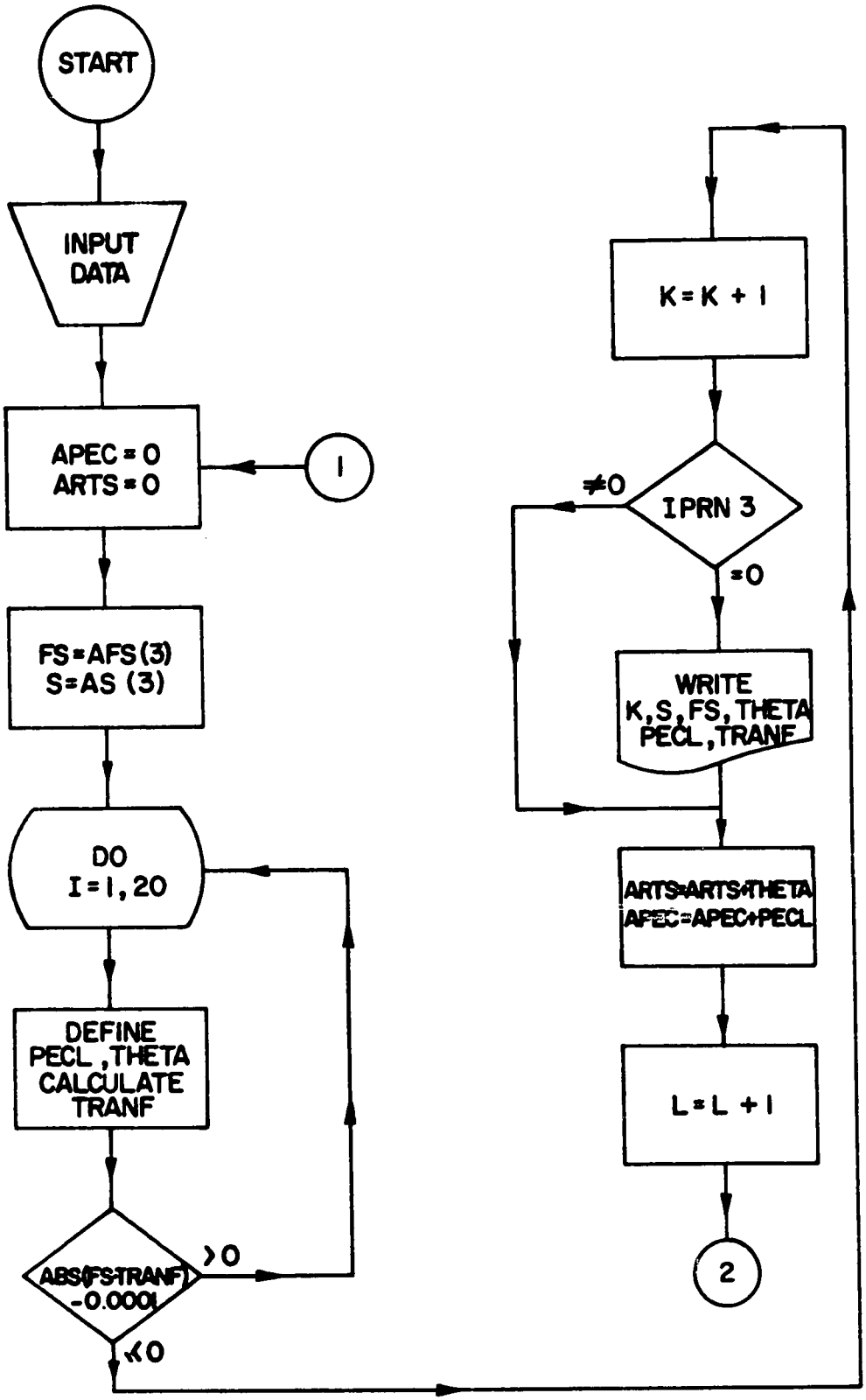
START
INPUT DATA
APEC = 0
ARTS = 0
1
FS = AFS(3)
S = AS (3)
DO
I = 1, 20
DEFINE
PECL , THETA
CALCULATE
TRANF
ABS(FS-TRANF) -0.0001
>0
<0
K = K + 1
IPRN 3
≠0
=0
WRITE
K, S, FS, THETA
PECL, TRANF
ARTS=ARTS+THETA
APEC=APEC+PECL
L = L + 1
2

COMPAR Contd.

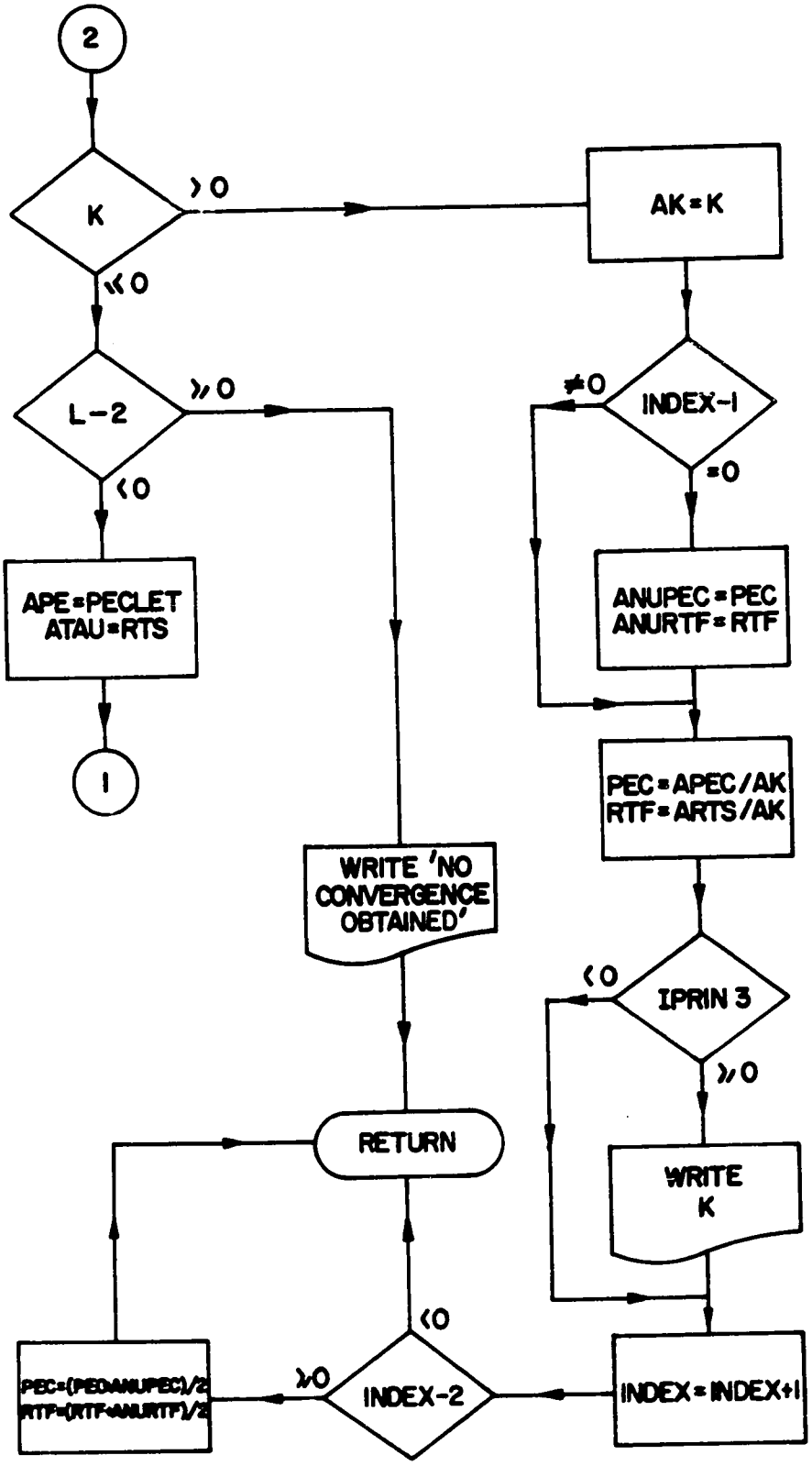

CALCULATION OF LIQUID MIXING RESULTS

```
C
C
C       M A I N   P R O G R A M
C       -----------------------
C
C       CALCULATES RESULTS BY MOMENT ANALYSIS  AND
C       TRANSFER FUNCTION ANALYSIS FOR DIFFUSION MODEL
C       WITH INFINITE AND FINITE BED BOUNDARY CONDITIONS
C
C
C       DIMENSION  STATEMENT
C
      DIMENSION PE1(100), PE2(100), PE3(100), PEP1(100), PEP2(100),
     1 PEP3(100), UH1(100), UH2(100), UH3(100), TAU1(100),
     2 TAU2(100), TAU3(100), HOLD1(100), HOLD2(100), HOLD3(100),
     3 HOL1(100), HOL2(100), HOL3(100), U1(100), U2(100),
     4 U3(100)
      COMMON Y1(100), Y2(100), ARUN(100), IDIAP(100), IHITE(100),
     1 AFLOW(100), AFLOG(100), ATEMP(100), ASFAC(100), NUMA1(100),
     2 NUMA2(100), R(13,2), AS(10), AFS(10), DLX1, DLX2, NUM1, NUM2,
     3 DIAP, HITE, FLOW, RUN, TEMP, XN2, ATERM, WHN, SFACTR, NNN,
     4 INDEX, IPUNCH, IPRINT, IPRIN1, IPRIN2, IPRIN3, IPRIN4, IJK,
     5 FLOL, FREET, FREEH, TABLE(9,2) ,ATRUH(100),KUSUM
C
C      NOMENCLATURE  FOR  CONTROL  CARDS
C      --------------------------------
C
C      IREAD    =  -1  READS DATA WHEN GAS FLOW IS UNKNOWN,
C               0 WHEN PRECALCULATED
C      IPUNCH   =  -1  SUPPRESSES PUNCHED OUTPUT FROM MOMENT
C               ANALYSIS SUBROUTINE,  0 FOR PUNCH
C      IPRINT   =  -1  SUPPRESSES PRINTING FROM CURVE-FIT
C               SUBROUTINE, 0 FOR PRINT
C      IPRIN1   =  -1  SUPPRESSES INTERMEDIATE PRINT OUT FROM
C               MOMENT ANALYSIS SUBROUTINE, 0 FOR PRINT
C      IPRIN2   =  -1  SUPPRESSES INTERMEDIATE PRINT OUT FROM
C               TRANSF SUBROUTINE, 0 FOR PRINT
C      IPRIN3   =  -1  SUPPRESSES INTERMEDIATE PRINT OUT FROM
C               COMPAR SUBROUTINE, 0 FOR PRINT
C      IPRIN4   =  -1  SUPPRESSES FINAL MATRIX PRINT OUT,
C               0  FOR  PRINT
C      ATERM    =  VALUE IN %AGE OF THE MAXIMUM IN ARRAY
C      IMAX     =  -1  FOR TERMINATING THE BREAKTHROUGH CURVE
C      NNN      =   COUNTER FOR CALCULATIONS
C      KKK      =  TOTAL NUMBER OF SETS OF DATA TO BE PROCESSED
C      IJK      =  TOTAL NUMBER OF POINTS FOR TRANSFER
C               FUNCTION ANALYSIS, MAXIMUM 10, UNLESS DIMENSIONS
C               INCREASED
C
       IREAD    = -1
       IPUNCH   = -1
       IPRINT   = -1
       IPRIN1   = -1
       IPRIN2   = -1
       IPRIN3   = -1
       IPRIN4   = 0
       IMAX     = -1
       ATERM    = 0.1
       IJK      = 10
       KKK=731
       NN       = 0
       NNN      = 0
C
C      READ DATA FROM CARDS
C
       READ(5,11)((R(L,M),L=1,13),M=1,2)
    11 FORMAT(8F10.0/5F10.0/13F5.4)
       WRITE(6,2)((R(L,M),L=1,13),M=1,2)
     2 FORMAT(1H1,13F10.1/13F10.4)
       READ(5,999) DP,G,DENS,WDEN,OMEG,DIAC
   999 FORMAT(6F10.5)
       WRITE(6,24) DP,G,DENS,WDEN,OMEG,DIAC
    24 FORMAT(1H //40X, 'DP =', F12.5//40X, 'G =', F13.5//40X,
     1 'DENS =', F10.5//40X, 'WDEN =', F10.5//40X, 'OMEG =',
     2 F10.5//40X, 'DIAC =', F10.5////)
       READ(5,99999)((TABLE(I,J),I=1,9),J=1,2)
 99999 FORMAT(8F10.5)
C
       III  =  100
       IF ( KKK .LT. 100 ) III  = KKK
    18 DO  5  I  =  1  ,  III
       NN  =  NN  +  1
       NNN =  NNN +  1
       IF ( IREAD .EQ. 0 )  GO  TO  56
       READ( 5 , 66 ) RUN, FLOL, TEMP, PS, ODIF, WBTP, DIAP, HITE,
     1 NUM2, IXP1, NUM1, XP2, (Y2(J) , J = 1 , NUM2 ) ,
     2 (Y1(J) , J = 1 , NUM1 )
    66 FORMAT(A4,F7.3,F5.1,F5.0,F10.4,F6.1,F5.2,F6.2,
     1 3I3,7X,F5.7,/(12F6.2))
C      FLOL    LIQUID FLOW RATE GPM
C      TEMP    TEMPERATURE DEGREES C.
C      PS      STATIC PRESSURE MM. OF N-HEPTANE
C      ODIF    INCLINED TUBE DIFFERENTIAL, INCHES
C      HITE    GRID SPACING , INCHES
C      1 REFERS TO INPUT, 2 REFERS TO OUTPUT
C      IXP1    DELAY IN PULSE INJECTION IN 0.01 SECS.
C      XP2     DELAY IN OUTLET PULSE ARRIVAL ,SECS.
C      XN2     NET DELAY FOR THE SECOND PULSE
C
       KUSUM=0
       XP1 = IXP1
       XP2 =  XP2   -  0.08   +  0.1354
       XN2  = XP2 - XP1 * 0.01
       DLX1  =  0.01
       DLX2  =  0.1354
C
C      CALCULATE FLOW RATES
C
```

```
      CALL  FLOW ( TEMP, PS, DCIF, WMN, DP, G, DENS, WDEN,
     1 OMEG, DIAO, MMMM, WETP )
      FLOW  = FLOL  *  8.345  *  60.  *  144./((22.*2.75**2)/7.)
      WMN   = WMN  *  144. / ((  22.  *  2.75**2 ) / 7. )
      GO  TO  76
   96 READ( 5, 1 ) RUN, FLOW, WMN, TEMP, NUM1, NUM2, DIAP,
     1HITF, XN2, OLX1, OLX2, PE, PEP, X1B, X2B,
     2X1BB, X2BB, UH, U, TAU, HOLD, HOLP,
     3(Y1(J), J = 1 , NUM1 ) , (Y2(J), J = 1 , NUM2 )
    1 FORMAT(A4,F8.1,F6.1,F4.1,2I2,F3.1,F5.2,F5.3, 8X ,F4.2,
     1F9.7,F7.3,F8.5,/,5F8.5,F6.4,F8.5,2F9.8,4X,/,(19F4.1))
   76 IF ( OLX2 .LT. 0.136 )  GO  TO  9
      OLX2      = 0.1354
    9 ARUN(I)   = RUN
      AFLOW(I)  = FLOW
      AFLOG(I)  = WMN
      ATEMP(I)  = TEMP
      IDIAP(I)  = DIAP / 0.24995
      IHITE(I)  = HITE / 5.4999
      NUMA1(I)  = NUM1
      NUMA2(I)  = NUM2
C
C     CALCULATE TRUE BED HEIGHT AND TIME OF FREE FALL
C
      IF(IHITE(I).EQ.1) GO TO 88888
      GMF=1570.*((DIAP)**1.5)*( 10.**(-0.000043*FLOW))
      CALL LOCK(VELOC)
      TRUEH=0.00315*((WMN-GMF)/GMF)* (GMF**1.2)
      TRUEH=TRUEH*5.5 *5.5
      FREEH=HITE-TRUEH
      FREET=FREEH/VELOC*(1./12.)
      FREEH=TRUEH
      GO TO 66666
C
88888 FREEH=HITE
      FREET=0.
66666 WRITE(6,11111) GMF, WMN, FREEH, HITE, FREET, VELOC
11111 FORMAT(1H , 7F10.2)
      ATRUN(I)=FREEH
C
      CALL MOMENT(PE1(NN), TAU1(NN), PEP1(NN), UH1(NN), U1(NN),
     1 HOLD1(NN), HOL1(NN), IMAX)
      CALL TRANSF(PE1(NN), TAU1(NN), PE2(NN), TAU2(NN),
     1 PEP2(NN), UH2(NN), U2(NN), HOLD2(NN), HOL2(NN),
     2 PE3(NN), TAU3(NN), PEP3(NN), UH3(NN), U3(NN),
     3 HOLD3(NN), HOL3(NN))
      ASFAC(I)  = SFACTR
    5 CONTINUE
      IF ( IPRIN4 )  7 ,  8 ,  8
    8 CONTINUE
C
C         PRINT SECTION
C
      WRITE( 6 , 6 )
    6 FORMAT(1H1//,20X, ' CALCULATED RESULTS FOR MOMENT '
     1'ANALYSIS ARE GIVEN IN THE FOLLOWING TABLE/S'//)
      CALL OUTPUT(PE1, PEP1, UH1, U1, TAU1, HOLD1,
     1 HOL1, III)
      WRITE( 6 , 26 )
   26 FORMAT(1H //,20X,' CALCULATED RESULTS FOR TRANSFER FUNCTION'
     1' ANALYSIS -- INFINITE BED CONDITIONS',/35X,
     2 'ARE GIVEN IN THE FOLLOWING TABLE/S',//)
      CALL OUTPUT(PE2, PEP2, UH2, U2, TAU2, HOLD2,
     1 HOL2, III)
      KUSUM=1
      WRITE( 6 , 36 )
   36 FORMAT(1H //,20X,' CALCULATED RESULTS FOR TRANSFER FUNCTION'
     1' ANALYSIS -- FINITE BED CONDITIONS',/35X,
     2 'ARE GIVEN IN THE FOLLOWING TABLE/S',//)
      CALL OUTPUT(PE3, PEP3, UH3, U3, TAU3, HOLD3,
     1 HOL3, III)
C
    7 NN=0
      IK  =  KKK  -  NNN
      IF (  IK  -  100  )  13 ,  14 ,  14
   13 IF (  IK  . EQ .  0 )  GO  TO  15
      III  =  IK
   14 GO  TO  18
   15 STOP
C
      END
```

```
C
C
      SUBROUTINE  TRANSF(PE, TAU, PECLET, RTS, PECLEP, UHS,
     1 US,  HOLDS, HOL1S, PEC, RTF, PEP, UH, U, HOLDF,
     2 HOL1F)
C
C     DATA REDUCTION BY TRANSFER FUNCTION ANALYSIS
C
      DIMENSION X(100), Y(100), X1(100), X2(100), XVALS(10),
     1 YVALS(10), WTS(10), XFIXED(1), YFIXED(1), COEFFS(2),
     2 AFS1(10), AFS2(10)
      COMMON Y1(100), Y2(100), ARUN(100), IDIAP(100), IWITE(100),
     1 AFLOW(100), AFLOG(100), ATEMP(100), ASFAC(100), NUMA1(100),
     2 NUMA2(100), R(13,2), AS(10), AFS(10), DLX1, DLX2, NUM1, NUM2,
     3 DIAP, WITE, FLOW, RUN, TEMP, XN2, ATERM, WHN, SFACTR, NNN,
     4 INDEX, IPUNCH, IPRINT, IPRIN1, IPRIN2, IPRIN3, IPRIN4, IJK,
     5 FLOL,FREEF,FREEH
C
C     DEFINE TIME ARRAYS FOR BOTH THE PULSES
C
      INDEX  = 0
      X1(1)=FREEF
      DO 22 I = 2 , NUM1
      K1 = I - 1
   22 X1(I) = X1(K1) + DLX1
      X2(1)  = XN2
      DO 2 I = 2 , NUM2
      K1 = I - 1
    2 X2(I) = X2(K1) + DLX2
C
C     CALCULATE AREA UNDER THE BREAKTHROUGH CURVES
C
      CALL AREA(Y1,NUM1,DLX1,AR1,0)
      CALL AREA(Y2,NUM2,DLX2,AR2,0)
      SFACTH = AR2/AR1
      AL   =  10.
      KCOUNT = 0
   17 IF ( KCOUNT  -  5  )  44 ,  55 ,  55
   44 IF (  INDEX  -  2  )  66 ,  88 ,  55
   88 CALL PARAM(PEC,RTF,PEP,UH,U,DIAP,FREEH,HOLDF,HOL1F,
     1 FLOW)
      PECLET  =  (  APECLE  +  PECLET  )  /  2.
      RTS     =  (  ARTSFN  +  RTS     )  /  2.
      CALL PARAM(PECLET,RTS,PECLEP,UHS,US,DIAP,FREEH,
     1 HOLDS, HOL1S, FLOW)
      GO  TO  55
C
C     CALCULATE TRANSFER FUNCTION FOR THE SYSTEM
C
   66 IF(  INDEX  -  1  )  666 ,  606 ,  666
  606 APECLE  =  PECLET
      ARTSFN  =  RTS
  666 DO  10  J  =  1 ,  IJK
      S = J
      S = 0.09 / TAU   +   S * 0.01 / TAU
      S = S  * AL
      DO 33 I = 1 , NUM1
      S1 = -S*X1(I)
   33 X(I) = (Y1(I))*SFACTR*(1./(EXP(-S1)))
      CALL AREA(X,NUM1,DLX1,FS1,1)
      DO 3 I = 1 , NUM2
      S2 = -S*X2(I)
    3 Y(I) = (Y2(I))*(1./(EXP(-S2)))
      CALL AREA(Y,NUM2,DLX2,FS2,1)
      FS = FS2/FS1
      YVALS(J) = 1./(ALOG(1./FS))
      XVALS(J) = S*1./((ALOG(1./FS1))*(ALOG(1./FS)))
      AS(J)    = S
      AFS1(J)  = FS1
      AFS2(J)  = FS2
      AFS(J)   = FS
   10 CONTINUE
C
C     FIT CURVE USING CURVFT SUBROUTINE
C
      DO 6 I = 1 , IJK
    6 WTS(I) = 1.
      NPTS = IJK
      ISCALE = 1
      MAXDEG = 1
      NFIXED = 0
      NCOEFF = 2
      CALL CURVFT(XVALS,YVALS,WTS,NPTS,ISCALE,MAXDEG,
     1XFIXED,YFIXED,NFIXED,COEFFS,NCOEFF,IPRINT)
      AL = AL/3.
      KCOUNT = KCOUNT + 1
C
C     CALCULATE PROCESS PARAMETERS
C
    7 RTS = COEFFS(2)
      PECLET = -1./COEFFS(1)
C
C     PRINT SECTION
C
      IF (  IPRIN2  )  20 ,  21 ,  21
C
   21 CONTINUE
   77 CALL PARAM(PECLET,RTS,PECLEP,UHS,US,DIAP,FREEH,HOLDS,
     1 HOL1S, FLOW)
      WRITE( 6 , 555 )
  555 FORMAT(1H //, 43X, 'S',  8X, 'FS1',  7X, 'FS2',  7X,
     1 'FS', //)
      WRITE( 6 , 5 )(AS(J), AFS1(J), AFS2(J), AFS(J),J=1,IJK)
    5 FORMAT(1H , 35X, 4F10.3)
      WRITE( 6 , 5 ) COEFFS
      WRITE( 6, 500 )
  500 FORMAT(1H /25X,'RUN     UHS     PECLET    FLOW      WHN     ',
     1'SFACTR   US    RTS     HOLDS     HOL1S     PECLEP    FREET')
```

```
      WRITE( 6 , 11 ) RUN, UHS, PECLET, FLOW, WHN, SFACTR,
     1 US, RTS, HOLDS, HOLIS, PECLEP, FREFT
   11 FORMAT(1H /, 25X, A4, F10.5, F8.3, F10.1, F8.1,
     1F10.4, F6.3, F7.4, 2F10.6,2F8.5,///)
C
   20 CONTINUE
C
      CALL CCMPAR(PE, TAU, PECLET, RTS, PEC, RTF, K)
C
      GO  TO  17
   55 RETURN
C
      END
C
C
      SUBROUTINE PARAM(PECLET, RTS, PECLEP, UHS, US, DIAP,AHITE,
     1 HOLDS, HOLIS, FLOW)
C
C     CALCULATE PROCESS PARAMETERS
C
      PECLEP=PECLET*DIAP/AHITE
      UHS = 1./RTS
      US=AHITE/(12.*RTS)
      FLCL =FLOW*((22.*2.75**2)/7.)/(8.345*60.*144.)
      HOLDS = FLCL * 0.13368 * RTS/60.
      HOLIS=HOLDS/(AHITE*0.1649885/12.)
C     HOLDS= TOTAL HOLDUP ,CU. FT.
C     HOLIS= DIMENSIONLESS TOTAL HOLDUP
C     FLCL=  GPM
C     FLOW=  LBS./HR. FT**2
C     US=    VELOCITY
      RETURN
C
      END
C
C
C     SUBROUTINE CCMPAR(PE, TAU, PECLET, RTS, PEC, RTF, K)
C     ----------------------------------------------------
C
C     FINITE LENGTH DIFFUSION MODEL ----
C
C
C     TRANSFER FUNCTION ANALYSIS USING PREVIOUSLY CALCULATED
C     MODEL PARAMETERS FROM INFINITE BED CONDITIONS
C
C
      COMMON Y1(100), Y2(100), ARUN(100), IDIAP(100), IHITE(100),
     1 AFLOW(100), AFLCG(100), ATEMP(100), ASFAC(100), NUMA1(100),
     2 NUMA2(100), R(13,2), AS(10), AFS(10), DLX1, DLX2, NUM1, NUM2,
     3 DIAP, HITE, FLOW, RUN, TEMP, XN2, ATERM, WHN, SFACTR, NNN,
     4 INDEX, IPUNCH, IPRINT, IPRIN1, IPRIN2, IPRIN3, IPRIN4, IJK
      APEC = 0.
      ARTS = 0.
      L  =  0
      K  =  0
C
C     DEFINE PECLET AND RESIDENCE TIME
C
      APE  = PE
      ATAU = TAU
    2 PECL1  =  APE  -  APE / 5.
      TAU1   =  ATAU -  ATAU/5.
      FS = AFS(3)
      S  =  AS(3)
      DO  30  I  =  1 ,  20
      AI = I
      THETA = TAU1 + 2.*ATAU /100. * AI
      DO  30  J  =  1 ,  20
      AJ = J
      PECL = PECL1 + 2. *APE /100. * AJ
C
C     EVALUATE TRANSFER FUNCTION FOR AXIALLY DISPERSED PLUG FLOW
C     MODEL WITH FINITE LENGTH BOUNDARY CONDITIONS
C
      BETA = SQRT(1. + 4.*THETA*S/PECL)
      TRANF  = 4. * BETA / ((( 1. + BETA ) ** 2 ) * (EXP( -PECL *
     1( 1. - BETA ) / 2. )) - (( 1. - BETA ) ** 2 ) * EXP( -PECL *
     2( 1. + BETA ) / 2. ))
      IF ( ABS ( FS - TRANF  )  -  0.0001 ) 31, 31, 30
   31 CONTINUE
      K = K + 1
      IF ( IPRIN3 .EQ. 0 )  GO TO 1
      GO  TO  3
    1 WRITE( 6 , 7 ) K, S, FS, THETA, PECL, TRANF
    3 ARTS = ARTS + THETA
      APEC = APEC + PECL
   30 CONTINUE
      L = L + 1
```

```
      IF(K)  55 , 55 , 66
   55 IF(L - 2)  44 , 77 , 77
C
C     REPEAT FOR NEW VALUES OF PECL AND THETA
C
   44 APE  =  PECLET
      ATAU =  RTS
      GO  TO  2
   66 AK = K
      IF (  INDEX . EQ . 1  )  GO  TO  88
      GO TO 99
   88 ANUPEC  = PEC
      ANURTF  =  RTF
   99 PEC  =  APEC / AK
      RTF    = ARTS / AK
      IF ( IPRIN3 ) 11 ,  12 ,  12
   12 WRITE( 6 , 5 ) K
   11 INDEX  =  INDEX  +  1
      IF( INDEX  -  2 )  78 ,  76 ,  76
   76 PEC =  (  PEC  +  ANUPEC ) / 2.
      RTF  = ( RTF  +  ANURTF ) / 2.
      GO  TO  78
   77 WRITE( 6 , 6 ) NNN ,  S
    5 FORMAT(1H /,25X, 'TOTAL NUMBER OF SETS SATISFYING THE'
     1 ' FINITE BED CONDITIONS = ', I3, /)
    6 FORMAT(1H , 'NO CONVERGENCE OBTAINED ---  NNN =',I4,
     1 '  S =',  F6.4)
    7 FORMAT(1H /25X, 'K =', I5, 3X, 'S =', F8.5, 3X,'FS =',
     1 F8.5, 3X, 'THETA =', F7.4, 3X, 'PECL =', F7.3, 3X,
     2 'TRANF =', F8.5)
   78 RETURN
C
      END
```

```
C
C     TWO POINT MOMENT ANALYSIS PROGRAM
C     ---------------------------------
C
C     NOMENCLATURE
C     ------------
C
      SUBROUTINE MOMENT(PE, TAU, PEP, UH, U, HOLD, HOL1, IMAX)
C     --------------------------------------------------------
C
C     SUBSCRIPTS 1 AND 2 REFER TO INLET AND OUTLET PULSES RESPECTIVELY
C
C     N        NUMBER OF DATA POINTS
C     DLX      TIME INTERVAL FOR EACH DATA POINT
C     X        TIME AXIS
C     Y        VALUES OF CONCENTRATION
C     XY       ARRAY OF X * Y VALUES
C     XXY      ARRAY OF X**2 * Y
C
C     ALL AREAS UNDER CURVES ARE EVALUATED BY SIMPSONS RULE
C
C     AR         AREA UNDER X - Y CURVE
C     ARR        AREA UNDER X * Y  - X CURVE
C     ARS        AREA UNDER X**2 * Y  - X CURVE
C     M1A, M2B   FIRST MOMENTS
C     X1A, X2B   X BAR VALUES
C     X1BB,X2BB SECOND CENTRAL MOMENTS
C
      DIMENSION XY1(100), XY2(100), XXY1(100), XXY2(100)
      COMMON Y1(100), Y2(100), ARUN(100), IDIAP(100), IHITE(100),
     1 AFLOW(100), AFLCG(100), ATEMP(100), ASFAC(100), NUMA1(100),
     2 NUMA2(100), R(13,2), AS(10), AFS(10), DLX1, DLX2, NUM1, NUM2,
     3 DIAP, HITE, FLCH, RUN, TEMP, XN2, ATERM, WHN, SFACTR, NNN,
     4 INDEX, IPUNCH, IPRINT, IPRIN1, IPRIN2, IPRIN3, IPRIN4, IJK,
     5 FLOL,FREET,FREEH
C
C     DIAP     DIAMETER OF PACKING, INCHES
C     HITE     COLUMN HEIGHT, INCHES
C     U/H      VELOCITY/HEIGHT
C     U        VELOCITY OF WATER IN TCA, FT. / SEC.
C     PE       COLUMN PECLET NUMBER
C     PEP      PACKING PECLET NUMBER
C     TAU      MEAN RESIDENCE TIME, SECONDS
C     HOLD     HOLD-UP IN TCA, CU. FT OF WATER
C     HOL1     HOLD-UP IN TCS, CU. FT. / CU. FT. OF TCA VOLUME
C
      IF ( IMAX .EQ. -1 )  GO  TO  1
      GO  TO  2
C
C     CALCULATE THE HIGHEST NUMBER IN ARRAY
C
    1 DO 23 I = 1, NUM2
      IF(Y2(I+1)-Y2(I)) 22,22,23
   23 CONTINUE
```

```
   22 RAM=Y2(I)
      RAM  =  0.01 * ATERM * RAM
C
C     CALCULATE ATERMS OF THE MAXIMUM VALUE IN THE ARRAY AND
C     TERMINATE, MAKING THE NEXT NUMBER ZERO
C
      DO 29 I = 15,NUM2
      IF(Y2(I) - RAM) 30, 26,29
   29 CONTINUE
   30 Y2(I)=0.
      NUM2 = I
      GO TO 27
   26 Y2(I+1) = 0.
      NUM2 = I +1
   27 CONTINUE
C
C     FIND ODD AND EVEN NUM1 AND NUM2, MAKE ODD
C     BY ADDING ANOTHER LAST ZERO
C
      F=NUM1
      F=F/2.
      I=NUM1/2
      G1 = I
      IF(F-G1)19, 19, 20
   19 NUM1 = NUM1 + 1
      Y1(NUM1) = 0.
   20 CONTINUE
      E = NUM2
      E = E/2.
      I = NUM2/2
      H = I
      IF(E-H) 21, 21, 28
   21 NUM2 =NUM2 + 1
      Y2(NUM2) = 0.
   28 CONTINUE
C
C     COMPUTE ZEROTH, FIRST AND SECOND MOMENTS
C
    2 X1 = FREET
      CALL AREA(Y1, NUM1, DLX1, AR1, 0 )
      CALL AREA(Y2, NUM2, DLX2, AR2, 0 )
      DO 6 J=1,NUM1
      XY1(J)=X1*Y1(J)
      XXY1(J)=(X1**2)*Y1(J)
    6 X1=X1+DLX1
      CALL AREA(XY1, NUM1, DLX1, ARR1, 1 )
      CALL AREA(XXY1, NUM1, DLX1, ARS1, 1 )
      X2=0.0
      DO 8 I=1,NUM2
      XY2(I)=X2*Y2(I)
      XXY2(I)=(X2**2)*Y2(I)
    8 X2=X2+DLX2
      CALL AREA(XY2, NUM2, DLX2, ARR2, 1 )
      CALL AREA(XXY2, NUM2, DLX2, ARS2, 1 )
      SFACTR  =  AR2 / AR1
      XN1=0.
      W1B=ARR1/AR1
      X1B=W1B+XN1
      X1BB=(ARS1/AR1)-(W1B**2)
      W2B=ARR2/AR2
      X2B=W2B+XN2
      X2BB=(ARS2/AR2)-(W2B**2)
      UH=1./(X2B-X1B)
      PE=2.0/(((UH*1.)**2)*(X2BB-X1BB))
      TAU =1./UH
      CALL PARAM(PE, TAU, PEP, UH, U, DIAP, FREEH, HOLD,
     1 HOL1, FLOW )
      IF (  IPRINT  )  5 , 9 ,  9
    9 CONTINUE
C
C          PRINT SECTION
C
      WRITE(6,99)NNN, DIAP, HITE
   99 FORMAT(1H , 55X, 'SERIAL NUMBER', I4, /,
     150X,'DIAP# @,F3.1,5X,'COLUMN HITE# @,F5.2)
      IF( IREAD .EC. 0 )  GO  TO  110
      WRITE(6,15)RUN,FLOL,TEMP,PS,ODIF,NUM1,DLX1,NUM2,DLX2,XN2
   15 FORMAT(40X,'RUN# @,A4,2X,'LIQUID FLOW#@,F6.3,2X,'TEMP# @,F4.1,2X,'
     1PS# @,F4.0,/27X,'ORIFICE DIFF# @,F7.4,2X,'NUM1# @,I2,1X,'DELX1# @,
     2F4.2,2X,'NUM2#@,I2,2X,'DELX2# @,F8.6,2X,'XN2# @,F4.2,/)
  110 WRITE(6,10)
   10 FORMAT(1H ,      3HRUN,2X,5HX1BAR,5X,5HX2BAR,4X,6HX1BBAR,4X,
     16HX2BBAR,5X,3HU/H,5X,2HPE,7X,4HFLOL,5X,4HFLOG,3X,1HI,5X,4HSFAC,
     2'    U     TAU        HOLD       HOL1     PEP@ )
      WRITE( 6 , 11 ) RUN, X1B, X2B, X1BB, X2BB, UH, PE,
     1 FLOW, NNN, MMMM, SFACTR, U, TAU, HOLD, HOL1, PEP
   11 FORMAT(1H ,A4,F8.5,F9.5,F9.5,F10.5,F10.5,F8.3,F10.1,F8.1,I3,
     1 F10.2, F6.3,F7.4,2F10.6,F8.5,/)
      IF (  IPUNCH  )  4 ,  3 ,  3
    3 CONTINUE
      WRITE(7,7) RUN,FLOW,WHN,TEMP,NUM1,NUM2,DIAP,HITE,XN2,SFAC,DLX1,
     1DLX2,PE,PEP,X1B,X2B,X1BB,X2BB,UH,U,TAU,HOLD,HOL1,NNN,
     2(Y1(I),I=1,NUM1),(Y2(I),I=1,NUM2)
    7 FORMAT(A4,F8.1,F6.1,F4.1,I2,I2,F3.1,F5.2,F5.3,F8.5,F4.2,
     1 F9.7,F7.3,F8.5,/,5F8.5,F6.4,F8.5,2F9.8,I4,/,(19F4.1))
    4 CONTINUE
      IF(NUM1-NUM2) 512,512,511
  511 K=NUM2 + 1
      DO 514 J = K,NUM1
  514 Y2(J) = 0.
      GO TO 51
  512 K = NUM1 + 1
      DO 513 J = K, NUM2
  513 Y1(J) = 0.
   51 CONTINUE
      IF(NUM1-NUM2) 100,101,101
  100 NNNN  =  NUM2
      GO TO 333
```

```
  101 NNNN  =  NUM1
  333 WRITE(6,16)(I,Y1(I),Y2(I), I = 1,NNNN)
   16 FORMAT(1H ,30X,11C,5A,F8.2,20X,F8.2)
      WRITE(6,123)
  123 FORMAT(1H1,/)
    5 RETURN
C
      END
```

```
C
C
      SUBROUTINE AREA(A , N , DEL , AR , K )
      --------------------------------------
C
C
C     AREA UNDER THE CURVE BY SIMPSON'S RULE
C
C
      DIMENSION A(100)
C
      IF(K) 5, 1, 5
C
C     FIND THE MAXIMUM VALUE IN THE ARRAY
C
    1 AMAX = 0.
      DO 3 I = 1, N
      IF(AMAX - A(I)) 2, 2, 3
    2 AMAX = A(I)
    3 CONTINUE
C
C     TRANSFORMING TO NON-DIMENSIONAL FORM
C
      DO 4 I = 1, N
    4 A(I) = A(I)/AMAX
C
C     CALCULATE AREA UNDER THE CURVE
C
    5 AN = N - 2
      AR = 0.
      DO 6 I = 1, AN, 2
    6 AR = ((DEL/3.)*(A(I) + 4.0*A(I + 1 ) + A(I + 2))) + AR
      RETURN
C
      END
```

```
C
C
      SUBROUTINE OUTPUT(PEA, PEPA, UHA, UA, TAUA, HOLDA,
     1 HOLA, III)
C
C
      DIMENSION PEA(100), PEPA(100), UHA(100), UA(100),
     1 TAUA(100), HOLDA(100), HOLA(100)
      COMMON Y1(100), Y2(100), ARUN(100), IDIAP(100), IHITE(100),
     1 AFLOW(100), AFLOG(100), ATEMP(100), ASFAC(100), NUMA1(100),
     2 NUMA2(100), R(13,2), AS(10), AFS(10), DLX1, DLX2, NUM1, NUM2,
     3 DIAP, HITE, FLOW, RUN, TEMP, XN2, ATERM, WHN, SFACTR, NNN,
     4 INDEX, IPUNCH, IPRINT, IPRIN1, IPRIN2, IPRIN3, IPRIN4, IJK,
     5 FLOL, FREET, FREEH, TABLE(9,2) ,ATRUH(100),KUSUN
C
C
      IL  =  49
      II  =  1
      IF (  III  -  50 )  13 ,  12 ,  12
   13 IL  =  III  -  1
   12 IJ  =  II  +  IL
      WRITE( 6 , 10 )
      WRITE( 6, 11) (ARUN(I), IHITE(I), IDIAP(I), ATEMP(I),
     1 AFLOW(I), AFLOG(I), ASFAC(I), PEA(I), PEPA(I), UA(I),
     2 TAUA(I), ATRUH(I), HOLA(I),  I  =  II ,  IJ )
   10 FORMAT(1H /, 21X, 'RUN NO.   TEMP     FLOW     FLOG      SFAC
     ) 'PE       PEP     U      TAU      TRUH    HOL1',//)
   11 FORMAT(1H , 20X, A4,'H',I1,'D',I1,F6.1,F10.1,F8.1,F10.4,F8.3,
     1 F7.3, 2F6.3, F8.2,F10.6)
    1 FORMAT(1H1)
      WRITE( 6 , 1 )
      IF ( II .EQ. 51 ) GO  TO  14
      IF ( III  .GT.  50 )  GO  TO  18
      GO  TO  14
   18 IL  =  III  -  51
   17 II  =  51
      GO  TO  12
   14 CONTINUE
C
C          PUNCHED OUTPUT FOR EACH DATA SET
C
      IF(KUSUN.EQ. 0) GO TO 56
      WRITE( 7 , 46 )  (ARUN(I), IHITE(I), IDIAP(I), ATEMP(I),
     1 AFLOW(I), AFLOG(I), ASFAC(I), PEA(I), PEPA(I), UA(I),
     2 TAUA(I), ATRUH(I), HOLA(I),  I  =  1 ,  III )
   46 FORMAT(A4,'H',I1,'D',I1,F4.1,F8.1,F6.1,F6.2,F7.3,F8.5,
     1 F6.4, F7.4,  F8.2,F8.6)
   56 RETURN
C
      END
```

```
C
C
C     CALCULATE  AIR  FLOW  RATE
C     --------------------------
C
C
      SUBROUTINE FLOG ( TEMP, PS, PP, WHN, CP, G, DENS,
     1 WDEN, OMEG, DIAO, I, WBTP )
C
C
C     NOMENCLATURE
C     ------------
C
C     DP      PIPE DIAMETER,INCHES
C     DIAO    ORIFICE DIAMETER,INCHES
C     G         MOLECULAR WEIGHT RATIO
C     TEMP    TEMPRATURE OF THE RUN,DEG. C.
C     PP      INCLINED MANOMETER READING, MM
C     PS      MANOMETER READING FOR THE INLET PIPE PRESSURE, MM
C     VISC    VISC. OF GAS AT TEMP., CP.
C     DENS    DENSITY OF MANOMETER FLUID , LB/CU FT
C     WDEN    WATER DENSITY, LB/CU FT
C     OMEG    ANGLE OF INCLINATION OF THE MANOMMETER. DEGREES.
C
      COMMON Y1(100), Y2(100), ARUN(100), IDIAP(100), IWITE(100),
     1 AFLOW(100), AFLOG(100), ATEMP(100), ASFAC(100), NUMA1(100),
     2 NUMA2(100), R(13,2)
C
C     P       V.P. OF WATER AT TEMP, MM HG
C     SP      PRESSURE OF THE MIXTURE
C             INLET STATIC PRESSURE
C             ( MANOMETER+GAGE PRESSURE ), PSIA
C     Y       SP. WT. OF GAS AT TEMP
C     YA      SP. WT. OF DRY AIR AT TEMP
C     YS      SP. WT. OF WATER VAPOR ON SATURATION AT TEMP
C             LB/CU FT
C     PO      DIFFERENTIAL PRESSURE HEAD ACROSS THE ORIFICE,
C             MM OF MANOMETER FLUID
C     HMN     INCHES OF DIFERENTIAL OF MANOMETER FLUID
C             ( INCLINED )
C     HW      DIFFERENTIAL PRESSURE HEAD ACROSS THE ORIFICE,
C             IN. OF WATER AT 68 F
C     WHN     GAS FLOW RATE, LB/HR
C     SCFM    STANDARD CUBIC FEET PER MINUTE OF GAS
C
      WBTP  =  (  WBTP  -  32.  )  *  5.  /  9.
  900 BETA=DIAO/DP
      FA=1.
      F=1./(SQRT(1.-BETA**4))
      PL=8.965-2260./(WBTP+273.)
      P=10.**PL
      PT=(P*14.69)/760.
      TEMF=(TEMP*9./5.)+32.
      VISC=0.00002864*TEMF+0.01619
      TABS=TEMF+460.
      SP=14.696+(PS/335.)*(DENS/WDEN)*(14.696/33.9)
      YA=29.*SP/(10.73*TABS)
      YS=18.*SP/(10.73*TABS)
      Y=(YA*G*((SP)-PT))/SP+YS*(PT/SP)
      PN=PP
      PO=PP*SIN(OMEG*0.01743)
      HMN=PO
      HW=HMN*(DENS-Y)/62.3
      CD=0.65
      I=0
  100 WH=(359.*CD*F*FA*DIAO**2*(1.-(0.032/3.)*(HW/SP)))*SQRT(HW*Y)
      RE=(WH*48.)/(0.000672*3.14*DIAO*3600.*VISC)
      I=I+1
      DO 200 L=1,13
      DFRE=R(L,1)-RE
      IF(DFRE) 200,300,300
  200 CONTINUE
      WRITE(6,600)
  600 FORMAT('REYNOLDS NUMBAR TOO BIG FOR THE TABLE')
      COEF = 0.6702
      GO TO 900
  300 DFFR=R(L+1,1)-R(L,1)
      COEF = ((R(L+1,2) - R(L,2))/DFFR)*DFRE  + R(L,2)
  900 WHN=359.*COEF*F*DIAO**2*FA*(1.-((0.032/3.)*(HW/(SP))))*SQRT(HW*Y)
      IF ((ABS(WHN-WH))-0.01) 400, 400, 450
  450 CD=COEF
      IF ( I .GE. 400 )  GO  TO  400
      GO TO 100
  400 CONTINUE
      SCFM=(WHN*359.)/(29.*60.)
      RETURN
C
      END
```

```
C
      SUBROUTINE LOOK(VELOC)
C
C     INTERPOLATION FOR VELOCITY OF FREE FALL
C
      COMMON Y1(100),Y2(100), ARUN(100), IDIAP(100), IMITE(100),
     1 AFLOW(100), AFLOG(100), ATEMP(100), ASFAC(100), NUMA1(100),
     2 NUMA2(100), P(13,2), AS(10), AHS(10), DLX1, DLX2, NUM1, NUM2,
     3 DIAP, MITE, FLOW, RUN, TEMP, XN2, ATERM, WHN, SFACTR, NNN,
     4 INDEX, IPUNCH, IPRINT, IPRIN1, IPRIN2, IPRIN3, IPRIN4, IJK,
     5 FLOL, FACET, FREEM, TABLE(9,2)
C
C     VELOCITY=LIQUID VELOCITY OF FREE FALL  FPS
C     FLOW=  LIQUID FLOW RATE IN LBS./HR. FT.**2
C
      DO 1 I=1,9
      IF(FLOW-TABLE(I,1))3,2,1
    1 CONTINUE
    2 VELOC=TABLE(I,2)
      GO TO 4
    3  VELOC=((TABLE(I,2)-TABLE(I-1,2))/(TABLE(I,1)-TABLE(I-1,1)))*
     1(FLOW-TABLE(I,1))+TABLE(I,2)
C
    4 RETURN
      END
C
C
      SUBROUTINE ALUE(XX,NU,FS,PK,ALPHA,BETA,S)
      -----------------------------------------
C
      DIMENSION ALPHA(1),BETA(1),S(1)
C
C     EVALUE ROUTINE FOR CURVFT
C
      PZ=0.
      PK=1.
      FS=S(1)
      DO 1 I=1,NU
      TEMP=PK
      PK=(XX-ALPHA(I))*PK-BETA(I)*PZ
      PZ=TEMP
    1 FS=FS + PK*S(I+1)
      RETURN
C
      END
```

```
C
C
C     CURVE-FIT SUBROUTINE
C     --------------------
C
C
      SUBROUTINE CURVFT(XVALS,YVALS,WTS,NPTS,ISCALE,MAXDEG,XFIXED,
     1 YFIXED,NFIXED,COEFF,NCOEFF,IPRINT)
C
C
C     REMARKS
C        COEFFS MUST BE DIMENSIONED TO AT LEAST MAXDEG+1
C
      DIMENSION XVALS(1),YVALS(1),WTS(1),XFIXED(1),YFIXED(1),COEFF(1),
     1 Z(300),ALPHA(26),BETA(26),S(26),SGMSQ(26),
     2 P(300),PO(300),XG(300),YG(300),WG(300)
C
C
C     XVALS     DIMENSIONED ARRAY OF X COORDINATE
C     YVALS     DIMENSIONED ARRAY OF Y COORDINATE
C     WTS       DIMENSIONED ARRAY OF WEIGHT VALUES
C     NPTS      NUMBER OF POINTS TO BE FITTED
C     ISCALE    SCALING FOR 1,  NO SCALING FOR  0
C     MAXDEG    HIGHEST DEGREE OF POLYNOMIAL
C     XFIXED    DIMENSIONED ARRAY OF X COORDINATE OF FIXED POINTS
C     YFIXED    DIMENSIONED ARRAY OF Y COORDINATE OF FIXED POINTS
C     NFIXED    TOTAL NUMBER OF FIXED POINTS, CONSTRAINTS
C     COEFF     DIMENSIONED ARRAY OF COEFFS OF POLYNOMIAL
C     IPRINT    -1  SUPPRESSES PRINTING, 0 FOR PRINT
C
C
      FPTS=NPTS
      XO=0.0
      IF(ISCALE)5,5,8
C
C     NO SCALING
C
    5 GAMMA=1.0
      WMEAN=1.0
      GO TO 10
C
C     SCALE POINTS
C
    8 GAMMA=0.0
      WMEAN=0.0
      DO 9 J=1,NPTS
      XJ=XVALS(J)
      XO=XO+XJ
      GAMMA=GAMMA+ XJ*XJ
    9 WMEAN=WMEAN + WTS(J)
      GAMMA=SQRT(FPTS*GAMMA-XO*XO)/FPTS
      XO=XO/FPTS
      WMEAN=WMEAN/FPTS
C
```

```
   10 IF(NFIXED)11,11,15
C
C     NO FIXED POINT CONSTRAINTS
C
   11 DO 12 J=1,NPTS
      XG(J)=(XVALS(J)-XO)/GAMMA
      YG(J)=YVALS(J)
   12 WG(J)=WTS(J)/WMEAN
      GO TO 30
C
C     INCORPORATE CONSTRAINTS
C
   15 DO 16 J=1,NFIXED
      WG(J)=1.0
      XG(J)=(XFIXED(J)-XO)/GAMMA
   16 YG(J)=YFIXED(J)
      CALL  GEFYT(NFIXED+1,1,NFIXED,XG,YG,WG,S,P,PO,SGMSQ,ALPHA,BETA)
      RHO=0.0
      DO 18 J=1,NPTS
      RHO=RHO + WTS(J)
   18 XG(J)=(XVALS(J)-XO)/GAMMA
      RHO=FPTS/RHO
      S(NFIXED+1)=0.0
      DO 22 J=1,NPTS
      CALL ALUE(XG(J),NFIXED,FS,PK,ALPHA,BETA,S)
      IF(PK)20,19,20
   19 STOP 101
   20 YG(J)=(YVALS(J)-FS)/PK
   22 WG(J)=WTS(J)*PK*PK*RHO
C
C     MERGE
C
   30 KN=MAXDEG+1
      CALL GEFYT(KN,NFIXED+1,NPTS,XG,YG,WG,S,P,PO,SGMSQ,ALPHA,BETA)
      N=KN-1
      DO 31 J=1,NPTS
      CALL ALUE(XG(J),N,FS,PK,ALPHA,BETA,S)
   31 Z(J)=FS
      DO 32 I=1,N
      ALPHA(I)=ALPHA(I)*GAMMA + XO
   32 BETA(I)=BETA(I)*GAMMA
      AMDA=GAMMA
C
C     'CODA' ROUTINE
C
      NCOEFF=N+1
      DO 34 I=2,NCOEFF
      COEFF(I)=0.0
      P(I)=0.0
   34 PO(I)=0.0
      P(1)=0.0
      PO(1)=1.0
      COEFF(1)=S(1)
      DO 35 I=1,N
      T2=0.0
      II=I+1
      DO 35 J=1,II
      T1=(T2-ALPHA(I)*PO(J)-BETA(I)*P(J))/AMDA
      T2=PO(J)
      P(J)=PC(J)
      PO(J)=T1
   35 COEFF(J)=COEFF(J)+T1*S(I+1)
C
C     PRINT SECTION
C
      IF(IPRINT)50,36,36
C
   36 WRITE(6,100)
  100 FORMAT(1H1,31X,24HPOLYNOMIAL CURVE FITTING //  6X,1HX,18X,1HY,
     1 18X,2HF1,17X,2HF2)
      DO 38 J=1,NPTS
      XZ=XVALS(J)
      FZ=COEFF(NCOEFF)
      I=N
   37 FZ=FZ*XZ + COEFF(I)
      I=I-1
      IF(I)38,38,37
   38 WRITE(6,101)XVALS(J),YVALS(J),Z(J),FZ
  101 FORMAT(4E20.7)
      N2=N+2
      WRITE(6,102)( SGMSQ(I),I=1,N2)
  102 FORMAT(6HOSGMSQ,4E16.8)
      WRITE(6,104)SGMSQ(NCOEFF),N
  104 FORMAT(15HO MINIMUM SGMSQ= ,E16.8,11H FOR DEGREE,I3)
      WRITE(6,105)N
  105 FORMAT(3H1N=,I4)
      DO 41 I=1,NCOEFF
      II=I-1
   41 WRITE(6,106)II,COEFF(I)
  106 FORMAT(2H C, I3,2H =,E18.7)
   50 RETURN
C
      END
```

```
C
C
      SUBROUTINE GEFYT(N,NC,NM,XG,YG,WG,S,P,PO,SGMSC,ALPHA,BETA)
      ----------------------------------------------------------
C
C
C
      DIMENSION XG(1),YG(1),WG(1),S(1),P(1),PO(1),SGMSC(1),ALPHA(1),
     1 BETA(1)
C
C     ROUTINE CALLED BY CURVFT
C
      J=N-NC
      IF(J)1,2,2
    1 STOP 102
    2 IXACT=0
      J=J-NM
      IF(J)3,30,1
    3 IF(J-1)4,30,30
   30 IXACT=1
    4 BETA(NC)=0.0
      DSQ=0.0
      WPP=0.0
      DO 6 J=1,NM
      P(J)=1.0
      PO(J)=0.0
      WPP=WPP + WG(J)
      IF(IXACT) 5,5,6
    5 DSQ=DSQ + WG(J)*YG(J)*YG(J)
    6 CONTINUE
      K=NM*NC-1
      DO 20 I=NC,N
      IFR=K-I
      WYP=0.0
      WXPP=0.0
      DO 10 J=1,NM
      TEMP=WG(J)*P(J)
      IF(I-N)7,8,9
    7 WXPP=WXPP + TEMP*XG(J)*P(J)
    8 IF(IFR)10,9,9
    9 WYP=WYP + TEMP*YG(J)
   10 CONTINUE
      IF(IFR)12,11,11
   11 S(I)=WYP/WPP
   12 IF(IXACT)13,13,14
   13 DSQ=DSQ-S(I)*S(I)*WPP
      SGMSC(I)=DSQ/FLOAT(IFR)
      IF(I-NC)21,14,21
   21 IF(ABS(SGMSQ(I))-ABS(SGMSC(I-1)))14,14,22
   14 IF(I-N)15,20,20
   15 ALPHA(I)=WXPP/WPP
      WPPO=WPP
      WPP=0.
      DO 17 J=1,NM
      TEMP=(XG(J)-ALPHA(I))*P(J)-BETA(I)*PO(J)
      WPP=WPP + WG(J)*TEMP*TEMP
      PO(J)=P(J)
   17 P(J)=TEMP
      BETA(I+1)=WPP/WPPO
   20 CONTINUE
      RETURN
   22 N=I-1
      RETURN
C
      END
```

VI.3. CALCULATION OF INTERFACIAL AREAS OF MASS TRANSFER

```
C
C     IRITEC = 0 WRITES FROM CO2FLO
C     IRITEC = 1 NOWRITE
C     IRITES = 0 WRITES FROM FROM SO2FLO
C     IRITES = 1 NOWRITE
C     IRITER = 0 WRITES FROM REACTN
C     IRITER = 1 NOWRITE
C     IPNCHC = 0 PUNCHES FROM CO2FLO
C     IPNCHC = 1 NOPUNCH
C     IPNCHS = 0 PUNCHES FROM SO2FLO
C     IPNCHS = 1 NOPUNCH
C
      COMMON R(26,2),T(26,2),DP,G,DENS,WDEN,OMEG,TG,AL,TL, GCO2,
     1AI,CO2IN,CO2OUT,CO2LBS,TGS,TLS,ALS,GSO2,SO2IN,SO2OUT,SO2LBS,
     2HOLD(100,40),ALNPPC,ALNPPS,AMUWAT,AMUSLN,DWAT,HW,H,ALNKR,
     3REXPTC,REXPTS,GMF,TRUEHC,TRUEHS,TRUEH,EAREA,TVOL,AKGSO2,AKGCO2,
     4ANUKGS,AREAC,SPAREA,IPNCHC,IPNCHS,IPNCHR,IRITEC,IRITES,IRITER,
     5NNNNN ,DSOLN,TK,AKR,GC
C
      IRITEC = 0
      IRITES = 0
      IRITER = 0
      IPNCHC = 1
      IPNCHS = 1
      NNNNN = 32
C
C     READ DATA
C
      READ(5,1) DP,G,DENS,WDEN,OMEG,DIAO
    1 FORMAT(6F10.5)
      IIIII = 0
      WRITE(6,24) DP,G,DENS,WDEN,OMEG
   24 FORMAT(1H1/1H ,3HDP#,F10.5/1H ,2HG#,F10.5/1H ,5HDENS#,
     1F10.5/1H ,5HWDEN#,F10.5/1H ,5HOMEG#,F10.5)
      READ(5,3)((T(L,M),L=1,13),M=1,2)
    3 FORMAT(8F10.0/5F10.0/13F5.4)
      WRITE(6,127) ((T(L,M),L=1,13),M=1,2)
      READ(5,3) ((R(L,M),L=1,13),M=1,2)
      WRITE(6,127) ((R(L,M),L=1,13),M=1,2)
  127 FORMAT(1H1,13F10.1/13F10.4)
  700 IIIII  = IIIII + 1
      CALL CO2FLO(TG,TL,AL,GC,AI,CO2IN,CO2OUT,IIIII,KKKKK)
      CALL SO2FLO(TGS,TLS,ALS,GS,SO2IN,SO2OUT,IIIII,KKKKK)
      CALL REACTN(IIIII,KKKKK,GS)
      IF(IIIII.EQ.NNNNN) GO TO 601
      GO TO 700
  601 DO 600 MNPQ = 1 , 25 , 12
      NPQR = MNPQ + 11
      WRITE(6,50)((HOLD(I,J),J=MNPQ,NPQR),I=1,NNNNN)
  600 CONTINUE
   50 FORMAT(1H1,///(12E11.3))
      CALL PRINTR(ZN,ZM)
      STOP
C
      END
```

```
C
C
      SUBROUTINE CO2FLO(TEMPG,TEMPL, WATFLO, GMASS,TOTALK,
     1GASIN,VOUT, IIIII,KKKKK)
C
C     CALCULATES FLOW RATES AND ABSORPTION DATA FOR CO2-NAOH SYSTEM
C     -------------------------------------------------------------
C
      DIMENSION FLOWN(50),CO21(100),CO22(50),CO23(50),GASFLO(50),
     1CO2M(50),CO24(50)
      COMMON R(26,2),T(26,2),DP,G,DENS,WDEN,OMEG,TG,AL,TL, GCO2,
     1AI,CO2IN,CO2OUT,CO2LBS,TGS,TLS,ALS,GSO2,SO2IN,SO2OUT,SO2LBS,
     2HOLD(100,40),ALNPPC,ALNPPS,AMUWAT,AMUSLN,DWAT,HW,H,ALNKR,
     3REXPTC,REXPTS,GMF,TRUEHC,TRUEHS,TRUEH,EAREA,TVOL,AKGSO2,AKGCO2,
     4ANUKGS,AREAC,SPAREA,IPNCHC,IPNCHS,IPNCHR,IRITEC,IRITES,IRITER,
     5NNNNN ,DSOLN,TK,AKR,GC
C
C     DP       PIPE DIAMETER,INCHES
C     DIAO     ORIFICE DIAMETER IN INCHES
C     G        MOLECULAR WEIGHT RATIO
C     TEMP     TEMPERATURE OF THE RUN,DEGREES CENTIGRADE
C     PP       INCLINED MANOMETER READING, INCHES
C     PS       MANOMETER READING FOR THE INLET PIPE PRESSURE, MM
C     DENS     DENSITY OF MANOMETER FLUID, LBS PER CU FT
C     WDEN     DENSITY OF WATER, LBS PER CU FT
C     OMEG     ANGLE OF INCLINATION OF THE MANOMETER, DEGREES
C     P        PRESSURE OF SATURATED VAPOR AT TEMP,MM HG
C     WHN      GAS FLOW RATE, LB/HR
C     SCFM     STANDARD CUBIC FEET PER MINUTE OF GAS
C
C     READ DATA
C
  700 READ(5,999) NAME,TEMP,TEMPL,PP1,PP2,PS,FLOW,GASV1,GASV2,
     1PP3,PP4,ALKA1,CARB1,ALKA2,CARB2,KKKKK
  999 FORMAT(I2,F4.1,3F5.2,F6.2,F8.2,2F6.2,F4.2,F5.2,F6.2,F5.2,2F6.2,I1)
C
C     CALCULATE GAS FLOW
C
      GMOLWT = 44.
      DIAO =1.5
      TEMPG=TEMP
      PP=PP1+PP2/64.-PP3-PP4/64.
      IF(KKKKK.EQ.1) DIAO =2.
      CALL ORIFIS(DIAO, TEMP,TEMPL, PP, PS, GASV1, GASV2,
     1GMOLWT,KKKKK, WHN, GMASS, GASIN, GASOUT,PN,TABS,SP,Y,P)
      SCFM=(WHN*359.)/(29.*60.)
      GASFLO(IIIII)=GMASS
      GCO2 = GMASS
C
C     CALCULATE AMOUNT ABSORBED
C
      V=10.
  888 CARB1  = CARB1/5.
      SOLUTN = ALKA1 * 0.97324 /50. + 1.50605*40./50.
```

```
      ALKA1 = 10. * SOLUTN / 0.97324
      CARB2  = CARB2/5.
      SOLUTN = ALKA2 * 0.97324 /50. + 1.50605*40./50.
      ALKA2 = 10. * SOLUTN / 0.97324
  777 ACIDV=0.5*(ALKA1+CARB1)+0.5*(ALKA2+CARB2)
      TOTALK=ACIDV*0.97324/V
      FLOWN(IIIIII)=FLOW/(SQRT(1.087 *6.8/6.7260))*1.087
      WATFLO = FLOWN(IIIIII)
      CO21(IIIIII)=40.*44.*.97324*FLOWN(IIIIII)*(ALKA1-ALKA2)/(1.087*453.6
     1 *80.*62.4)*28.316* 0.1
      CO22(IIIIII)=GMASS*44.*(GASV2-GASV1)/2900.
      CO23(IIIIII)=CO21(IIIIII)*(CARB2-CARB1)/(ALKA1-ALKA2)
      IF(CO23(IIIIII).EQ.0.) CO23(IIIIII) = CO21(IIIIII)
      IF(CO21(IIIIII).LT.0.)CO21(IIIIII)=CO23(IIIIII)
      CO2M(IIIIII)= (CO21(IIIIII)+ CO23(IIIIII))/2.
      CO2LBS=CO2M(IIIIII)
      GASIN = GASIN/(1. - P/760.)
      CO2ING=GMASS*0.164955*GASIN /( Y*100.)
      CO2OTG=CO2ING-CO2LBS*0.16495*359.*TABS*14.696/(44.*492.*SP)
      VOUT=CO2OTG/(CO2OTG+(CO2ING*(1.-GASIN /100.)/(GASIN /100.)))*100.
      PPCO2=(GASIN +VOUT)/2.
      CO24(IIIIII)= 100. - VOUT
C
C     PRINT SECTION
C
      IF(IRITEC.EQ.0) GO TO 111
      GO TO 222
  111 WRITE(6,10) PN, HW, WHN, SCFM, TEMP, GMASS, PS, IIIII,
     1TEMPL,FLOW,GASV1,GASV2,ALKA1,CARB1,ALKA2,CARB2,DIAO
   10 FORMAT(1H ,2F8.3,5F8.1, I3,F9.1,7F8.2,F3.1)
  222 IF(IPNCHC.EQ.0) GO TO 333
      GO TO 444
  333 WRITE(7,401) TEMPG,PP,TEMPL,FLOWN(IIIIII),GMASS,PPCO2,TOTALK,
     1GASIN,  VOUT, V,CO2M(IIIIII),IIIII
  401 FORMAT(F5.1,F7.4,F5.1,F10.1,F7.1,F7.2,F7.3,2F7.2,F4.1,F8.2,I3)
  444 IF(IIIII.EQ.NNNNN) GO TO 600
      GO TO 11111
  600 WRITE(6,650) (FLOWN(IN),CO21(IN),CO22(IN),CO23(IN),CO2M(IN),
     1 CO24(IN),GASFLO(IN), IN, IN = 1 , NNNNN)
  650 FORMAT(1H1,///(7F15.5,I5))
C
11111 RETURN
C
C     GMOLWT  MOLECULAR WEIGHT OF GAS BEING ABSORBED
C     GASIN   GAS CONCENTRATION AT THE INLET
C     GASOUT  GAS CONCENTRATION AT THE OUTLET
C     CO2     GAS ARSORBED LBS CO2/HR-FT**2
C     PPCO2   P.P OF CO2, %AGE
C     ACIDV   ACID VOLUME REQUIRED TO NEUTRALIZE V CC OF SAMPLE
C     TOTALK  TOTAL ALKALINITY, GM MOL/LITER
C
      END
```

```
C
C
      SUBROUTINE SO2FLO(TEMPG,TEMPL,WATFLO,GMASS,
     1 VOUT,GASOUT, IIIII,INDEX)
C
C     CALCULATES FLOW RATES AND ABSORPTION DATA FOR SO2-NAOH SYSTEM
C     -------------------------------------------------------------
C
      DIMENSION FLOWN(50),CO21(50),CO22(50),CO23(50),GASFLO(50)
C
      COMMON R(26,2),T(26,2),DP,G,DENS,WDEN,OMEG,TG,AL,TL, GCO2,
     1AI,CO2IN,CO2OUT,CO2LBS,TGS,TLS,ALS,GSO2,SO2IN,SO2OUT,SO2LBS,
     2HOLD(100,40),ALNPPC,ALNPPS,AMUWAT,AMUSLN,DWAT,HW,H,ALNKR,
     3REXPTC,REXPTS,GMF,TRUEHC,TRUEHS,TRUEH,EAREA,TVOL,AKGSO2,AKGCO2,
     4ANUKGS,AREAC,SPAREA,IPNCHC,IPNCHS,IPNCHR,IRITEC,IRITES,IRITER,
     5NNNNN ,DSOLN,TK,AKR,GC
C
C
C     SO2IN  SO 2  INTO COLUMN  GRAM-MOLES / SEC.
C     SO2OUT SO 2 OUT OF COLUMN  GRAM-MOLES / SEC.
C     SO2ABS SO 2 ABSORBED IN COLUMN GRAM-MOLES / SEC.
C     SO2LBS SO 2 ABSORBED IN COLUMN LBM/HR-FT**2
C     SO2ING SO 2 INTO COLUMN FT**3/HR
C     SO2OTG SO 2 OUT OF COLUMN FT**3/HR
C
C
C     READ DATA
C
  700 READ(5,999)VA,VB,NAME,TEMP,TEMPL1,TEMPL2,IPP1,IPP2,VS,PS,FLOW,
     1 GASV1,GASV2,IPP3,IPP4,VLA,VLB,INDEX
  999 FORMAT(2F5.2,I2,1X,3F5.2,2I2,F7.2,F4.2,F7.2,2F6.3,I1,I2,1X,2F6.2,
     1I2)
C
C     CALCULATE  GAS  FLOW
C
      GMOLWT = 64.
      DIAO = 1.5
      IF(INDEX.EQ.1)DIAO=2.0
      TEMPL = (TEMPL1 + TEMPL2)/2.
      TEMPG=TEMP
      PP = FLOAT(IPP1) + FLOAT(IPP2)/64.0-FLOAT(IPP3)-FLOAT(IPP4)/64.
      CALL ORIFIS(DIAO, TEMP,TEMPL, PP, PS, GASV1, GASV2,
     1GMOLWT, INDEX, WHN, GMASS, GASIN, GASOUT,PN,TABS,SP,Y, P)
      SCFM=(WHN*359.)/(29.*60.)
      GASFLO(IIIIII)=GMASS
      GSO2 = GMASS
C
C     CALCULATE AMOUNT ABSORBED
C
      ANORMT=1./9.
      ANORMI=VS*ANORMT*0.1
      VOLIIN=(VA*ANORMI-VLA*ANORMT)/10.
      SO2IN=(VOLIIN*0.03203*FLOW*0.165*(30.48)**3)/(64.*62.4*3600. )
      VOLIOT=(VB*ANORMI-VLB*ANORMT)/10.
```

```
      SO2OUT=SO2IN*VOLIOT/VOLIIN
      SO2ABS=SO2OUT-SO2IN
      SO2LBS=SO2ABS*64.*3600./(453.6*0.165)
      SO2ING=GMASS*0.164955*GASOUT/(Y*100.)
      SO2OTG=SO2ING*SO2LBS*0.16495*359.*TABS*14.696/(64.*492.*SP)
      VOUT=SO2OTG/(SO2OTG+(SO2ING*(1.-GASOUT/100.)/(GASOUT/100.)))*100.
      CO21(IIIIII) = SO2ABS
      CO22(IIIIII) = SO2LBS
      CO23(IIIIII) = VOUT
      FLOWN(IIIIII)=FLOW/(SQRT(1.087 *6.8/6.7260))*1.087
      WATFLO = FLOWN(IIIIII)
C
C     PRINT  OUT  SECTION
C
      IF(IRITES.EQ.0) GO TO 111
      GO TO 222
  111 WRITE(6,10) PN, HW, WHN, SCFM, TEMP, GMASS, PS, IIIII,
     1TEMPL,FLOW,GASV1,GASV2,VOUT,VLA,VLB ,DIAO
      GASV1  = 100. - VOUT
   10 FORMAT(1H ,2F8.3,5F8.1, I3,F9.1,8F8.2,F3.1)
  222 IF(IPNCHS.EQ.0) GO TO 333
      GO TO 444
  333 CONTINUE
      WRITE(7,401) TEMPG,PP,TEMPL,FLOWN(IIIIII),GMASS,VOUT,GASOUT,
     1SO2LBS ,IIIII
  401 FORMAT(F5.1,F7.4,F5.1,F10.1,F7.1,14X,2F7.2,4X,  F8.2,I3)
C
  444 IF(IIIIII.EQ.NNNNNN) GO TO 600
C
      GO TO 11111
  600 WRITE(6,650) (FLOWN(IN),CO21(IN),CO22(IN),CO23(IN),
     1 GASFLO(IN), IN, IN = 1 , NNNNN)
  650 FORMAT(1H1,///(5E20.5,I5))
C
11111 RETURN
C
      END
```

```
C
      SUBROUTINE REACTN (N,KKKKK,GS)
C
C     CALCULATES EFFECTIVE INTERFACIAL AREA OF MASS TRANSFER
C     ------------------------------------------------------
C
      COMMON R(26,2),T(26,2),DP,G,DENS,WDEN,DMEG,TG,AL,TL, GCO2,
     1AI,CO2IN,CO2OUT,CO2LBS,TGS,TLS,ALS,GSO2,SO2IN,SO2OUT,SO2LBS,
     2HOLD(100,40),ALNPPC,ALNPPS,AMUWAT,AMUSLN,DWAT,HW,H,ALNKR,
     3REXPTC,REXPTS,GMF,TRUEHC,TRUEHS,TRUEH,EAREA,TVOL,AKGSO2,AKGCO2,
     4ANUKGS,AREAC,SPAREA,IPNCHC,IPNCHS,IPNCHR,IRITEC,IRITES,IRITER,
     5NNNNN ,DSOLN,TK,AKR,GC
C
C
C     TL      TEMPERATURE DEG. C.
C     TK      TEMPERATURE DEG. K.
C     AI      IONIC STRENGTH
C     F       CONCENTRATION OF SOLUTION IN FORMALITY
C     AMUSLN  VISCOSITY OF NAOH SOLUTION C.P.
C     DWAT    DIFFUSIVITY OF CARBON DIOXIDE IN WATER (CM**2 / SEC.)*10**5
C     DWAT .  DIFFUSIVITY OF CARBON DIOXIDE IN NAOH  (CM**2 / SEC.)*10**5
C     AKR     REACTION VELOCITY CONSTANT, LITERS/(GM-MOLE-SEC.)
C     ALNKR   LOG (AKR)
C     AKLR    LIQUID MASS TRANSFER COEFF WITH REACTION,CM/SEC
C     AKG'S   GAS MASS TRANSFER COEFFICIENT,GM-MOL/SEC ATM CM**3
C     HHW     RATIO OF H TO HW
C     HW      HENRY'S LAW CONSTANT FOR WATER  G-MOLES/L-ATMOS.
C     H       HENRY'S LAW CONSTANT FOR NAOH   G-MOLES/L-ATMOS.
C     CSTR    EQUILIBRIUM CONCENTRATION  G-MOLES/CC.
C     R       RATE OF ABSORBTION    G-MOLES/(SEC. CM**2)
C     REXPTL  EXPERIMENTAL RATE OF ABSORBTION  GM.-MOLES CO 2 / SEC.
C     TRUEH   TRUE BED HEIGHT  FT.
C     TVOL    TRUE BED VOLUME CM**3
C     AREAC   EFFECTIVE INTERFACIAL AREA,CM**2/CM**3
C     SPAREA  SPECIFIC AREA   CM**2 / CM**3
C     GMF     MINUMUM FLUIDIZATION VELOCITY  LBM./(HR.-FT**2)
C     PPCO2   CO 2 PRESENT EXPRESSED AS A PERCENTAGE
C
      DIAP=0.75
C     F MUST BE LESS THAN 8.
C     CANNOT HANDLE MORE THAN 100 SETS OF DATA WITHOUT CHANGING DIMENSION
C
C     CALCULATE LOG-MEAN DRIVING FORCE
C
      ALNPPC=(CO2IN-CO2OUT)/ALOG(CO2IN/CO2OUT)  *0.01
      ALNPPS=(SO2IN-SO2OUT)/ALOG(SO2IN/SO2OUT)  *0.01
      TGK=TG+273.13
C
C     CALCULATE  VISCOSITY OF THE SOLUTION
C
      TT=TL-8.435
      AMUWAT=100./(2.1482*(TT+SQRT(8078.4+TT**2))-120.)
      F=AI
      IF(F.GT.4.) GO TO 10
```

```
      IF(F.GT.2.) GO TO 20
C
      AMUSLN=AMUWAT*((F*0.3)+1.00)
      GO TO 30
   10 AMUSLN=AMUWAT*(((F-4.)*1.0625)+2.78)
   20 AMUSLN=AMUWAT*(((F-2.)*0.575)+1.59)
   30 CONTINUE
C
C     CALCULATE  DIFFUSIVITY OF THE GAS IN SOLUTION
C
      DWAT=(TL-10.)*0.04358 + 1.2368
      DSOLN=DWAT*(AMUWAT/AMUSLN)**0.85
      TK=TL +273.13
C
C     CALCULATE  REACTION VELOCITY CONSTANT
C
      ALNKR=13.635 - (2895./TK) + 0.133*AI
      AKR=10.**ALNKR
C
C     CALCULATE  SOLUBILITY OF CO2, IN THE SOLUTION
C
      A=0.01 + ((0.017-0.01)/10.)*(TL-15.)
      HHW=10.**(-(0.094+0.061-AI*AI)
      HW=10.**((1140./TK)-5.3)
      H=HHW*HW
      AKLR=SQRT(DSOLN*AKR*AI*0.00001)
      REXPTC=CO2LBS*0.163*453.6/(3600.*44.)
      REXPTS=SO2LBS*0.163*453.6/(3600.*64.)
C
C     CALCULATE BED HEIGHT
C
      GMF=1570. * ((DIAP)**1.5) * (10.**(-0.000043 * AL))
      TRUEHC=0.00015*((GC   - GMF)/GMF)*(GMF**1.2)
      TRUEHS=0.00015*((GS   - GMF)/GMF)*(GMF**1.2)
      IF ( TRUEHC . LT . 0. )  TRUEHC  = 0.
      IF ( TRUEHS . LT . 0. )  TRUEHS  = 0.
      TRUEH=(TRUEHC+TRUEHS)/2.
      TRUEH=(TRUEH*5.5 +5.5)/12.
      EAREA=3.1416*16.**0.089*((16.5/12.)-TRUEH)/12.
C
C     CALCULATE INTERFACIAL AREA OF MASS TRANSFER
C
      TVOL=0.165 * TRUEH * (30.48**3)
      AKGCO2=REXPTC/(ALNPPC*TVOL)
      AKGSO2=REXPTS/(ALNPPS*TVOL)
      ANUKGS=AKGSO2*SQRT(0.165/0.151)
      AREAC=AKGCO2*ANUKGS/((ANUKGS-AKGCO2)*H*AKLR)*1000.
      EAREA=EAREA/TVOL
      SPAREA=AREAC-EAREA
C
C     PRINT OUT SECTION
C
      IF(IRITER.NE.0) GO TO 57
C
   56 WRITE(6,50)AL,GC,TRUEHC,AI,AKR,H,REXPTC,SPAREA
C
      WRITE(6,50)ALS,GS,TRUEHS,REXPTS,ALNPPC,ALNPPS,AKLR,
     1AKGCO2,AKGSO2,ANUKGS,AREAC
C
C     HOLD EVERYTHING
C
   57 HOLD(N,1)=TL
      HOLD(N,2)=TG
      HOLD(N,3)=DSOLN
      HOLD(N,4)=DWAT
      HOLD(N,5)=AMUSLN
      HOLD(N,6)=AMUWAT
      HOLD(N,7)=HHW
      HOLD(N,8)=HW
      HOLD(N,9)=TRUEH
      HOLD(N,10) = SPAREA
      HOLD(N,11) = EAREA
      HOLD(N,12) = AL
      HOLD(N,13) = AKGCO2
      HOLD(N,14) = AKGSO2
      HOLD(N,15) = ANUKGS
      HOLD(N,16) = AREAC
      HOLD(N,17) = GMF
      HOLD(N,18) = TRUEHC
      HOLD(N,19) = TRUEHS
      HOLD(N,20) = REXPTC
      HOLD(N,21) = REXPTS
      HOLD(N,22) = AI
      HOLD(N,23) = AKR
      HOLD(N,24) = H
      HOLD(N,25) = GC
      HOLD(N,26) = GS
      HOLD(N,27) = DIAP
      HOLD(N,28) = ALNPPC
      HOLD(N,29) = ALNPPS
      HOLD(N,30) = AKLR
      HOLD(N,31) = TLS
      HOLD(N,32) = TGS
      HOLD(N,33) = CO2IN
      HOLD(N,34) = CO2OUT
      HOLD(N,35) = SO2IN
      HOLD(N,36) = SO2OUT
   50 FORMAT(8E12.3)
C
C
C
      RETURN
      END
```

```
C
      SUBROUTINE FINDCD(RE,W,COEF)
C
C     ITERATES FOR COEFFICIENT OF DISCHARGE
C     -------------------------------------
C
      DIMENSION W(26,2)
C
      COMMON R(26,2),T(26,2),DP,G,DENS,WDEN,OMEG,TG,AL,TL, GCO2,
     1AI,CO2IN,CO2OUT,CO2LBS,TGS,TLS,ALS,GSO2,SO2IN,SO2OUT,SO2LBS,
     2HOLD(100,40),ALNPPC,ALNPPS,AMUWAT,AMUSLN,DWAT,HW,H,ALNKR,
     3REXPTC,REXPTS,GMF,TRUEHC,TRUEHS,TRUEH,EAREA,TVOL,AKGSO2,AKGCO2,
     4ANUKGS,ARFAC,SPAREA,IPNCHC,IPNCHS,IPNCHR,IRITEC,IRITES,IRITER,
     5NNNNN ,DSOLN,TK,AKR,GC
C
      DO 200 L=1,13
      DFRE=W(L,1)-RE
      IF(DFRE)200,300,300
  200 CONTINUE
  300 IF(L.GT.1) GO TO 500
      DFFR=W(L+1,1)-W(L,1)
      COEF=((W(L+1,2)-W(L,2))/DFFR)*(RE-W(L,1))+W(L,2)
      GO TO 600
  500 DFFR = W(L,1) - W(L-1,1)
      COEF=((W(L,2)-W(L-1,2))/DFFR)*(RE-W(L,1))+W(L,2)
  600 CONTINUE
C
C
      RETURN
      END
```

```
      SUBROUTINE ORIFIS(DIAO, TEMP,TEMPL, PP, PS, GASV1, GASV2,
     1GMOLWT, INDEX, WHN, GMASS, GASIN, GASOUT,PN,TABS,SP,Y,P)
      COMMON R(26,2),T(26,2),DP,G,DENS,WDEN,OMEG,TG,AL,TL, GCO2,
     1AI,CO2IN,CO2OUT,CO2LBS,TGS,TLS,ALS,GSO2,SO2IN,SO2OUT,SO2LBS,
     2HOLD(100,40),ALNPPC,ALNPPS,AMUWAT,AMUSLN,DWAT,HW,H,ALNKR,
     3REXPTC,REXPTS,GMF,TRUEHC,TRUEHS,TRUEH,EAREA,TVOL,AKGSO2,AKGCO2,
     4ANUKGS,ARFAC,SPAREA,IPNCHC,IPNCHS,IPNCHR,IRITEC,IRITES,IRITER,
     5NNNNN ,DSOLN,TK,AKR,GC
C     VISC    VISCOSITY OF GAS AT TEMP, CENTIPOISES
C     SP      PRESSURE OF THE  MIXTURE,STATIC + ATMOSPHERIC,PSIA
C     Y       SP. WT. OF GAS AT TEMP AND SP, LBS PER CU FT
C     YA      SP. WT. OF DRY AIR AT TEMP, LBS PER CU FT
C     YS      SP. WT. OF WATER VAPOUR AT TEMP AND SP,LBS PER CU FT
C     PO      ORIFICE DIFFERENTIAL, MM OF MANOMETER FLUID
C     HMN     ORIFICE DIFFERENTIAL ON INCLINED SCALE, INCHES
C     HW      PRESSURE DIFFERENTIAL ACROSS ORIFICE,INCHES WATER AT 68 F
  500 BETA=DIAO/DP
      FA=1.
      F=1./(SQRT(1.-BETA**4))
      WBTP=TEMP
      PL=8.965-2260./(WBTP+273.)
      P=10.**PL
      PT=(P*14.69)/760.
      TEMF=(TEMP*9./5.)+32.
      VISC=0.00002864*TEMF+0.01619
      TABS=TEMF+460.
      SP=14.696+(PS/305.)*(DENS/WDEN)*(14.696/33.9)
      GASIN=100.-GASV1
      GASOUT=100.-GASV2
      YA=(GASV1/100.+(1.-GASV1/100.)*(GMOLWT/29.))*29.*SP/(10.73*TABS)
      YS=18.*SP/(10.73*TABS)
      Y=(YA*G*((SP)-PT))/SP+YS*(PT/SP)
      PN=PP
      PO=PP*SIN(OMEG*0.01743)
      HMN=PO
      HW=HMN*(DENS-Y)/62.3
      CD=0.65
  100 WH=(359.*CD*F*FA*DIAO**2*(1.-(0.032/3.)*(HW/SP)))*SQRT(HW*Y)
      RE=(WH*48.)/(0.000672*3.14*DIAO*3600.*VISC)
      IF(INDEX.EQ.1) GO TO 666
      CALL FINDCD(RE,T,COEF)
      GO TO 555
  666 CALL FINDCD(RE,R,COEF)
  555 WHN=359.*COEF*F*DIAO**2*FA*(1.-((0.032/3.)*(HW/(SP))))*SQRT(HW*Y)
      IF((WHN-WH)-0.01) 400,400,450
  450 CD=COEF
      GO TO 100
  400 CONTINUE
      GMASS = WHN* 1./0.164955
      RETURN
C
      END
```

```
      SUBROUTINE APRNT(IA,IB,IC,ID,II,I)
C
      COMMON R(26,2),T(26,2),DP,G,DENS,WDEN,OMEG,TG,AL,TL, GCO2,
     1A1,CO2IN,CO2OUT,CO2LBS,TGS,TLS,ALS,GSO2,SO2IN,SO2OUT,SO2LBS,
     2HOLD(100,40),ALNPPC,ALNPPS,AMUWAT,AMUSLN,DWAT,HW,H,ALNKR,
     3REXPTC,REXPTS,GMF,TRUEHC,TRUEHS,TRUEH,EAREA,TVOL,AKGSO2,AKGCO2,
     4ANUMGS,APFAC,SPAREA,IPNCHC,IPNCHS,IPNCHR,IRITEC,IRITES,IRITER,
     5NNNNN ,DSOLN,TK,AKR,GC
C
      WRITE(6,2)
    2 FORMAT(1H1,//////////35X,'TABLE IV INTERFACIAL AREA DETERMINATION'
     1)
      IF(IC.GT.0) WRITE(6,11)
   11 FORMAT(1H ,50X,'(CONTINUED)')
      IF (IA.EQ.0) GO TO 6
      IF((IA.GE.1).AND.(IB.EQ.0).AND.(IA.EQ.4)) GO TO 6
      IF((IA.GE.1).AND.(IB.GE.1).AND.(IC.LE.4).AND.(IB.EQ.4)) GO TO 19
   10 WRITE(6,15)
   15 FORMAT(1H ,40X, 'EXPERIMENTAL DATA (CONTINUED)'
      GO TO 10
    6 WRITE(6,5)
    5 FORMAT(1H ,45X,   'EXPERIMENTAL DATA'
   19 III = II - 1
      IF(III)20, 25, 30
   20 WRITE(6,21)
   21 FORMAT(/28X,  'ABSORPTION OF CARBON DIOXIDE IN SODIUM HYDROXIDE SO
     1LUTION'      )
      IA = IA +1
      IF(IA.EQ.4) GO TO 40
      GO TO 35
   25 WRITE(6,26)
   26 FORMAT(/29X, 'ABORRPTION OF SULPHER DIOXIDE IN 2N SODIUM HYDROXIDE
     1 SOLUTION '   )
      IB = IB +1
      IF (IB.EQ.4) GO TO 40
      GO TO 35
   30 WRITE(6,31)
   31 FORMAT(/28X,  'EXPERIMENTAL DATA AND CALCULATED RESULT FOR ABSORPT
     1ION')
      IC = IC +1
      IF (IC.EQ.4) GO TO 40
   35 WRITE(6,36)
   36 FORMAT( 45X,'IN MOBILE BED CONTACTOR'/1H ,48X,'DP = 0.75 INCHES'/)
      GO TO 60
   40 WRITE(6,41)
   41 FORMAT( 45X, 'IN FIXED BED CONTACTOR'/1H ,48X,'DP = 0.75 INCHES'/)
  600 II = II +1
C
   60 CONTINUE
      IE = ID + 7
      IF(I.LE.4) GO TO 90
      IF(I.LE.8) GO TO 91
      WRITE(6,93)
      WRITE(6,203)(N,HOLD(N,12),HOLD(N,25),HOLD(N,13),HOLD(N,15),
     1 HOLD(N,22),HOLD(N,24),HOLD(N,3),HOLD(N,23),HOLD(N,10),N=ID,IE)
  203 FORMAT(1H ,/,13X,I2,F9.0,F6.0,  2F9.2,F7.2,F9.4,F9.2,F13.1,F10.3)
      GO TO 101
   90 WRITE(6,94)
      WRITE(6,201)(N,HOLD(N,12),HOLD(N,25),HOLD(N,20),HOLD(N,22),
     1 HOLD(N,1),HOLD(N,2),HOLD(N,28),N=ID,IE)
  201 FORMAT(1H ,/,15X,I4,F12.1,F8.1,F13.4,F8.2,2F10.1,F10.3)
      GO TO 101
   91 WRITE(6,95)
      WRITE(6,202)(N,HOLD(N,12),HOLD(N,26),HOLD(N,21),HOLD(N,31),
     1 HOLD(N,32),HOLD(N,29),N=ID,IE)
  202 FORMAT(1H ,/,15X,I4,F12.1,F10.1,E13.4,F10.1,F11.1,F15.3)
      GO TO 101
C
   93 FORMAT(/,12X,' RUN   LIQUID  GAS     KG      KG     ',
     1'LIQUID SOLUBILITY DIFFUSIVITY REACTION INTERFACIAL',
     2/,12X,'NUMBER  FLOW    FLOW     (CO2)   (SO2) ',
     3'CONCN                          VELOCITY    AREA',
     4/,49X,'GM-MOL/L',12X,'10**5',
     5 6X,  'CONSTANT',/,14X,'  LBS/HR-FT**2 GM-MOL/(SEC ATM CM**3)','
     6 GM-MOL/L-ATM CM**2/SEC L/GM-MOL-SEC CM**2/CM**3'/)
   94 FORMAT(/,15X,'  RUN    LIQUID     GAS      RATE OF     LIQUID    LI
     1QUID     GAS   LOG MEAN GAS',/,15X,' NUMBER   FLOW      FLOW     ABS
     2ORPTION   CONCN.     TEMP        TEMP    CONCENTRATION',
     3//,15X,'           LBS/HR-FT**2      GM-MOL/SEC  GM-MOL/L.     C',
     4'            C          %  '/)
   95 FORMAT(/,15X,'  RUN     LIQUID      GAS       RATE OF      LIQUID',
     1'       GAS      LOG  MEAN  GAS',  /,15X,' NUMBER     FLOW       FLOW
     2    ABSORPTION      TEMP         TEMP      CONCENTRATION',
     3//,15X,'             LBS/HR-FT**2       GM-MOL/SEC        C
     5C          %'/)
  101 CONTINUE
      IF((IA.EQ.4).AND.(IB.EQ.0)) GO TO 97
      IF((IA.EQ.4).AND.(IB.EQ.4).AND.(IC.EQ.0)) GO TO 97
      GO TO 96
   97 ID = 1
      GO TO 98
   96 ID  =  ID  +  8
   98 CONTINUE
C
      RETURN
      END
```

```
      SUBROUTINE PRINTR(AN,BN)
      COMMON R(26,2),T(26,2),DP,G,DENS,WDEN,OMEG,TG,AL,TL, GCO2,
     1AI,CO2IN,CO2OUT,CO2LBS,TGS,TLS,ALS,GSO2,SO2IN,SO2OUT,SO2LBS,
     2HOLD(100,40),ALNPPC,ALNPPS,AMUWAT,AMUSLN,DWAT,HW,H,ALNKP,
     3PSXPTC,REXPTS,GMF,TRUEHC,TRUEHS,TRUEH,EAREA,TVOL,AKGSO2,AKGCO2,
     4ANUMGS,ARFAC,SPAREA,IPNCHC,IPNCHS,IPNCHP,IRITEC,IRITES,IRITER,
     5NNNNN ,DSOLN,TK,AKR,GC
      IA = 0
      IB = 0
      IC = 0
      ID = 1
      II = 0
      DO 700 IN = 1, 32
      HOLD(IN,28) = 100.*HOLD(IN,28)
      HOLD(IN,29) = 100.*HOLD(IN,29)
  700 CONTINUE
      DO 5 I = 1,12
    5 CALL APRNT(IA,IB,IC,ID,II,I)
      STOP
      END
```

VI.4. CALCULATION OF PHYSICAL MASS TRANSFER COEFFICIENTS

```
C
C
C     THIS PROGRAM CALCULATES MASS TRANSFER COEFFICIENTS
C     ----------------------------------------------
C
C
      DIMENSION W(36,2), HOLD(50,20)
C
C     TVOL       COLUMN VOLUME, LITERS
C     REXPTL     RATE OF ABSORPTION, GM-MOLES/HR
C     AKLA,AKA   MASS TRANSFER COEFFICIENT, HR,-1
C     GMF        MINIMUM FLUIDIZATION GAS VELOCCITY,LBS/HR-FT**2
C     ANOX       NO. OF TRANSFER UNITS
C     REL        REYNOLDS NUMBER
C     ALAMDA     ABSORPTION FACTOR
C     IPRINT = 1     PRINTS
C     IPRINT = 0     NOPRINT
C
      WRITE(6,12345)
12345 FORMAT(1H1)
      M = 0
      IPRINT = 0
      PERCNT = 0.0001
      DP = 0.75
      GA = 68000000.
      READ(5,1) ((W(I,J),I=1,36),J=1,2)
    1 FORMAT(16F5.1)
  222 FORMAT(1H , (12F10.3))
      WRITE(6,222) W
    2 READ(5,10)AL,G,XIN,XOUT,III,TL
   10 FORMAT(2F10.1,2F10.7,10X,I5,F10.2)
      DELT = 0.1
      ANOX = .85
      ANOX1 = ANOX
      ANOX2 = ANOX
      M = 0
      DIAP = DP/12.
C
C     FIND BED HEIGHT
C
      GMF = 1570. * ((DP)**1.5)*(10.**(-0.000043*AL))
      DELTA =(G-GMF)/GMF
      IF(DELTA.LT.0.) DELTA=0.
      HEIGHT = 0.00015*(DELTA)*(GMF**1.2)
      HEIGHT = HEIGHT*5.5 +5.5
      HITE = HEIGHT/12.
      REL = (DIAP * AL)/2.42
C
C     FIND LIQUID PECLET NUMBER
C
      IF(DELTA.EQ.0.) GO TO 14
      CALL FINOCO(DELTA,W,PEPEC)
   13 PEO = 1.06 *(REL**0.41)*(GA**(-0.095))
      PE = PEPEO*PEO
      P = PE * HEIGHT /DP
      GO TO 15
   14 P = 1.06 * (REL**0.41)*(GA**(-0.095))
      P = P * HEIGHT / DP
   15 CONTINUE
C
C     FIND NO. OF TRANSFER UNITS WITH LIQUID MIXING
C
      H = 10.**((1140./(TL + 273.13))-5.3)
      H = 1000. /( H * 18.)
      ALAMDA = (29.*AL)/(18.*G *H)
      EXPANS = XOUT/XIN
   20 A = P + ALAMDA * ANOX
      AA = A/2.
      B = ( 1. - ALAMDA ) * ANOX * P
      RT = SQRT((AA**2 + B))
      ALAM2 = AA + RT
      ALAM3 = AA - RT
      F2 = 1. + ALAM2/ANOX - ( ALAM2**2/(ANOX*P ))
      F3 = 1. + ALAM3/ANOX - ( ALAM3**2/(ANOX*P ))
      D1 = (ALAM2 * F3 - ALAM3 * F2) * (EXP(A))
      D2 = ALAM3 * ( EXP(ALAM3))
      D3 = - ALAM2 * ( EXP(ALAM2))
      D = D1 + ALAM3*(1.-ALAM2/P)*(EXP(ALAM3))-ALAM2*(1.-ALAM3/P)*
     1 (EXP(ALAM2))
      F1 = D1 / D
      F2 = D2 / D
      F3 = D3/D
      M = M+1
      IF(M.GT.2) XODXI = XODXI2
      IF(M.GT.1) GO TO 41
   40 XODXI = F1 + F2*(EXP(ALAM2)) + F3*(EXP(ALAM3))
   61 IF((ABS(XODXI - EXPANS)*100./EXPANS)-PERCNT)150,150,63
   41 XODXI2 = F1 + F2*(EXP(ALAM2)) + F3*(EXP(ALAM3))
C
C     INTERMEDIATE PRINT OUT
C
      IF(IPRINT.EQ.0) GO TO 62
      WRITE(6,600)XODXI,XODXI2,EXPANS,DELT,ANOX1,ANOX2,4
  600 FORMAT(1H ,6F15.3,I5)
   62 IF((ABS(XODXI2-EXPANS)*100./EXPANS)-PERCNT)151,151,63
   63 IF(M-1)280,70,280
   70 ANOX2 = ANOX1 + DELT
      ANOX = ANOX2
      GO TO 20
  280 IF((XODXI2 - EXPANS).GT.0.) GO TO 210
      IF((XODXI  - EXPANS).LT.0.) GO TO 80
      GO TO 81
  210 IF((XODXI  - EXPANS).LT.0.) GO TO 81
   80 IF((ABS(XODXI2-EXPANS))-(ABS(XODXI-EXPANS)))81,110,75
   75 DELT = -DELT
      GO TO 70
   81 IF(XODXI-EXPANS)82,82,83
   82 IF(XODXI2-EXPANS)90,90,95
```

```
   83 IF(XODXI2-EXPANS)95,95,90
   90 ANOX1 = ANOX2
      ANOX2 = ANOX2 + DELT
      ANOX = ANOX2
      GO TO 20
   95 ANOX2 = ANOX1 + DELT/2.
      DELT = DELT/2.
      ANOX = ANOX2
      IF(N.GT.999) GO TO 110
      GO TO 20
  150 ANOX = ANOX1
      GO TO 152
  151 ANOX = ANOX2
  152 AKA = ANOX * AL /(HITE * 62.4)
C
C     FIND NO. OF TRANSFER UNITS WITH NO LIQUID MIXING
C
      REXPTL = (XIN -XOUT)*AL*G.165*28.32/62.4
      ALNDRV = (XIN -XOUT)/ ALOG(XIN /XOUT)
      TVOL = G.165*HITE*28.32
      AKLA = REXPTL/(ALNDRV*TVOL)
      ANOXP = AKLA * HITE * 62.4 / AL
      HOLA = HITE / ANOX
      HOLP = HITE / ANOXP
C
C     FINAL PRINT OUT
C
      IF(IPRINT.EQ.C) GO TO 701
      WRITE(6,12345)
      WRITE(6,350)M,N,XODXI2,EXPANS,P,AKA,ANOX,AKLA,ANOXP,
     1 HOLA,HOLP,AL,G,TL
  350 FORMAT(1H ,215, 2F10.5, 2F10.2, F10.4, F10.2, 3F10.4,2F10.1,F10.1)
  701 N = N + 1
C
C     HOLD EVERYTHING FOR PRINTOUT IN TABULAR FORM
C
      HOLD(N,1) = AL
      HOLD(N,2) = G
      HOLD(N,3) = XODXI2
      HOLD(N,4) = EXPANS
      HOLD(N,5) = ANOX
      HOLD(N,6) = AKA
      HOLD(N,7) = HOLA
      HOLD(N,8) = ANOXP
      HOLD(N,9) = AKLA
      HOLD(N,10) =HOLP
      HOLD(N,11) =P
      HOLD(N,12) = XIN*100.
      HOLD(N,13) = XOUT*100.
      HOLD(N,14) = TL
      HOLD(N,15) = DP
      HOLD(N,16) = ALNDRV
      HOLD(N,17) = REXPTL
      HOLD(N,18) = TVOL
      HOLD(N,19) = HITE
      HOLD(N,20) = REL
C
C
      IF(N.LT.42) GO TO 2
      CALL PRINTR(HOLD,N)
      WRITE(6,700)((HOLD(I,J),J=1,11),I=1,N)
  700 FORMAT(1H ,2F10.1,3F12.5,F12.2,2F12.5,F12.2,F12.5,F10.2)
      GO TO 500
  110 WRITE(6,111)
  111 FORMAT(1H ,'NO CONVERGENCE')
  500 STOP
C
      END
C
C
      SUBROUTINE FINDCO(RE,W,COEF)
      DIMENSION W(36,2)
      DO 200 L = 1,36
      DFRE = W(L,1) - RE
      IF(DFRE)200,300,300
  200 CONTINUE
  300 IF(L.GT.1) GO TO 500
  400 DFFR = W(L+1,1)- W(L,1)
      COEF=((W(L+1,2)-W(L,2))/DFFR)*(RE-W(L,1))+W(L,2)
      GO TO 600
  500 DFFR = W(L,1) - W(L-1,1)
      COEF = ((W(L,2) - W(L-1,2))/DFFR)*(RE-W(L,1))+W(L,2)
  600 CONTINUE
C
C
      RETURN
      END
```

```
      SUBROUTINE PRINTR(HOLD,I)
      DIMENSION HOLD(50,20)
C
      ID = 1
      NI = 0
   11 WRITE(6,1)
    1 FORMAT(1H1,  ////////////////,25X,'TABLE V  LIQUID-SIDE MASS TRANSF
     6ER COEF'
     1FICIENT DETERMINATION',/45X,'FOR MOBILE BED CONTACTOR',//
     213X,'EXPERIMENTAL DATA AND CALCULATED RESULTS FOR DESORPTION OF CA
     3RBONDIOXIDE FROM WATER'/)
      IF(NI.EQ.0)  GO  TO  3
      WRITE(6,2)
    2 FORMAT(1H ,50X,'(CONTINUED)',/)
    3 WRITE(6,4)
    4 FORMAT(1H ,10X,'RUN     LIQUID    GAS        LIQUID',9X,' TRANSFER
     1 UNITS     MASS TRANSFER    HEIGHT OF',/9X,'NUMBER     FLOW   ',
     2'  FLOW    CONCENTRATION                                  COEFFICIENT  TRAN
     4NSFER UNITS',/,20X,'L         G       XIN       XOUT          ',
     5'                  K A',12X,'H',/,41X,'10**2',11X,'N',9X,'N',
     612X,'L',14X,'OL',/20X,'LBS/HR-FT**2      GM-MOL/L,'
     511X,'OX',8X,'OXP',9X,'HR**(-1)      FT',/)
      NI = NI + 1
      IE = ID + 10
      IF(NI.EQ.4) IE = IE - 2
      WRITE(6,5)(N,HOLD(N,1),HOLD(N,2),HOLD(N,12),HOLD(N,13),
     1 HOLD(N,5),HOLD(N,8),HOLD(N,6),HOLD(N,7),N=ID,IE)
      ID = ID + 11
      IF(NI.EQ.4) GO TO 6
      GO  TO  11
    5 FORMAT(1H ,I12,F11.0,F9.0,2F9.4,F9.3,F11.3,F12.1,F14.3,/)
    6 WRITE(6,12345)
12345 FORMAT(1H1)
      RETURN
      END
```

APPENDIX III.1

GALVANOMETER AMPLIFIER

Operating Instructions

Preliminary

Switch on negative 44 volts power supply.
Switch on filament supply.
Switch on 105 and 250 volt supplies.
Allow to warm and stabilize for 40 minutes.

Zero

Switch all function switches to GND.
Switch all averager switches to OFF.
Switch all galvanometer switches to OFF.
Rotate all amplitude controls fully CCW (min.).

1 - Reference Channel

(a) Galvanometer switch to ON.
(b) Push zero button on back and adjust coarse zero control for null on recorder.
(c) Release zero button and adjust fine zero control for null on recorder.
(d) Galvanometer switch to OFF.

2 - Channel 1

(a) Galvanometer switch to ON.
(b) Push zero button on back and adjust coarse zero control for null on recorder.
(c) Release zero button and adjust fine zero control for null on recorder.
(d) Galvanometer switch to OFF.

3 - Channel 2

Same as Channel 1

4 - Channel 3

Same as Channel 1

5 - Channel 4

Same as Channel 1

6 - Channel 5

Same as Channel 1

NOTE: It is important that the Reference Channel be adjusted first.

Calibration

(a) All function switches to CALIBRATE.
(b) All galvanometer switches to OFF.
(c) Adjust all galvanometers for a mechanical zero.
(d) Rotate the reference channel amplitude control fully CCW (min.).
(e) Turn galvanometer switches for channels 1 to 5 to ON. (Ref. to OFF).
(f) Adjust amplitude controls for channels 1 to 5 such that each galvanometer will deflect equally (i.e. five units).
(g) Without altering these five settings, turn the reference channel amplitude control CW until one or more galvanometers return to a zero position.
(h) Adjust the potentiometers under the chassis to return the remaining galvanometers to zero.

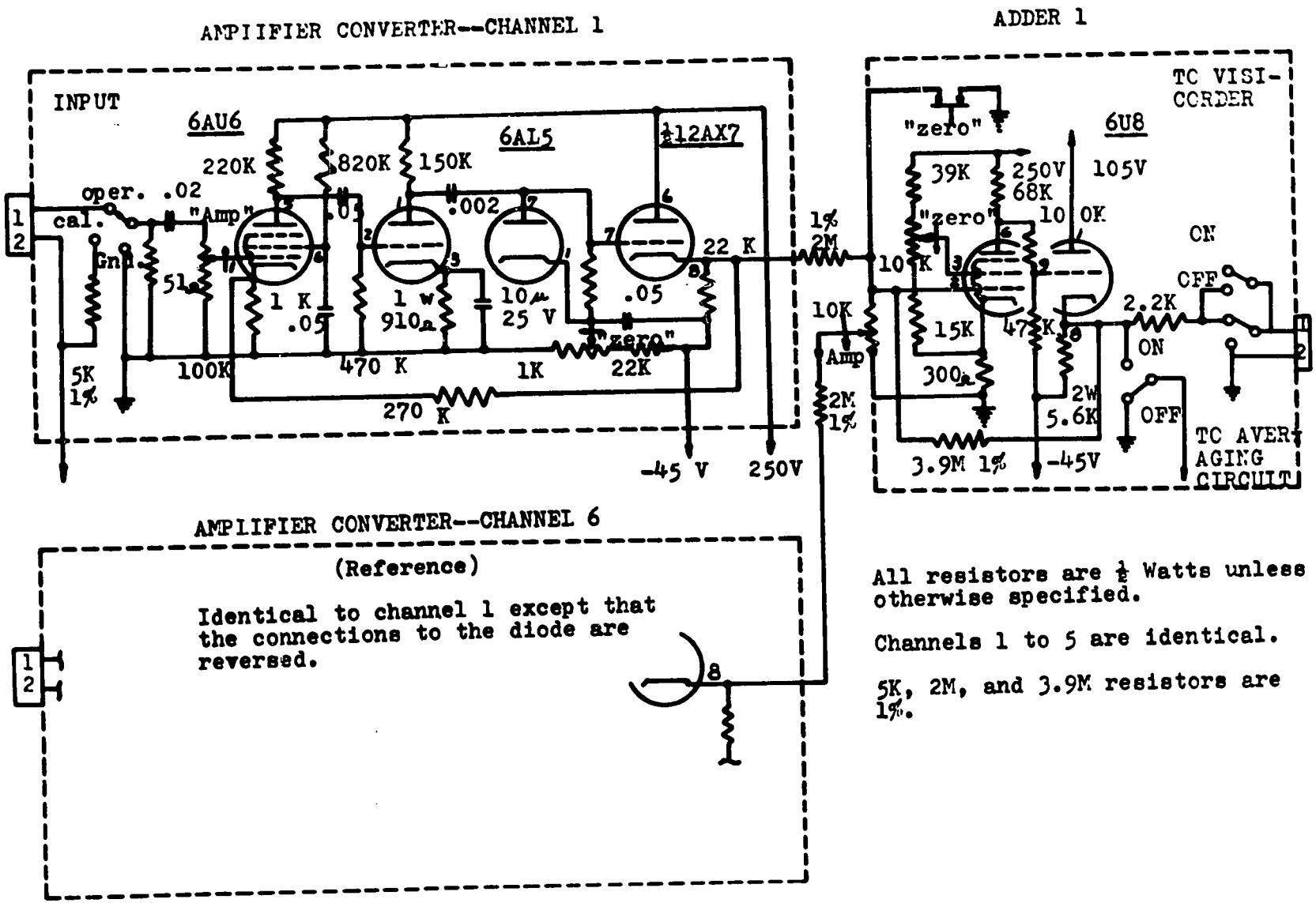

FIGURE A-1: CIRCUIT DIAGRAMS FOR AMPLIFIER DEMODULATOR

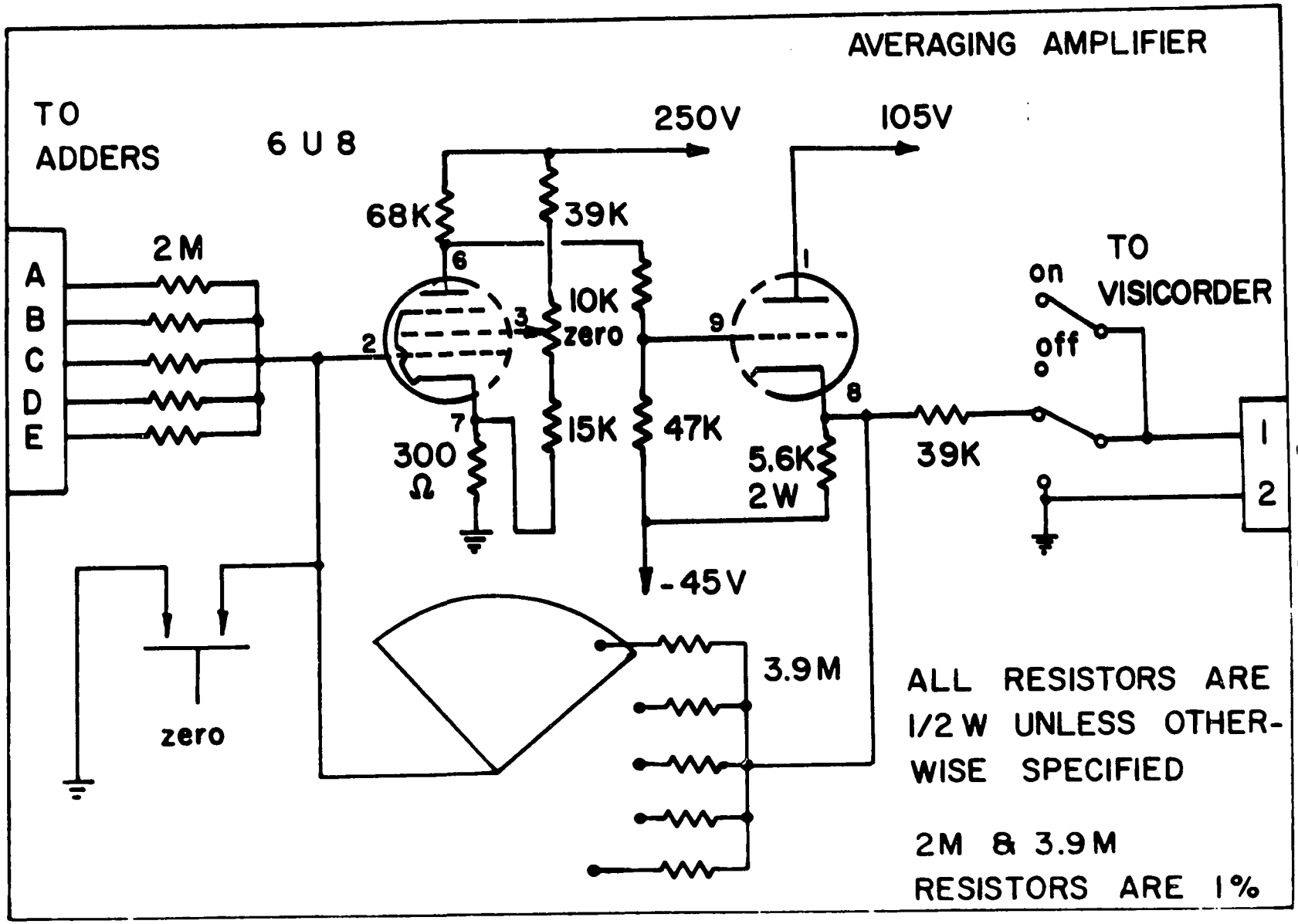
AVERAGING AMPLIFIER
TO ADDERS
6 U 8
250V
105V
68K
39K
2M
A
B
C
D
E
6
2
3
10K zero
9
1
on
off
TO VISICORDER
7
300 Ω
15K
47K
8
5.6K 2W
39K
1
2
-45V
zero
3.9M
ALL RESISTORS ARE 1/2 W UNLESS OTHERWISE SPECIFIED
2M & 3.9M RESISTORS ARE 1%

APPENDIX III.3

DYMEC SYSTEM TURN-ON FOR SINGLE CHANNEL, DC VOLT MONITOR

A. POWER SWITCHES
1. main switch pushbutton-in
2. voltmeter power switch-on; WAIT 60 sec.
3. amplifier power switch-on
4. scanner, "manual" pushbutton latched, "reset" pushbutton pressed to bring home light (red neon) on

FOR MAXIMUM ACCURACY A 1 HOUR+ WARM-UP NECESSARY

B. CONNECTIONS AND PROGRAMMING
1. input connected to channel 1 in rear panel through connecter; pos. to #3 lead, neg. to #2 lead and #1 (for Guarding) SCANNER HOME LIGHT MUST BE ON
2. plug board behind scanner panel programmed for appropriate channel, being careful that only one of each FUNCTION, RANGE, SAMPLE PERIOD used scanner pushbutton latched for selected channel, other 24 unlatched.

C. CALIBRATION AND ZEROING

VOLTMETER (each time instrument turned on, after warm-up)

a. Counter Check

100 KC STD (rear panel)	INT
FUNCTION	FREQU.
ATTEN.	CHECK
SAMPLING RATE	CW from STOP

Check reading for each of 3 fixed sample periods

.01 sec.	10.0 KC reading	
.1 sec.	10.00 KC reading	(1 count)
1.0 sec.	10.000 KC reading	

b. Zero Adjustment

LOOKC STD (rear Panel)	INT
FUNCTION	VOLT
RANGE	ZERO
SAMPLE PERIOD	1 sec
SAMPLING RATE	CW from STOP

Set front pane Zero adjustment for zero (1 count) on the digital display.

c. Full-Scale Adjustment (after Zero)

RANGE INT+1V set front panel CAL+ for +1000 mv indication on digital readout

RANGE INT-1V set front panel CAL- for -1000 mv indication on digital readout

D. SYSTEM OPERATION

Voltmeter -	RANGE	1V
	FUNCTION	EXT SEL
	ATTEN	
	SAMPLE PERIOD	EXT SEL
	SAMPLING RATE	FULL CW
Amplifier -	MODE	EXT SEL
Tape Punch -	POWER	ON for punch and print
Coupler -	AUTOMATIC	latched
	NON-PUNCH	unlatched

NOTE: Check Manual for possible Amplifier Zero Control and operational check -- these not needed daily.

APPENDIX IV

EVALUATION OF PHYSICO-CHEMICAL PROPERTIES OF CARBON DIOXIDE - SODIUM HYDROXIDE SYSTEM

(a) Estimation of Diffusivity: The diffusivity of carbon dioxide in the reacting system of interest here may be estimated from the values of diffusivity which have been reported for a variety of non-reacting systems. The diffusion coefficient was estimated from the equation:

$$D_{solution} = D_{water} \left(\frac{\mu_{water}}{\mu_{solution}} \right)^{0.85} \qquad (A-1)$$

Equation (A-1) was developed by Nigsing et al. (155) for the systems carbon dioxide-sodium sulphate and carbon dioxide-magnesium sulphate, and has been further verified indirectly for the carbon dioxide-sodium hydroxide system. The diffusivity of carbon dioxide in water as an empirical function of temperature has been given by Thomas and Adams (156) as

$$D_w = 0.044\ T_L + 0.80 \qquad (A-2)$$

where $10^o < T_L < 30^oC$

(b) Estimation of Solubility of Carbon dioxide, H.

It is not possible to measure by conventional analytical techniques the solubility of a gas in solutions with which it reacts. However, it is possible to infer the solubility of carbon dioxide in reacting solutions from the

available information on the solubility in neutral salt solutions and theoretical considerations. The solubility of gases in non-reacting electrobyte solutions can be estimated by the expression:

$$\log_{10} (H/H_w) = K_s I \qquad (A-3)$$

where $K_s = i_+ + i_- + i_G$

and

H = solubility in given electrolyte solution

H_w = solubility in water,

I = Ionic strength,

i_+, i_-, i_G = contributions due to cation, anion, and gas, respectively.

The values of i for carbon dioxide and for ions of interest, Na^+ and OH^-, at 15 and 25°C have been reported by Van Krevelen and Hoftyzer (157).

The solubility H (g mole/liter-atm.) of carbon dioxide in water is given by

$$\log_{10} H_w = \frac{1140}{T} - 5.30 \qquad (A-4)$$

T in degrees K,

whence

$$H = H_w \times 10^{-K_s I} \qquad (A-5)$$

The solubility values, H, computed from equation (A-5) has been found to compare very well with those obtained

from measurements of transient rates of absorption of carbon dioxide in reacting solutions. In fact, values of H have been extracted from experimental values of H_∞/D by using the computed values of D. Equation (A-5) can therefore be used to predict with reasonable accuracy the solubility of carbon dioxide in reacting solutions.

(c) Estimation of Reaction Velocity constant, k_2.

Carbon dioxide undergoes second-order reaction with hydroxyl ions, OH^-, and the absorption of carbon dioxide into caustic soda solution conforms to the above model. In the earlier stages of absorption, carbon dioxide diffuses into a solution containing an almost uniform concentration of OH^- ions, with which it undergoes the reaction:

$$CO_2 + OH^- \longrightarrow HCO_3^- \qquad \text{(A-6)}$$

which is first-order with respect to CO_2 and to OH^-. This reaction is followed by

$$HCO_3^- + OH^- \longrightarrow CO_3^{--} + H_2O \qquad \text{(A-7)}$$

The second stage is an ionic reaction and is very much faster. Thus, provided the concentration of OH^- is sufficiently high ($> 0.1N$) for the equilibrium concentration of HCO_3^- to be negligible, the overall reaction is

$$CO_2 + 2\,OH^- \longrightarrow CO_3^{--} + H_2O \qquad \text{(A-8)}$$

which can be considered to be first-order with respect to CO_2 and to OH^-, and having the velocity constant of reaction (A-6). Provided that the OH^- ions are not substantially

depleted in the neighbourhood of the surface, the reaction will be pseudo-first-order with a velocity constant $k = k_2 [OH^-]$. The rate of consumption of hydroxyl ions due to both stages of the reaction is twice the rate of absorption of carbon dioxide as given by equation (A-8).

A number of workers (155, 158-9) have studied the rate of hydration of carbon dioxide at infinite dilution and expressed the result by

$$\log_{10} k_{OH^-_\infty} = 13.635 - \frac{2895}{T} \qquad \text{(A-9)}$$

where T is in degrees K.

The rate of reaction of carbon dioxide in solution containing OH^- ions is complicated by the effects of ionic strength and composition on the rate constant, k_{OH^-}, at finite OH^- concentration in the solution. The variation of rate constant with ionic strength of the solution at a given temperature is given by Nijsing et al. (155) as

$$k_{OH^-} = k_{OH^-_\infty} \times 10^{\alpha I} \qquad \text{(A-10)}$$

where α = 0.18 for KOH solution

= 0.133 for NaOH solution.

The value of reaction velocity constant has, therefore, been calculated from

$$\log k_2 = \log k_{OH^-}$$

$$= 13.635 - \frac{2895}{T} + 0.133\, I \qquad \text{(A-11)}$$

The applicability of equation (A-11) has been discussed by Roberts and Danckwerts (158) and Porter et al (61).

APPENDIX V

AXIAL DISPERSION AND TRANSFER FUNCTION ANALYSIS

The transfer function, F(s), for a linear system gives the response of the system to an impressed signal. If s is expressed as a complex variable, $i\omega$, the real and imaginary parts of F(s) can be written as:

$$F(s) = X + iY$$

whence amplitude, $A = |F(s)| = (X^2 + Y^2)^{0.5}$

and phase angle , $\phi = \tan^{-1} \frac{Y}{X}$

Bode diagrams (variation of amplitude and phase angle with frequency of impressed signal, ω) can be obtained. One can thus derive steady-state frequency response from the transient response to a pulse signal. By comparing the computed frequency response (from pulse testing data) with the frequency response solution (Equation (3.22)) to the diffusion Equation (2.22) with finite-bed boundary conditions one can obtain residence time, τ, and Peclet number, P. This, however, does not offer any advantage in data processing over direct trace-matching of the original pulse data. The type of frequency response technique described above can be used to analyze two-point concentration-time data for finite-bed boundary conditions with a tracer input signal of any form, including a completely random signal.

Transfer function analysis using a real, positive value of s however provides a simpler data processing scheme. The use of real, positive values of s in Equation (3.7) in fact reduces the relative importance of the tail of the breakthrough curves in influencing the values of τ and P. It is, however, important to realize that the use of a very large value of s has the effect of almost completely eliminating the weighting of the data at large t because of exponential decay factor e^{-st} in Equation (3.7). Michelsen and Ostergaard (103) have shown that a value of the product, $s\tau$, between 1 and 2 gives the most accurate results by this analysis. This range of values has therefore been used in the present analysis of data.

The details of the actual data processing are presented next in three parts.

I. As moment analysis gives an approximate solution for the case of infinite-bed boundary conditions, a program for moment analysis was used to obtain rough estimates of τ and P for each experimental. (This estimate for P and τ was also used in debugging the data processing by the more accurate transfer- function analysis programs.)

II. A series of values of s was defined using the initial estimates of τ from moment analysis such that the product $s\tau$ varied between 1 and 2. This series of values of s was used to obtain corresponding experimental values of F(s) according to Equation (3.7). The values of P and τ for each run were then obtained

according to Equation (3.8) which is valid for infinite-bed boundary conditions.

III. The values of τ and P from the above were used as the initial estimate in the application of transfer-function analysis for finite-bed boundary conditions. This procedure was as follows:

- select a mean value of s from previous program,
- vary P and τ by $\pm$ 20% in 20 steps each,
- compute 400 values for F(s) for the finite-bed model from Equation (3.12) using the above single value of s and the 400 sets of values of P and τ.
- compare these values of F(s) with the single experimental value of F(s) for the same value of s as computed from Equation (3.7), and retain and average all those combinations of τ and P which meet the criterion

$$|F(s)_{exptl.} - F(s)_{calculated}| \leq 0.0001$$

- repeat the above process for a second value of s, and obtain the arithmetic mean of the two. The values of τ and P thus obtained are reported as corrected residence time and Peclet number in this thesis.

Since MBC did not show very high liquid mixing, the magnitude of these corrections was less than 5% of their values obtained by transfer-function analysis using infinite-bed boundary conditions.